



PHD

**Sex differences in the effects of kappa opioid receptors agonists and acute stress on the mouse brain**

Ma, Qianhan

*Award date:*  
2020

*Awarding institution:*  
University of Bath

[Link to publication](#)

**Alternative formats**

If you require this document in an alternative format, please contact:  
[openaccess@bath.ac.uk](mailto:openaccess@bath.ac.uk)

Copyright of this thesis rests with the author. Access is subject to the above licence, if given. If no licence is specified above, original content in this thesis is licensed under the terms of the Creative Commons Attribution-NonCommercial 4.0 International (CC BY-NC-ND 4.0) Licence (<https://creativecommons.org/licenses/by-nc-nd/4.0/>). Any third-party copyright material present remains the property of its respective owner(s) and is licensed under its existing terms.

**Take down policy**

If you consider content within Bath's Research Portal to be in breach of UK law, please contact: [openaccess@bath.ac.uk](mailto:openaccess@bath.ac.uk) with the details. Your claim will be investigated and, where appropriate, the item will be removed from public view as soon as possible.

# **Sex differences in the effects of kappa opioid receptor agonists and acute stress on the mouse brain**

**Qianhan Ma**

**A thesis submitted for the degree of Doctor of  
Philosophy**

**University of Bath**

**Department of Pharmacy & Pharmacology**

**May 2019**

## **COPYRIGHT**

Attention is drawn to the fact that copyright of this thesis rests with the author. A copy of this thesis has been supplied on condition that anyone who consults it is understood to recognise that its copyright rests with the author and that they must not copy it or use material from it except as permitted by law or with the consent of the author.

This thesis may be made available for consultation within the University Library and may be photocopied or lent to other libraries for the purposes of consultation.

# Table of Contents

<b>Table of figures and tables .....</b>	<b>v</b>
<b>Acknowledgements .....</b>	<b>xi</b>
<b>Abstract .....</b>	<b>xii</b>
<b>List of Abbreviations .....</b>	<b>xiv</b>
<b>1 General Introduction .....</b>	<b>1</b>
Hypothesis and aims .....	2
1.1 Stress .....	3
1.1.1 A risk factor for psychiatric disease .....	3
1.1.2 Stress and the HPA axis .....	4
1.1.3 Brain regions involved in stress .....	6
1.1.4 Stress in anxiety and depression .....	7
1.1.5 Role of stress in addiction .....	9
1.1.6 Animal models of stress .....	12
1.2 Kappa opioid receptor .....	13
1.2.1 What is the kappa opioid receptor? .....	13
1.2.2 Distribution of KOPrs .....	14
1.2.3 Role of KOPrs in stress .....	16
1.2.4 Role of KOPrs in addiction .....	19
1.3 Sex differences .....	22
1.3.1 Sex differences of opioid receptors in pain and analgesia .....	22
1.3.2 Sex differences in response to stress .....	24
1.3.3 Sex differences in KOPr and stress .....	26
1.3.4 Sex differences in KOPrs and addiction .....	27
1.4 Transgenic animal strains .....	29
1.4.1 cFos .....	29

1.4.2	cFos-GFP and GAD-GFP transgenic mice .....	30
1.4.3	The advantages of using cFos-GFP mice .....	31
<b>2</b>	<b>General Methods .....</b>	<b>32</b>
2.1	Animals .....	33
2.2	Genotyping .....	33
2.3	Antibodies .....	34
2.4	Restraint stress .....	35
2.5	Forced Swim Stress (FSS) .....	35
2.6	Kappa opioid receptor ligands .....	36
2.7	Protein extraction and Western blotting .....	36
2.8	RNA Isolation .....	37
2.9	Reverse transcription PCR (RT-PCR) .....	38
2.10	Immunocytochemistry .....	39
2.11	Blood sampling .....	40
2.12	Corticosterone analysis .....	41
2.13	Data quantification and statistical analysis .....	42
2.14	Reagents and materials .....	42
<b>3</b>	<b>Optimisation of methods used to quantifying cFos activation .....</b>	<b>43</b>
3.1	Introduction .....	44
3.2	Methods .....	45
3.2.1	Animals .....	45
3.2.2	<i>In vivo</i> stressor .....	45
3.2.3	Immunohistochemistry .....	45
3.2.4	Quantification and statistical analysis .....	45
3.3	Results .....	46
3.3.1	Validation of anti-GFP antibody .....	46
3.3.2	Expression of GFP following <i>in vivo</i> stress .....	47
3.3.3	Expression of cFos mRNA following <i>in vivo</i> stress .....	50
3.3.4	Immunohistochemical localisation of cFos and GFP expression .....	51

3.3.5	Optimisation of immunohistochemical methodology .....	54
3.4	Discussion .....	59
<b>4</b>	<b>The effect of kappa opioid receptor activation and <i>in vivo</i> stressor in male mice .....</b>	<b>61</b>
4.1	Introduction .....	62
4.2	Methods .....	65
4.2.1	Immunohistochemistry .....	65
4.3	Results .....	67
4.3.1	The effect of U50,488 in male PFCx .....	67
4.3.2	The effect of FSS in male PFCx .....	71
4.3.3	The effect of U50,488 in male NAc .....	74
4.3.4	The effect of FSS in male NAc .....	78
4.3.5	Overlapping expression of cFos and GFP in PFCx and NAc .....	81
4.3.6	The effect of U50,488 in male hippocampus .....	86
4.3.7	The effect of FSS in male hippocampus .....	92
4.3.8	The effect of U50,488 in male amygdala .....	97
4.3.9	The effect of FSS in male amygdala .....	103
4.3.10	Summary of different stimuli in male mice .....	108
4.4	Discussion .....	110
<b>5</b>	<b>The effect of kappa opioid receptor activation and <i>in vivo</i> stressor in female mice .....</b>	<b>116</b>
5.1	Introduction .....	117
5.2	Methods .....	118
5.2.1	Immunohistochemistry .....	118
5.3	Results .....	119
5.3.1	The effect of U50,488 and FSS in female PFCx .....	119
5.3.2	The effect of U50,488 and FSS in female NAc .....	124
5.3.3	The effect of U50,488 and FSS in female hippocampus .....	129
5.3.4	The effect of U50,488 and FSS in female amygdala .....	139

5.4	Discussion .....	149
<b>6</b>	<b>Identification of activated neurons in response to stress .....</b>	<b>156</b>
6.1	Introduction .....	157
6.2	Methods .....	158
6.2.1	Immunohistochemistry .....	158
6.3	Results .....	159
6.4	Discussion .....	167
<b>7</b>	<b>Effect of acute stress and kappa opioid receptor activation on plasma corticosterone in adult male and female mice .....</b>	<b>170</b>
7.1	Introduction .....	171
7.2	Methods .....	173
7.2.1	Animals .....	173
7.2.2	FSS and KOPr ligand treatment .....	173
7.2.3	Blood collection and corticosterone analysis .....	173
7.2.4	Statistical analysis .....	173
7.3	Results .....	174
7.4	Discussion .....	178
<b>8</b>	<b>General Discussion .....</b>	<b>181</b>
8.1	Sex differences in KOPr expression .....	183
8.2	Sex differences in KOPr activation and signaling .....	184
8.3	Sex differences in stress-induced cFos expression .....	187
8.4	Future work .....	190
	<b>References .....</b>	<b>196</b>
	<b>Published abstracts .....</b>	<b>214</b>

## Table of figures and tables

<b>Chapter 1 .....</b>	<b>1</b>
<b>Figure 1.1</b> Overview of the hypothalamic-pituitary-adrenal (HPA) axis .....	5
<b>Figure 1.2</b> Schematic diagram of the location and function of brain regions that are important in mediating stress responses .....	6
<b>Figure 1.3</b> Illustration of the rewarding mesolimbic dopamine pathway in the brain .....	10
<b>Table 1.1</b> Summary of ligands that activate on KOPr .....	13
<b>Figure 1.4</b> The distribution of KOPrs and KOPr system in major circuits implicated in stress and addiction responses .....	15
<b>Figure 1.5</b> Schematic diagram of HPA axis and expressions of KOPrs, GRs and MRs .....	16
<b>Figure 1.6</b> Schematic diagram of mechanism underlies KOPrs-modulated dopamine transmission from VTA to NAc .....	21
<b>Figure 1.7</b> Illustration of transcription factor cFos gene induction .....	29
<b>Figure 1.8</b> Schematic diagram of cFos gene and cFos-GFP transgene structure in response to stressor stimuli .....	30
 <b>Chapter 2 .....</b>	 <b>32</b>
<b>Table 2.1</b> The genetic sequences of forward and reverse primer sequences for $\beta$ -actin (internal positive control) and GFP (transgene) .....	34
<b>Table 2.2</b> Gene specific forward and reverse primers designed for one step RT-PCR .....	39
 <b>Chapter 3 .....</b>	 <b>43</b>
<b>Figure 3.3.1</b> Validation of anti-GFP antibody .....	47
<b>Figure 3.3.2</b> GFP expression following two hours restraint stress .....	49
<b>Figure 3.3.3</b> Expression of cFos mRNA after <i>in vivo</i> stressor .....	51
<b>Figure 3.3.4</b> Coronal sections of the dorsal and ventral hippocampus in mouse brain immunostained for cFos and GFP .....	53

<b>Figure 3.3.5</b> Example images of stress-induced cFos and cFos-driven GFP expression in the PFCx in male mice .....	55
<b>Figure 3.3.6</b> Two different methods of quantifying the effects of stress on cFos and cFos-driven GFP expression in the PFCx in mice .....	56
<b>Figure 3.3.7</b> Example images of stress-induced cFos and cFos-driven GFP expression in the hippocampal CA1 region in male mice .....	57
<b>Figure 3.3.8</b> Two different quantifying methods for analysing FSS-induced cFos and GFP expression in the CA1 region of the hippocampus in male mice .....	58
 <b>Chapter 4</b> .....	<b>61</b>
<b>Figure 4.1</b> Illustration of immunohistochemistry procedures for male C57BL/6 cFos-GFP mice following pharmacological or physical <i>in vivo</i> stressors .....	66
<b>Figure 4.2A</b> Coronal section of mouse brain showing prefrontal cortex .....	68
<b>Figure 4.2B</b> The Effect of U50,488 (20mg/kg) on cFos and GFP expression in PFCx in the presence of norBNI (10mg/kg) in male cFos-GFP mice .....	69
<b>Figure 4.2C</b> Quantified fluorescent signals of cFos and GFP expression following U50,488 (20mg/kg) in PFCx .....	70
<b>Figure 4.3A</b> The Effect of 15-minute FSS on cFos and GFP expression in PFCx in the presence of norBNI (10mg/kg) .....	72
<b>Figure 4.3B</b> Quantified fluorescent signals of cFos and GFP expression following FSS in PFCx .....	73
<b>Figure 4.4A</b> Coronal section of mouse brain showing nucleus accumbens .....	75
<b>Figure 4.4B</b> Illustration of cFos and GFP expression in NAc core after U50,488 (20mg/kg) treatment in the presence of norBNI (10mg/kg) .....	76
<b>Figure 4.4C</b> Quantification of fluorescent cFos and GFP signals following U50,488 (20mg/kg) in NAc core .....	77
<b>Figure 4.5A</b> Demonstration of cFos and GFP expression following 15-minute FSS in NAc core in the presence of norBNI (10mg/kg) .....	79
<b>Figure 4.5B</b> Quantified fluorescent signals of cFos and GFP expression following FSS in NAc core .....	80
<b>Figure 4.6A</b> Overlapping images of cFos-expressing neurons (red), GFP-expressing neurons (green) and cFos/GFP co-localised in the same neurons in PFCx and NAc core .....	83



<b>Figure 4.6B</b> Overlapping images of cFos-expressing neurons (red), GFP-expressing neurons (green) and cFos/GFP co-localised in the same neurons in PFCx and NAc core .....	84
<b>Figure 4.6C</b> Percentage of overlapping neurons in total neurons in PFCx (A) and NAc core (B) .....	85
<b>Figure 4.7A</b> Coronal section of mouse brain showing dorsal hippocampus .....	87
<b>Figure 4.7B</b> Fluorescent images of cFos and GFP expression in CA1 region of dorsal hippocampus after U50,488 (20mg/kg) treatment in the absence or presence of norBNI (10mg/kg) .....	88
<b>Figure 4.7C</b> Quantification of fluorescent cFos and GFP signals following U50,488 (20mg/kg) in hippocampal CA1 region .....	89
<b>Figure 4.7D</b> Fluorescent images of cFos and GFP expression in dentate gyrus of dorsal hippocampus after U50,488 (20mg/kg) treatment in the presence or absence of norBNI (10mg/kg) .....	90
<b>Figure 4.7E</b> Quantification of fluorescent cFos and GFP signals following U50,488 (20mg/kg) in hippocampal dentate gyrus .....	91
<b>Figure 4.8A</b> Fluorescent images of cFos and GFP expression in CA1 region of dorsal hippocampus after 15-minute FSS .....	93
<b>Figure 4.8B</b> Quantified fluorescent cFos and GFP signals following 15-minute FSS in hippocampal CA1 region .....	94
<b>Figure 4.8C</b> Fluorescent images of cFos and GFP expression in dentate gyrus of dorsal hippocampus after 15-minute FSS .....	95
<b>Figure 4.8D</b> Quantified fluorescent cFos and GFP signals following 15-minute FSS in dentate gyrus of hippocampus .....	96
<b>Figure 4.9A</b> Coronal section of mouse brain containing amygdala .....	98
<b>Figure 4.9B</b> Fluorescent images of cFos and GFP expression in CeA after a single U50,488 (20mg/kg) administration .....	99
<b>Figure 4.9C</b> Quantified fluorescent cFos and GFP signals following U50,488 treatment in CeA .....	100
<b>Figure 4.9D</b> Fluorescent images of cFos and GFP expression in BLA after a single U50,488 (20mg/kg) administration .....	101
<b>Figure 4.9E</b> Quantified fluorescent cFos and GFP signals following U50,488 treatment in BLA .....	102
<b>Figure 4.10A</b> Fluorescent images of cFos and GFP expression in CeA following FSS.....	104

<b>Figure 4.10B</b> Quantified fluorescent cFos and GFP signals following 15-minute FSS in CeA .....	105
<b>Figure 4.10C</b> Fluorescent images of cFos and GFP expression in BLA following FSS .....	106
<b>Figure 4.10D</b> Quantified fluorescent cFos and GFP signals following 15-minute FSS in BLA .....	107
<b>Table 4.1</b> Summary of cFos and cFos-induced GFP expression in different brain regions following KOR activation, U50,488 and in vivo forced swim stress (FSS) .....	109
 <b>Chapter 5</b> .....	<b>116</b>
<b>Table 5.1</b> Comparison between male and female cFos-GFP mice on cFos and GFP expression in PFCx following U50,488 or FSS treatment.....	119
<b>Figure 5.1A</b> Fluorescent images of cFos and GFP expression in female PFCx after U50,488 treatment .....	120
<b>Figure 5.1B</b> Quantification of fluorescent cFos and GFP signals following U50,488 in female PFCx .....	121
<b>Figure 5.1C</b> Fluorescent images of cFos and GFP expression in female PFCx after 15-minute FSS .....	122
<b>Figure 5.1D</b> Quantification of fluorescent cFos and GFP signals following FSS in female PFCx .....	123
<b>Table 5.2</b> Comparison between male and female cFos-GFP mice on cFos and GFP expression in NAc core following U50,488 or FSS treatment .....	124
<b>Figure 5.2A</b> Fluorescent images of cFos and GFP expression in female NAc core after U50,488 injection .....	125
<b>Figure 5.2B</b> Quantification of fluorescent cFos and GFP signals following U50,488 in female NAc core.....	126
<b>Figure 5.2C</b> Fluorescent images of cFos and GFP expression in female NAc core after FSS .....	127
<b>Figure 5.2D</b> Quantification of fluorescent cFos and GFP signals following FSS in female NAc core.....	128
<b>Table 5.3</b> Comparison between male and female cFos-GFP mice on cFos and GFP expression in CA1 region of hippocampus following U50,488 or FSS treatment .....	130
<b>Table 5.4</b> Comparison between male and female cFos-GFP mice on cFos and GFP expression in dentate gyrus following U50,488 or FSS treatment .....	130

<b>Figure 5.3A</b> Fluorescent images of cFos and GFP expression in female CA1 region of hippocampus after U50,488 injection .....	131
<b>Figure 5.3B</b> Quantification of fluorescent cFos and GFP signals following U50,488 in female hippocampal CA1 .....	132
<b>Figure 5.3C</b> Fluorescent images of cFos and GFP expression in female hippocampal CA1 region after FSS .....	133
<b>Figure 5.3D</b> Quantification of fluorescent cFos and GFP signals following FSS in female hippocampal CA1 region .....	134
<b>Figure 5.3E</b> Fluorescent images of cFos and GFP expression in female dentate gyrus region of hippocampus after U50,488 injection .....	135
<b>Figure 5.3F</b> Quantification of fluorescent cFos and GFP signals following U50,488 in female hippocampal dentate gyrus .....	136
<b>Figure 5.3G</b> Fluorescent images of cFos and GFP expression in female dentate gyrus region of hippocampus FSS .....	137
<b>Figure 5.3H</b> Quantification of fluorescent cFos and GFP signals following FSS in female hippocampal dentate gyrus .....	138
<b>Table 5.5</b> Summary of U50,488 or FSS-induced effects in CeA in both male and female cFos-GFP mice .....	140
<b>Table 5.6</b> Summary of U50,488 or FSS-induced effects in BLA in both male and female cFos-GFP mice .....	140
<b>Figure 5.4A</b> Fluorescent images of cFos and GFP expression in CeA following a single U50,488 (20mg/kg) administration .....	141
<b>Figure 5.4B</b> Quantified fluorescent cFos and GFP signals following U50,488 treatment in CeA in female mice .....	142
<b>Figure 5.4C</b> Typical expression pattern of cFos and GFP in CeA from female mice after FSS .....	143
<b>Figure 5.4D</b> Quantified fluorescent cFos and GFP signals following FSS in CeA in female mice .....	144
<b>Figure 5.4E</b> Fluorescent images of cFos and GFP expression in BLA of female mice following a single U50,488 (20mg/kg) treatment .....	145
<b>Figure 5.4F</b> Quantified fluorescent cFos and GFP signals following U50,488 injection in BLA of female mice .....	146
<b>Figure 5.4G</b> Fluorescent images of cFos and GFP expression pattern in BLA of female mice after FSS .....	147

<b>Figure 5.4H</b> Quantification of fluorescent signals following FSS in BLA in female mice .....	148
--	-----

<b>Table 5.7</b> Summary of cFos and cFos-induced GFP expression in different brain regions in female mice following KOPr activation (50,488) and <i>in vivo</i> stress (FSS) .....	149
---	-----

<b>Table 5.8</b> Summary of the sex differences in the expression of cFos and GFP following U50,488 and FSS treatment .....	150
---	-----

## **Chapter 6 .....156**

<b>Figure 6.1</b> Fluorescent images of cFos-expressing neurons (red), GABAergic neurons (green) and cFos/GABAergic neurons overlapping in male PFCx following U50,488 and FSS .....	161
--	-----

<b>Figure 6.2</b> Fluorescent images of cFos-expressing neurons (red), GABAergic neurons (green) and cFos/GABAergic neurons overlapping in male NAc following U50,488 and FSS .....	162
---	-----

<b>Figure 6.3</b> Total number of cFos-expressing neurons that were induced by U50,488 or FSS in male PFCx and NAc .....	163
--	-----

<b>Figure 6.4</b> Fluorescent images of cFos-expressing neurons (red), GABAergic neurons (green) and cFos/GABAergic neurons overlapping in female PFCx following U50,488 and FSS .....	164
--	-----

<b>Figure 6.5</b> Fluorescent images of cFos-expressing neurons (red), GABAergic neurons (green) and cFos/GABAergic neurons overlapping in female NAc following U50,488 and FSS .....	165
---	-----

<b>Figure 6.6</b> Total number of cFos-expressing neurons that were induced by U50,488 or FSS in female PFCx and NAc .....	166
--	-----

## **Chapter 7 .....170**

<b>Figure 7.1</b> Experimental design for male and female mice treated with either stress (15 mins FSS) or KOPr agonist (U50,488) in the presence or absence of norBNI pre-treatment .....	174
--	-----

<b>Figure 7.2</b> Effect of forced swim stress (FSS) and U50,488 (20mg/kg) on corticosterone levels in male cFos-GFP transgenic mice .....	176
--	-----

<b>Figure 7.3</b> Effect of forced swim stress (FSS) and U50,488 (20mg/kg) on corticosterone levels in female cFos-GFP transgenic mice .....	177
--	-----

## Acknowledgements

Firstly, I would especially like to thank my supervisor Dr Chris Bailey, for all his great guidance and help during my PhD, for his kind support not only during my research and thesis writing, but also any other difficulties encountered in my life. This work would not have been achieved without his constant feedback and help.

I would also like to thank my supervisors Dr Sarah Bailey and Prof Sue Wonnacott who have always supported and encouraged me in numerous ways throughout my PhD.

Many thanks to all the technical staff in 4 South annex animal unit for their patient help and support, special thanks to Martin and Lesley for spending time with me on blood sampling, it would not be possible to do without your support.

Special thanks to all PhD students in the 5W PhD office, who made me laugh and made my difficult time more cheerful. Particularly to Jo, for being such a supportive lab mate when I first started my research life and being such a great friend throughout my PhD. With special mention to Fritz, thank you for all the laughs and sharing fascinating stories, getting me through difficult days in the lab and keeping me going.

Last but not the least, I would like to thank my family, my parents who have always believed in me and encourage me during my studies and throughout this PhD process.

I am grateful for all your continuous and generous support!

## Abstract

Stress is a risk factor for the development of psychiatric disorders (e.g. depression, anxiety) and drug addiction. Stress induces the release of endogenous neuropeptide, dynorphin, which primarily activates kappa opioid receptor (KOPr) and produces aversive and depressive-like behaviours in rodents. Stress-induced depressive-like behaviours and stressed-induced potentiation of drug self-administration are inhibited, at least in part, by blocking KOPrs, showing that KOPr plays an important role in mediating stress responses and motivational behaviours, and acts as a potential therapeutic target for the treatment of affective disorders. However, accumulating studies have reported that stress-induced behavioural effects or stress-induced KOPrs activation are sex dependent. In this study, the effects of acute forced swim stress (FSS) and activation of KOPr by the selective agonist, U50,488 (20mg/kg, i.p.) on neuronal activation in different brain regions (prefrontal cortex (PFCx), nucleus accumbens (NAc), hippocampus and amygdala) were investigated in both male and female mice.

Adult (9-13 weeks old) male and female C57BL/6 cFos-GFP transgenic mice were used, where the cFos acts as a neuronal activity marker and drives the production of green fluorescent protein (GFP) upon neuron activation. FSS and U50,488-induced neuronal activity (cFos or cFos-driven GFP expression) was detected by immunohistochemistry. Our data showed that there is an overlap in brain regions that are activated by U50,488 and FSS in male mice, with significant increases in cFos and cFos-driven GFP expression seen in the PFCx, NAc and basolateral amygdala following both types of stimuli. Only U50,488, not FSS, induced significant cFos expression in the hippocampal CA1 region and central amygdala in male mice. Different patterns were observed in female mice; in the PFCx, neither U50,488 nor FSS induced significant cFos expression. In the NAc, only FSS, not U50,488, increased cFos expression. Other regions in females, including hippocampal CA1, central amygdala and basolateral amygdala, showed similar cFos expression patterns that were seen in male mice. Generally, KOPr activation-induced cFos or GFP expression was significantly blocked by pretreatment KOPr antagonist, norBNI (10mg/kg, i.p.), whereas FSS-induced effects were not affected by norBNI. Overall, this study

provided a better understanding of stress mechanisms, especially in PFCx and NAc, highlighting that PFCx and NAc are the regions that showed different effects following KOPr activation and *in vivo* stressor between male and female mice, which may underlie sex differences in stress-induced behaviours.

## List of Abbreviations

<b>ACSF</b>	Artificial cerebrospinal fluid
<b>ACTH</b>	Adrenocorticotrophic hormone
<b>ANOVA</b>	Analysis of variance
<b>AP-1</b>	Activator protein-1
<b>BDNF</b>	Brain-derived neurotrophic factor
<b>BLA</b>	Basolateral amygdala
<b>BSA</b>	Bovine serum albumin
<b>CeA</b>	Central amygdala
<b>CIS</b>	Chronic immobilisation stress
<b>CPA</b>	Conditioned place aversion
<b>CPP</b>	Conditioned place preference
<b>CREB</b>	Cyclic adenosine monophosphate response element-binding protein
<b>CFH</b>	Corticotropin releasing factor
<b>CRH</b>	Corticotropin releasing hormone
<b>CRHR1</b>	Corticotropin releasing hormone receptor 1
<b>CRHR2</b>	Corticotropin releasing hormone receptor 2
<b>DA</b>	Dopamine
<b>DNA</b>	Deoxyribonucleic acid
<b>DOPr</b>	Delta opioid receptor
<b>DYN</b>	Dynorphin
<b>EDTA</b>	Ethylenediaminetetraacetic acid
<b>EGFP</b>	Enhanced green fluorescent protein
<b>ELISA</b>	Enzyme-linked immunosorbent assay
<b>FSS</b>	Forced swim stress
<b>GABA</b>	$\gamma$ -aminobutyric acid
<b>GFAP</b>	Glial fibrillary acidic protein
<b>GFP</b>	Green fluorescent protein
<b>GPCR</b>	G-protein coupled receptor
<b>GR</b>	Glucocorticoid receptor
<b>HIP</b>	Hippocampus



<b>HPA</b>	Hypothalamic Pituitary Adrenal
<b>ICSS</b>	Intracranial self-stimulation
<b>IEG</b>	Immediate early gene
<b>IHC</b>	Immunofluorescent histochemistry
<b>i.p.</b>	Intraperitoneal
<b>KOPr</b>	Kappa opioid receptor
<b>LH</b>	Learned helplessness
<b>LTP</b>	Long term potentiation
<b>mPFC</b>	Medial prefrontal cortex
<b>mRNA</b>	Messenger ribonucleic acid
<b>MOPr</b>	Mu opioid receptor
<b>MR</b>	Mineralocorticoid receptor
<b>NAc</b>	Nucleus accumbens
<b>NMDA</b>	N-methyl-D-aspartate
<b>NorBNI</b>	Norbinaltorphimine
<b>PCR</b>	Polymerase chain reaction
<b>PFCx</b>	Prefrontal cortex
<b>PTSD</b>	Post traumatic stress disorder
<b>PVDF</b>	Polyvinylidene fluoride
<b>PVN</b>	Paraventricular nucleus
<b>RIPA</b>	Radio immunoprecipitation assay
<b>RNA</b>	Ribonucleic acid
<b>RS</b>	Restraint stress
<b>RT-PCR</b>	Reverse transcription polymerase chain reaction
<b>SDS</b>	Sodium dodecyl sulfate
<b>SDS-PAGE</b>	Sodium dodecyl sulfate polyacrylamide gel electrophoresis
<b>TBST</b>	Tris buffered saline tween 20
<b>TH</b>	Tyrosine hydroxylase
<b>VGLUT2</b>	Vesicular glutamate transporter 2
<b>VTA</b>	Ventral tegmental area
<b>WMT</b>	Water maze task

# **Chapter 1 General Introduction**

# Hypothesis and aims

There is a strong association between sex and stress-induced behavioural responses, and the sex differences in stress-induced kappa opioid receptor activation. It is hypothesised that *in vivo* stress or pharmacological activation of KOPr, induces neuronal activity at the molecular level is sex dependent.

To test this hypothesis, the following aims are addressed in this project:

1. To determine the brain regions activated by stress in cFos-GFP mice and optimise the techniques that can be used in determining neuronal activity.
2. To determine any differences between a physical stressor and pharmacological KOPr activation in male cFos-GFP mice.
3. To investigate any sex differences in the effects of stress and KOPr activation on neuronal activation pattern between male and female cFos-GFP mice, and investigate if pre-treatment of KOPr antagonist, norBNI would block stress-induced effects in both sexes.
4. To identify the types of stress-activated neurons by using GAD-GFP transgenic mice and measure the levels of stress-induced steroid hormone e.g. corticosterone in response to both forced swim stress and a single KOPr agonist treatment.

In this study, I have quantified immunofluorescent labelling for cFos-GFP mice on different brain regions, including prefrontal cortex, hippocampus, amygdala and nucleus accumbens following stress, or KOPr activation. These are key regions involved in neural circuitry mediating the response to stress and KOPr activation. These studies will provide us with greater insight into the roles of these brain regions in both stress, and the behavioural effects KOPr activation, and whether the effects differ between sexes.

# 1.1 Stress

## 1.1.1 A risk factor for psychiatric disease

Stress is a well-known risk factor for the development of psychiatric disorders, drug addiction and triggers drug relapse. Acute or chronic stressors have been known to be involved in the pathogenesis of psychiatric diseases, such as depression and anxiety disorders, which are also strongly associated with drug dependence. Statistics show that there were 19.7% of people in the UK affected by anxiety disorder and mental illness, and more than 2 million people affected by substance abuse in the UK in 2014/15 (Evans *et al.*, 2016, NHS Digital, 2017). Depression is one of the most serious and prevalent mental disorders that affects approximately 21% of the total population in developed countries (Wong *et al.*, 2001).

Stress plays an important role in regulating brain structure and function through a number of mediators, including brain-derived neurotrophic factor (BDNF), excitatory amino acid neurotransmitters, endocannabinoids and glucocorticoids, resulting in neuronal restructuring by altering synapse density for stress adaptation (McEwen *et al.*, 2015). For example, it was shown that repeated stress could cause reorganisation of dendrites in the hippocampus and prefrontal cortex, leading to impaired cognitive behaviours (Radley *et al.*, 2004). Prolonged stress causes neuronal loss in the medial amygdala and expansion of dendrites in the basolateral amygdala, which are believed to be important changes implicated in depression and anxiety-like behaviours (Bennur *et al.*, 2007). Overall, it is becoming clear that stress has a significant impact on the development of both drug abuse and psychiatric disorders.

### 1.1.2 Stress and the HPA axis

The hypothalamic-pituitary-adrenal (HPA) axis is activated during a physical or emotional stressor and plays a crucial role in regulating and adapting the stress responses (Figure 1.1). The HPA axis induces the release of corticotrophin releasing hormone (CRH) from the hypothalamic paraventricular nucleus (PVN), which stimulates the anterior pituitary and causes the release of adrenocorticotrophic hormone (ACTH). The released ACTH enters into the systemic circulation and promotes the synthesis and release of glucocorticoids from the cortex of the adrenal glands. The main glucocorticoid in humans is cortisol, while corticosterone is the main glucocorticoid in rodents e.g. mice, rats (Herman *et al.*, 2016). The released glucocorticoids secreted into the systemic circulation act on mineralocorticoid receptors (MRs) with a high affinity to regulate basal glucocorticoids levels and bind to glucocorticoid receptors (GRs) with a lower affinity. GRs are widely expressed throughout the brain, including cortex, hypothalamus, hippocampus and amygdala, while MRs are heavily distributed in hippocampus and hypothalamus (Keller *et al.*, 2017). Importantly, activation of GRs also inhibits the release of CRH and ACTH, resulting in reduced further release of cortisol and inhibition of stress responses. This negative feedback mechanism is an important mechanism for stress adaptation and allostatic processes in the body, illustrated in figure 1.1. (Herman *et al.*, 2016, Keller *et al.*, 2017).

Although activation of the HPA axis plays a crucial role in adapting stress responses, the exposure of prolonged and repeated stress could lead to excessive release of glucocorticoids into the systemic circulation. The dysregulation of MRs or GRs and hyperactivity of the HPA axis has been implicated in the development of depression and could be pathological in other psychiatric disorders, such as anxiety and cognitive dysfunction (Herman *et al.*, 2016). Previous studies have shown that the levels of cortisol in the plasma are elevated in 40-60% of patients with depression, suggesting that there is a strong association between overactivation of the HPA axis, elevated cortisol levels, and depression (Deuschle *et al.*, 1997, Murphy BE. 1991, Moica *et al.*, 2016).

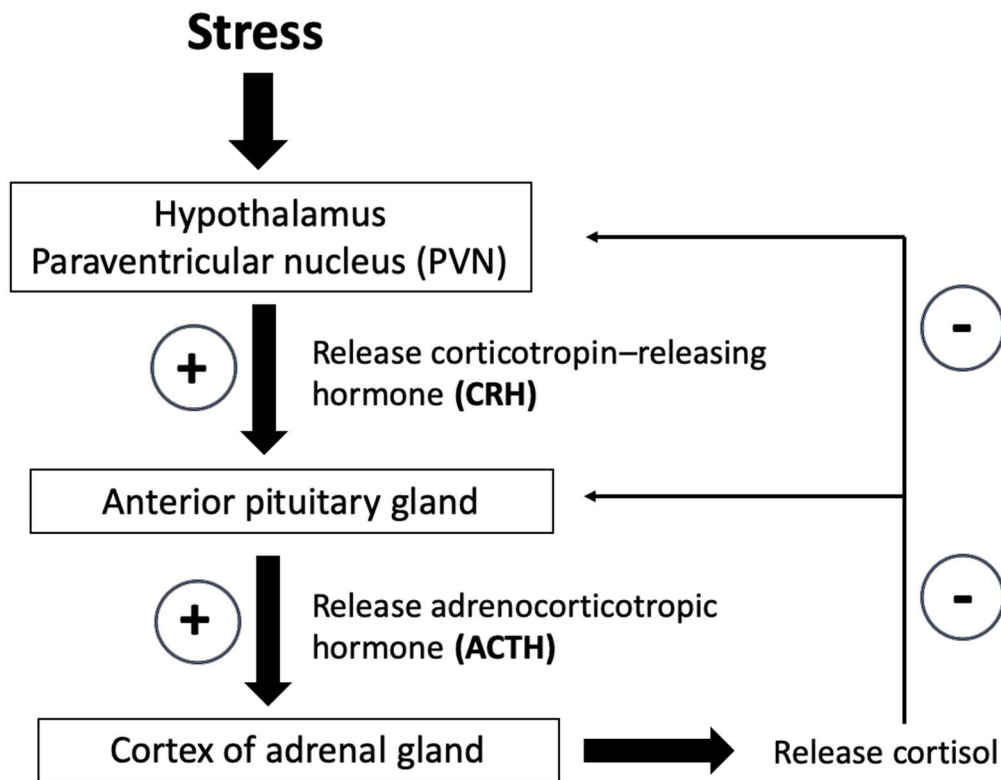


**Figure 1.1 Overview of the hypothalamic-pituitary-adrenal (HPA) axis. “+” indicates positive feedback, “-” indicates negative feedback. Stressors induce the release of CRH from PVN, which are transported to the anterior pituitary and cause ACTH release into the systemic circulation. The release of ACTH stimulates the production and secretion of glucocorticoids (cortisol in man, corticosterone in rodent e.g. rats or mice) at the adrenal cortex, which in turns cause a negative feedback mechanism on PVN and anterior pituitary gland, resulting in reduction of further cortisol release.**

### 1.1.3 Brain regions involved in stress

The brain is the primary and central organ mediating stress responses and regulating physiological responses to both social and physical stressors. Three of the primary brain regions involved in mediating behavioural responses to stressors are the prefrontal cortex (PFCx), hippocampus and amygdala (Figure 1.2). These regions are responsible for generating various stress-related responses, and stressors have been shown to directly alter gene transcription or active epigenetic modifications in these brain regions (McEwen *et al.*, 2010). For example, in the hippocampus and PFCx, chronic stressors have been shown to cause shrinkage of dendrites, which could lead to impaired memory and cognitive behaviours (Radley *et al.*, 2004). Whereas prolonged stress causes dendritic expansion in the basolateral amygdala and spine reduction in the medial amygdala, which are thought to be implicated in depression and anxiety-like behaviours (Bennur *et al.*, 2007, McEwen *et al.*, 2013).

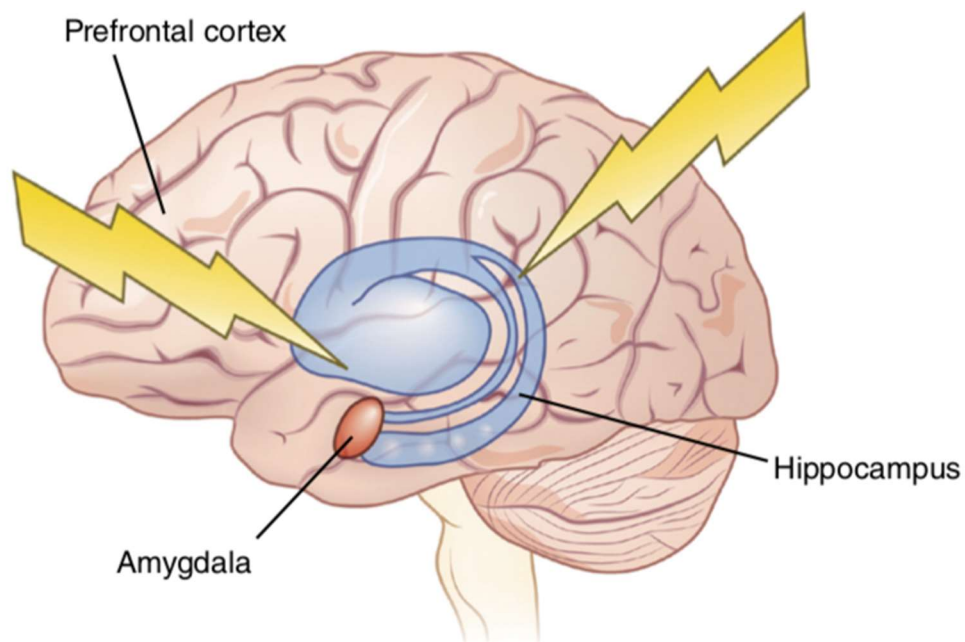


**Figure 1.2 Schematic diagram of the location and function of brain regions that are important in mediating stress responses.**

*Diagram from McEwen et al., 2015*

In addition, stress-induced glucocorticoids activate MRs and GRs, which are widely expressed throughout the brain, particularly in the CA1 region of hippocampus. Interestingly, Lowy and colleagues used *in vivo* microdialysis to show that extracellular glutamate levels in the hippocampus were significantly elevated by restraint stress, and this effect was inhibited by adrenalectomy or in MR knockout mice, indicating that glutamate levels are dependent on adrenal steroids and activation of MRs and GRs produce non-genomic effects (Lowy *et al.*, 1993, Karst *et al.*, 2005). This process might explain neuronal loss and dendritic remodelling in the hippocampus following chronic stress (McEwen *et al.*, 1999). Similarly, stress-induced excessive release of glutamate and NMDA activation is responsible for dendritic reorganisation in the medial prefrontal neurons (Martin *et al.*, 2011). Other studies also showed that central infusion of corticotropin-releasing factor (CRF) into basolateral amygdala (BLA) induces anxiety-like behaviours, suggesting that the amygdala is one of the key brain regions that mediates stress-induced responses (Jochman *et al.*, 2005).

Overall, stress-induced release of hypothalamic CRF and glucocorticoids from the adrenal glands affect prefrontal, hippocampal dendritic remodelling, and regulate synaptic plasticity and neuronal activity in the amygdala and CA1 region of hippocampus during stress responses (Chen *et al.*, 2006, McEwen *et al.*, 2015).

#### **1.1.4 Stress in anxiety and depression**

According to the psychiatric dictionary, depression is defined as ‘a mental condition characterised by feelings of severe despondency and dejection’, while anxiety is defined as ‘a nervous disorder marked by excessive uneasiness and apprehension, typically with compulsive behaviour or panic attacks’. Stress is known to be a major risk factor for clinical depression (Grant *et al.*, 2013). Although the precise mechanisms for how stress can result in anxiety and depression (Russell *et al.*, 2018), prolonged stress induces structural remodelling of dendrites and synaptic connections in the hippocampus, PFC and amygdala, which are implicated in cognitive impairment and affective disorders, such as depression and anxiety (McEwen *et al.*, 2016). Early studies revealed that chronic stress induced dendritic



shrinkage in and loss of spines in CA3 region and dentate gyrus of the hippocampus in rats (McEwen 1999), which was further supported by other evidence, demonstrating that chronic stress-induced neuronal reorganisation and dendritic shrinkage were not only found in dentate gyrus and CA3 region, but also in the hippocampal CA1 region in rats (Sousa *et al.*, 2000, Brunson *et al.*, 2005). Studies reported that the volume of hippocampus was significantly reduced in patients with depression (Bremner *et al.*, 2000, Shah *et al.*, 1998).

In addition to altering dendritic morphology in the hippocampus, stress also has been shown to affect memory functions and synaptic plasticity. Rats that were exposed to chronic stress showed spatial learning and memory deficits in the water maze task (Sousa *et al.*, 2000). Similar to the findings in rats, humans who are diagnosed with depression and hypercortisolaemia showed impaired hippocampus-dependent memory (Starkman *et al.*, 1992). Further evidence showed that stress induced impairment of long-term potentiation (LTP) in both mice and rats in the CA1 region and dentate gyrus of the hippocampus (Shors *et al.*, 1994, Garcia *et al.*, 1997). It has also been shown that stress not only impaired LTP, but also induced long-term depression (LTD) in the hippocampal CA1 region in rats (Xu *et al.*, 1997). Such stress-induced synaptic plasticity facilitates the development of depression and anxiety.

In addition to affecting the hippocampus, chronic immobilisation stress (CIS) induced dendritic expansion in the basolateral amygdala (BLA) in rats, and repeated restraint stress caused spine density reduction in the medial amygdala in mice (Vyas *et al.*, 2002, Bennur *et al.*, 2007), as well as causing neuronal remodelling and dendritic reduction in the medial prefrontal cortex (mPFC) in rats (Radley *et al.*, 2004). These findings suggest that chronic stress could affect the structural modelling of hippocampus, amygdala and mPFC regions in the brain, resulting in a higher chance of development of mood disorders such as anxiety and depression. Importantly, stress-induced HPA activity can be regulated by mPFC (Brake *et al.*, 2000) and dysregulation of HPA axis is strongly associated with mood-related disorders, such as depression and anxiety, patients with these disorders are characterised with high

levels of CRH and cortisol, blunted ACTH function in response to CRH and reduced hippocampal volume (Varghese *et al.*, 2001).

#### **1.1.5 Role of stress in addiction**

Addiction is considered to be a chronic, relapsing disorder characterized by compulsive drug-seeking and drug-taking, despite serious negative consequences (Nestler 1992; Cami and Farre, 2003). Behavioural studies e.g. self-administration or conditioned place preference (CPP) experimental paradigms have been used to study the reinforcing and rewarding properties following administration of drugs of abuse, which showed that the key mechanisms underlying the rewarding pathways of addictive drugs are related to the mesocorticolimbic dopamine pathway (Nestler 1992). The major components of this pathway are a projection of dopaminergic neurons from the ventral tegmental area (VTA) to the nucleus accumbens (NAc) in the ventral striatum and to the PFCx (Nestler 1992, Adinoff 2004) (Figure 1.3), as early animal studies in rats revealed that local administration of opiates into VTA or NAc developed CPP, also, lesions of the VTA-NAc pathway blocked cocaine self-administration and blocked intravenous opiate-induced CPP development (Pettit *et al.*, 1984, Wise *et al.*, 1987, Koob *et al.*, 1988). These studies established that the mesolimbic dopamine system plays a crucial role in drug-induced reward effect. In addition to VTA and NAc regions, microinjection of cocaine into the mPFC in rats induced reinforcing properties in a dose-dependent manner, which implies that reinforcement process of cocaine is also mediated, at least in part, by the mPFC (Goeders *et al.*, 1983). Although dopaminergic input to the nucleus accumbens is thought to be responsible for the initial rewarding properties of drugs of abuse (Di Chiara *et al.*, 1988), the development and expression of addiction-related behaviours also involves other brain regions, such as the hippocampus and amygdala (Barr *et al.*, 2014). Other evidence also showed that lesions of the amygdala and nucleus accumbens impaired cocaine self-administration, and humans with cocaine addiction showed impaired recognition memory, suggesting that both hippocampus and amygdala are also implicated in drug reward mechanisms (Bolla *et al.*, 2003, Whitelaw *et al.*, 1996).

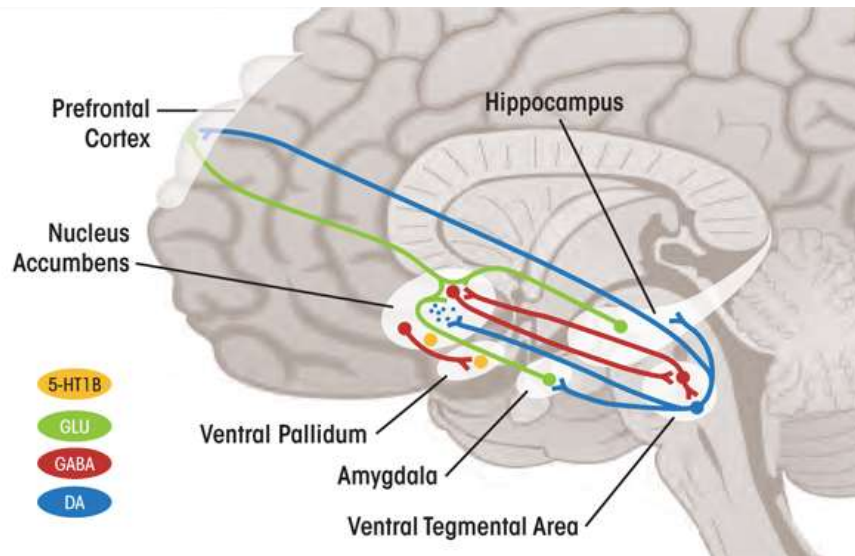


**Figure 1.3 Illustration of the rewarding mesolimbic dopamine pathway in the brain.** Dopaminergic neurons (DA, showed in blue circuit) in the ventral tegmental area (VTA) project to nucleus accumbens (NAc), hippocampus, amygdala and prefrontal cortex. GABAergic neurons (GABA, shown in red circuit) originate in the NAc and project directly to VTA and amygdala. NAc receives strong glutamatergic transmission (GLU, shown in green) from prefrontal cortex (PFCx), hippocampus and amygdala. 5-HTergic neurons (5-HT1B, shown in yellow) are populated in NAc and ventral pallidum.

*Diagram from Alim et al., 2012*

There is increasing evidence that stress also plays a key role in motivation to seek and take drugs of abuse, with stress now seen as a key risk factor for drug addiction development (Sinha, 2008). For example, animal studies revealed that stressful experiences could modulate extracellular dopamine release, indicating the strong correlation between stress and mesolimbic dopamine transmission, which could promote drug self-administration and enhances vulnerability to drug addiction (Sinha, 2008). In addition, rats with acute footshock stress-induced high levels of CRF and corticosterone are much more likely to self-administer cocaine (Erb *et al.*, 1996). Although the exact mechanism that underlies how stress overlaps with mesolimbic pathway is not fully understood, recent studies suggest that stress-induced CRF in the NAc and elevated glucocorticoids facilitates signalling in the mesolimbic dopaminergic pathway (Koob *et al.*, 2018).

The brain regions implicated in mediating stress-related and addiction-related behaviours are somewhat overlapping i.e. mesocorticolimbic dopaminergic systems. As described earlier, NAc is a key region in mesolimbic dopaminergic pathway, involved in motivation and rewarding properties. Electrophysiological studies in mice showed that glutamatergic transmission was enhanced in the NAc after two-day cold water forced swim stress (Campioni *et al.*, 2009). More importantly, acute restraint stress significantly induced immediate early genes cFos and FosB in the NAc in rats (Perrotti *et al.*, 2004). Altogether, these stress-induced effects in the NAc might contribute to stress-induced reinstatement of drug intake and also emphasise the strong correlation between mechanisms that underlying stress and drug addiction-related behaviours.

Therefore, the brain regions PFCx, hippocampus, NAc and amygdala are key regions that are involved in both stress responses and drug dependence development. The relationship between stress and the opioid receptor system, as well as their common neurochemical effects in the PFCx, hippocampus, amygdala and NAc are the focus of this project.

#### **1.1.6 Animal models of stress**

Animal models are extremely useful and beneficial for understanding pathophysiology that underlies the mechanisms of psychiatric diseases and development of potential therapeutic treatment. Animal models of psychiatric diseases, such as depression and schizophrenia have been developed using a wide range of methods, including pharmacological approaches, genetic modification, environmental manipulations and electrical stimulation (Nestler and Hyman, 2010). Forced swim, restraint and tail suspension are widely used as short-term acute physical stressors (Nestler and Hyman, 2010). A major limitation of these stressors is that it only applies short-term stress on normal animals, which is different to depression in humans. However, these physical stressors can also be applied chronically to enable the study of chronic stress and the effects on the brain. A further model used for chronic stress is 'chronic unpredictable stress' where animals are exposed to physical stressors (such as restraint) in combination with environmental stressors such as cold temperature, changes in lighting conditions, water and food restriction. Repeated physical stressors and chronic unpredictable stress paradigms have been shown to produce a depression-like phenotype that could be blocked by antidepressant administration (Jaggi *et al.*, 2011, Willner, 2016).

Therefore, there are numerous different ways to induce stress in rodents. As mentioned above, chronic stress is a complex process, which involves adaptive process in the HPA activation and remodelling of the brain region structures (Campos *et al.*, 2013). Since acute and chronic stress induces different physiological effects in rodents, it is impossible to directly compare the acute and chronic-induced physiological or behavioural effects. As previous studies in C57BL/6 mice demonstrated that two hours restraint stress or forced swim stress (15 minutes) significantly induced high levels of corticosterone levels (Wittmann *et al.*, 2009, Sadler and Bailey, 2016). In this project, we used acute restraint and forced swim stress to evaluate the impact of stress on neuronal activity in the brain.

## 1.2 Kappa opioid receptor

### 1.2.1 What is the kappa opioid receptor?

KOPrs are part of the opioid receptor family of G-protein coupled receptors (GPCRs), which consist of the  $\mu$  (mu) opioid receptor (MOPr),  $\delta$  (delta) opioid receptor (DOPr) and  $\kappa$  (kappa) opioid receptor (KOPr). The KOPr is primarily activated by endogenous neuropeptide dynorphin (DYN), which is released from large dense vesicles at synaptic and extra-synaptic sites in response to stress, i.e. stress induces the release of DYN levels (Shirayama *et al.*, 2004). The DYN-activated KOPrs couple to inhibitory Gi alpha subunit proteins (G $\alpha$ i), which inhibits adenylyl cyclase, hence decreases neuronal activity by inhibiting voltage-gated Ca<sup>2+</sup> channels and activating voltage gated K<sup>+</sup> channels, resulting in reduced release of neurotransmitters and synaptic transmission (Bruchas *et al.*, 2010). Electrophysiological and neurochemical studies have shown that activation of KOPr in the VTA decreases the release of dopamine and dopaminergic transmission in the NAc (Shippenberg *et al.*, 2007). It also produces anxiety-like and pro-depressive behaviours, such as increased immobility in the forced swim test, also produces negative affective states, such as dysphoria, sedation and anxiety (Carlezon *et al.*, 2006). The KOPr and endogenous ligand DYN are highly expressed in the NAc, PFCx and VTA regions (Shippenberg *et al.*, 2007). The mechanism of stress-induced DYN release is not fully understood, but high level of DYN was detected in the hippocampus, amygdala and PVN in hypothalamus of rodents (Lin *et al.*, 2006, Knoll *et al.*, 2010, Van't Veer *et al.*, 2013).

Endogenous peptide	Agonist ligands	Antagonist ligands
<b>Dynorphin A:</b> Tyr-Gly-Gly-Phe-Leu-Arg-Arg-Ile-Arg-Pro-Lys-Leu-Lys	U50,488	Norbinaltorphimine (norBNI)
	U69,593	Naloxone (non-selective)
<b>Dynorphin B:</b> Tyr-Gly-Gly-Phe-Leu-Arg-Arg-Gln-Phe-Lys-Val-Val-Thr	Bremazocine	Buprenorphine (non-selective)

**Table 1.1 Summary of ligands that activate on KOPr.** Two different forms of dynorphin (A and B), which are derived from precursor protein prodynorphin with different amino acid sequences. Naloxone also acts on  $\mu$  opioid receptor and  $\delta$  opioid receptor. Buprenorphine acts as a partial agonist on  $\mu$  opioid receptor and antagonist on  $\delta$ ,  $\kappa$  opioid receptor.

### 1.2.2 Distribution of KOPrs

Identification of KOPrs in the key brain regions that are implicated in depression, anxiety and addiction would further facilitate the further potential therapeutics development. Increasing evidence have shown that KOPrs are widely expressed throughout the brain, and the central and peripheral nervous systems.

For example, autoradiographic studies in male Sprague-Dawley rats have shown that KOPrs are particularly expressed in limbic brain areas, including the NAc, hippocampus, frontal cortex, VTA, basolateral amygdala and hypothalamus at relatively high levels (Fan *et al.*, 2002). This localisation of KOPrs in NAc and hippocampus was also supported by DYN immunocytochemistry studies in adult male Sprague-Dawley rats, demonstrating that acute stress increased DYN immunoreactivity in the NAc, CA1, CA3 regions and dentate gyrus of the hippocampus (Shirayama *et al.*, 2004). Early studies of northern blot analysis in male Sprague-Dawley rats showed that KOPr mRNA was expressed in the hypothalamus, cortex, hippocampus, amygdala and NAc (George *et al.*, 1994). Quantitative *in vitro* autoradiography in the guinea pig brain also revealed that high levels of KOPr expression were observed in cortex, substantial nigra and NAc, while hypothalamus, hippocampus and amygdala express moderate levels of KOPr (Wang *et al.*, 2001). More importantly, quantitative autoradiography of KOPr binding in wildtype mice revealed high levels of KOPrs are expressed in the NAc, claustrum and hypothalamus, moderate levels of KOPrs expression are found in the PFCx and amygdala, relative low levels of binding were observed in the hippocampus (Kitchen *et al.*, 1997, Clarke *et al.*, 2001).

Altogether, these results demonstrated the regional distribution of KOPrs expression in the brain, highlighting the emotional and motivational role of KOPrs in psychiatric disorders and drug addiction, as well as modulate the circuits between different brain regions in stress responses and anxiety, addiction behaviours (Figure 1.6).

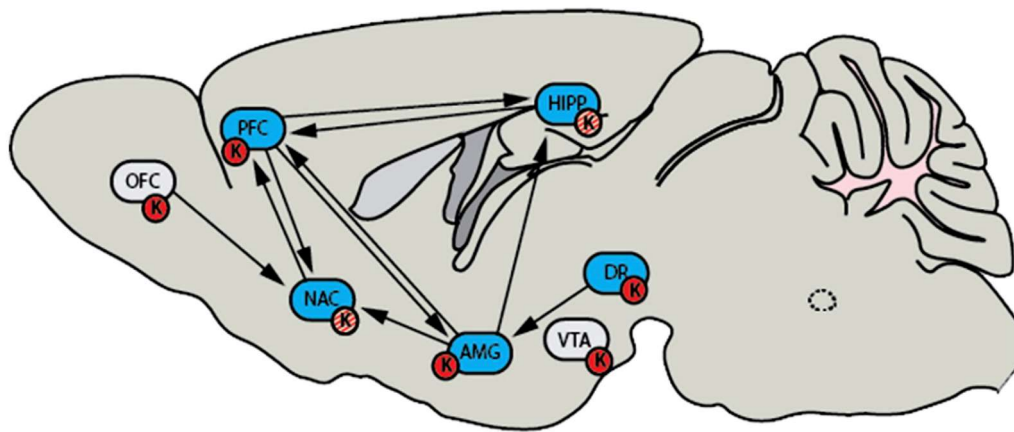


**Figure 1.4 The distribution of KOPrs and KOPr system in major circuits implicated in stress and addiction responses.** Regions involved in mediating aversive and dysphoric are labelled with red circles, regions labelled with red and white circles are implicated in depressive-like behaviours and reinforcing properties. **PFC**, prefrontal cortex, **OFC**, orbital frontal cortex, **NAc**, nucleus accumbens, **AMG**, amygdala, **VTA**, ventral tegmental area, **HIPP**, hippocampus, **DR**, dorsal raphe nucleus.

*Diagram from Crowley et al., 2015*



### 1.2.3 Role of KOPrs in stress

Activation of KOPrs causes aversive, anxiety-like and depressive-like behaviours in rodents and in humans (Pfeiffer *et al.*, 1986, Carlezon *et al.*, 2006). Accumulating evidence proposed that KOPr system induces these effects by regulating HPA axis (Van't Veer *et al.*, 2013). For example, a reduction in CRF mRNA expression in PVN of the hypothalamus and decreased corticosterone levels were detected in wildtype mice pre-treated with KOPr antagonist, norBNI, and acute swim stress-induced increases in corticosterone levels were reduced in prodynorphin knockout mice, which suggested that KOPr activation plays an important role in HPA axis regulation (Wittmann *et al.*, 2009). Similar evidence was also revealed in rats i.e. lowered corticosterone levels were measured in rats following norBNI pre-treatment in response to food restriction stress (Allen *et al.*, 2013). Importantly, it has been shown that KOPrs expression pattern overlaps with the regions that are involved in HPA activity, shown in figure 1.5, suggesting that KOPrs activation induces stress-like effects by modulating glucocorticoid release in HPA axis (Van't Veer *et al.*, 2013).

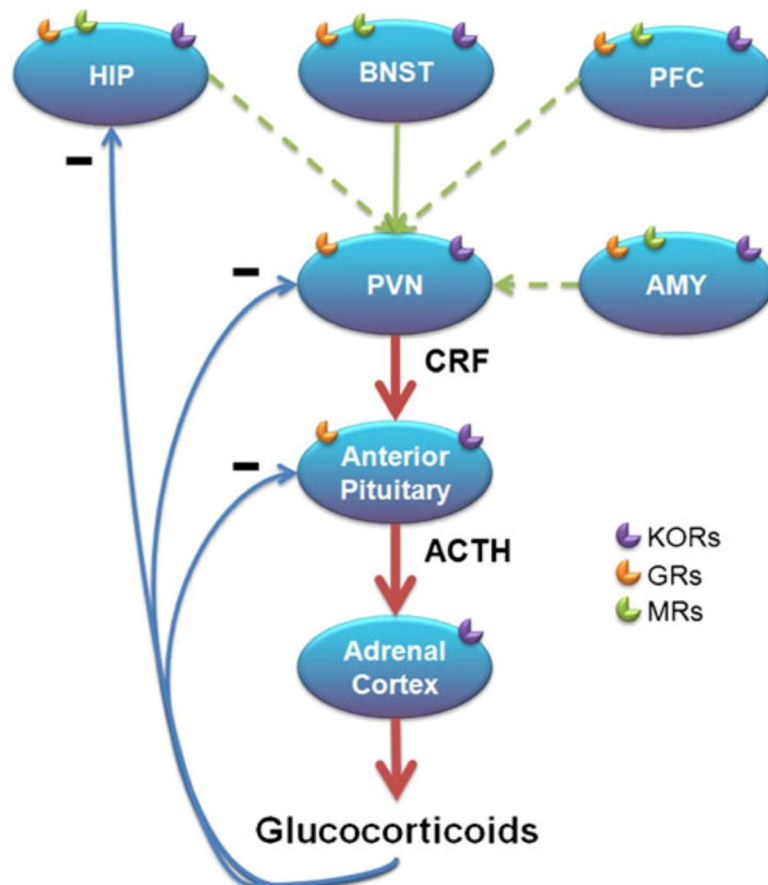


**Figure 1.5 Schematic diagram of HPA axis and expressions of KOPrs, GRs and MRs.** Glucocorticoid release regulated by negative feedback via MRs and GRs. KOPr expression overlaps with HPA axis. **KOPrs**, kappa opioid receptors, **GRs**, glucocorticoid receptors, **MRs**, mineralocorticoid receptors, **ACTH**, adrenocorticotrophic hormone, **CRF**, corticotropin-releasing factor, **HIP**, hippocampus, **BNST**, bed nucleus of the stria terminalis, **PFC**, prefrontal cortex, **PVN**, paraventricular nucleus of hypothalamus, **AMY**, amygdala. Red arrows indicate positive feedback, blue arrows indicate negative feedback, green arrows indicate indirect connections from brain regions to the PVN in HPA axis.

*Diagram from Van't Veer et al., 2013*

At the molecular level, forced swim stress-induced CRF release or intracerebroventricular injection of CRF significantly increased activation and phosphorylation of KOPr in the VTA, amygdala, NAc and hippocampus regions, shown by Western blot analysis in mice, indicating that DYN/KOPr system plays a key mediating role in stress responses (Land *et al.*, 2008).

Stress induces the release of endogenous opioid peptide, DYN and activation of the KOPr system has also been reported to be strongly associated with behavioural responses in animal models of depression, anxiety and aversive effects. For example, footshock stress or forced swim stress produced aversive behaviours in conditioned aversion paradigm in male C57BL/6 mice, which could be reversed by selective KOPr antagonist, norBNI pre-treatment (Land *et al.*, 2008). Also, administration of norBNI decreased immobility in the FST dose dependently in male Sprague-Dawley rats (Mague *et al.*, 2003). Social defeat stress-induced analgesia responses and potentiation of cocaine-conditioned place preference (CPP) were also shown to be blocked by KOPr antagonism in wildtype C57BL/6 male mice and in mice with prodynorphin gene disruption (McLaughlin *et al.*, 2003, McLaughlin *et al.*, 2006a), suggesting that KOPr activation is important in mediating responses induced by acute stress.

There is also accumulating evidence showing that the KOPr antagonist, norBNI, blocks stress-induced potentiation of drug-dependent CPP and drug self-

administration. Consistent with these effects, prodynorphin knockout mice did not show the forced swim stress-induced cocaine CPP potentiation, which further confirms that KOPr system plays an important role in inducing motivational effects of stress (McLaughlin *et al.*, 2003, Sperling *et al.*, 2010, Smith *et al.*, 2012, Graziane *et al.*, 2013). In addition, activation of KOPr by the agonist, U50,488, potentiated cocaine CPP in mice, which mimics the effects caused by stress, confirming that KOPr activation is important and strongly associated with stress-induced reinforcing properties of addictive drugs (McLaughlin *et al.*, 2006b).

In adult male rats study, bilateral microinfusion of norBNI directly into the ventricles or NAc induced antidepressant effects in the FST in a dose-dependent manner (Pliakas *et al.*, 2001), similar to the antidepressant effects as seen in a learned helplessness (LH) paradigm following microinjection of norBNI directly into the NAc (core and shell) or hippocampal CA3 and dentate gyrus regions (Shirayama *et al.*, 2004), suggesting that norBNI-induced inhibition of KOPr in the NAc or hippocampus could lead to enhanced dopamine transmission. Site specific administration of norBNI into the BLA blocked stress-induced anxiety-like behaviours in the elevated plus maze (EPM), highlighting the important role of KOPr system in the amygdala in mediating anxiety behaviours in response to stress (Bruchas *et al.*, 2009). These studies indicate the expression of KOPr in the BLA, hippocampus and NAc and the potential role of dynorphin/KOPr in mesolimbic dopamine system, as well as potential therapeutic target for depression treatment (Shirayama *et al.*, 2004).

Overall, this evidence suggest that acute stress-induced physical and behavioural responses are mediated, at least in part, by dynorphin/KOPr activation and signalling, and the motivational and emotional role of KOPr in animal behavioural responses represent a potential drug target for psychiatric disorders. For example, KOPr antagonists have been proposed as potential novel drug treatments for depression and anxiety disorders. KOPr antagonists have also been suggested as potential treatments for drug addiction.

#### 1.2.4 Role of KOPrs in addiction

As described above, KOPrs are important in regulating stress-induced motivational behaviours, increasing evidences has shown that KOPr signalling is not only involved in stress-induced neurological effects, but also strongly associated with craving and rewarding properties of addictive drugs, such as cocaine, heroin and alcohol (Nestler *et al.*, 2005, Bruchas *et al.*, 2010, Lalanne *et al.*, 2014). Dysregulation of dynorphin/KOPr signalling is characterised in drug-seeking behaviours and drug dependence, and KOPr has been studied as a potential therapeutic target for the treatment of drug addiction (Nestler *et al.*, 2005, Lalanne *et al.*, 2014).

In an early animal studies in Sprague-Dawley rats, microinjection of KOPr agonist U50,488 directly into VTA, NAc and mPFC produced conditioned place aversion (CPA) in a dose dependent manner (Bals-Kubik *et al.*, 1993), similar effects were observed in C57BL/6 mice, which showed that pre-treatment of U50,488 effectively abolished morphine conditioned place preference (CPP) (Funada *et al.*, 1993), suggesting that KOPr might play an important role in anti-rewarding effects in motivation of drugs of abuse. In addition to that, direct administration of norBNI into CA3 region of the hippocampus improved ethanol-induced spatial learning and memory impairments in rats in the water maze task (WMT), proving that KOPrs also play a key role in mediating the effects of alcohol on impaired learning and memory (Kuzmin *et al.*, 2013). Glick and colleagues reported that i.p. injection of U50,488 (10mg/kg) prior to drugs testing showed reduced cocaine and morphine self-administration, supporting the previous evidence for the inhibitory role of KOPr in rewarding properties of drug addiction (Glick *et al.*, 1995), as well as suggesting that KOPr may act as a promising and novel pharmacological target for opioid addiction treatment.

However, other studies demonstrated that the effects of KOPr on rewarding properties of drug addiction depended on timing, e.g., administration of the KOPr agonist, U50,488 15 minutes prior to cocaine significantly blocked cocaine-induced CPP, which was consistent with earlier evidence, whereas administration of U50,488 60 minutes before cocaine significantly potentiated cocaine-induced CPP in C57BL/6 mice, which was inhibited by KOPr antagonist, norBNI pre-administration or KOPr

gene disruption (McLaughlin *et al.*, 2006b). These results suggested that the timing between KOPr activation and cocaine treatment was crucial, resulting in both facilitatory or inhibitory effects of KOPr agonist on drug-induced CPP and highlighting the difficulties for KOPr clinical studies in the treatment of drugs of abuse (McLaughlin *et al.*, 2006b).

It is hypothesised that the mechanism underlying the KOPr-induced effects on addiction-related behaviours and drug-induced reward is by regulating the mesolimbic pathway. KOPrs are expressed on dopaminergic neurons in the mesolimbic pathway, and activation of KOPrs in these neurons results in decreased neurotransmission and inhibition of dopamine release in the NAc. This process is thought to be responsible for mediating the aversive effects of KOPr agonists (Trifilieff *et al.*, 2013). Within the NAc, infusion of KOPr agonist, U69,593 into the NAc in rats demonstrated decreased dopamine release in the NAc using microdialysis (Spanagel *et al.*, 1992), and systemic administration of U69,593 in rats also showed reduction in extracellular dopamine concentrations in the mPFC (Tejeda *et al.*, 2013). The KOPr agonist, U69,593-induced CPA was abolished in knockout mice with deletion of KOPr on dopaminergic neurons, confirming that KOPr on dopaminergic neurons are necessary and sufficient to mediate aversive behaviours (Chefer *et al.*, 2013), the network of KOPr-regulated dopaminergic transmission in the mesolimbic pathway is shown in Figure 1.6. *In vivo* microdialysis studies in rats showed that systemic administration of KOPr agonist, salvinorin A, decreased extracellular dopamine concentrations in the NAc and regulating dopamine transmission in the NAc, which is a key component of mesolimbic rewarding system, supporting the idea that KOPrs activation modulates rewarding properties of addictive drugs (Carlezon *et al.*, 2006). More importantly, as described above, KOPr antagonist, norBNI was reported to block stress-dependent reinstatement of cocaine-induced CPP in mice, highlighting the important role of KOPr in drug-seeking behaviours (McLaughlin *et al.*, 2003). Furthermore, another KOPr antagonist (non-selective, partial MOPr agonist), buprenorphine has also been shown to reduce cocaine self-administration and increase extracellular concentration of dopamine in the NAc, providing evidence that

KOPr activation is strongly associated with drug addiction behaviours and involved in regulating mesolimbic pathway (Brown *et al.*, 1991, Robinson 2006).

These neurochemical and behavioural evidence in animal studies proposed that KOPr antagonists could be developed for potential therapies for drug addiction treatment. However, there are still difficulties remain unsolved, addiction is a chronic process that involves time-dependent alterations and adaption of neuronal circuitry in the brain, the better understanding of the effects of KOPr antagonists on different stages of the addiction development is required, which would facilitate an early development of an effective treatment for addiction (Shippenberg *et al.*, 2009).

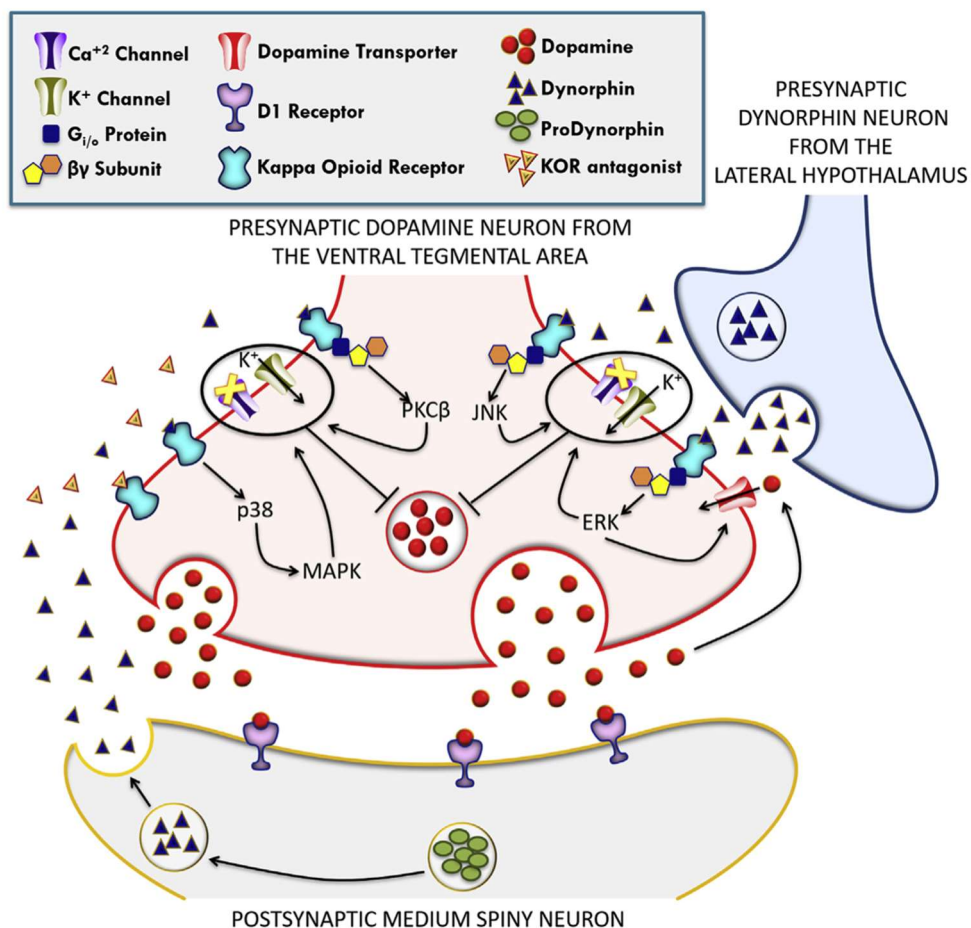


**Figure 1.6 Schematic diagram of mechanism underlies KOPrs-modulated dopamine transmission from VTA to NAc.** Activation of KOPrs (coupled to G<sub>i/o</sub>) on dopaminergic neurons leads to decreased release of dopamine in NAc. The dopaminergic transmission is reduced by activating K<sup>+</sup> channels and inhibiting Ca<sup>2+</sup> channels, resulting in hyperpolarisation of the neurons. The dopamine transporters are also stimulated to increase dopamine reuptake following KOPr activation.

Diagram from Margolis *et al.*, 2019

## 1.3 Sex differences

Statistics indicate that women are more prevalent to develop certain psychiatric disorders such as depression and anxiety, compared to men (Mergl *et al.*, 2015). Accumulating studies have reported that sex is a key factor that determines different effects of stress and opioids on behaviours and analgesic responses both in animal and human studies. These sex differences effects may result from different molecular mechanisms at the receptor level, neural mechanism in the brain networks and sex hormone levels (Bolea-Alamanac *et al.*, 2018). This section focuses on the sex differences in stress, KOPr activation and depression, addiction responses, suggesting the evidence that may underlie these sex differences.

### 1.3.1 Sex differences of opioid receptors in pain and analgesia

In addition to dysphoria, depressive-like behaviours and increased immobility following KOPr activation, DYN/KOPr system has been also reported to be involved in nociception and to produce analgesic effects by inhibiting synaptic transmission in pain circuits (Meng *et al.*, 2005). KOPrs are also found to be expressed in the dorsal horn of the spinal cord, dorsal root ganglia and rostral ventromedial medulla (RVM) and sensory thalamus, which are important regions involved in pain circuitry (Gutstein *et al.*, 1998, Winkler *et al.*, 2006). A number of studies showed that both physical and psychological stressors induce analgesia in animals via activating KOPr signalling (Takahashi *et al.*, 1990, Menendez *et al.*, 1993). However, it has been recently revealed that the effects of dynorphin-induced analgesia are influenced by sex. For example, Liu and colleagues showed that intrathecal administration of yohimbine, a selective  $\alpha_2$  adrenoceptors antagonist, produced an anti-nociceptive effect by releasing dynorphin and activating the KOPr system, which in turn attenuated formalin-elicited nociception in male rats, but no effect was observed in females (Liu *et al.*, 2013). Early studies on mice showed that administration of U50,488, a selective kappa opioid receptor agonist, produced more analgesia in male mice than female mice on the hot-plate (Kavaliers *et al.*, 1987). One recent study in C57BL/6N mice demonstrated KOPr activation by selective KOPr agonist, U50,488 produced a great anti-nociceptive effect in male mice, but not in female mice in the

tail flick assay. These sex-dependent analgesic effects induced by KOPr activation is regulated by estradiol levels and G protein-coupled receptor kinase 2 (GRK2) activity, which might underlie the sex differences in KOPr function in analgesic responses (Abraham *et al.*, 2018).

Whereas in human clinical studies reported the opposite effects, administration of mixed KOPr and MOPr agonists, pentazocine and nalbuphine produced significantly greater and prolonged analgesia in women subjects than in men after dental surgery, suggesting that kappa opioid receptor activation-induced analgesia is sex dependent and patient sex might have an impact on the efficacy of clinical opioid analgesics (Gear *et al.*, 1996). The distinct sex difference effects observed between rodents and humans could due to different study designs and pain models were involved and different ligands were used.

Altogether, this evidence indicates that KOPr-mediated analgesic effects depend on sex, strain, species and pain models. The mechanisms underlying the sex differences observed in KOPr-induced anti-nociception could result from sex chromosomes, gonadal hormones, distribution and expression levels of KOPrs in the brain, and the mechanisms underlying these sex-dependent effects still remain elusive.



### 1.3.2 Sex differences in response to stress

Epidemiological studies have shown that women have higher vulnerability to stress-related psychiatric conditions than men, such as post-traumatic stress disorder (PTSD) and depression. The prevalence of depression in women is almost twice that in men in the global analysis (Kessler, 2003, Albert, 2015). Although, the mechanisms underlying these sex differences in chronic stress-related psychiatric disorders are not fully understood, studies have suggested that sex differences in stress sensitivity could result from different corticotropin-releasing factor (CRF) function, which is one of the key modulators in the HPA axis in response to stress, described in section 1.1.2.

For example, in male and female Sprague-Dawley rats, Bangasser and colleagues showed that at receptor level, there is an enhanced CRF receptor signalling (greater CRF receptor coupling to Gs protein) in non-stressed female rats, which was not significantly affected by swim stress, but in male rats, CRF signalling is largely increased following swim stress (Bangasser *et al.*, 2010), also, stress-induced CRF receptor internalisation was only observed in male rats, not in females, indicating that females have higher sensitivity to low levels of CRF and decreased ability to adapt to excessive levels of CRF, which might be an important molecular mechanisms that underlie higher vulnerability of females to develop psychiatric disorders and sex differences in response to stress (Bangasser *et al.*, 2010). In addition, other evidence reported that there were higher basal ACTH and CRF expression in the PVN in female rats than males, especially in the presence of high levels of estrogen (Iwasaki-Sekino *et al.*, 2009). In response to foot shock stress or restraint stress (RS), female rats showed higher levels of plasma ACTH and corticosterone than male rats (Viau *et al.*, 2005, Iwasaki-Sekino *et al.*, 2009). These studies indicate different secretion of ACTH and corticosterone in response to stress between male and female rodents, suggesting that the function of stress-related PVN region and HPA axis-regulated hormone release are sex-dependent, which are implicated in sex differences in stress-induced psychiatric disorders.

In contrast to rodent's data, human studies reported that adult men showed significantly higher basal ACTH levels compared to age-matched women (Back *et al.*,

2008). In response to an acute psychological stress e.g. public speaking, academic exam, male subjects also showed greater release of ACTH and cortisol than female subjects (Kudielka *et al.*, 2005, Uhart *et al.*, 2006). These opposite findings between rodents and human highlight sex differences in stress-activated HPA activation and the importance of future investigations of the mechanisms underlying stress-induced psychiatric disorders in human.

Two important mediators of the antidepressant therapeutic targets, brain-derived neurotrophic factor (BDNF) and cyclic adenosine monophosphate response element-binding protein (CREB) levels were investigated in response to foot shock stress in both male and female rats (Lin *et al.*, 2009), which showed reduced CREB levels in the hippocampus and amygdala following this stress in male rats, but these effects were not observed in female rats. However, BDNF levels were not affected following chronic stress in male PFCx but were significantly decreased in female PFCx. Finally, during the stress response, stress-induced morphological changes were only found in male hippocampus, but not in female rats (Lin *et al.*, 2009), these results further showed that sex is an important factor in mediating different effects in response to stress, suggest the further development of antidepressants could be sex dependent. Early studies have also shown that female rats had more rapid and significant increases in corticosterone levels than male rats during forced swimming stress (Kant *et al.*, 1983), and female rats were more sensitive to HPA axis activation than male rats after prenatal stress (Weinstock *et al.*, 1992). More recent studies on behavioural tests revealed that chronic stress significantly decreased sucrose preference and reduced time spent in the centre of open field tests in female rats, compared to the control groups, whereas male rats did not produce these effects in the behavioural test (Lu *et al.*, 2015).

Collectively, these findings in both human and animals proved the importance of sex differences in mediating stress-related behavioural responses and stress-induced glucocorticoids release in the brain.

### 1.3.3 Sex differences in KOPr and stress

Stress-induced effects are strongly associated with KOPr activation, stress induces behavioural responses, at least in part, by activating dynorphin/KOPr system. As shown in the previous section, sex differences have been observed in animal behaviours in response to stress, and it is proposed that KOPr activation plays a role in mediating sex dependent behavioural response to stress. An increasing number of studies have been performed to investigate how sex influences the effects of KOPr activation.

Activation of KOPrs produces depressive-like and anxiety-like states, blockade of KOPrs have been showed to improve stress-induced depressive-like behaviours and dysphoric states in animal studies. Consequently, the KOPr is proposed as a potential therapeutic target for the treatment of psychiatric disorders, such as depression and anxiety. However, several studies revealed the sex differences in the effects of KOPrs function on stress-induced behavioural responses. In recent animal studies on C57BL/6J and California mice, the KOPr selective antagonist, norBNI, blocked forced swim stress-induced immobility in a sex dependent manner, where male mice showed reduced immobility in the FST. This was not found in female mice, indicating that KOPr plays a greater role in mediating stress-induced effects in males, and forced swimming-induced immobility might be less dependent on KOPr signalling in female mice. This evidence confirms the importance of KOPr in mediating sex differences in stress-induced behavioural responses (Laman-Maharg *et al.*, 2018).

It also has been shown that the effect of KOPr activation by U50,488 treatment on motivational behavioural was not only sex dependent, but also dose dependent, female California mice demonstrated CPA with a low dose of U50,488 (2.5mg/kg), but CPP to a high dose of U50,488 (10mg/kg), whereas male mice only formed CPA to the high dose of U50,488 (10mg/kg) (Robles *et al.*, 2014), which are supported by other studies on the sex differences in KOPr activation-induced behaviours, showing that low dose of U50,488 (2.5mg/kg) induced CPA in naïve female California mice, not in male mice, whereas naïve male mice only showed aversive effects following high dose of U50,488 (10mg/kg) treatment (Laman-Maharg *et al.*, 2017), indicating

that females are more sensitive to KOPr agonist than male mice. More importantly, after long-term social defeat stress, female mice no longer demonstrated aversive properties with 2.5mg/kg of U50,488 treatment, no place aversion was observed with increased dose of U50,488 (10mg/kg), however, stressed male mice showed aversive effects in the presence of U50,488 (10mg/kg) treatment (Laman-Maharg *et al.*, 2017). These findings suggest that long-term stress may attenuate KOPr-mediated aversive properties in female mice, highlighting the importance of sex differences in the effects of chronic stress on KOPr function, and future study of how short or long-term stress could affect KOPr activation-mediated behaviours between males and females is needed.

Although it has been shown that KOPr activation-mediated sex differences are dependent on estradiol levels and GRK2 activity (Abraham *et al.*, 2018). The mechanisms that underlying different KOPr function between males and females are still not fully understood, further understanding of KOPrs distribution and expression levels, as well as the influences of sex chromosomes on KOPr function could facilitate the development of effective analgesic drugs for males and females (Rasakham *et al.*, 2011).

#### **1.3.4 Sex differences in KOPrs and addiction**

Similar to the sex differences in KOPr system-mediated stress responses, there are also evidence on sex differences in KOPr activation-induced addictive behaviours. It is known that dopamine release in the mesolimbic pathway is crucial in mediating motivated behaviours, however, recent study investigated the effect of KOPr activation on dopamine release in both male and female rats, which showed that administration of U50,488 suppressed dopamine release in the NAc more effectively in male mice, compared to the females (Conway *et al.*, 2019). Also, KOPr activation by a selective KOPr agonist, U50,488 induced anhedonic effects and decrease in motivated behaviour in adult Sprague-Dawley male rats, but significantly less effects were observed in female rats, which is independent of gonadal hormones (Russell *et al.*, 2014), these effects were measured with intracranial self-stimulation (ICSS), an

operant paradigm that is used for rodents to examine changes in rewarding function (Carlezon and Chartoff, 2007).

In addition, administration of KOPr agonist prior to cocaine treatment potentiated cocaine-induced place preference in male mice (McLaughlin *et al.*, 2006), it was proposed that cocaine-induced rewarding properties would produce different effects in female mice, which was showed by early studies from Sershen and colleagues, who reported that a KOPr agonist produced behavioural responses in a sex dependent manner, pre-treatment with KOPr agonist, spiradoline potentiates locomotor activity following cocaine treatment only in male mice, not in female mice (Sershen *et al.*, 1998). Interestingly, opposite effects were observed in guinea pigs in the same study, where KOPr agonist, U50,488 significantly decreased cocaine-induced locomotor activity in females, not males (Wang *et al.*, 2011).

All these inconsistent findings in sex differences in KOPr system-mediated stress responses and addictive behaviours emphasise the importance of sex-dependent therapeutics for addiction and affective disorders treatment.

## 1.4 Transgenic animal strains

### 1.4.1 cFos

Following exposure to a variety of stimuli, activated neurons alter gene expression by inducing a number of immediate early gene (IEGs), including cFos, c-Jun and zif268 (Senba *et al.*, 1997). cFos has low basal expression levels and is rapidly induced in response to different stimuli, it is widely used as a neuronal activity marker, i.e. upregulation of cFos gene expression indicates recent neuronal activities. Therefore, monitoring expression of cFos has been useful in identifying brain regions that are activated by a wide range of stimuli or regions involved in behavioural responses and pharmacological states (Gall *et al.*, 1998). Since cFos is initially and transiently induced following a wide range of stimuli, it is an important neuronal marker not only for indicating recent neural activity, but also widely used to map neuronal changes and circuitry during development and identify the types of neurons activated by specific treatment in the brain networks (Hoffman *et al.*, 1993, Rinaman *et al.*, 1997).

cFos is a proto-oncogene and belongs to a transcription FOS family with other members including FosB, FosB2,  $\Delta$ FosB, Fra-1 and Fra-2. It is activated rapidly and responsible for converting extracellular signals into changes of gene expression. cFos normally forms a heterodimer with another transcription factor c-Jun, a complex called activator protein-1 (AP-1), which has specific DNA binding sites that regulate target gene expression (Curran *et al.*, 1988) (Figure 1.7).

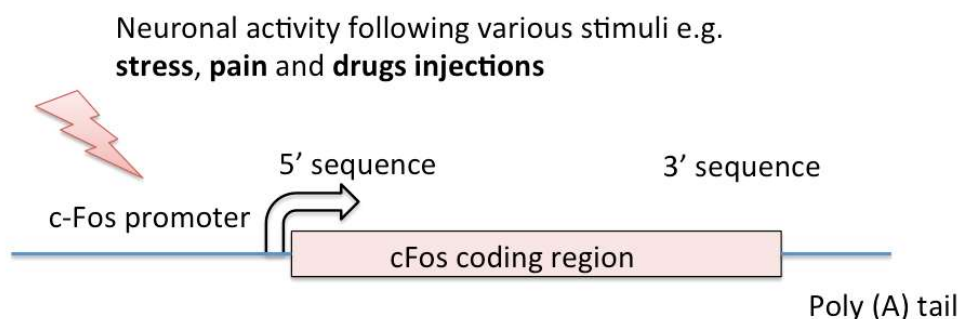


**Figure 1.7 Illustration of transcription factor cFos gene induction.** Activation of cFos promoter initiates the production of cFos gene from 5' to 3' following different stimuli.

### 1.4.2 cFos-GFP transgenic mice

In order to understand the neuronal changes involved in stress and drug addiction-related responses, the expression of the IEG cFos was used as a measure of recent neuronal activity. In this study, previously developed cFos-GFP transgenic mice were used (Barth *et al.*, 2004). In these mice the cFos promoter is coupled to the coding region for enhanced green fluorescent protein (EGFP), illustrated in figure 1.8. Since the promoter and coding region from the cFos gene were fused in frame to EGFP, expression of GFP directly follows the cFos production in activated neurons.

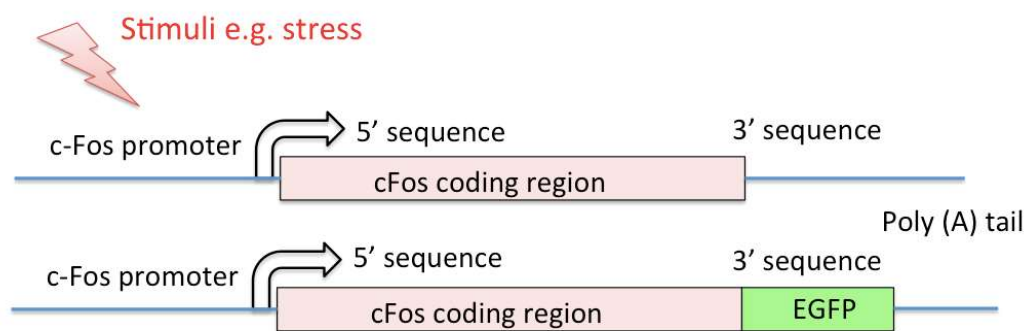


**Figure 1.8 Schematic diagram of cFos gene and cFos-GFP transgene structure in response to stressor stimuli.**

*Diagram adapted from Barth et al., 2004*

In addition,  $\gamma$ -aminobutyric acid (GABA) is the predominant inhibitory neurotransmitter in the central nervous system. In order to better understand the distribution and characterise GABAergic neurons, Tamamaki and colleagues developed glutamic acid decarboxylase - green fluorescence protein (GAD-GFP) knock-in mouse. As GAD is only expressed in GABAergic neurons, GFP expression in these mice is restricted to GABAergic neurons only (Tamamaki *et al.*, 2003). These mice therefore enable us to visualise GABAergic neurons and identify whether the neurons are GABAergic neurons or non-GABAergic neurons in immunocytochemistry experiments (Chapter 6).

### **1.4.3 The advantages of using cFos-GFP mice**

The use of cFos-GFP transgenic mice facilitates identification of the brain regions and individual neurons activated by different stimuli; also cFos-GFP mice facilitate characterisation of activated neurons by performing electrophysiology or FACS sorting techniques. Upon neuronal activation, expression of both cFos protein and GFP in these transgenic mice would allow us to perform co-labelling of both proteins with immunofluorescent histochemistry (IHC) to quantify the number of GFP positive (GFP+) and GFP negative (GFP-) neurons. Considering the short half-life of cFos protein (Kovacs *et al.*, 1998), GFP was previously determined to have a relatively longer half-life in cultured cells from mice (Corish *et al.*, 1999). The more stable GFP properties allow us to identify the temporal sequence of brain regions that have been activated.



## **Chapter 2 General Methods**

## 2.1 Animals

All studies used either male or female adult C57BL/6 cFos-GFP (Chapter 3, 4, 5 and 7) (Barth *et al.*, 2004) or GAD-GFP transgenic mice (Chapter 3 and 6) (Tamamaki *et al.*, 2003). Original cFos-GFP mice were purchased from Jackson Laboratories (Bar Harbor, Maine, USA). Original GAD-GFP mice were a kind gift from Dimitri Kullman (UCL, UK) and were rederived by Charles River (Margate, UK). All animals used in this study were bred in-house from heterozygous males bred with wild type C57BL/6 females (Charles River UK).

All positive transgenic male or female mice used in the experiments were between 9 weeks and 13 weeks old. Mice were housed in groups of 2 to 5 with water and food available *ad libitum* in a temperature and humidity-controlled environment under a 12-hours light-dark cycle (lights on at 7 a.m.), all experiments were carried out during the light phase. All mice were handled and weighed one day before stress procedures (section 2.4 and 2.5) or drug treatment (section 2.6). All procedures were approved by the Animal (Scientific Procedures) Act 1986 and the University of Bath's ethical review process.

## 2.2 Genotyping

GAD-GFP mice were genotyped by using GFP goggles (BLS, Budapest, Hungary) when mice were <3 days post-partum. cFos-GFP mice were genotyped using polymerase chain reaction (PCR) amplification. Ear punch biopsy samples were collected from 3 weeks old male and female mice. DNA was extracted by adding 75µl of alkaline lysis reagent (25mM NaOH, 0.2mM disodium EDTA, pH 12), heat block at 95°C for 20 minutes. After heating, samples were cooled at 4°C and followed by adding 75µl of neutralising reagent (40mM Tris-HCl, pH 5) into each sample (Truett *et al.*, 2000). The extracted DNA were used for PCR reaction, which was carried out by using Taq DNA polymerase with standard Taq (Mg-free) buffer kit (New England Biolabs, M0320S), dNTP mix (10mM) (Thermo Fisher Scientific, R0191) and previously designed gene specific primers (Sigma-Aldrich, UK; summarised in Table 2.1). For PCR reaction, 2.5

$\mu$ l 1x standard Taq (Mg-free) buffer (containing 10mM Tris-HCl, 50mM KCl, pH 8.3), 2  $\mu$ l MgCl<sub>2</sub> (1.5mM) solution, 0.5  $\mu$ l dNTPs (10mM), 2.5  $\mu$ l GFP forward primer (10 $\mu$ M), 2.5  $\mu$ l GFP reverse primer (10 $\mu$ M), 1.25  $\mu$ l  $\beta$ -actin forward primer (10 $\mu$ M), 1.25  $\mu$ l  $\beta$ -actin reverse primer (10 $\mu$ M), 0.25  $\mu$ l Taq polymerase, 8.25  $\mu$ l RNase-free water and 4  $\mu$ l DNA sample were added in each PCR tube. The PCR tubes were placed in a PCR machine (MJ Research, PCT-200) with following reaction cycling conditions: 95°C for 30 seconds (denaturation), 40 cycles of 95°C for 15 seconds (denaturation), 60°C for 30 seconds (annealing), 68°C for 30 seconds (extension), followed by 68°C for 5 minutes for final elongation. The PCR products were separated on 1% agarose gel with ethidium bromide (0.2  $\mu$ g/ml, Sigma-Aldrich, UK) under 120V for 40 minutes. Finally, the DNA bands were visualised and imaged using GeneSnap (SynGene) software under UV exposure.

Primer	Sequences 5'- 3'	Size	References
$\beta$ -Actin	<b>Forward:</b> CTAGGCCACAGAATTGAAAGATCT	324	The Jackson Laboratory
	<b>Reverse:</b> GTAGGTGGAAATTCTAGCATCATCC	324	
GFP	<b>Forward:</b> AAGTTCATCTGCACCACCG	173	The Jackson Laboratory
	<b>Reverse:</b> TCCTTGAAGAAGATGGTGCG	173	

**Table 2.1** The genetic sequences of forward and reverse primer sequences for  $\beta$ -actin (internal positive control) and GFP (transgene).

## 2.3 Antibodies

Commercially available primary antibodies used were: rabbit anti-actin antibody (Abcam, ab1801), rabbit anti-cFos antibody (Santa Cruz Biotechnology Inc., SC-52), which was discontinued mid-way through the project and replaced with rabbit anti-cFos antibody (Cell Signalling Technology, #2250), chicken anti-GFP (Green Fluorescent Protein) antibody (Abcam, ab13970). Secondary antibodies were:

IRDye® 800CW Donkey anti-Rabbit IgG (H+L) (LICOR, #926-32213) and IRDye® 680RD Donkey anti-Chicken IgG (H+L) (LICOR, #926-32218). Goat anti-Rabbit antibody Alexa Fluor 568 (ThermoFisher Scientific, A11011) and Goat anti-Chicken antibody Alexa Fluor 488 (Abcam, ab150169).

## 2.4 Restraint stress

Restraint stress was used as an acute stressor by placing the body into a modified 50ml ventilated syringe for 2 hours (Kim and Han, 2006). The mouse body was stabilised by using the syringe plunger so that it can remain in the confined space. After 2 hours restraint stress, the mice were sacrificed by cervical dislocation, and the brains were dissected and removed for biochemical analysis, including protein extraction for western blotting (Section 2.7) and RNA extraction for RT-PCR (Section 2.8 and 2.9). All non-stressed control mice were just handled and weighed.

## 2.5 Forced Swim Stress (FSS)

The forced swim test (FST) was used as an acute stressor (Contet *et al.*, 2006). The FST was carried out in a glass beaker (height 34 cm, diameter 22 cm) with total volume 10 litres; the glass beaker was filled with water to approximately two thirds of the total beaker volume (height 23 cm), the water temperature was adjusted to  $25 \pm 1^{\circ}\text{C}$ . The mice were gently placed on the water in the beaker and allowed to swim for 15 minutes. After 15 minutes, the mice were removed from the water and dried before being placed into an empty holding cage with heated blanket underneath. The mice were further dried in the holding cage for at least 10 minutes before moving back to the home cage. The glass beaker was washed with 70% ethanol, rinsed with water at least 3 times and refilled with fresh water after each mouse. The mice were killed 2 hours after stressing and the brains were removed for biochemical analysis with Western blotting (section 2.7) and RNA isolation (section 2.8) or proceeded to immunocytochemistry (section 2.10). All non-stressed control mice were just handled and weighed.

## 2.6 Kappa opioid receptor ligands

U50,488 was used as a selective KOPr agonist (Vonvoigtlander *et al.*, 1983) (Tocris, Avonmouth, UK), and was administered intraperitoneally (i.p.) at 20 mg/kg (Marrone *et al.*, 2016). Norbinaltorphimine (norBNI) was used as a selective KOPr antagonist (Portoghese *et al.*, 1987) (Tocris, Avonmouth, UK) and was administered i.p. at 10 mg/kg (McLaughlin *et al.*, 2003). All drugs were dissolved in 0.9% w/v saline (Hameln Pharmaceuticals, Gloucester, UK) and administered via i.p. route at a volume of 10 ml/kg. NorBNI is characterised with a slow onset of activity (peaking at 24 hours) and long-lasting effects for 3-4 weeks (Endoh *et al.*, 1992), therefore norBNI injections were administered 24 hours before stress or U50,488 treatment.

## 2.7 Protein extraction and Western blotting

In initial experiments (Chapter 3), brain GFP expression was quantified using Western blotting. Mice were killed by cervical dislocation and the brains were rapidly removed, the hippocampi and/or PFCx were dissected and immediately placed on dry ice. Samples were kept at -80°C before processing. Protein was extracted from brain tissues by using 10 volumes of Radioimmunoprecipitation (RIPA) buffer (including 10 mM Tris-HCl, pH 7.4, 1 mM EDTA, 1% Triton X-100, 0.1% sodium deoxycholate, 0.1% SDS, 140 mM NaCl, 1 mM PMSF). The protein concentration of the supernatant was determined using BCA protein assay (Pierce, Rockford, IL) (Bailey and Toth 2004).

Proteins (20µg) were separated by 10% SDS-PAGE (sodium dodecyl sulphate polyacrylamide gel electrophoresis), followed by transferring the separated protein onto PVDF (Polyvinylidene difluoride) membrane. The membranes were blocked by 5% BSA (bovine serum albumin) at room temperature for 1 hour, then the blots were incubated with primary anti-GFP (diluted 1:5000) or anti-Actin antibody (diluted 1:1000) in TBST (Tris Buffered Saline Tween 20) containing 2.5% BSA overnight at 4°C. The next day, the membrane blots were rinsed with TBST 6 times (5 minutes each time) and incubated with fluorescence-conjugated secondary antibody (diluted 1:5000) in TBST containing 2.5% BSA for 1 hour at room temperature. The proteins

of interest were then detected by LI-COR Bioscience Odyssey with 685nm and 785nm wavelength.

## 2.8 RNA Isolation

In initial experiments (Chapter 3), GFP was quantified using reverse transcription polymerase chain reaction (RT-PCR). Mice were killed by cervical dislocation and the brains were rapidly removed, the hippocampi were dissected and immediately placed on dry ice. Samples were kept at -80°C before processing. Hippocampal RNA was isolated from brain tissues by adding 0.5 ml TRIzol (Invitrogen) and the mixtures were homogenised by a pellet pestle. Another 0.5 ml TRIzol was added and the mixtures were passed through a 23G needle (1 ml of TRIzol per 50-100 mg tissue). 20 µl glycogen (1 mg/ml) was added to the sample and mixed briefly. The homogenised sample was left for 5 minutes at room temperature. 200 µl chloroform was then added to the sample in fume hood and vigorously shook by hand for 15 seconds and left at room temperature for 2-3 minutes. The mixture was centrifuged at  $12,000 \times g$  for 15 minutes at 4°C, which allows the mixture to separate into a lower red phenol-chloroform phase and a colourless upper phase. The upper aqueous phase was collected into a new tube in fume hood and the lower phase was discarded. RNA was precipitated by adding 0.5 ml 100% propa-2-ol, the mixture was then incubated at room temperature for at least 30 minutes. After 30 minutes' incubation, the mixture was centrifuged at  $12,000 \times g$  for 15 minutes at 4°C and the supernatant was removed. A further 1 ml of 75% ethanol per 1 ml TRIzol was added, followed by briefly vortexing. The mixture was centrifuged again at  $7,500 \times g$  for 5 minutes at 4°C. The liquid was removed, and the pellet was left to air dry for 5-10 minutes, the pellet was then re-suspended with 30µl RNase free water by passing solution through a pipette tip several times. Finally, the mixture was incubated at 55-60°C for 10-15 minutes and stored at -80°C until use.

DNA digestion was then carried out in order to remove DNA from extracted RNA solution. For each RNA sample, 4 µl reaction buffer (New England Biolabs), 1 µl RNasin (40U/µl, Fementas), 4 µl DNase (1U/µl, Fementas) and 1 µl RNase free water

were added and incubated at 37°C for 30 minutes. 10 µl glycogen (1mg/ml) and 100 µl 100% ethanol were added to each sample to precipitate RNA, followed by at least 30 minutes incubation at room temperature. The mixture was centrifuged at 12,000 × g for 15 minutes at 4°C and the supernatant was removed. The pellet was washed with 250 µl 75% ethanol, followed by briefly vortex and the sample was centrifuged at 12,000 × g for 5 minutes at 4°C. The supernatant was removed, and the pellet was left to air dry for at least 15 minutes at 37°C. Finally, the RNA pellet was re-suspended in 20 µl RNase free water and the samples were stored at -80°C until use.

## **2.9 Reverse transcription PCR (RT-PCR)**

Reverse transcription PCR was carried out by using SuperScript® One-step RT-PCR with Platinum® *Taq* DNA polymerase kit (Invitrogen), which allows detection of the expression of a specific gene of interest by amplifying its sequence, using the previously designed gene specific primers (Sigma-Aldrich, UK; summarised in Table 2.2). For PCR reaction, 12.5 µl 2 x reaction buffer (including 0.4mM dNTP, 2.4mM MgSO<sub>4</sub>), 10.1 µl RNase-free water, 0.4 µl RT/*Taq* mix, 0.5 µl forward primer (10µM), 0.5 µl reverse primer (10µM) and 1 µl template RNA sample (0.2 µg/µl) were added in each PCR tube. The PCR tubes were placed in a PCR machine (MJ Research, PCT-200) underwent the following reaction cycling conditions: 50°C for 30 minutes (reverse transcription for cDNA synthesis), 94°C for 2minutes (denaturation), 40 cycles of 94°C for 15 seconds (denaturation), 60°C for 30 seconds (annealing), 72°C for 30 seconds (extension), followed by final elongation at 72°C for 5 minutes. The PCR products were separated on 1% agarose gel with ethidium bromide (0.2 µg/ml, Sigma-Aldrich, UK) under 100V for 50 minutes - 1 hour, then the gene of interest (separated DNA bands) on the gel were visualised using GeneSnap (SynGene) software under UV exposure.

Primer	Sequences 5'- 3'	Product size	References
$\beta$ -Actin	<b>Forward:</b> ACCAACTGGGACGATATGGAGAAGA	214	Schmittgen <i>et al.</i> , 2000
	<b>Reverse:</b> TACGACCAGAGGCATACAGGGACAA	214	
c-Fos	<b>Forward:</b> TCCGGTTCCTTCTATGCAGC	129	Primer BLAST
	<b>Reverse:</b> GTAAGTAGTGCAGCCCGGAG	129	

**Table 2.2** Gene specific forward and reverse primers designed for one step RT- PCR. Primers were designed by using primer-designing tool (Primer-BLAST) or adopted from published sequences.

## 2.10 Immunocytochemistry

Mice were treated with either a single i.p. injection of selective KOPr agonist (U50,488, 20mg/kg) or acute *in vivo* stressor (forced swim stress or restraint stress). Immediately after restraint stress, or, 2 hours after forced swim stress or KOPr agonist injection, mice were anesthetised with i.p. injection of pentobarbital (100mg/kg) and perfused intracardially with a solution of 0.1M of phosphate buffered saline (PBS), pH 7.4, followed by 4% paraformaldehyde (PFA), pH 7.4. The brain was removed and placed in a specimen bottle and post-fixed and stored in 4% PFA at 4°C. The brain tissue was permeated with 30% sucrose in PBS solution at 4°C overnight (16 hours) one day before immunohistochemistry. The brain tissues were cut into coronal sections (40 $\mu$ m) on a vibratome, including PFC (Bregma +2.22 mm), NAc (Bregma +1.34 mm), dorsal hippocampus (Bregma -1.94 mm) and amygdala (Bregma -1.94 mm). For each mouse, one slice was taken for each brain region. The slices were rinsed in 0.01 M PBS, pH 7.4. Tissue sections were blocked in 0.01 M PBS



containing 0.1% Triton X-100 and 5% donkey serum for 2 hours at room temperature. After that, the tissue slices were incubated with affinity-purified primary antibodies (cFos, 1:500, GFP, 1:1000) in 0.01 M PBS containing 0.1% Triton X-100 and 2.5% donkey serum at 4°C overnight (16 hours).

The following day, tissue slices were washed with 0.01 M PBS at least four times for 10 minutes. The slices were incubated with either IRDye® 800CW Donkey anti-Rabbit antibody (diluted 1:1000) and IRDye® 680RD Donkey anti-Chicken antibody (diluted 1:1000) (Chapter 3 for LICOR images), or Alexa Fluor 568 Goat anti-Rabbit antibody (diluted 1:500) and Alexa Fluor 488 Goat anti-Chicken antibody (diluted 1:500) (Chapter 4, 5 and 6 for fluorescent microscope images) in 0.01 M PBS containing 0.1% Triton X-100 and 2.5% donkey serum for 2 hours at room temperature. The tissue slices were washed four times over 2 hours and mounted with Vectashield (Vector Laboratories) on microscope slides. The infrared immunoreactivity was detected by scanning the whole brain slides at 700 nm or 800 nm wavelength, infrared images were acquired with 21 µm resolution and set with 'highest' quality (Eaton *et al.*, 2016). The fluorescence immunoreactivity was detected using a Leica DMI4000B inverted wide-field fluorescent microscope at 200x magnification.

Fluorescent signals in regions of interest are directly proportional to the amount of protein on the brain slices; thus, the observed signal intensities were directly measured in ImageJ software. Two methods of quantification were trialled initially (see Chapter 3). In each experiment, shown in Chapters 4-6, background signals were measured and cFos or GFP signals data were normalised relative to corresponding background signals.

## 2.11 Blood sampling

The tail incision method was used for blood sampling in this study (Flutterm *et al.*, 2000; Sadler and Bailey 2016). All blood samples were collected between 9:00h and 13:00h. Mice were carefully held and cupped by one person and the operator

stabilised the mouse by gently holding the tail on the bench. A small nick (approximately 2mm in width, 0.5mm in depth) was made on the lateral tail vein using a razor blade, perpendicular to the tail, approximately 2cm from the tip of the tail. Blood samples were then collected by using heparinised capillary tubes (Hawksley, Sussex, UK), approximately 40µl of blood was collected from each mouse. All blood samples were then transferred to microcentrifuge tubes containing EDTA (3µg/µl) and stored on ice. Samples were then centrifuged at 2000 relative centrifuge force (rcf) for 20 minutes at 4°C. After centrifugation, plasma was collected and stored at -20°C until corticosterone analysis.

## 2.12 Corticosterone analysis

The corticosterone concentrations in each sample were determined by performing enzyme-linked immunosorbent assay (ELISA) according to the manufacturer's instructions (IBL International, Hamburg, Germany) (Sadler *et al.*, 2016). Plasma samples were diluted 10x and added to a 96 well plate (with standards of known corticosterone concentration), where wells were coated with an anti-corticosterone antibody. Enzyme conjugate (corticosterone conjugated to horseradish peroxidase) was added into each well and the well plate was mixed for 10 seconds, followed by 1-hour incubation at room temperature and washed 3 times. Lastly, the enzyme substrate solution (tetramethylbenzidine) was added to each well and incubated for 15 minutes at room temperature, the enzymatic reaction was terminated by adding a stop solution into each well. The final optical density was read at  $450 \pm 10$  nm using a microtiter plate reader (FLUOstar Optima, BMG Labtech). All samples were run in duplicate, with average values taken. The standard curve was calculated and constructed using MARS data analysis software (BMG Labtech) with a 4-parameter logistics curve fit, the average values from each sample duplicate were used to calculate the corticosterone concentrations directly from the standard curve.

## **2.13 Data quantification and statistical analysis**

Normalised data were analysed with one-way (treatment) analysis of variance (ANOVA) followed by post-hoc Sidak's test for each brain area in Chapter 4, 5 and 6. The effect of *in vivo* stressor and U50,488 on corticosterone levels were analysed using two-way (treatment x time) ANOVA followed by Sidak's test in Chapter 7. All data are presented as mean  $\pm$  SEM and significance levels were  $P < 0.05$ .

## **2.14 Reagents and materials**

All reagents and materials were purchased from suppliers as mentioned above. All other reagents and materials were purchased from Signal-Aldrich (Poole, UK), except PVDF membrane, glycogen and paraformaldehyde (PFA) powder which were purchased from Thermo Fisher Scientific (Loughborough, UK), and agarose powder which was purchased from Dutscher Scientific (Brumath, France).

## **Chapter 3 Optimisation of methods used to quantify cFos activation**

### 3.1 Introduction

As described in Chapter 1, multiple brain regions are involved in the primary responses to stress, and there is considerable overlap between stress-related brain regions and those that express KOPr and/or are activated by systemic administration of KOPr agonists or by dynorphin release. These brain regions include the PFCx, amygdala, NAc and hippocampus.

cFos is an immediate early gene that is often seen as a marker of neuronal activation. Numerous studies have shown that acute stress can induce a significant increase in cFos expression. For examples, acute restraint stress induced significant induction of cFos mRNA in the hippocampus and PFCx (Melia *et al.*, 1994, Ryabinin *et al.*, 1995, Del Bel *et al.*, 1998), and in immunohistochemistry studies, cFos protein expression was increased by acute restraint and forced swim stress in the hippocampus (Ryabinin *et al.*, 1995, Pace *et al.*, 2005).

In this study we are using expression of cFos as a marker for neuronal activity, which will allow us to investigate the pattern of cFos activation / neuronal activation in response to stress and KOPr agonist administration. The initial aim of this study was to determine appropriate experimental procedures that robustly and reproducibly enable us to quantify cFos expression (mRNA or protein) following an acute stressor. After identifying an appropriate technique, this can then be used in subsequent experiments to quantify stressor/KOPr agonist-induced cFos-positive neurons.

## **3.2 Methods**

### **3.2.1 Animals**

In this chapter, male adult (9-13 weeks old, 25-30g) C57BL/6 cFos-GFP (Barth *et al.*, 2004) were used, which were originally purchased from Jackson Laboratories (Bar Harbor, Maine, USA). GAD-GFP (12 weeks old, 26g) (Tamamaki *et al.*, 2003) transgenic mouse (Charles River, Margate, UK) were used for the anti-GFP antibody validation (Abcam, ab13970) experiment.

### **3.2.2 *In vivo* stressor**

Restraint stress (section 2.4) and forced swim stress (section 2.5) were used as acute stressors to induce the cFos mRNA and cFos-driven GFP expression, which were detected by using RT-PCR (section 2.8, 2.9), Western blotting (section 2.7) and immunohistochemistry (section 2.10).

### **3.2.3 Immunohistochemistry**

The immunohistochemistry details were described in chapter 2, section 2.10. In this chapter, the mouse prefrontal cortex (Bregma +2.22 mm), dorsal (Bregma -1.94 mm) and ventral hippocampal (Bregma -2.80 mm) slices were cut using a vibratome. For each mouse, one slice was taken for each region, these slices were dual-labelled with anti-cFos and anti-GFP antibodies (section 2.3), followed by incubation with infrared-labelled secondary antibodies: IRDye® 800CW Donkey anti-Rabbit antibody (diluted 1:1000) and IRDye® 680RD Donkey anti-Chicken antibody (diluted 1:1000) for LICOR images (section 2.3) or goat anti-rabbit Alexa fluor 568 antibody (diluted 1:500) and goat anti-chicken Alexa fluor 488 antibody (diluted 1:500) (section 2.3).

### **3.2.4 Quantification and statistical analysis**

Band intensities were measured in pixel/band and normalised to corresponding actin values by using ImageJ. In immunohistochemistry, two methods of quantifying the stress-induced cFos and cFos-induced GFP were shown in this chapter for comparison: the relative fluorescent signals (section 4.2.2) by using ImageJ and

manually counting the number of fluorescent-positive neurons. The data were analysed with unpaired Student's *t* test. All data are presented as mean  $\pm$  SEM and significance levels were  $P < 0.05$ .

## 3.3 Results

### 3.3.1 Validation of anti-GFP antibody

The long-term aim of this study was to use cFos-GFP transgenic mice, where GFP expression is under the control of the cFos promoter. In this way, quantifying GFP expression is an index of previous cFos expression. In initial experiments, the anti-GFP antibody was validated. To do this, we used GAD67-GFP transgenic mice (Tamamaki *et al.*, 2003), which constitutively express GFP in all GABAergic neurons in the brain. As GABAergic neurons are ubiquitously expressed in the brain and account for a relatively large portion of neurons, GFP expression in the brains of these animals is widespread and so GAD67-GFP transgenic mice are useful as a positive control for anti-GFP antibody validation.

Subjects were one male adult wild type C57BL/6 mouse and one male adult GAD-GFP transgenic mouse; both PFCx and hippocampus were dissected from each mouse and immediately proceeded to protein extraction in solubilisation buffer, followed by separation and analysis by Western blotting using anti-GFP antibody, with actin controls. As shown in Figure 3.3.1, no GFP signal was observed in wild type PFCx and hippocampus samples, whereas robust GFP signals were shown in GAD67-GFP transgenic PFCx and hippocampus samples at 27kDa, which suggests that the specific anti-GFP antibody is functional and specific.

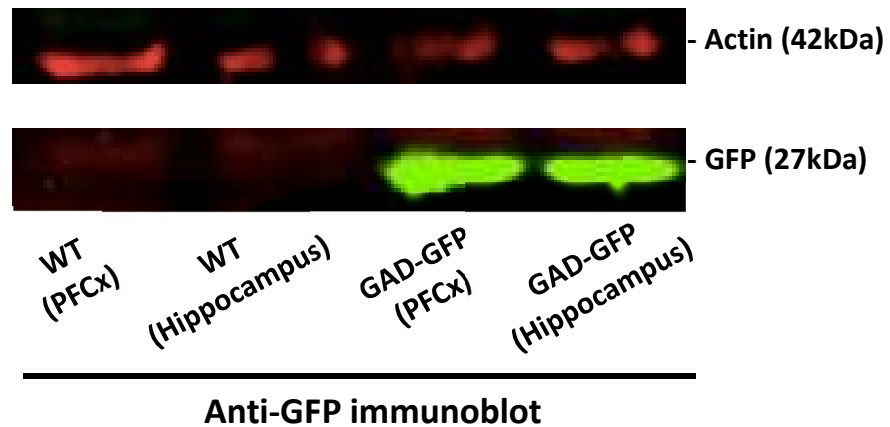


**Figure 3.3.1 Validation of anti-GFP antibody.** Male adult (12 weeks) GAD-GFP transgenic mouse and wild type (WT) mouse were used. Both PFCx and hippocampus were obtained from each type of mouse. Tissues underwent Western blotting for GFP detection.

### 3.3.2 Expression of GFP following *in vivo* stress

Once the anti-GFP antibody had been validated, it was then used to attempt to detect cFos-driven GFP induction following an acute *in vivo* restraint stressor, a well-established model to induce depression and anxiety-like behaviours which has previously been shown to induce cFos expression in a variety of brain regions. In initial studies, the acute stressor used was restraint stress, previously shown to increase cFos expression in the hippocampus (Melia *et al.*, 1994).

Three cFos-GFP transgenic animals were exposed to restraint stress, then killed by cervical dislocation immediately after, 2 hours after or 4 hours after. The hippocampi were dissected and then processed for Western blotting using an anti-GFP antibody, with actin control. Control cFos-GFP animals were not exposed to restraint stress but were killed at the same time as restraint stress-treated animals. Two GAD-GFP transgenic animals were used as positive controls.

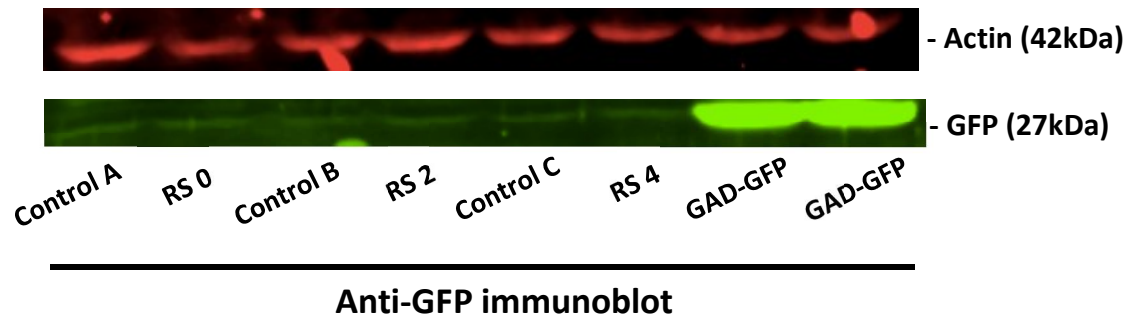


Figure 3.3.2A demonstrates that there was no robust increase in GFP expression after two hours restraint stress, compared to non-stressed mice (control A, B or C). Also the expression of GFP immediately after stress (RS 0) is similar to that of 2 hours (RS 2) or 4 hours (RS 4) post stress (Figure 3.3.2A). In the same Western blot gel, hippocampal protein samples taken from two GAD-GFP transgenic mice were also analysed as a positive control and show strong GFP bands signals at 27kDa. Figure 3.3.2B shows quantification of the Western blot shown in Figure 3.3.2A. Here there is a slight increase in the relative GFP/Actin signal immediately after stress (RS 0), which then declines after two- or four hours post-stress (RS 2, RS 4). One possible reason for this might be GFP is degrading over the time period, however, previous studies have shown that GFP protein is relatively stable, and so would be unlikely to degrade significantly over 2-4 hours (Barth *et al.*, 2004). As in these preliminary validation experiments the sample size was effectively 1, we cannot say for sure whether GFP was increase at RS 0, but, the overall increase in GFP signal was minimal.

Overall, these data fail to detect a robust increase in cFos-driven GFP expression in the hippocampus, following two hours restraint stress. This is in contrast to previous studies that have demonstrated cFos expression induced by restraint stress (Melia *et al.*, 1994, Ryabinin *et al.*, 1995). The reasons why this approach did not yield favourable results for us is unclear.

The same experiment was repeated for cFos/GFP protein detection following forced swim as the stressor (rather than restraint stress) with both wild-type C57BL/6 mice and cFos-GFP transgenic mice, using both anti-cFos and anti-GFP antibodies. However, it showed a similar pattern to restraint stress, in that no consistent difference was seen between control and stress-treated animals (data not shown). We therefore used a different technique (RT-PCR) to attempt to quantify increases in cFos expression after an acute stressor.

**A**



**B**

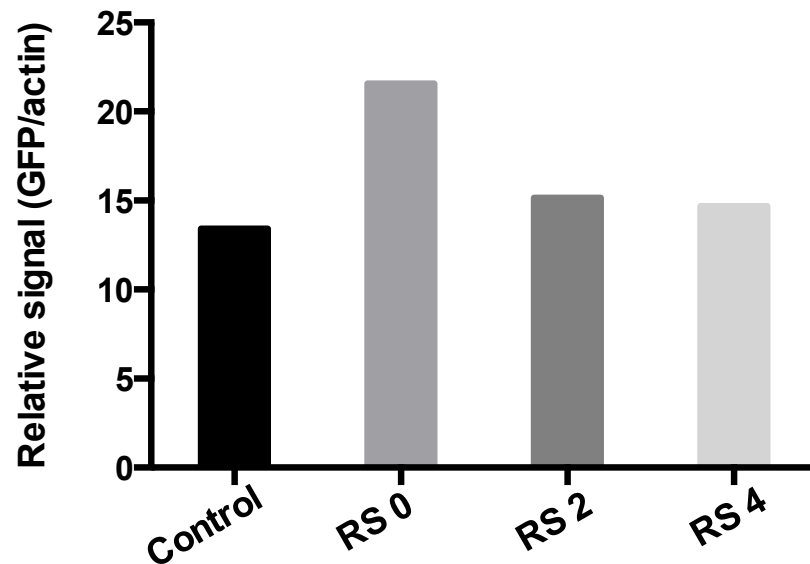


**Figure 3.3.2 GFP expression following two hours restraint stress. (A)** Six male adult (12 weeks) C57BL/6 cFos-GFP transgenic mice; three were untreated, serving as controls (control A, B and C), three underwent two-hour restraint stress (RS) and were killed either immediately (RS 0) after stress, or two hours (RS 2) or four hours (RS 4) after stress. Hippocampi were dissected and cFos-driven GFP measured using Western blotting. Two untreated GAD-GFP transgenic mice duplication were used as positive controls for GFP detection. **(B)** Quantitation of expression of GFP represented by relative signal (GFP/Actin).

### 3.3.3 Expression of cFos mRNA following *in vivo* stress

Since *in vivo* stressor stimulus did not profoundly affect the GFP expression examined using Western blots (Figure 3.3.2), it was then investigated whether an *in vivo* stressor (two hours restraint stress) could induce an observable increase in hippocampal cFos mRNA expression. This experiment used six cFos-GFP transgenic mice that were either untreated (3 controls) or exposed to two hours restraint stress as above (3 restraint stress treated). Immediately following *in vivo* restraint stress, mice were killed by cervical dislocation, the hippocampi were dissected and processed for mRNA analysis using RT-PCR.

Figure 3.3.3A represents the cFos mRNA bands observed in all six samples (3 controls, 3 restraint stress treated), with actin controls. However, as with previous Western blotting experiments, there was no significant difference between the control and stress-treated samples (Figure 3.3.3B). Notably, the RS 1 sample showed a slight increase in intensity, compared to the control 1 sample, whereas the opposite effect was observed between control 3 and RS 3 samples i.e. the intensity of control 3 is higher than that of RS 3 bands (Figure 3.3.3A), suggesting either that the two hours restraint stress did not produce robust increases in cFos mRNA levels, or that this method of detection is unsuitable. Furthermore, the same experiment was also carried out for cFos mRNA detection following forced swim wild-type C57BL/6 mice, but a similar pattern was observed (data not shown). Thus, further studies using a different technique, immunohistochemistry, were performed in order to derive a protocol to reproducibly quantify cFos expression following acute stress.

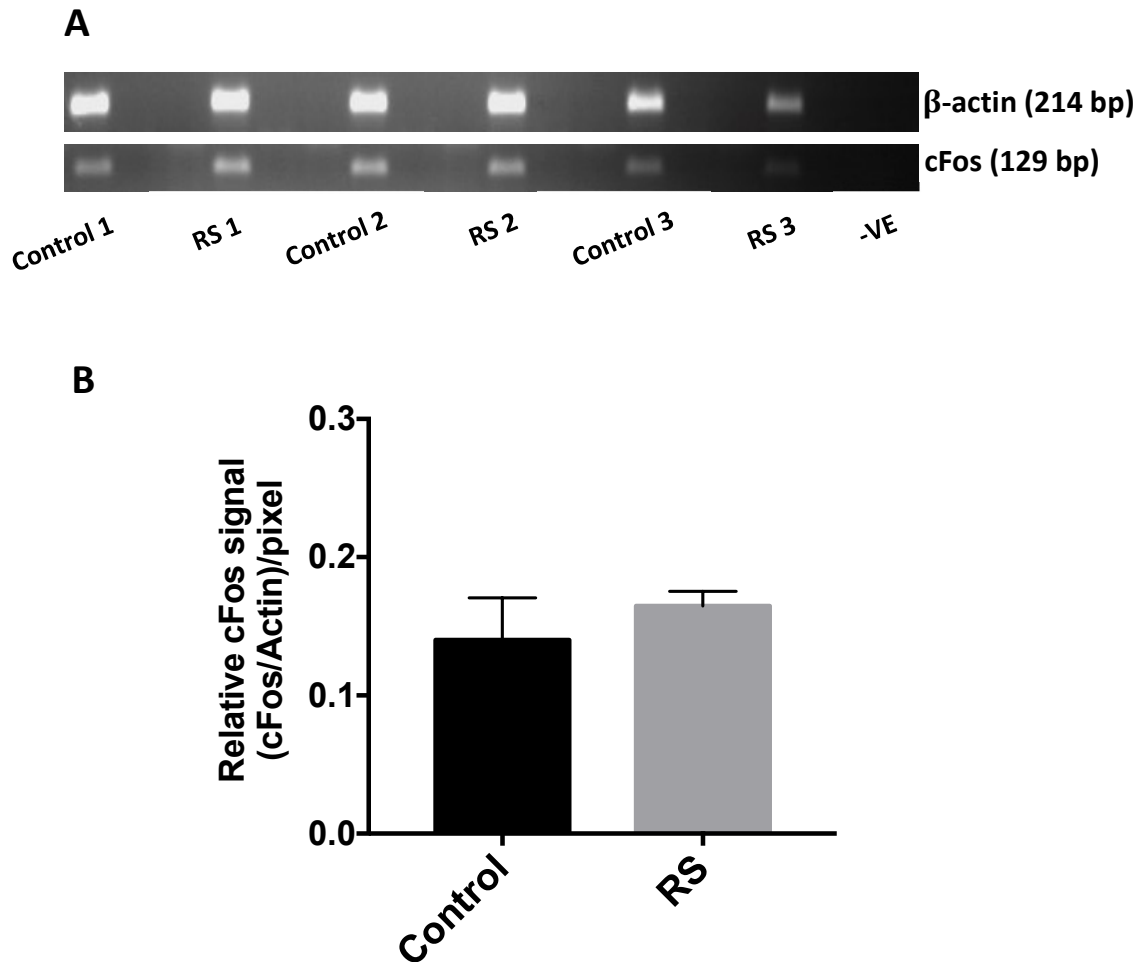


**Figure 3.3.3 Expression of cFos mRNA after *in vivo* stressor.** **(A)** Subjects were six male adults (10-12 weeks) C57BL/6 cFos-GFP transgenic mice. Three were untreated (control 1, 2 and 3) and three were underwent two-hour restraint stress (RS 1, 2 and 3). All mice were killed immediately after restraint stress. Hippocampi were dissected and processed to RNA extraction and RT-PCR. RNase free water acted as negative control (-VE). **(B)** Quantification of cFos mRNA after restraint stress between control and RS groups, represented by relative signal (cFos/actin). All data are shown as mean  $\pm$  SEM,  $n = 3$  animals per treatment group, unpaired Student's  $t$  test.

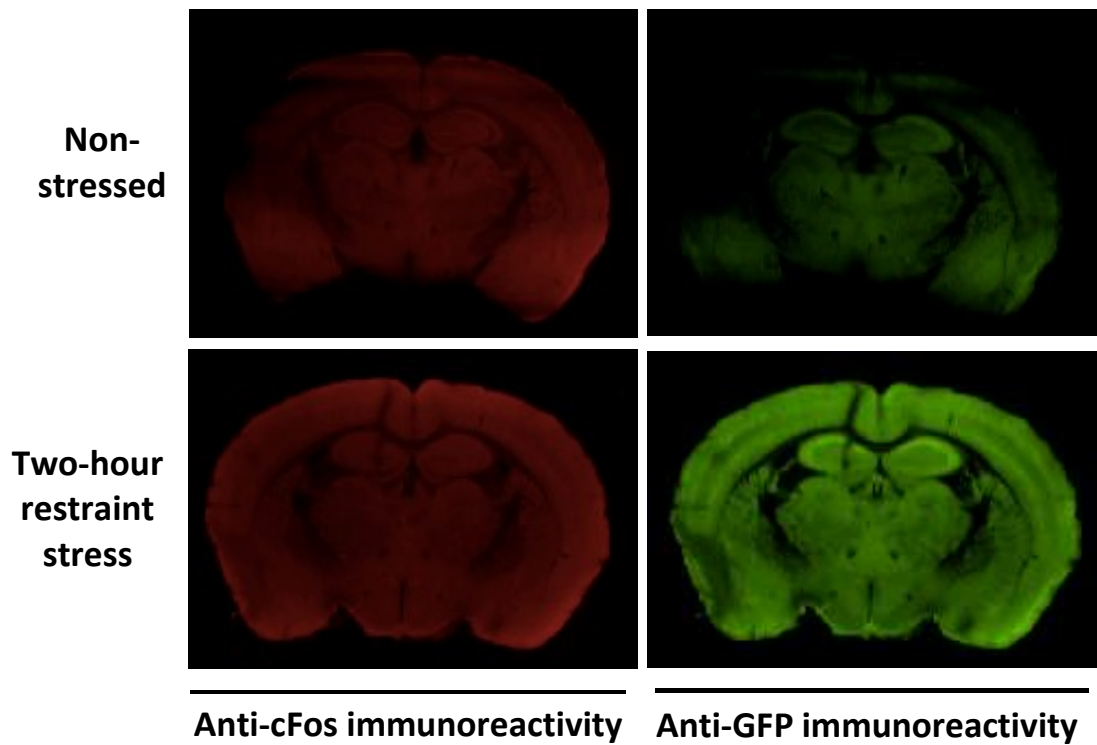
### 3.3.4 Immunohistochemical localisation of cFos and GFP expression

As there were no detectable stress-induced increases in cFos or cFos-driven GFP effects observed in Western and mRNA analysis in the previous sections (Section 3.3.2 & 3.3.3), immunohistochemical techniques were then used to attempt to

detect any cFos or cFos-driven GFP expression changes induced by stress, as previous immunohistochemistry studies have successfully demonstrated acute stress-induced increases in cFos expression in the hippocampus and PFCx in rats (Ryabinin *et al.*, 1995, Pace *et al.*, 2005).

Adult male (12 weeks) cFos-GFP C57BL/6 mice underwent two-hour restraint stress, with non-stressed controls. After two hours, the mice were anaesthetised with pentobarbital (100mg/kg), followed by cardiac perfusion fixation. Coronal brain sections (40µm) were taken, containing either dorsal or ventral hippocampus and were co-stained with both rabbit anti-cFos and chicken anti-GFP antibodies, followed by incubation of fluorophore-labelled secondary antibodies, 800CW donkey anti-rabbit and 680RD donkey anti-chicken antibodies. The slices were mounted on microscope slides and imaged using LI-COR Odyssey, shown in Figure 3.3.4. In the hippocampus, both dorsal and ventral hippocampus showed an increase in cFos and cFos-driven GFP immunoreactivity signals following acute two hours restraint stress, compared to the controls (Figure 3.3.4), indicating that two hours restraint stress induced an overall increase expression of cFos and cFos-driven GFP in the hippocampus in these mice. This immunohistochemical technique provides a promising methodology to detect the stress-induced effects in different brain regions in the following studies.

## Dorsal hippocampus sections



## Ventral hippocampus sections

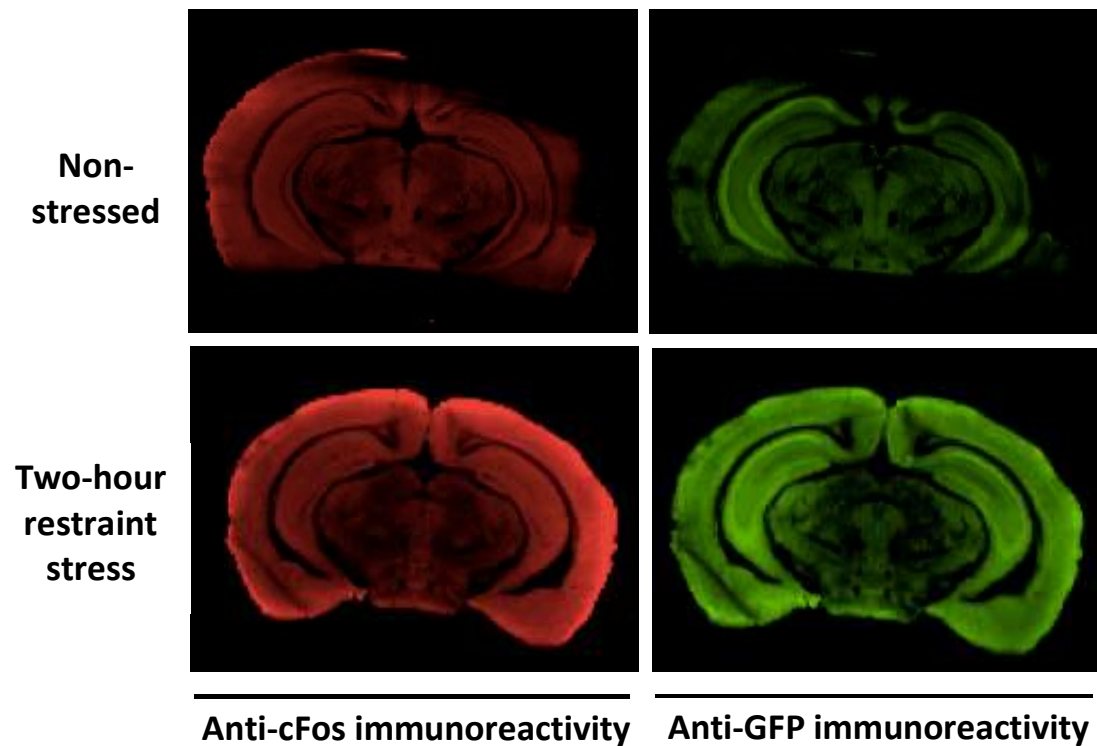


**Figure 3.3.4 Coronal sections of the dorsal (Bregma -1.94 mm) and ventral (Bregma -2.80 mm) hippocampus in mouse brain immunostained for cFos and GFP.** One adult male C57BL/6J cFos-GFP transgenic mouse underwent 2-hour restraint stress, with one untreated mouse as control. 40  $\mu$ m tissue sections were stained with both anti-cFos and anti-GFP antibodies, followed by appropriate fluorescent secondary antibodies. cFos and GFP immunoreactivity on each slice was detected with the LI-COR Odyssey with 21 $\mu$ m resolution and 1mm offset. Adult male C57BL/6J cFos-GFP transgenic mice were treated with either two-hour restraint stress or no stress time-

### **3.3.5 Optimisation of immunohistochemical methodology**

The previous section (3.3.4) demonstrated that immunohistochemistry could be used to detect and measure the effects of stress on cFos and cFos-driven GFP expression in cFos-GFP transgenic mice. Although the LICOR detection method allowed us to visualise cFos and cFos-driven GFP expression in whole brain section, it lacks resolution on the single cell level. In order to detect cFos and cFos-driven GFP immunoreactivity with higher resolution at an individual neuronal level, regular immunofluorescence microscope was used. The same primary antibodies were used as in the previous section (rabbit anti-cFos and chicken anti-GFP antibodies) but with secondary antibodies conjugated to different fluorophores to permit visualisation using a conventional immunofluorescence microscope, rather than in the infrared range (as with LICOR). Secondary antibodies used were goat anti-rabbit Alexa fluor 568 antibody and goat anti-chicken Alexa fluor 488 antibody.

cFos-GFP transgenic mice (n=6 animals per treatment group) underwent a single acute stress stressor (forced swim) with non-stressed controls. 2 hours later, animals were anaesthetised with pentobarbital (100mg/kg) followed by cardiac perfusion fixation. Brains were sectioned (40  $\mu$ m), immunolabelled, and imaged using a Leica DMI4000B inverted wide-field fluorescent microscope. Sample images in the PFCx are shown in figure 3.3.5, which shows apparent increases in both cFos and cFos-driven GFP following forced swim stress, compared to the non-stressed controls. The

fluorescence signals in these images were further quantified in two different ways: by measuring relative fluorescent signals in ImageJ software ([https://imagej.net/Image\\_Intensity\\_Processing](https://imagej.net/Image_Intensity_Processing)) and by counting the number of cFos or GFP-positive neurons manually, the quantified signals of both quantifying methods are demonstrated in figure 3.3.6 for comparison.

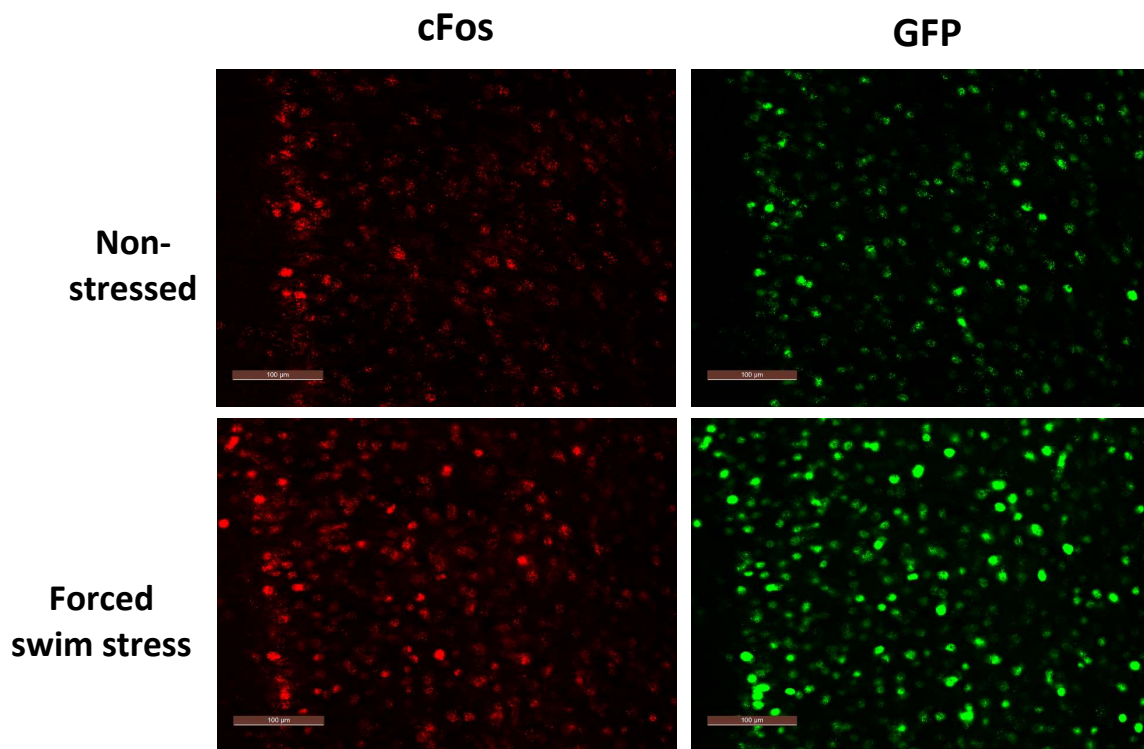


**Figure 3.3.5 Example images of stress-induced cFos and cFos-driven GFP expression in the PFCx in male mice.**

Coronal sections of PFCx (40μm) (Bregma +2.22 mm) were cut and immunolabelled with anti-cFos and anti-GFP antibodies. cFos (red) and cFos-driven GFP (green) immunoreactivity was visualised under wide-field fluorescent microscopy, and cFos and GFP expression was increased in response to 15 minutes forced swim stress in the PFCx, compared to the non-stressed controls. Scale bar = 100 μm.



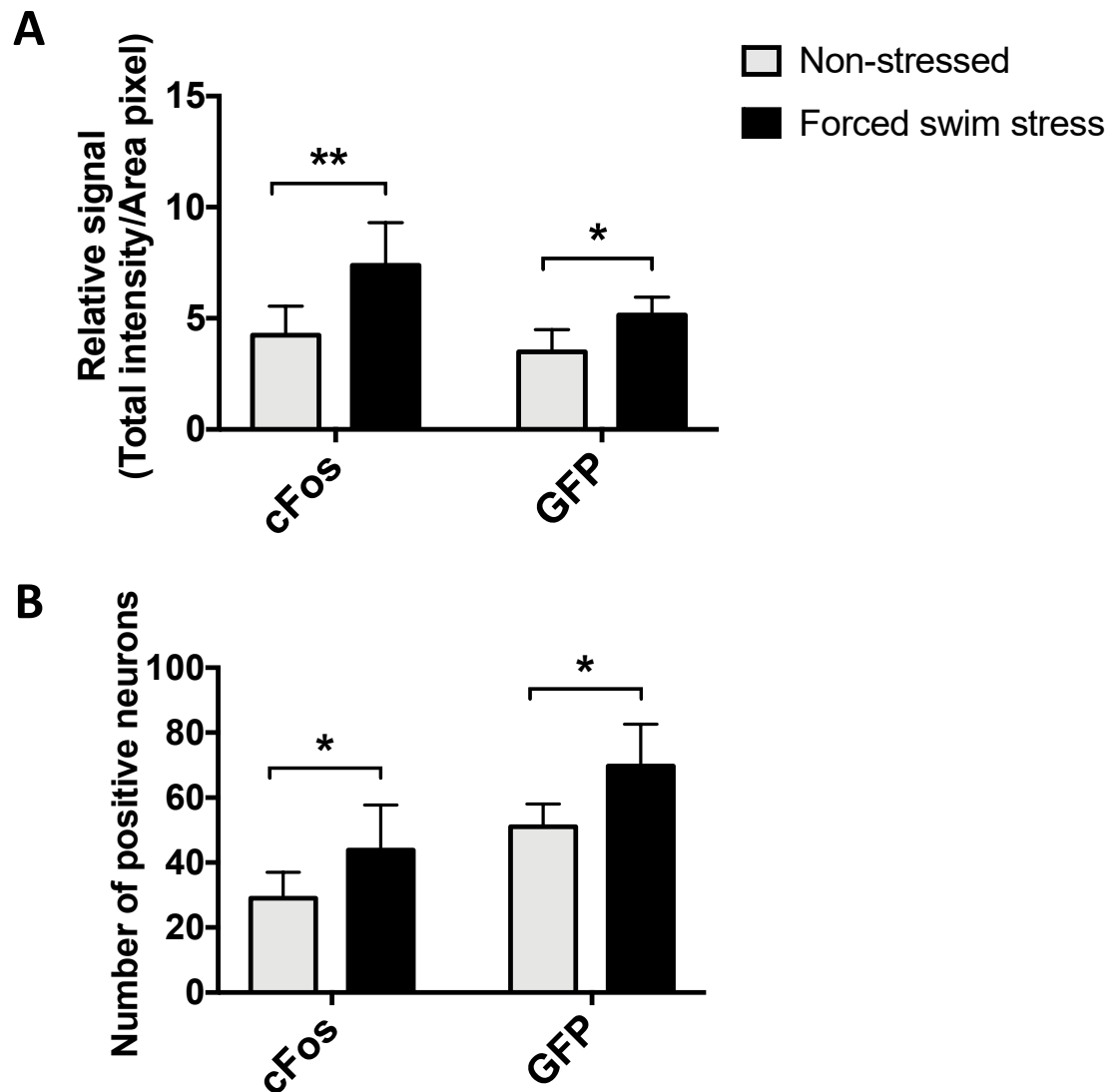


**Figure 3.3.6 Two different methods of quantifying the effects of stress on cFos and cFos-driven GFP expression in the PFCx in male mice.**

**A**, quantified fluorescent signals by measuring the relative signals. **B**, manually counting the number of positive neurons that express cFos or GFP immunoreactivity. All data are presented as mean  $\pm$  SEM. N = 6 animals per treatment group, unpaired Student's t test, \* =  $P < 0.05$ , \*\* =  $P < 0.01$ .

Figures 3.3.5 & 3.3.6 show that stress-induced increases in cFos and cFos-driven GFP expression (in cFos-GFP transgenic mice) can be successfully detected using this technique. Sample images are shown from PFCx, but similar results were observed in hippocampal CA1 region taken from the same animals (Figure 3.3.7), and quantified by two different methods for comparison (Figure 3.3.8). Further, in similar preliminary experiments, in mice treated with a single injection of the KOPr agonist,

U50,488 (20mg/kg), there was also a detectable and significant increase in cFos and cFos-driven GFP using this immunohistochemical method (data not shown). This provide us with a protocol with which stress- and KOPr agonist-induced neuronal activity can be detected. The images could then be quantified by two different methods, shown in figure 3.3.6 and 3.3.8, demonstrating that both of the quantification methods yield similar results, suggesting either of the quantification method works for this analysis in further similar preliminary experiments. Therefore, this immunohistochemical methods with fluorescent-labelled secondary antibodies and fluorescent microscope will be used in the following chapters.

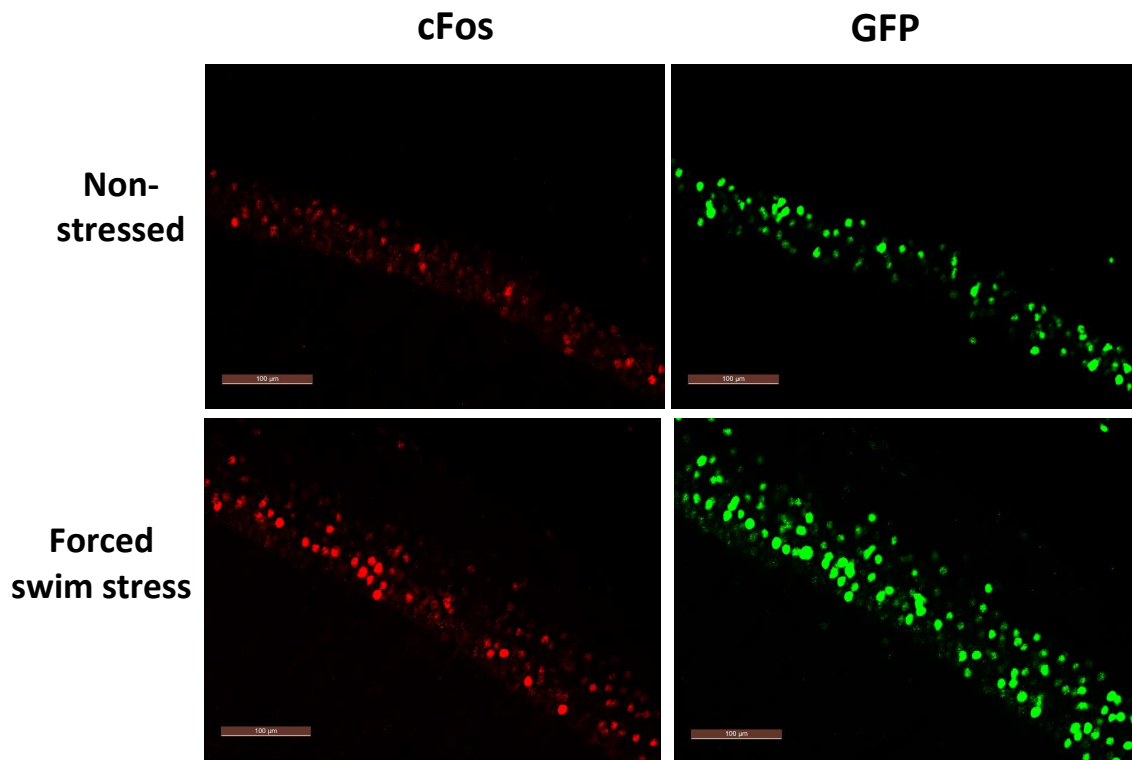


**Figure 3.3.7 Example images of stress-induced cFos and cFos-driven GFP expression in the hippocampal CA1 region in male mice.**

Similar to the PFCx images shown above, coronal sections of CA1 region (40µm) (Bregma -1.94 mm) were cut and co-stained with anti-cFos and anti-GFP antibodies. Comparing to the non-stressed samples, both cFos (red) and GFP (green) expression was increased after FSS in the hippocampus. Scale bar = 100µm.

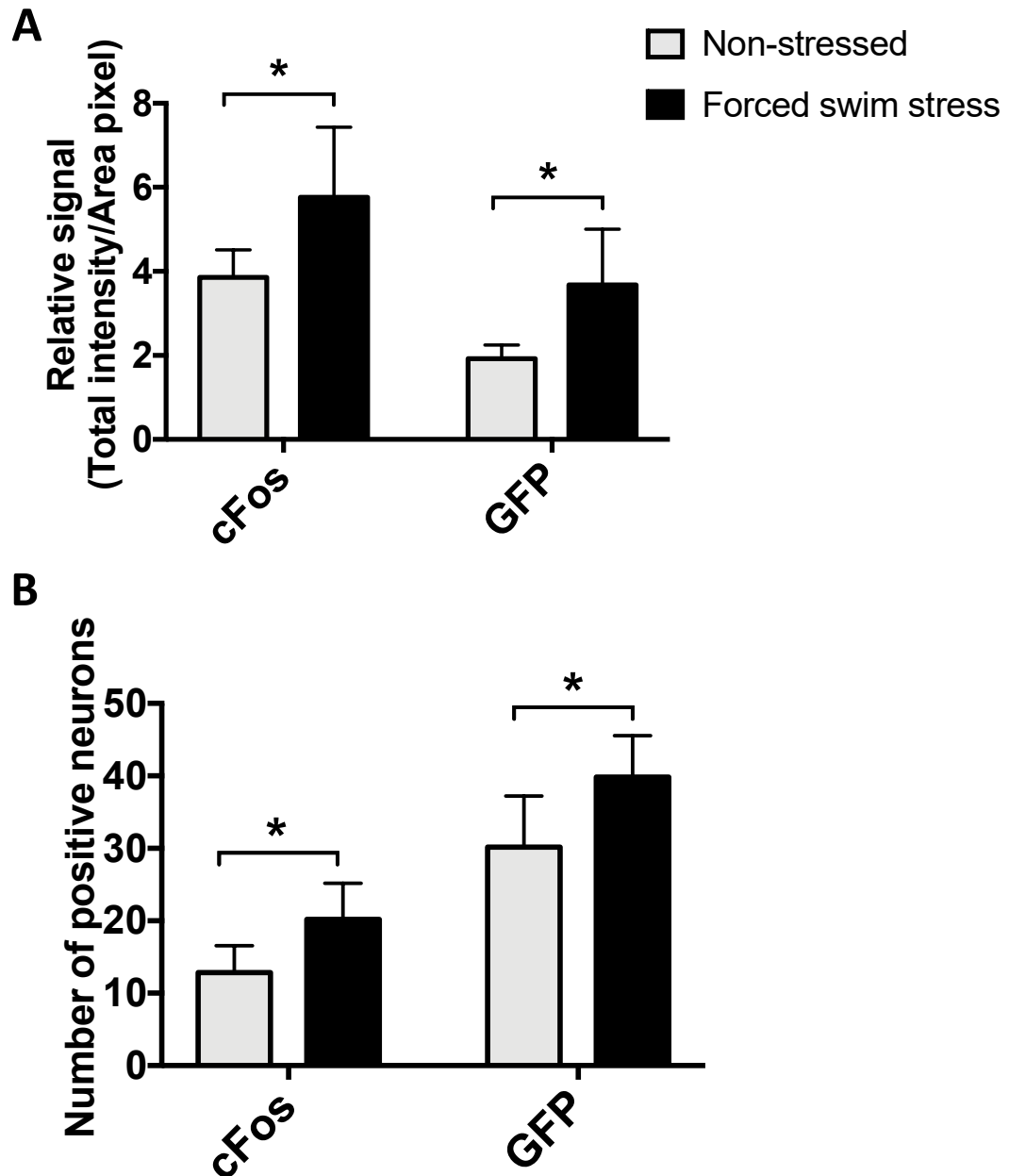


**Figure 3.3.8 Two different quantifying methods for analysing the FSS-induced cFos and GFP expression in the CA1 region of the hippocampus in male mice.**

**A**, fluorescent signals were quantified by measuring the relative signal.  
**B**, the number of cFos- or GFP-positive neurons were counted manually.  
N = 6 per treatment group, unpaired Student's t test, \* =  $P < 0.05$ .

### 3.4 Discussion

Different techniques were used to attempt to detect cFos and cFos-driven GFP expression in cFos-GFP expression following *in vivo* stressors, that could be used throughout this study. Our results from Western blotting and mRNA (RT-PCR) analysis failed to show a robust increase in either cFos or cFos-driven GFP expression immediately following acute restraint and forced swim stressors, which did not further support the earlier evidence in adult male rats, showing that acute restraint stress caused high levels of cFos protein expression in the PFCx using Western blotting (Perrotti *et al.*, 2004), or studies in adult male rats that showed increased expression of cFos mRNA in the hippocampus and PFCx immediately after acute two-hour restraint stress (Melia *et al.*, 1994, Ryabinin *et al.*, 1995). In addition, previous evidence demonstrated cFos mRNA expression reached a peak level after 30 minutes to 60 minutes post-stress, and this stress-induced cFos mRNA expression remarkably decreased after 120 minutes (Cullinan *et al.*, 1995), suggesting that stress intensity and duration or time course post-stress may directly affect the detection of cFos mRNA expression.

The reason why we failed to replicate these findings is unclear, but, one possible reason is that cFos expression might not be increase across the hippocampus as a whole. Pace and colleagues showed that changes in cFos expression after novel experience was region-specific, with an increase in cFos-positive cells in the CA1, CA2, CA3 and inner layer dentate gyrus regions in the hippocampus, but a significant decrease in cFos-positive neurons in the outer layer of the dentate gyrus (Pace *et al.*, 2005). These findings might explain why there was no obvious difference in cFos mRNA and protein levels between control and stressed mice, as the whole hippocampus was taken in these experiments for RNA and protein extraction and analysis, the elevated cFos gene levels in one subregion might be balanced with decreases in other subregions of the hippocampus. Therefore, both Western blotting and RT-PCR techniques might not be sensitive enough to detect the changes in stress-induced cFos expression within the hippocampus. In addition, as the whole

hippocampus was removed for RNA or protein extraction, it is unable to determine the stress-induced any effects in the subregions e.g. CA1 or dentate gyrus.

However, as an alternative to Western blotting and RT-PCR, several studies have revealed the effects of acute stress on cFos protein expression in different brain regions using immunohistochemistry (e.g. Ryabinin *et al.*, 1995, Pace *et al.*, 2005, Perrotti *et al.*, 2004, Briand *et al.*, 2010). For example, the overall number of cFos-positive neurons in the CA1 and CA2 regions of the hippocampus were increased after two-hour restraint stress in adult rats (Pace *et al.*, 2005), while other evidence showed 15 minutes restraint stress or 6 minutes forced swim stress significantly increased the number of cFos-positive immunoreactive neurons in the hippocampus, PFCx, NAc and amygdala in adult rats (Ryabinin *et al.*, 1995) and in adult mice (Briand *et al.*, 2010). Our data using immunohistochemical techniques (Section 3.3.4 & 3.3.5) not only provided us with the best method to investigate the stress-induced cFos expression effects in different brain subregions, but also showed a significant increase in cFos and cFos-driven GFP expression in the PFCx (Figure 3.3.5 & 3.3.6) and hippocampal CA1 region (Figure 3.3.7 & 3.3.8) in male cFos-GFP mice following an acute stress, which support the previous evidence on stress-induced effects in different brain areas in rodents. This method was then used to investigate cFos expression after an acute *in vivo* stressor and single administration of a KOPr agonist in both male and female mice in the following chapters.

## **Chapter 4 The effect of kappa opioid receptor activation and *in vivo* stressor in male mice**

## 4.1 Introduction

The previous chapter demonstrates that immunocytochemistry allowed us to detect cFos expression in the prefrontal cortex and hippocampus in brain slices after acute restraint stress. In this chapter, investigations into neuronal activity induced by acute forced swim stress or KOPr agonist treatment were performed. Using fluorescence microscopy in different brain regions in male mice, cFos immunoreactivity at an individual neuron level was quantified, using the method shown in the previous chapter.

As discussed in chapter 1, the PFCx, hippocampus (HPC) and amygdala are three primary regions that are important in mediating behavioural responses to stress (McEwen *et al.*, 2010), while dopaminergic input from VTA to the NAc is the key component for rewarding properties of drugs of abuse (Adinoff 2004). It has been shown that NAc is not only the key region involved in drug addiction, but also implicated in depression and anxiety (Perrotti *et al.*, 2004). Perrotti and colleagues showed increased cFos immunoactivity in the NAc in rats after acute restraint stress (Perrotti *et al.*, 2004). Similarly, other studies also demonstrated that acute forced swimming stress significantly induced cFos expression in the NAc and PFCx in male mice (Briand *et al.*, 2010). These data suggested the important role of NAc in the effects of acute *in vivo* stress, which may contribute to stress-induced enhancement of drug intake. In addition, both the hippocampus and the amygdala are also implicated in drug reward mechanisms and psychiatric diseases (Bolla *et al.*, 2003), for example, studies in male rats showed exposure of foot shock stress and 30 minutes of restraint stress significantly increased cFos expression in the NAc, hippocampus, central amygdala and basolateral amygdala (Funk *et al.*, 2006), highlighting the crucial role of these brain regions implicated in mediating stress responses and suggesting an association between stress and addiction-related behaviours.

Stress exposure induces the release of an endogenous neuropeptide dynorphin (DYN), which primarily activates kappa opioid receptors (KOPrs) and produces dysphoria, anxiety and depressive-like behaviours (Bruchas *et al.*, 2010). KOPr is a G<sub>i</sub> protein-coupled receptor (GPCR) and belongs to the opioid receptor family. Increasing evidences suggests that KOPrs play a major role in both stress responses and addiction-related behaviours, and dysregulation of KOPrs is involved in psychiatric disorders, such as depression and addiction (Bruchas *et al.*, 2010, Lalanne *et al.*, 2014). KOPrs are highly expressed throughout the limbic brain areas implicated in the development of depression, anxiety and addiction such as the VTA, NAc, PFCx, hippocampus and amygdala (Knoll & Carlezon, 2010).

A number of animal studies have shown that stress-induced dynorphin/KOPr system activation is a key component in the aversive stress behaviour and rewarding properties potentiation (McLaughlin *et al.*, 2003, Carey *et al.*, 2009, Shirayama *et al.*, 2004, Redila & Chavkin, 2008), thus, activation of KOPrs is used to mimic aversive effects of stress in animal models (Knoll & Carlezon, 2010). Importantly, antagonism of KOPr or disruption of prodynorphin gene significantly prevented stress-induced analgesia, reduced stress-induced immobility and blocked the stress-induced cocaine reinstatement (McLaughlin *et al.*, 2003, Redila & Chavkin, 2008), suggesting that KOPr antagonists have anti-depressant-like effects, thus, KOPrs represent a potential therapeutic target for the depression treatment. Additionally, Russell and colleagues showed that administration of KOPr agonist, U50,488 (10mg/kg) significantly induced cFos expression in the NAc and amygdala in male rats (Russell *et al.*, 2014). Other evidence in California male mice also reported U50,488-induced neuronal activation in the NAc by showing increased immunoactivity of p38 MAP kinase, an extracellular signal modulated MAP kinase that indicates the activation of KOPr (Robles *et al.*, 2014).

The aim of this chapter is to investigate the effects of a single injection of KOPr agonist (U50,488), in mice, on neuronal activity in various brain regions (PFCx, NAc, hippocampus, amygdala) and compare the brain regions activated by KOPr agonist with those activated by *in vivo* FSS. Neuronal activity will be assessed by quantifying



cFos expression in each brain region using immunohistochemistry. We hypothesise that, in mice, both a single injection of KOPr agonist and *in vivo* forced swim stress-induced dynorphin release would activate KOPrs *in vivo*, and would induce neuronal activation in a similar fashion in PFCx, NAc, hippocampus and amygdala (as indicated by increased cFos expression). We further hypothesise that pretreatment of the animals with the KOPr antagonist nor-binaltorphimine (norBNI) would block the effects of KOPr agonist and may also inhibit (at least in part) forced swim stress-induced effects in these brain regions.

## 4.2 Methods

### 4.2.1 Immunohistochemistry

Adult male (9-13 weeks old, 25-30g) C57BL/6 cFos-GFP transgenic mice (n = 6 animals per treatment group) were treated with either saline or KOPr antagonist, norBNI (10mg/kg; i.p.), after 24 hours, mice were treated with either a single injection of U50,488 (20mg/kg; i.p.) (Marrone *et al.*, 2016) or 15-minute forced swim stress. Two hours later, mice were then anesthetised with intraperitoneal injection of pentobarbital (100mg/kg; i.p.) and perfused intracardially with a solution of 0.1M of phosphate buffered saline (PBS), pH 7.4, followed by 4% paraformaldehyde (PFA), pH 7.4, illustrated in figure 4.1.

The brain was removed and placed in a specimen bottle and post-fixed and stored in 4% PFA at 4°C for immunocytochemistry, which was described in chapter 2 section 2.10. The coronal sections (40µm) of PFCx (Bregma +2.22 mm), NAc (Bregma +1.34 mm), amygdala (Bregma -1.94 mm) and hippocampal CA1 region and dentate gyrus (Bregma -1.94 mm) were cut on a vibratome. For each mouse, one slice was taken for each brain region. These slices were dual labelled with anti-cFos and anti-GFP antibodies (section 2.3), followed by fluophore-tagged secondary antibodies: goat anti-rabbit antibody Alexa Fluor 568 (diluted 1:500) and goat anti-chicken antibody Alexa Fluor 488 (diluted 1:500) (section 2.3).

The fluorescence immunoactivity was detected using Leica DMI4000B inverted wide-field fluorescent microscope at 200X magnification and fluorescence intensity quantified in regions of interest (ImageJ). Fluorescent signals are directly proportional to the amount of protein on brain slices; thus, the observed signal intensities for each brain region on each slice were the average values of the left and right signals, measured in ImageJ software. In each experiment, cFos or GFP expression signals were corrected to the background signals. All data are presented as mean  $\pm$  SEM and significance levels were  $P < 0.05$ , all data were analysed with the one-way (treatment) ANOVA followed by Sidak's test.

Saline (10ml/kg) **or** the KOPr antagonist norBNI (10mg/kg)



Adult **male** C57BL/6 cFos-GFP transgenic mice



**24 hours later**

**Pharmacological approach**

A single injection with **U50,488** (selective kappa opioid receptor agonist, 20mg/kg) or saline

**Physical in vivo approach**

15-minute forced swim stress (**FSS**) or no stress



**2 hours later**

Cardiac perfusion fixation and immunocytochemistry, labelling for **cFos** and **GFP**

**Figure 4.1** Illustration of immunocytochemistry procedures for adult male (9-13 weeks old) C57BL/6 cFos-GFP mice following pharmacological (U50,488, 20mg/kg, i.p.) or physical *in vivo* stressors (FSS).

## 4.3 Results

### 4.3.1 The effect of U50,488 in male PFCx

To investigate how kappa opioid receptor activation affects different brain regions in male mice. Adult male C57BL/6J cFos-GFP transgenic mice were pre-administered with either saline or the KOPr antagonist norBNI (10mg/kg, i.p.). After 24 hours, the mice were treated with either saline or KOPr agonist, U50,488 (20mg/kg; i.p.) (n = 6 animals per treatment group, i.e. 24 mice used in total). Two hours later, mice were killed and brains sectioned for immunocytochemistry. Typical expression patterns in the prelimbic area of the PFCx (layers 1-3, indicated in Figure 4.2A) are shown in Figure 4.2B.

These fluorescent signals were quantified as shown in Figure 4.2B. In male mice, cFos expression was significantly increased in the prelimbic area (layers 1-3) of PFCx following U50,488 treatment (Figure 4.2C), compared to the saline-treated control group. A similar increase was also observed in cFos-driven GFP expression (Figure 4.2C), demonstrating that the prelimbic area of PFCx was activated after a single injection of U50,488. In addition, administration of KOPr antagonist norBNI alone did not produce any significant effects on either cFos and GFP expression. More importantly, U50,488-induced effects were significantly blocked by 10mg/kg of norBNI pre-treatment (Figure 4.2C).

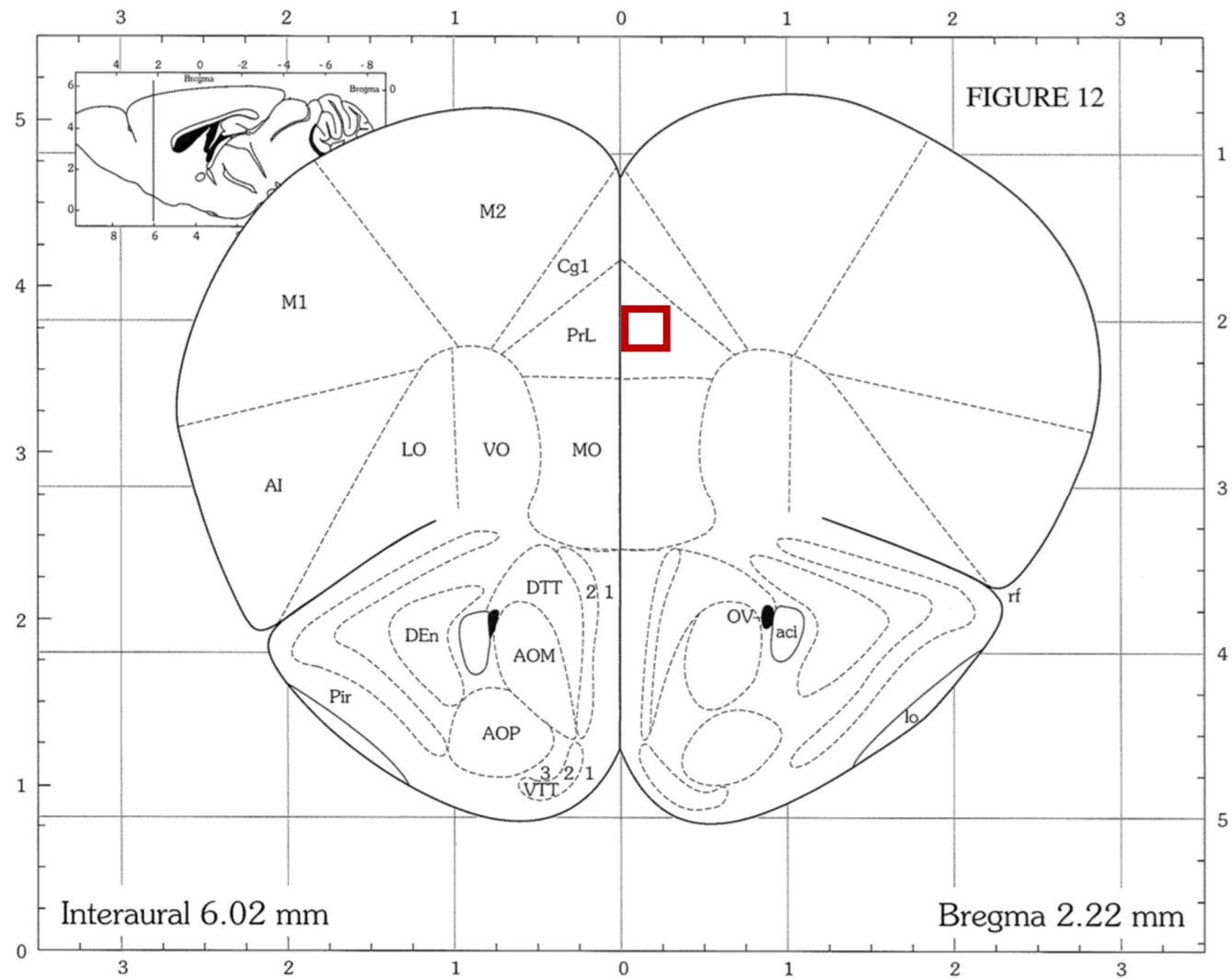


**Figure 4.2A Coronal section of mouse brain showing prefrontal cortex.** The red square indicates the location of the prelimbic area (layers 1-3), where all the fluorescent images were taken.

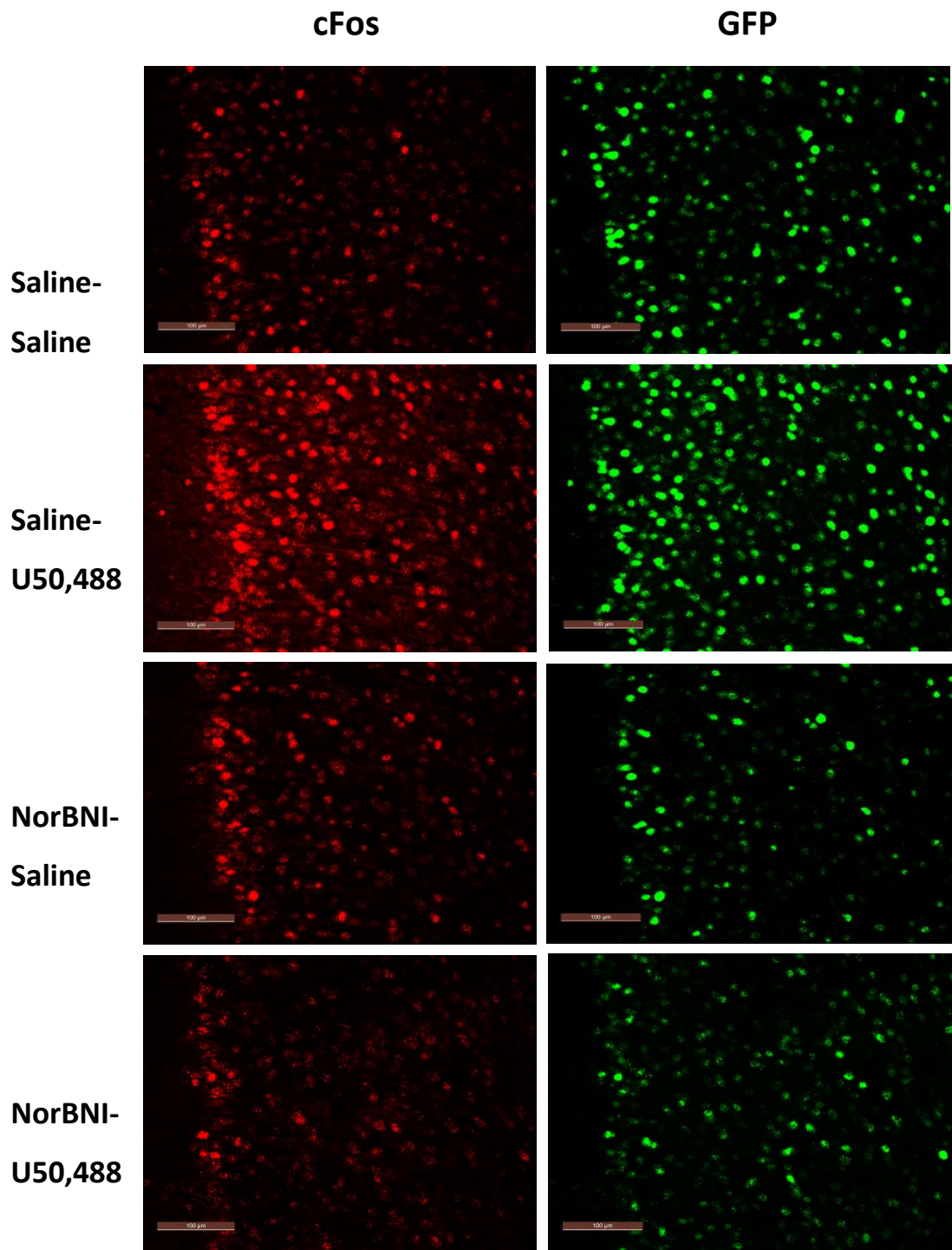


**Figure 4.2B The Effect of U50,488 (20mg/kg) on cFos and GFP expression in PFCx (Bregma +2.22 mm) in the presence of norBNI (10mg/kg) in male cFos-GFP mice.**

Example images of coronal sections of PFCx (40 $\mu$ m) in adult male C57BL/6J cFos-GFP transgenic mice, which were treated with either saline or norBNI (10mg/kg) 24 hours prior to the saline or U50,488 (20mg/kg) treatment. A single injection of U50,488 increased cFos and GFP fluorescent signals, compare to the control saline-treated groups. An effect that was blocked by pre-administration of norBNI. Scale bar = 100 $\mu$ m.

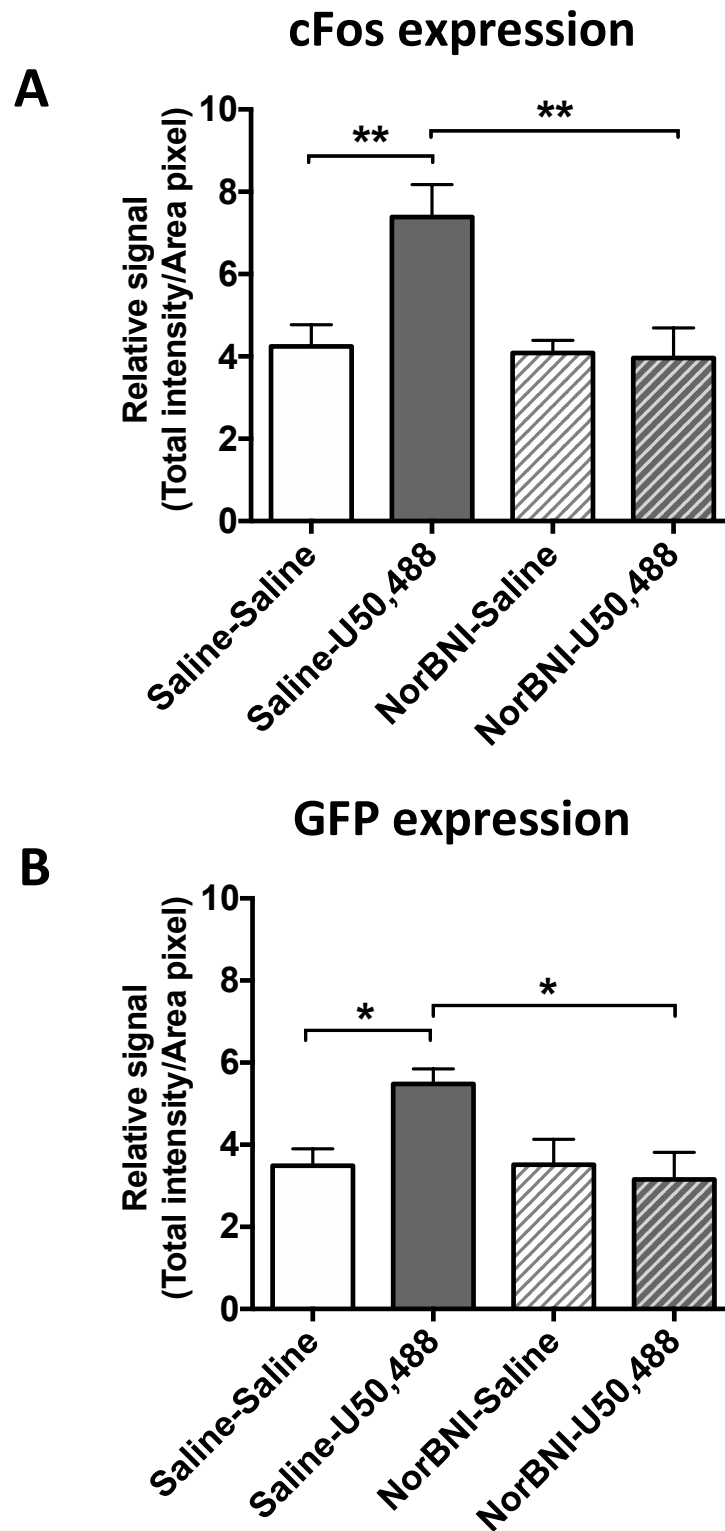


**Figure 4.2C Quantified fluorescent signals of cFos and GFP expression following U50,488 (20mg/kg) in PFCx in male mice.**

Fluorescent signals were relative signals, which were corrected to the background. U50,488 treatment significantly increased both **cFos (A)** and **GFP (B)** signals, which were significantly abolished by pre-administration of norBNI. All data are presented as mean  $\pm$  SEM, \* =  $P < 0.05$ , \*\* =  $P < 0.01$ . One-way ANOVA post-hoc Sidak's test,  $n = 6$  animals per treatment group.

### 4.3.2 The effect of FSS in male PFCx

In order to compare the effects observed following KOPr activation (Figure 4.2) with an *in vivo* stressor, mice underwent 15 minutes FSS, instead of U50,488 injection, and proceed to immunocytochemistry. Both cFos and cFos-driven GFP expression were increased in the prelimbic area (layer 1-3) of PFCx following FSS, compared to the non-stressed control groups. Samples images are shown in Figure 4.3A, with quantified data shown in Figure 4.3B. The effect of FSS was similar to the effect of U50,488 shown in Section 4.3.1, however, unlike with U50,488, pre-administration of norBNI (10mg/kg) did not significantly attenuate the FSS-induced increases in cFos or GFP expression (Figure 4.3B). Overall, these data suggest that the *in vivo* stressor, FSS, initiates neuronal activation in the PFCx in a similar manner to U50,488, although FSS-induced effects were unlikely to be mediated by activating the KOPr system, since the acute stress-induced neuronal activity were not significantly blocked by KOPr antagonist norBNI pre-treatment.



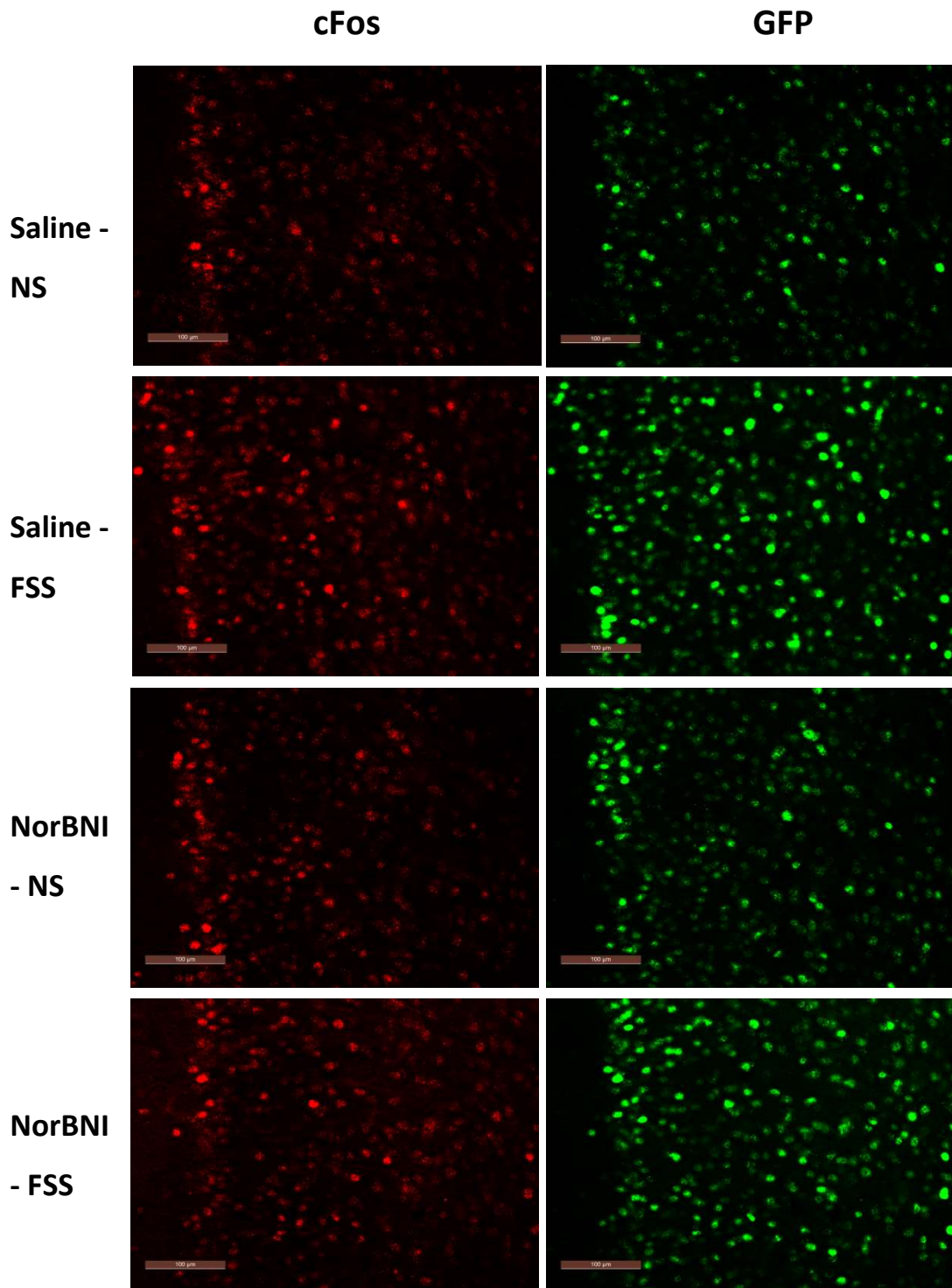


**Figure 4.3A The Effect of 15-minute FSS on cFos and GFP expression in PFCx in the presence of norBNI (10mg/kg).**

Adult male C57BL/6J cFos-GFP transgenic mice were treated with either saline or norBNI (10mg/kg) 24 hours prior to 15 minutes FSS or no stress (NS). 2 hours later, animals were killed and brains sectioned. Both cFos and GFP fluorescent signals were imaged under fluorescent microscope, FSS induced cFos and GFP expression, compare to the control non-stressed groups. Scale bar = 100μm.

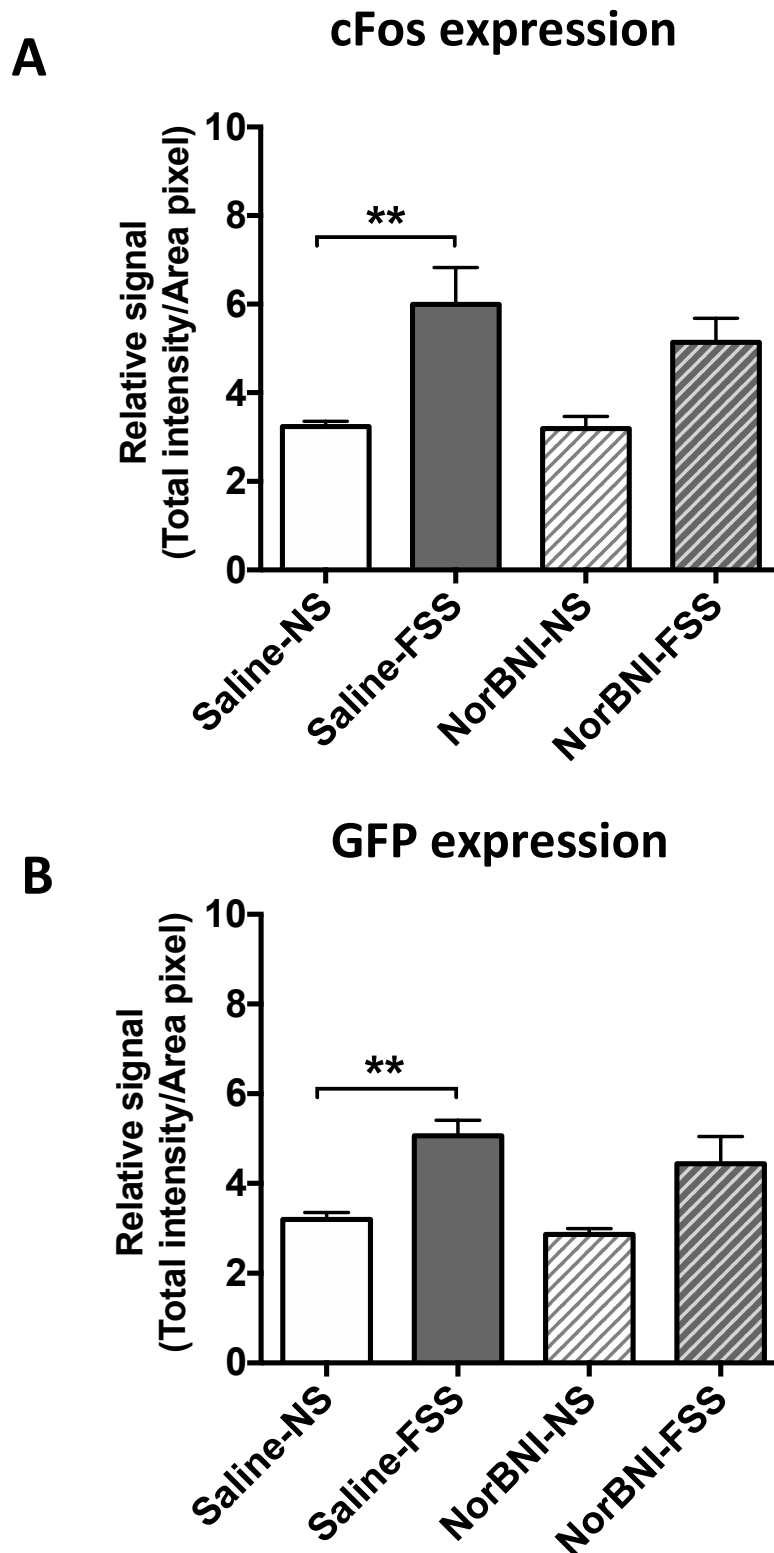


**Figure 4.3B Quantified fluorescent signals of cFos and GFP expression following FSS in PFCx.**

Fluorescent signals were relative signals, which were corrected to the background. 15-minute FSS significantly increased both **cFos (A)** and **GFP (B)** signals, which were not significantly decreased by pre-administration of norBNI. All data are presented as mean  $\pm$  SEM, \* =  $P < 0.05$ , \*\* =  $P < 0.01$ . One-way ANOVA post-hoc Sidak's test,  $n = 6$  animals per treatment group.

### **4.3.3 The effect of U50,488 in male NAc**

As we have seen significant effects of KOPr activation and *in vivo* stressor on neuronal activation in PFCx, we also investigated if these effects would produce a similar or different pattern in other brain regions i.e. nucleus accumbens core (Figure 4.4B). Comparing to the pattern we have seen in PFCx, similar patterns were observed in NAc: there was a significant effect of both cFos and GFP following a single injection of U50,488 (20mg/kg) (Figure 4.4C). These effects were also effectively abolished by pre-administration of norBNI (10mg/kg) and norBNI treatment alone did not produce any effect on both cFos and GFP expression (Figure 4.4C).

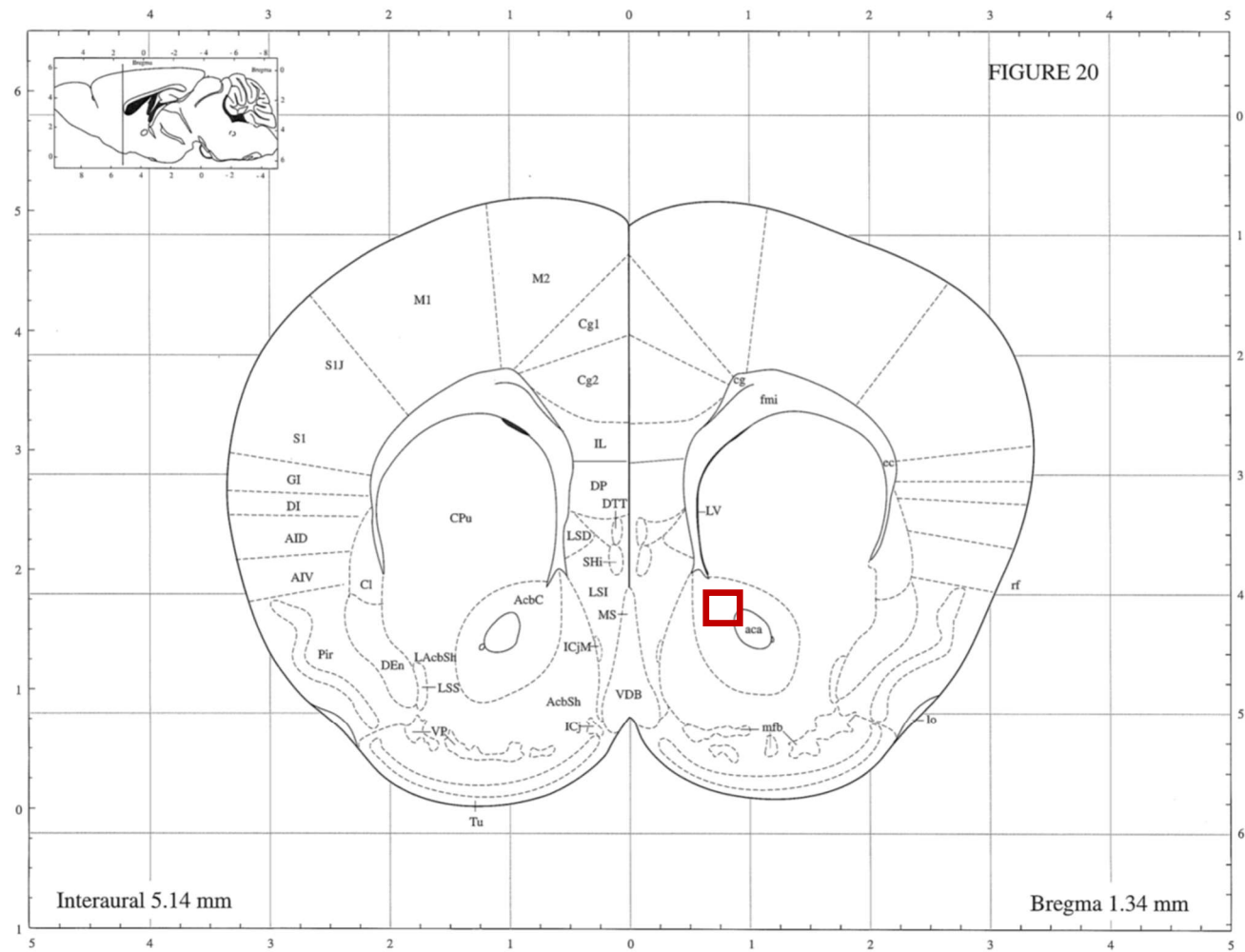


**Figure 4.4A Coronal section of mouse brain showing nucleus accumbens.** The red square indicates the location of nucleus accumbens core (NAC), where all the fluorescent images were taken.

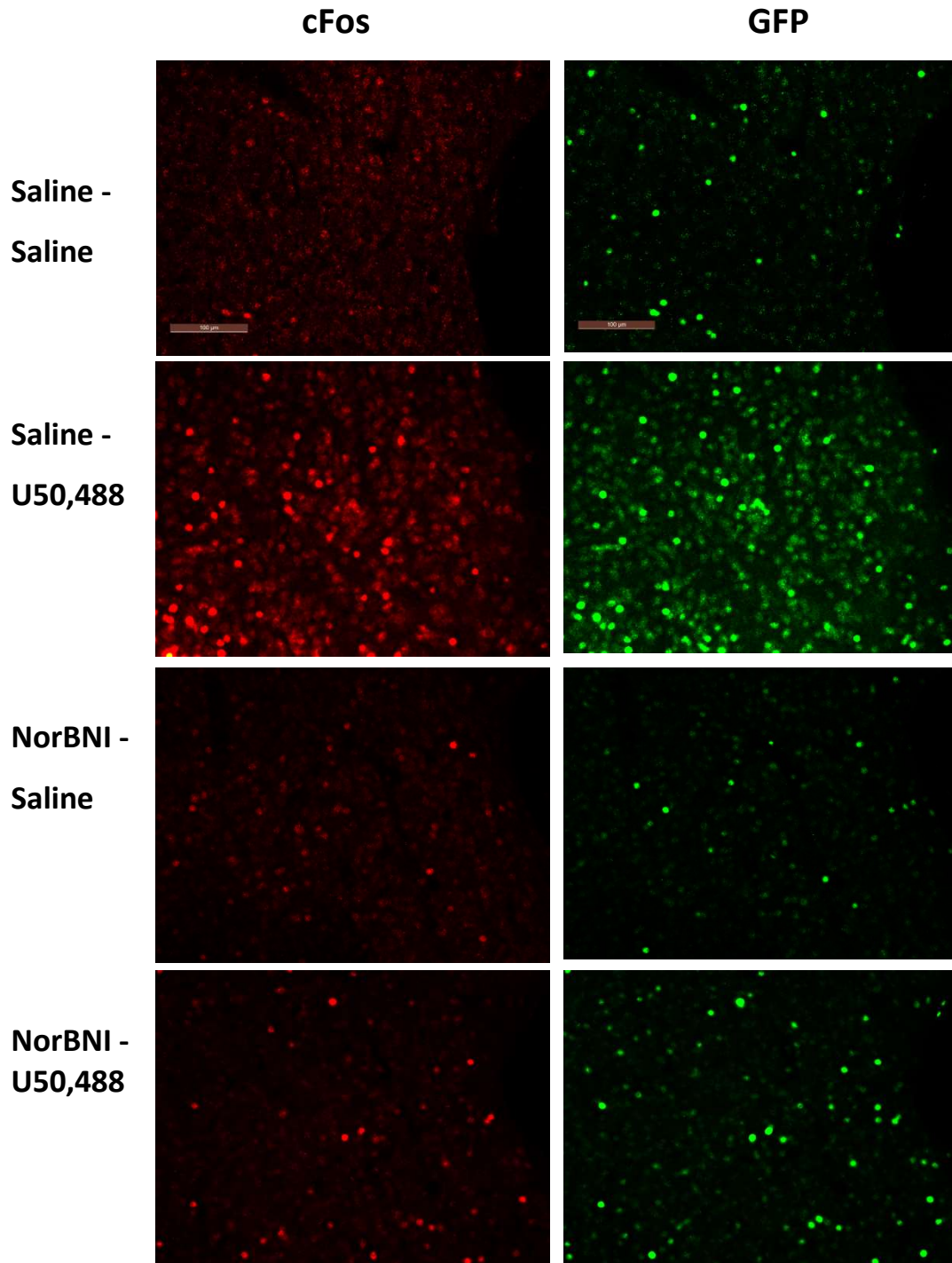


**Figure 4.4B Illustration of cFos and GFP expression in NAc core (Bregma +1.34 mm) after U50,488 (20mg/kg) treatment in the presence of norBNI (10mg/kg).** There was an increase in expression of both cFos and GFP after a single injection of U50,488 compared to the control saline-treated groups, similar to that seen in PFCx. The effect was blocked by pre-administration of norBNI. Scale bar = 100μm.

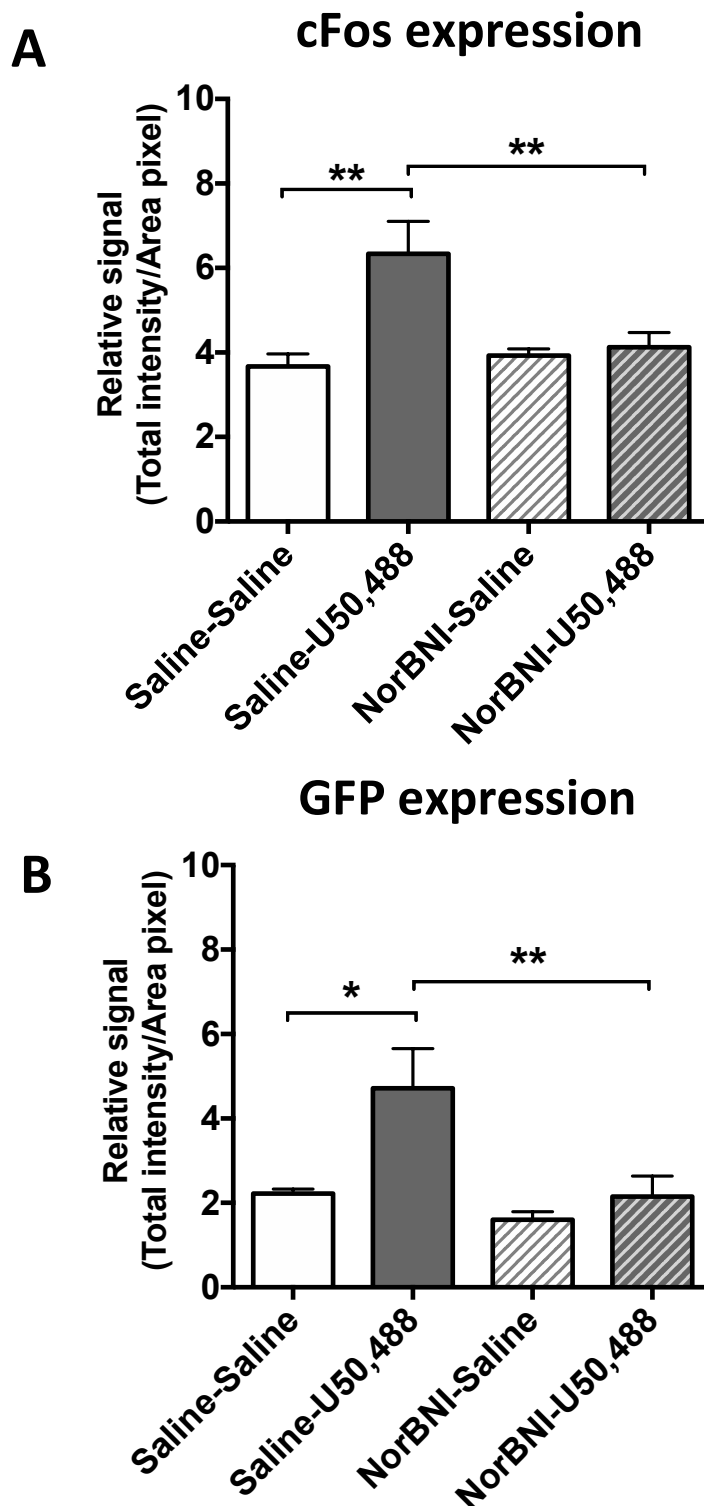


**Figure 4.4C** Quantification of fluorescent cFos and GFP signals following U50,488 (20mg/kg) in NAc core.

Fluorescent signals were relative signals, which were corrected to the background. U50,488 treatment significantly increased both **cFos (A)** and **GFP (B)** signals, which were effectively blocked by pre-administration of norBNI. All data are presented as mean  $\pm$  SEM, \* =  $P < 0.05$ , \*\* =  $P < 0.01$ . One-way ANOVA post-hoc Sidak's test,  $n = 6$  animals per treatment group.

#### **4.3.4 The effect of FSS in male NAc**

The effect of U50,488 on cFos and GFP expression in NAc was similar to that shown previously in PFCx (Section 4.3.3). The experiment was repeated after FSS, to compare cFos expression after pharmacological and physical stressors. Fluorescent images are shown in figure 4.5A. Again, there is a similar expression pattern on cFos and GFP expression following FSS stimulation in NAc as there was in PFCx i.e. both signals were effectively increased (Figure 4.5B). Interestingly, norBNI pre-administration showed significant reduction in cFos expression in NAc, an effect that was not seen in PFCx, although the blocking effect of norBNI was not observed in GFP signals. Overall, cFos and cFos-driven GFP was expressed following an *in vivo* stressor in NAc, as shown previously in PFCx. In NAc, but not PFCx, this neuronal activation might be partially caused by KOPr activation.



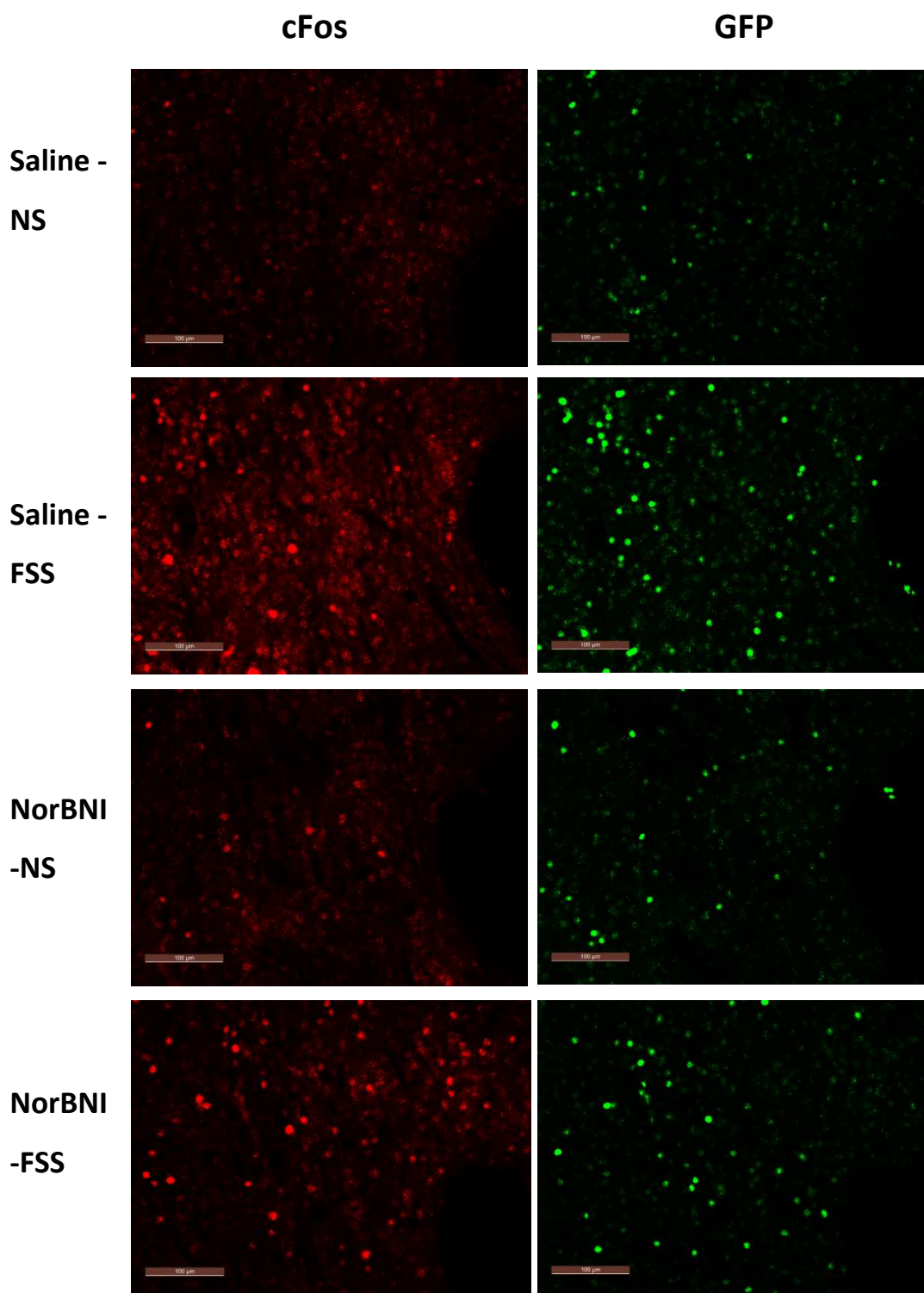


**Figure 4.5A Demonstration of cFos and GFP expression following 15-minute FSS in NAc core in the presence of norBNI (10mg/kg).**

C57BL/6J cFos-GFP transgenic mice were treated with either saline or norBNI (10mg/kg) 24 hours prior to 15 minutes FSS or no stress (NS). 2 hours later, animals were killed and brains sectioned. Both cFos and GFP fluorescent signals were imaged under fluorescent microscope, FSS induced cFos and GFP expression, compared to the control non-stressed groups. Scale bar = 100  $\mu$ m.



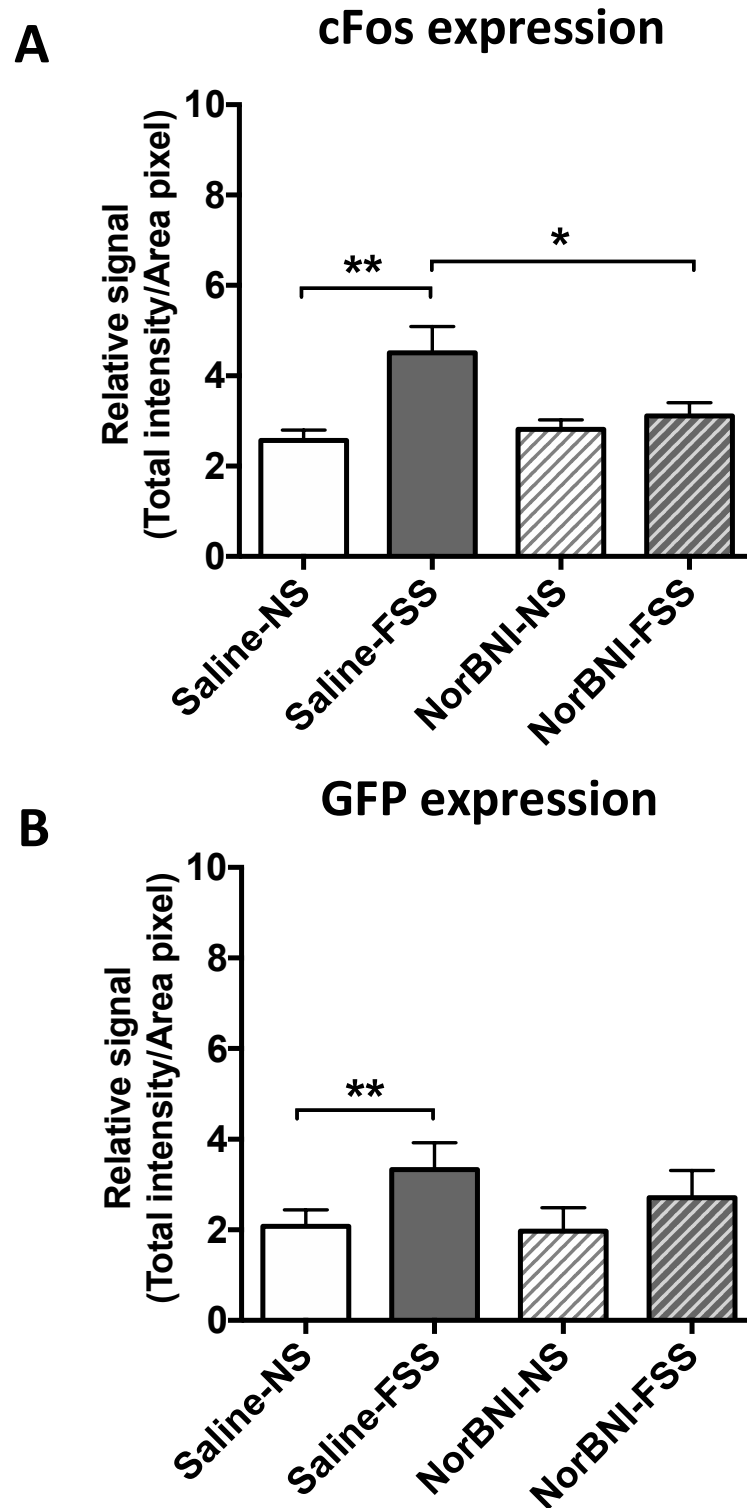


**Figure 4.5B Quantified fluorescent signals of cFos and GFP expression following FSS in NAc core.**

Relative fluorescent signals, which were corrected to the background. 15-minute FSS significantly increased both **cFos (A)** and **GFP (B)** signals. Prior treatment with norBNI significantly inhibited cFos, but not GFP expression. All data are presented as mean  $\pm$  SEM, \* =  $P < 0.05$ , \*\* =  $P < 0.01$ . One-way ANOVA post-hoc Sidak's test,  $n = 6$  animals per treatment group.

### 4.3.5 Overlapping expression of cFos and GFP in PFCx and NAc

As we have used cFos-GFP transgenic mice, where expression of GFP directly follows the cFos production in activated neurons (Chapter 1), this facilitates identification and mapping of the brain regions and individual neurons induced by different stimuli (FSS and kappa opioid receptor agonists). Also, as the half-life of cFos is much shorter than that of GFP, it also gives the possibility of looking at temporal changes in cFos expression. For example, if single neurons express GFP, but not cFos, this may mean that cFos expression occurred at an early stage, but that the cFos protein has already degraded at the time-point used here, with GFP expression persisting. For this reason, fluorescent images labelled with cFos and GFP (as shown earlier) were merged together, shown in figure 4.6A, 4.6B.

Figure 4.6A shows the cFos-expressing neurons (red), GFP-expressing neurons (green) and cFos/GFP overlapped images following a single U50,488 injection in PFCx and NAc. Yellow signals in the overlapping images show co-expression of both cFos and GFP in the same cell. The number of cells that were positive for cFos only, GFP only and both cFos and GFP (merged) were counted and presented as a percentage of total number of neurons (Figure 4.6C). In the PFCx, approximately 50% of neurons were positive for both cFos and GFP in control animals, with approximately 40% of neurons expressing GFP alone. Following U50,488 treatment, there was no significant change in the pattern of neurons that were positive for cFos alone, GFP alone or both cFos and GFP (Figure 4.6C).

In the NAc, in slices from control animals, there was a similar pattern of cells positive for cFos alone (~10%), GFP alone (~40%) and cFos+GFP (~50%). However, after U50,488 treatment, there was a significant increase in the proportion of cells that were positive for cFos alone (Figure 4.6C). The proportion of cells that were positive for GFP alone or cFos+GFP both decreased, but not significantly.

A different pattern was seen in sections taken from animals that had undergone 15-minute forced swim stressor (FSS) treatment; cFos alone (red), GFP alone (green) and both cFos + GFP (yellow) signals in PFCx and NAc (Figure 4.6B). In PFCx, after FSS, there was a significant increase in the proportion of cells positive for both cFos + GFP, and a significant decrease in cells positive for GFP alone (Figure 4.6C).

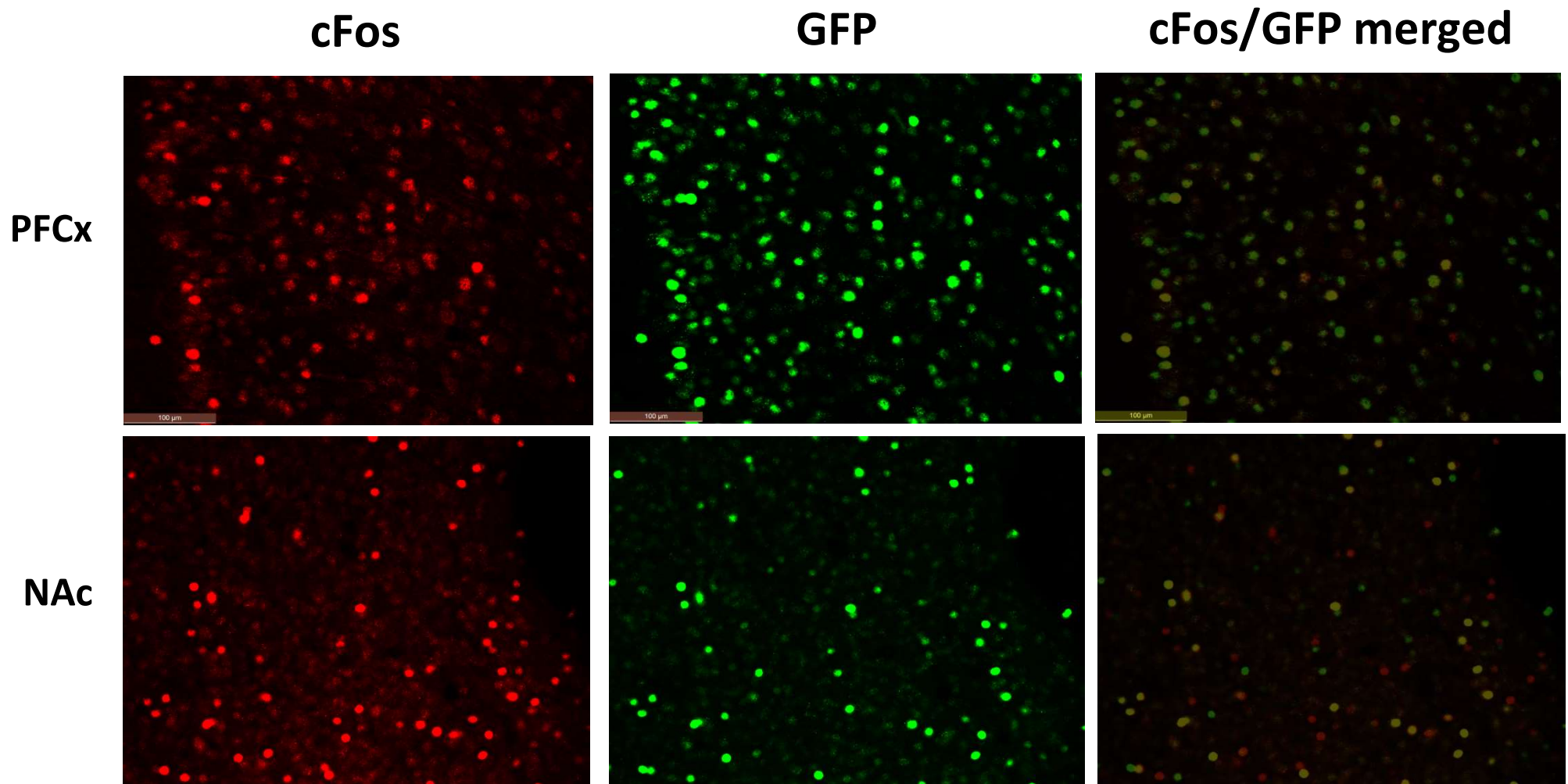


**Figure 4.6A** Overlapping images of cFos-expressing neurons (red), GFP-expressing neurons (green) and cFos/GFP co-localised in the same neurons in PFCx and NAc core. Co-expression of cFos and GFP shown in yellow indicates recent neuronal activity induced by a single injection of U50,488 (20mg/kg), scale bar = 100µm.

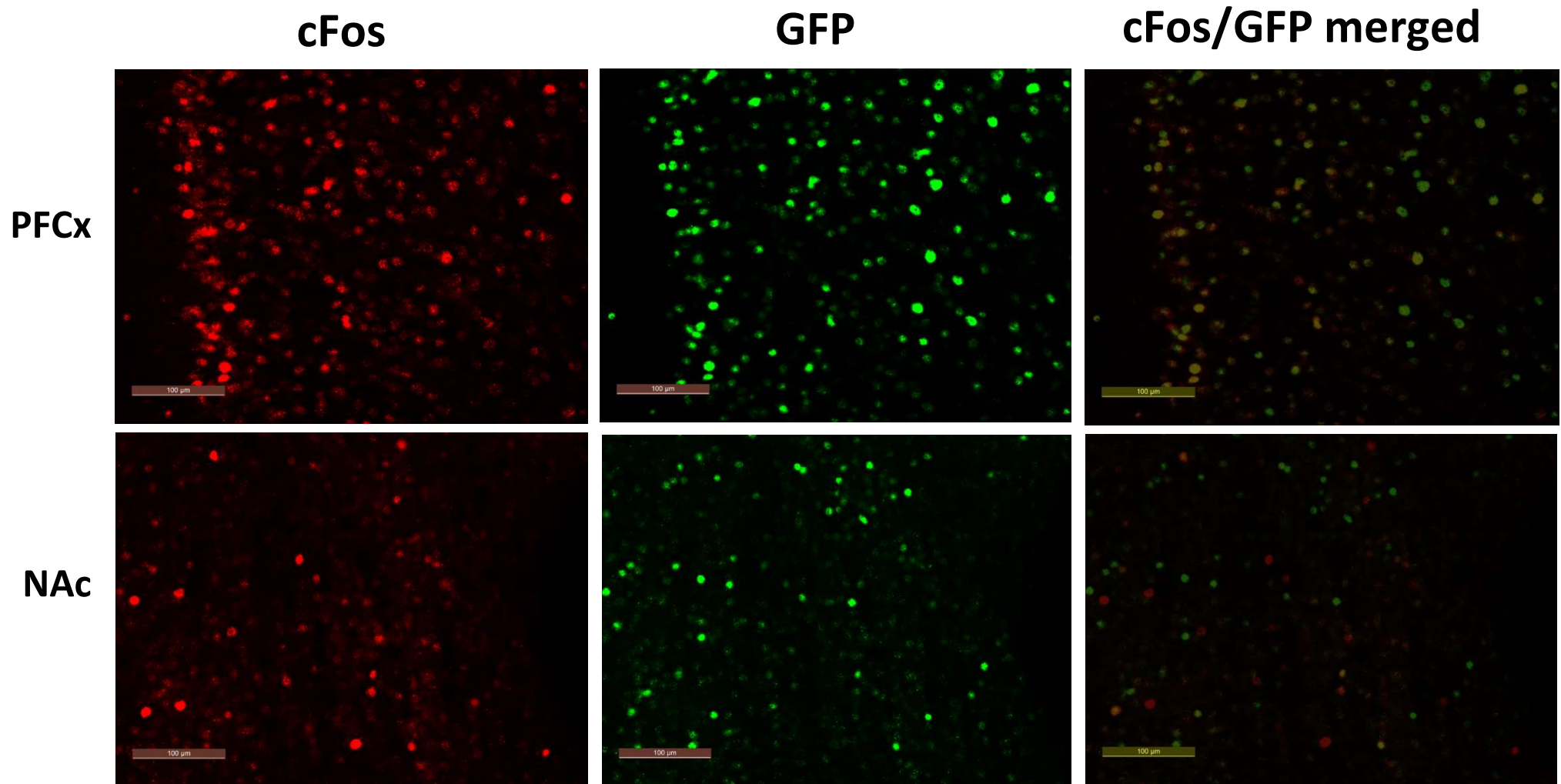


**Figure 4.6B** Overlapping images of cFos-expressing neurons (red), GFP-expressing neurons (green) and cFos/GFP co-localised in the same neurons in PFCx and NAc core.

cFos and GFP co-expression is shown in yellow indicates recent neuronal activity induced by **15-minute FSS**, scale bar = 100μm.

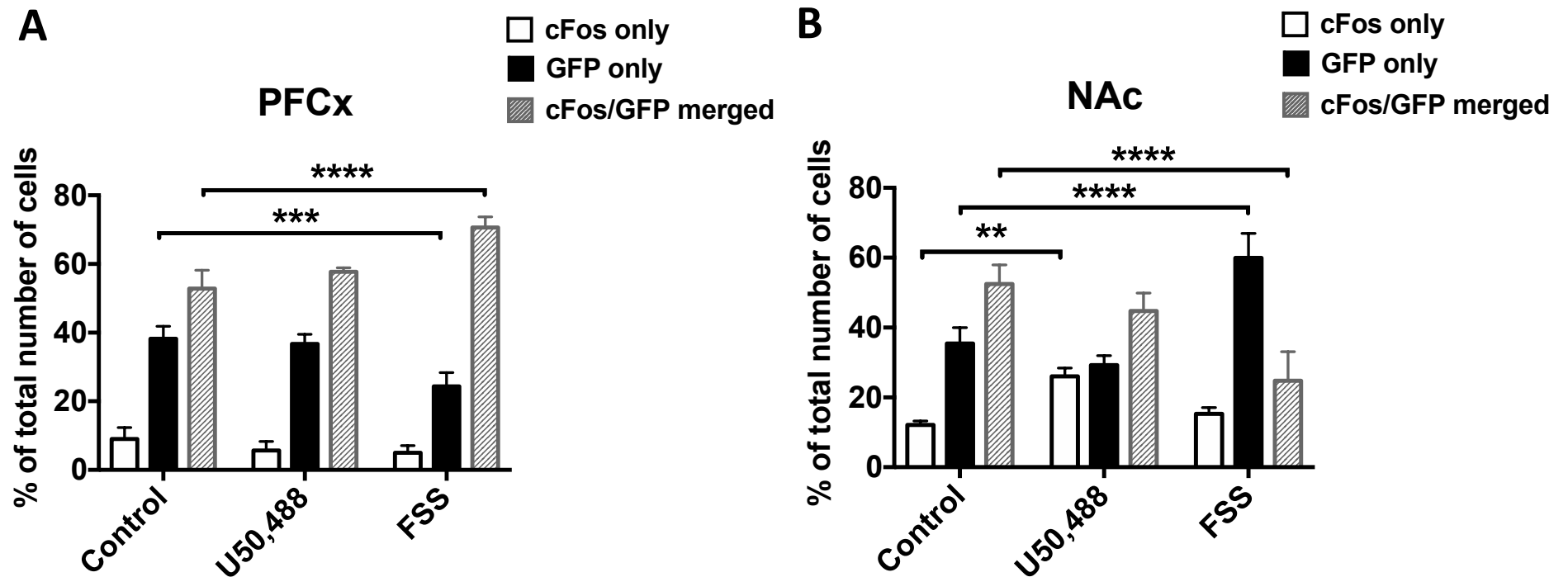


**Figure 4.6C Percentage of overlapping neurons in total neurons in PFCx (A) and NAc core (B).**

The cFos-positive, GFP-positive and cFos + GFP-positive neurons were counted separately and calculated as the percentage of total number of neurons for each treatment. The cFos + GFP-positive neurons indicated in grey bar represents cFos and GFP are co-expressed in the same cells. All data are presented as mean  $\pm$  SEM, one-way ANOVA post-hoc Sidak's test, \*\* =  $P < 0.01$ , \*\*\* =  $P < 0.001$ , \*\*\*\* =  $P < 0.0001$ .

#### **4.3.6 The effect of U50,488 in male hippocampus**

As discussed in Chapter 1, the hippocampus is also an important region that is involved in stress responses and affective-related disorders. The experiment above was repeated, and fluorescent images taken in CA1 region and dentate gyrus of dorsal hippocampus, indicated in figure 4.7A. The typical expression patterns are shown in figure 4.7B and 4.7D. Similar to the effects seen in PFCx and NAc (Section 4.3.1 – 4.3.4), in the CA1 region of hippocampus there was a significant increase in cFos and cFos-driven GFP expression following U50,488. Pre-administration of norBNI also inhibited these effects (Figure 4.7C). In contrast, in the dentate gyrus region of the hippocampus no changes in either cFos or GFP expression following U50,488 treatment were seen (Figure 4.7E).

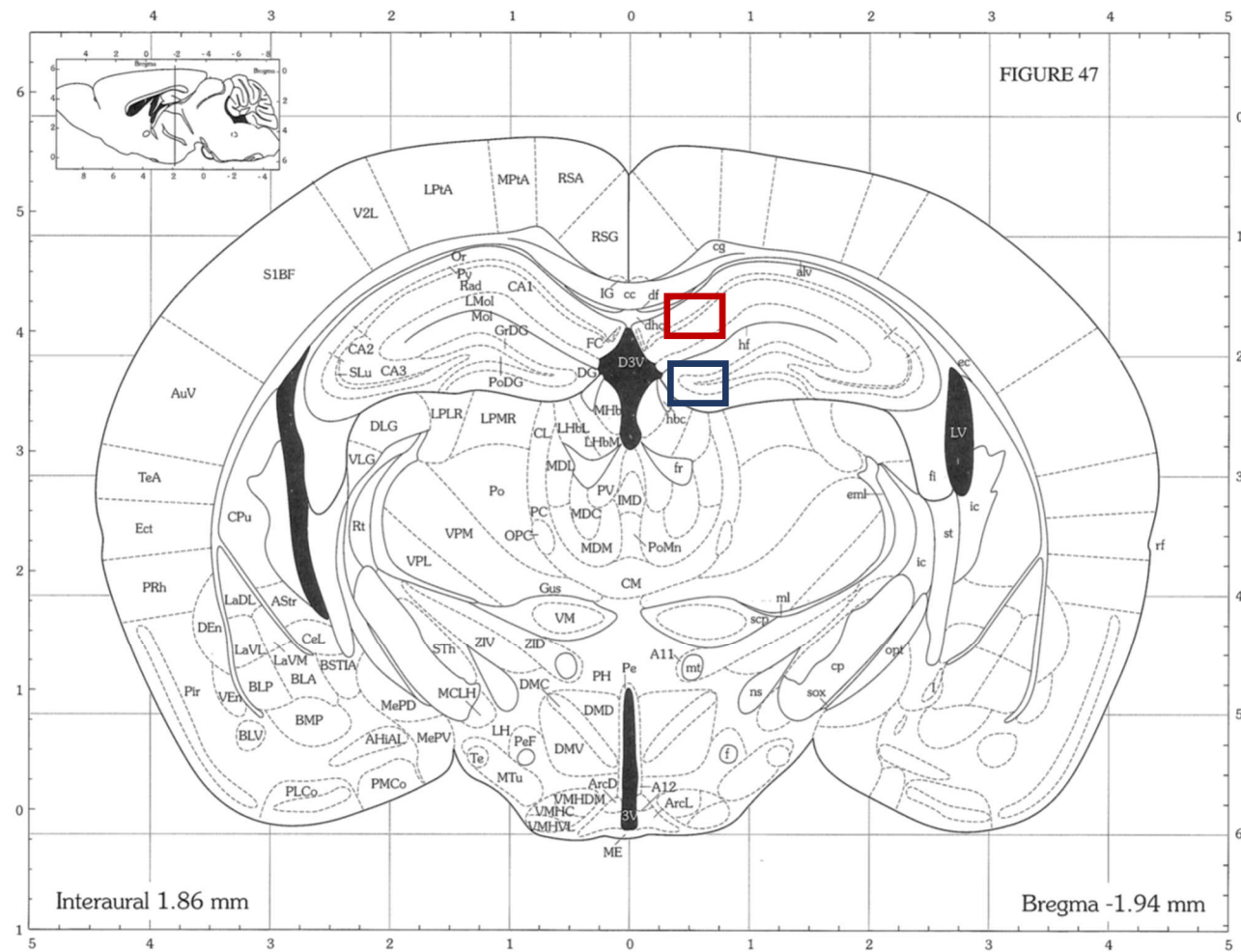


**Figure 4.7A Coronal section of mouse brain showing dorsal hippocampus.** The red rectangle indicates the location of CA1 region of dorsal hippocampus, the blue rectangle shows dentate gyrus of dorsal hippocampus, where all the fluorescent images were taken.



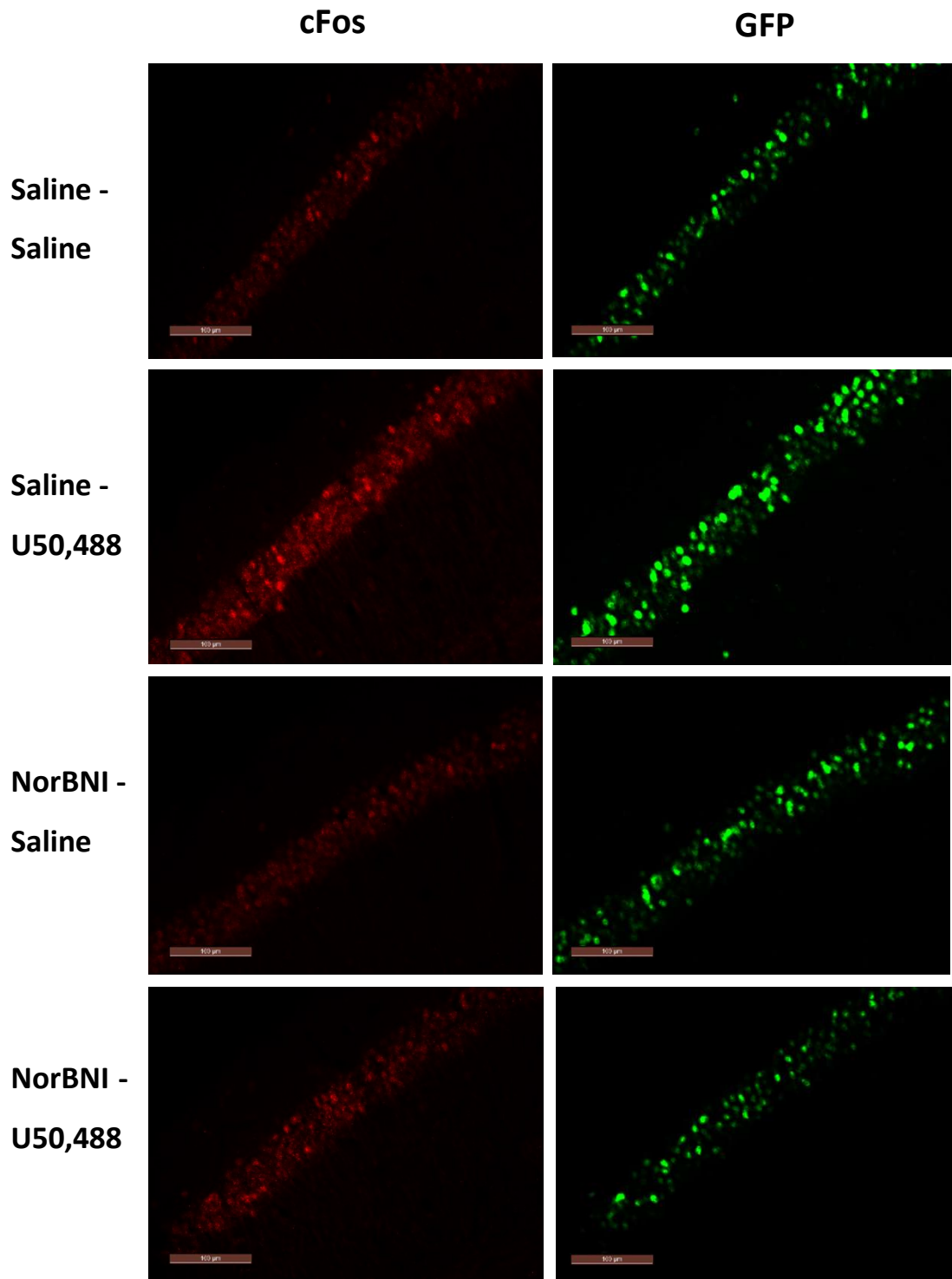


**Figure 4.7B** Fluorescent images of cFos and GFP expression in CA1 region of dorsal hippocampus (Bregma -1.94 mm) after U50,488 (20mg/kg) treatment in the absence or presence of norBNI (10mg/kg).

There was an increase in expression of both cFos and GFP after U50,488 treatment, compared to the control saline-treated groups. The effect was inhibited by pre-administration of norBNI. Scale bar = 100 $\mu$ m.

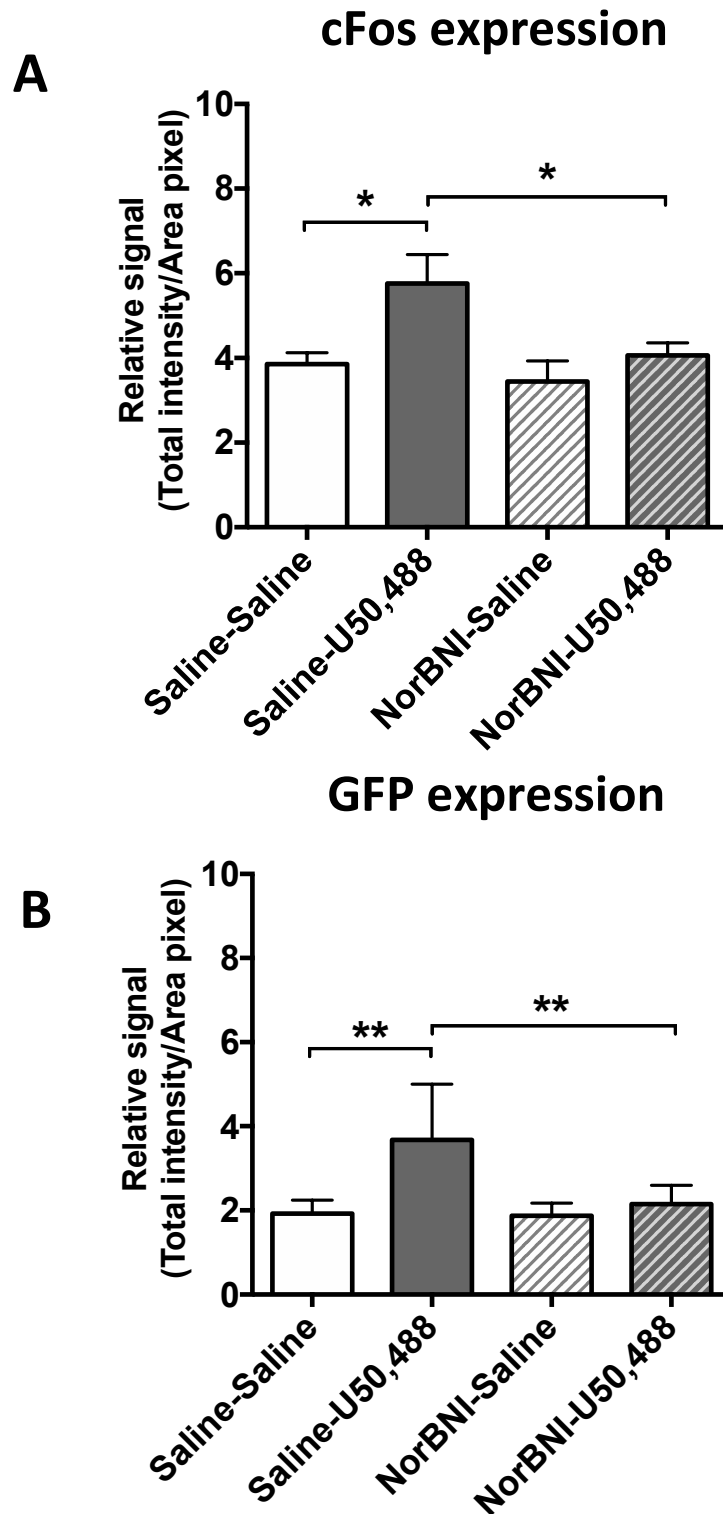


**Figure 4.7C Quantification of fluorescent cFos and GFP signals following U50,488 (20mg/kg) in hippocampal CA1 region.**

Fluorescent signals were relative signals, which were corrected to the background. U50,488 treatment significantly increased both **cFos (A)** and **GFP (B)** signals, which were effectively blocked by pre-administration of norBNI. All data are presented as mean  $\pm$  SEM, \* =  $P < 0.05$ , \*\* =  $P < 0.01$ . One-way ANOVA post-hoc Sidak's test,  $n = 6$  animals per treatment group.

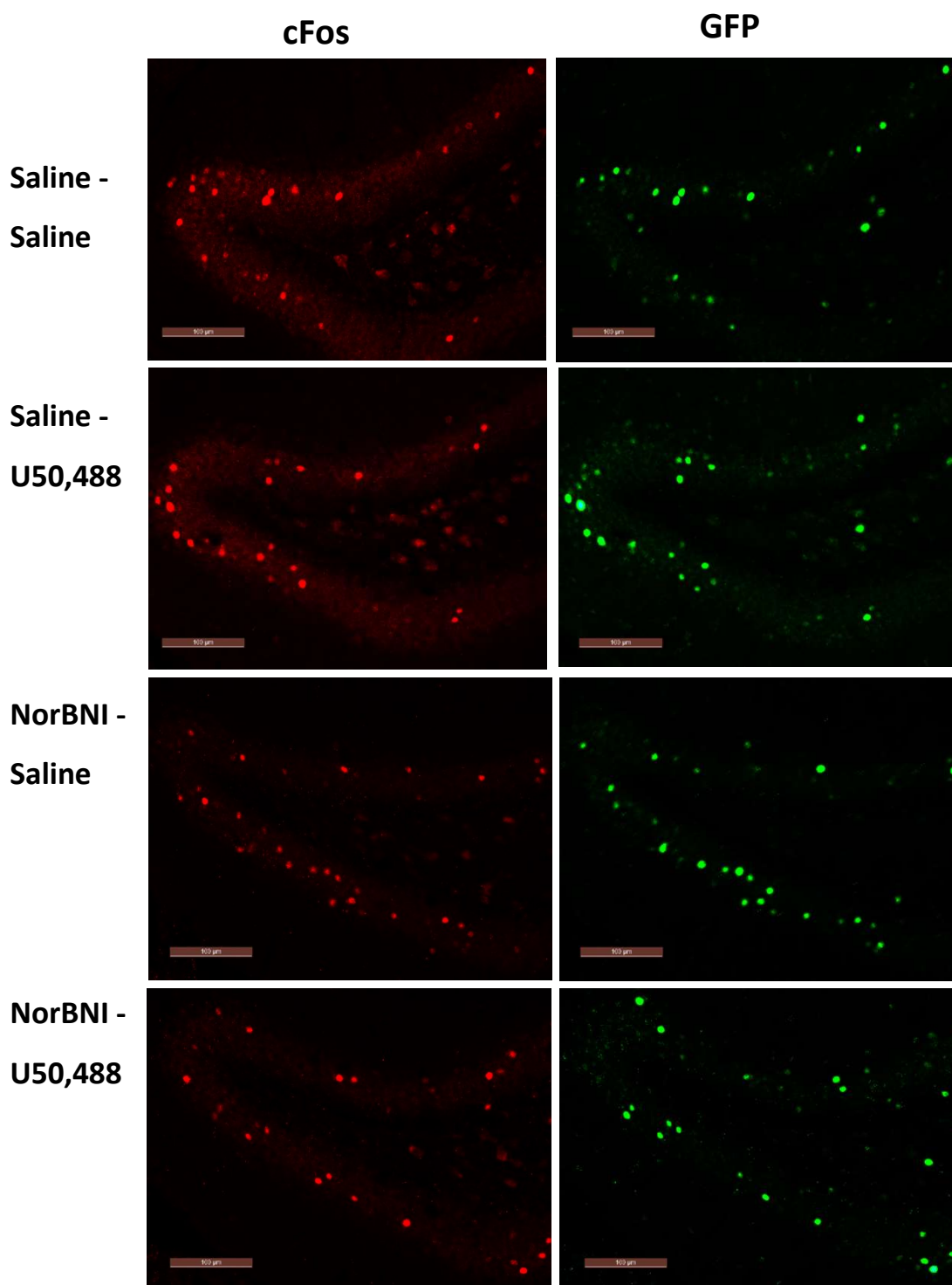


**Figure 4.7D** Fluorescent images of cFos and GFP expression in dentate gyrus of dorsal hippocampus (Bregma -1.94 mm) after U50,488 (20mg/kg) treatment in the presence or absence of norBNI (10mg/kg).

A single injection of U50,488 did not change expression of both cFos and GFP, compared to the control saline-treated groups, the presence of norBNI did not alter these effects. Scale bar = 100μm.

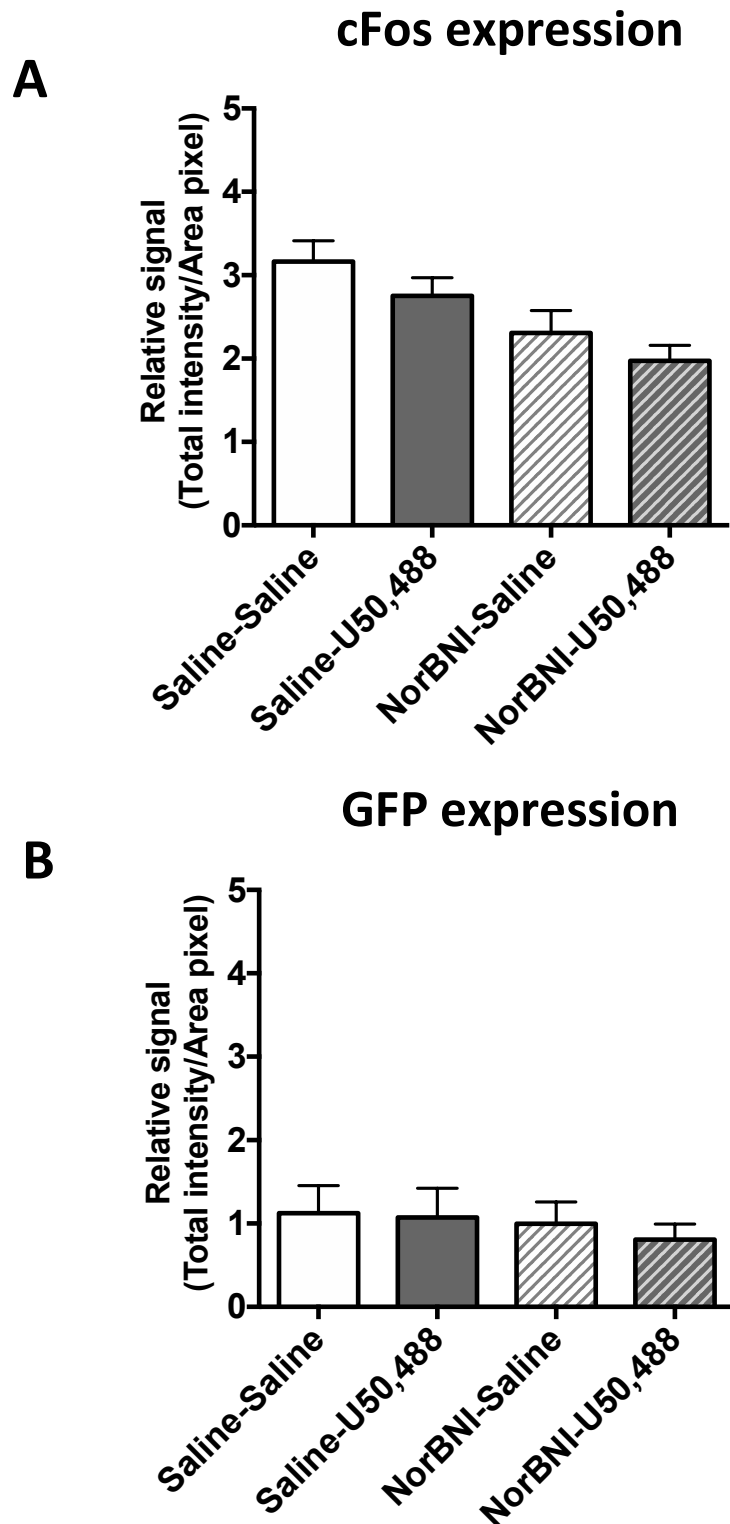


**Figure 4.7E Quantification of fluorescent cFos and GFP signals following U50,488 (20mg/kg) in hippocampal dentate gyrus.**

U50,488 treatment did not change both **cFos (A)** and **GFP (B)** signals. NorBNI also had no effect. All data are presented as mean  $\pm$  SEM. One-way ANOVA post-hoc Sidak's test, n = 6 animals per treatment group.

### 4.3.7 The effect of FSS in male hippocampus

As shown in Section 4.3.6, the effect of U50,488 treatment on hippocampal CA1 region was similar to that of in PFCx and NAc, but the hippocampal dentate gyrus did not respond to the U50,488 treatment. The experiment was then repeated in response to *in vivo* FSS. Sample images from the hippocampus are shown in figure 4.8A and 4.8C.

Surprisingly, *in vivo* FSS did not produce any effects on either cFos or GFP expression in hippocampal CA1 region and dentate gyrus (Figure 4.8B, 4.8D). Also, the presence of norBNI did not affect the cFos and GFP signals following FSS in the hippocampus. These effects were completely different from the effects observed in PFCx and NAc, which might suggest that the hippocampus is not the primary region involved in acute stressors.

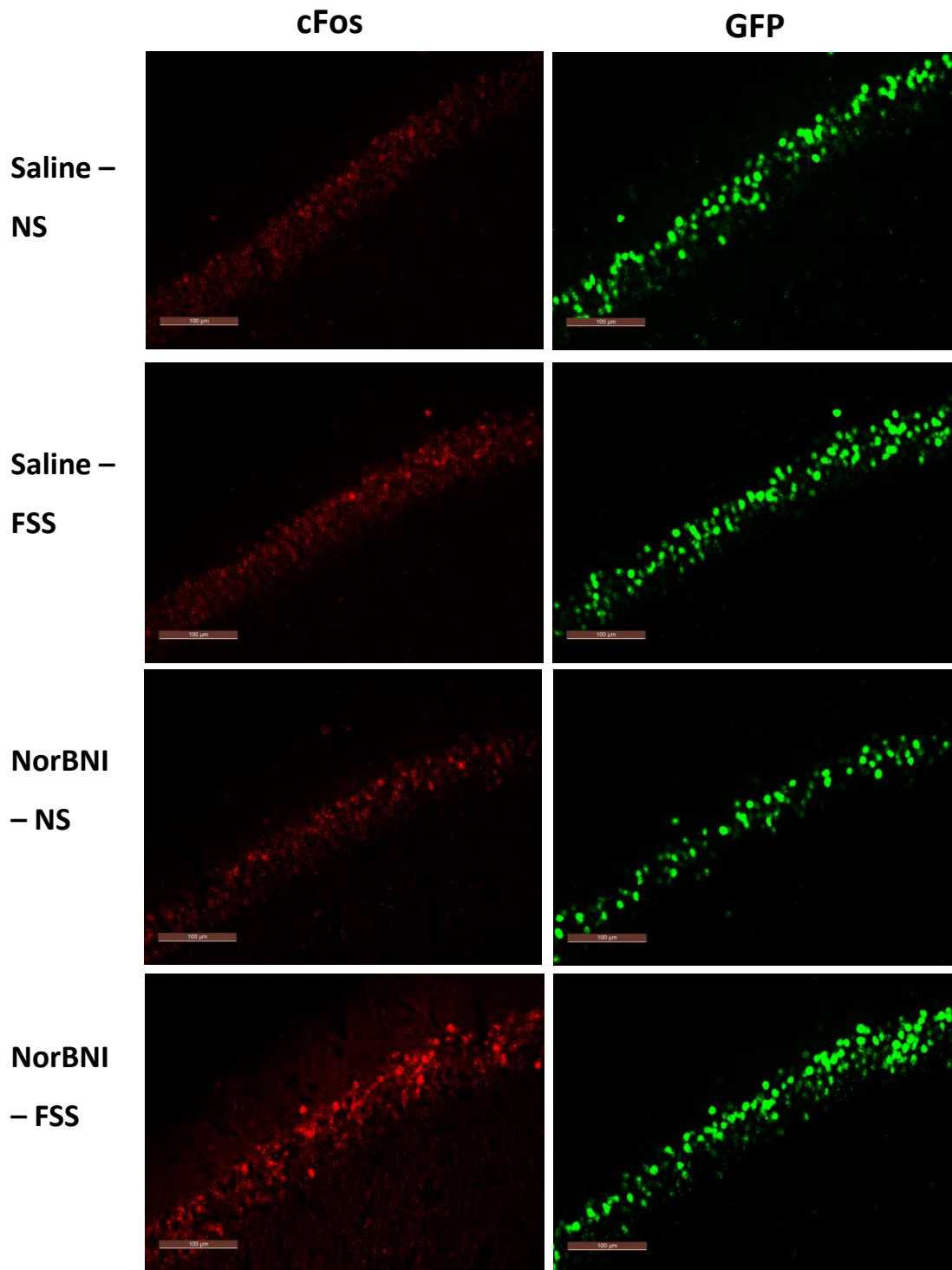


**Figure 4.8A** Fluorescent images of cFos and GFP expression in CA1 region of dorsal hippocampus (Bregma -1.94 mm) after 15-minute FSS.

No significant changes in either cFos or GFP signals after FSS, compared to the control non-stressed groups. Pretreatment with norBNI had no effect. Scale bar = 100 $\mu$ m.

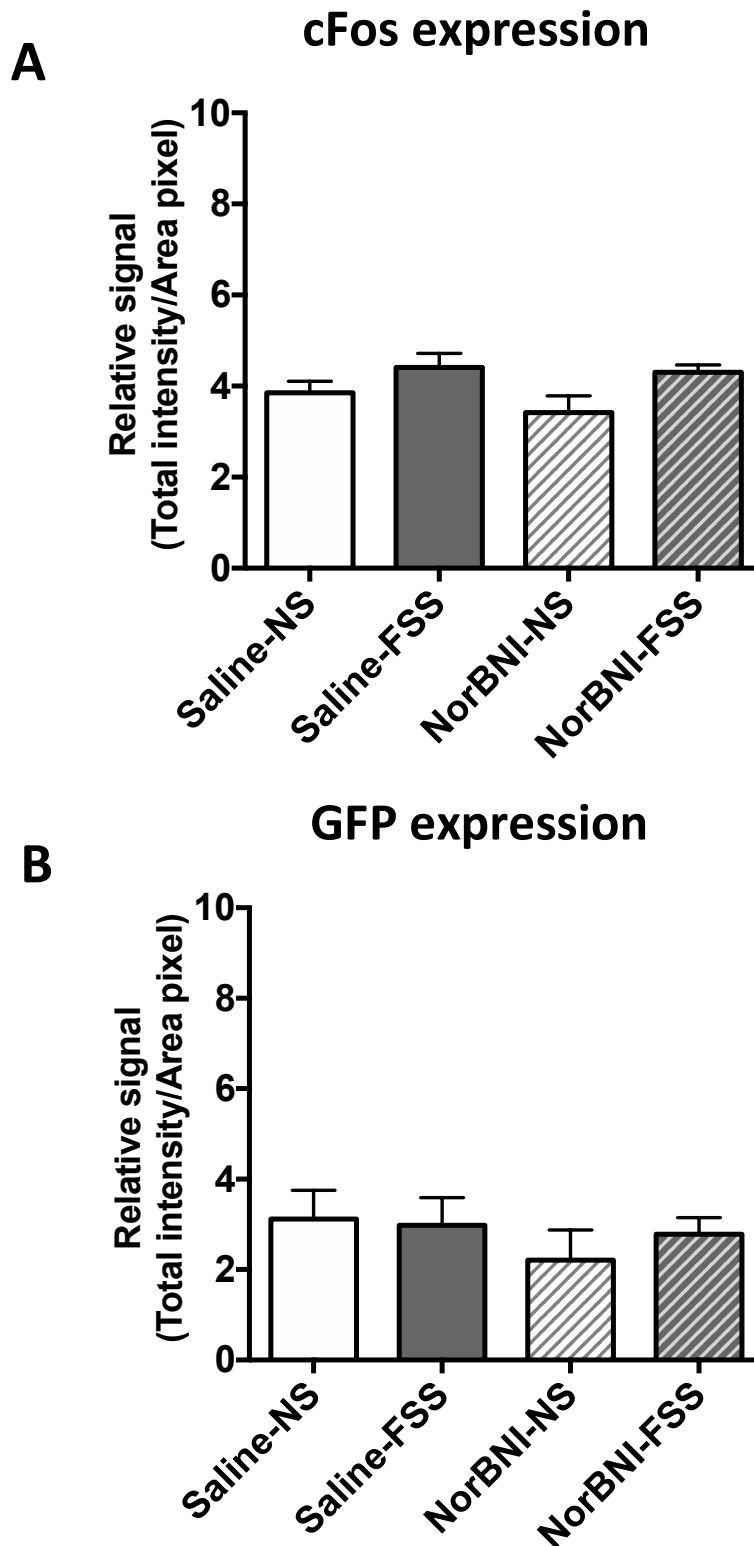


**Figure 4.8B Quantified fluorescent cFos and GFP signals following 15-minute FSS in hippocampal CA1 region.**

FSS did not significantly alter **cFos (A)** and **GFP (B)** signals in the absence or presence of norBNI (10mg/kg). All data are presented as mean  $\pm$  SEM. One-way ANOVA post-hoc Sidak's test,  $n = 6$  animals per treatment group.

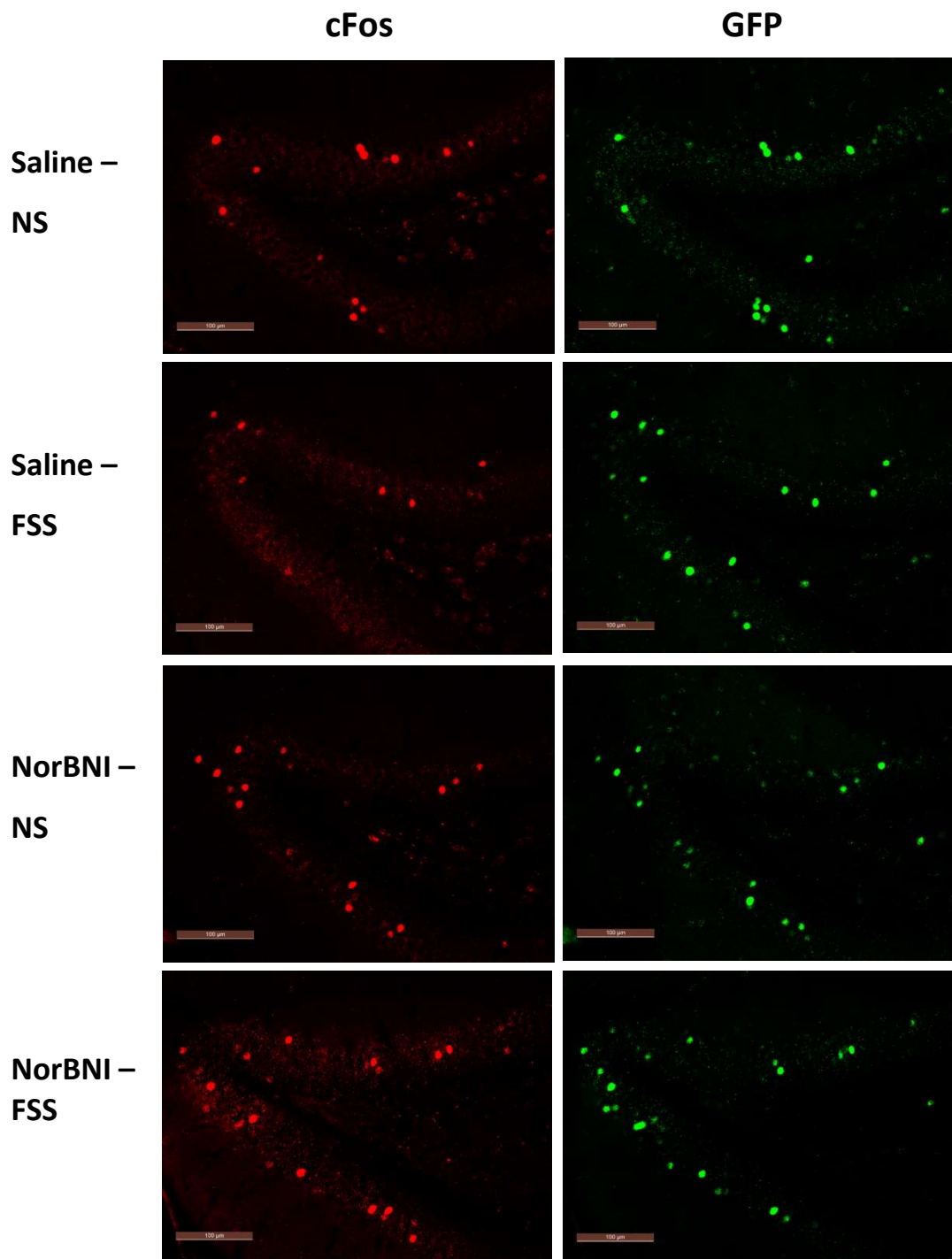


**Figure 4.8C** Fluorescent images of cFos and GFP expression in dentate gyrus of dorsal hippocampus (Bregma -1.94 mm) after 15-minute FSS. No significant changes in either cFos or GFP signals were seen after FSS, compared to the control non-stressed groups. NorBNI was without effect. Scale bar = 100µm.



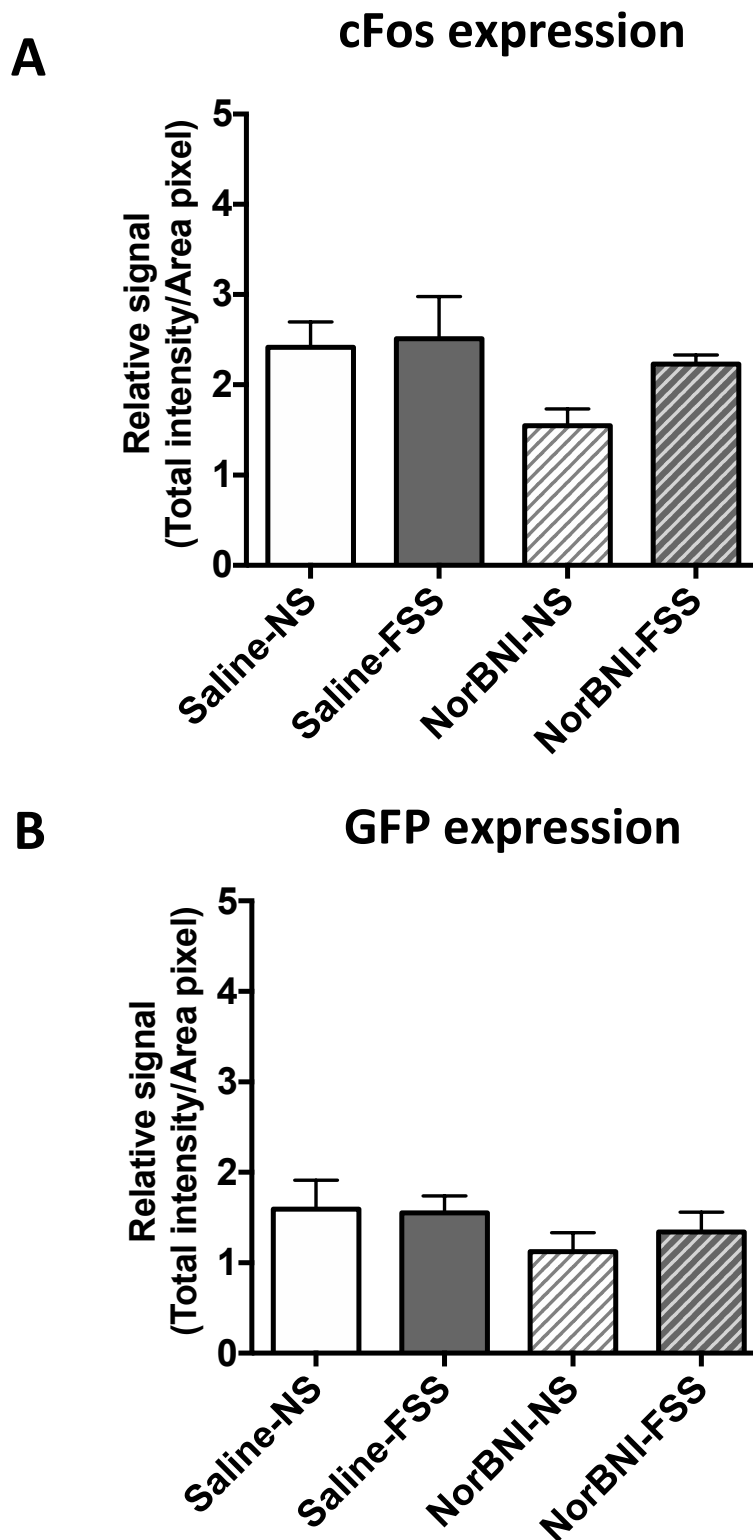


**Figure 4.8D Quantified fluorescent cFos and GFP signals following 15-minute FSS in dentate gyrus of hippocampus.**

FSS did not significantly alter either **cFos (A)** or **GFP (B)** signals in the absence or presence of norBNI (10mg/kg). All data are presented as mean  $\pm$  SEM. One-way ANOVA post-hoc Sidak's test,  $n = 6$  animals per treatment group.

#### **4.3.8 The effect of U50,488 in male amygdala**

It is known that the amygdala is an important region involved in anxiety and depression-related behaviours, as well as addiction-related behaviours, and high levels of KOPr mRNA have been detected in the amygdala (Chapter 1). We therefore investigated neuronal activity levels in both the central nucleus of the amygdala (CeA) and the basolateral nucleus of the amygdala (BLA) amygdala following a single injection of U50,488, indicated in figure 4.9A. Sample images in CeA are shown in figure 4.9B and BLA images are shown in figure 4.9D.

Similar to the effects that were shown in other brains regions i.e. PFCx, NAc and hippocampal CA1 region, U50,488 treatment significantly induced expression of cFos and cFos-driven GFP in CeA, as well as in BLA. Similarly, the U50,488-induced cFos and GFP expression in CeA and BLA were effectively blocked by pre-administration of KOPr antagonist norBNI (Figure 4.9C, 4.9E).

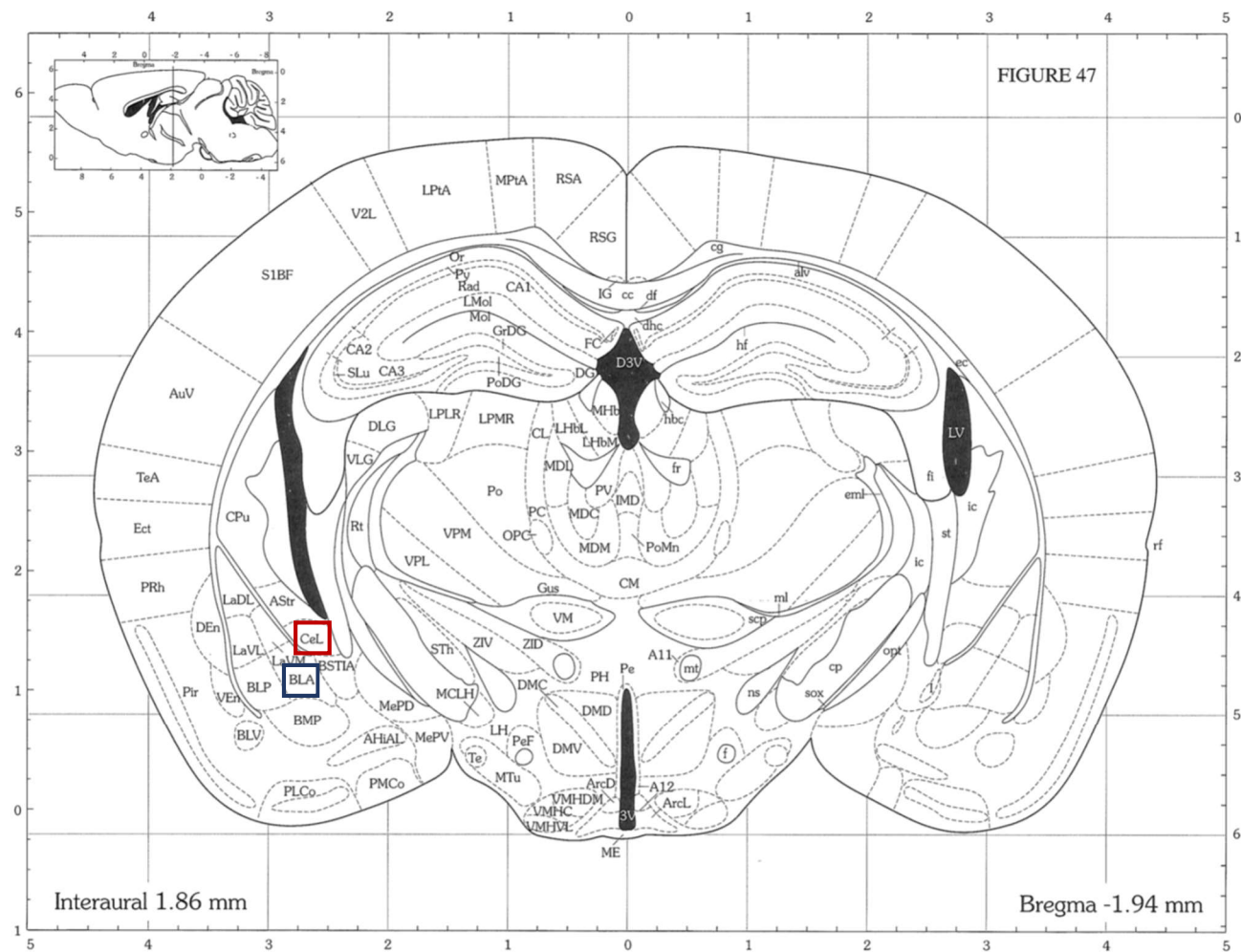


**Figure 4.9A Coronal section of mouse brain containing amygdala.** The red square indicates the location of central amygdala (CeA), the blue square shows basolateral amygdala (BLA), where all the fluorescent images were taken.

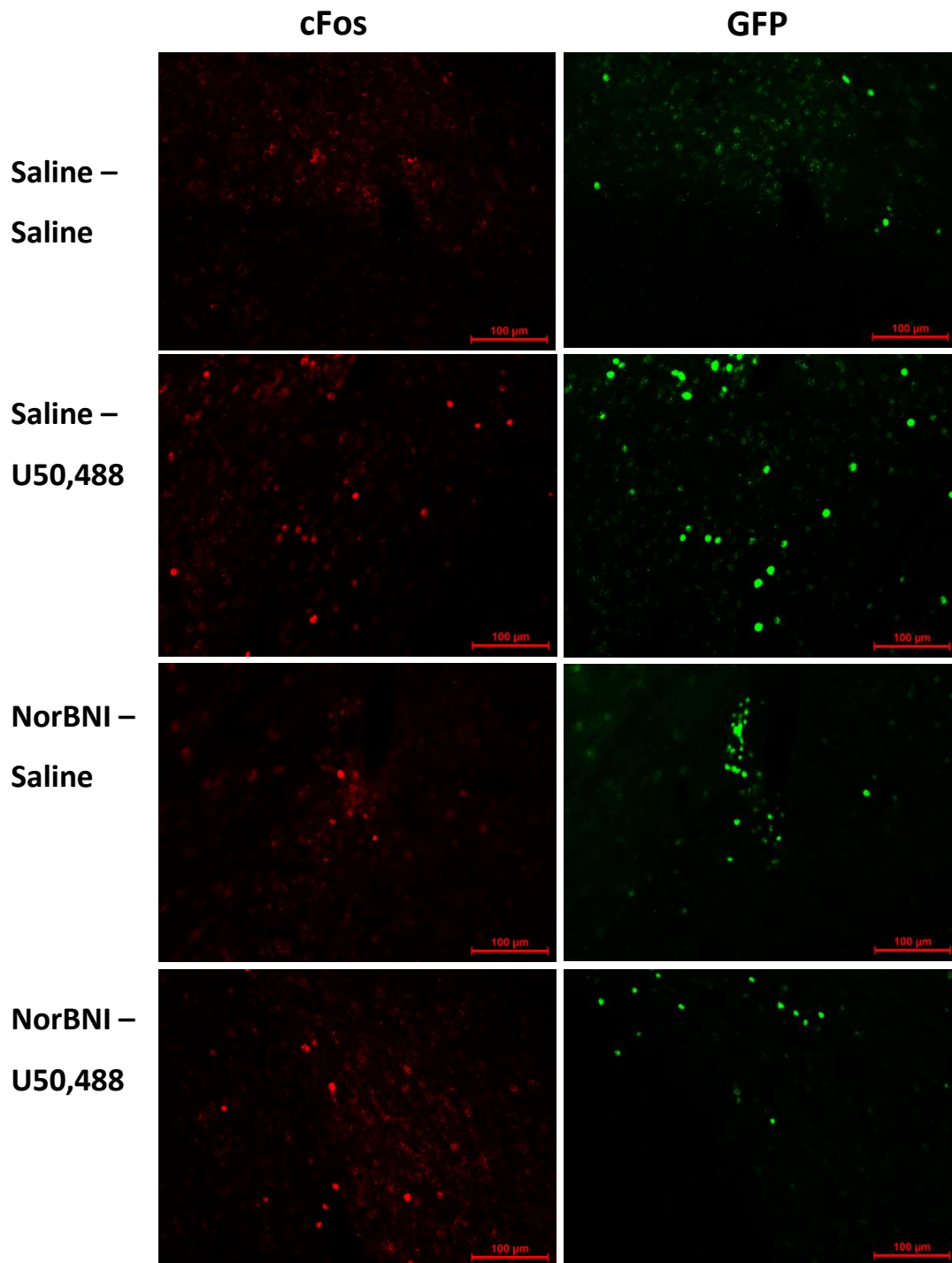


**Figure 4.9B** Fluorescent images of cFos and GFP expression in CeA (Bregma -1.94 mm) after a single U50,488 (20mg/kg) administration. A single injection of U50,488 induced both cFos and GFP, compared to the control saline-treated groups, an effect that was inhibited by norBNI. Scale bar = 100μm.

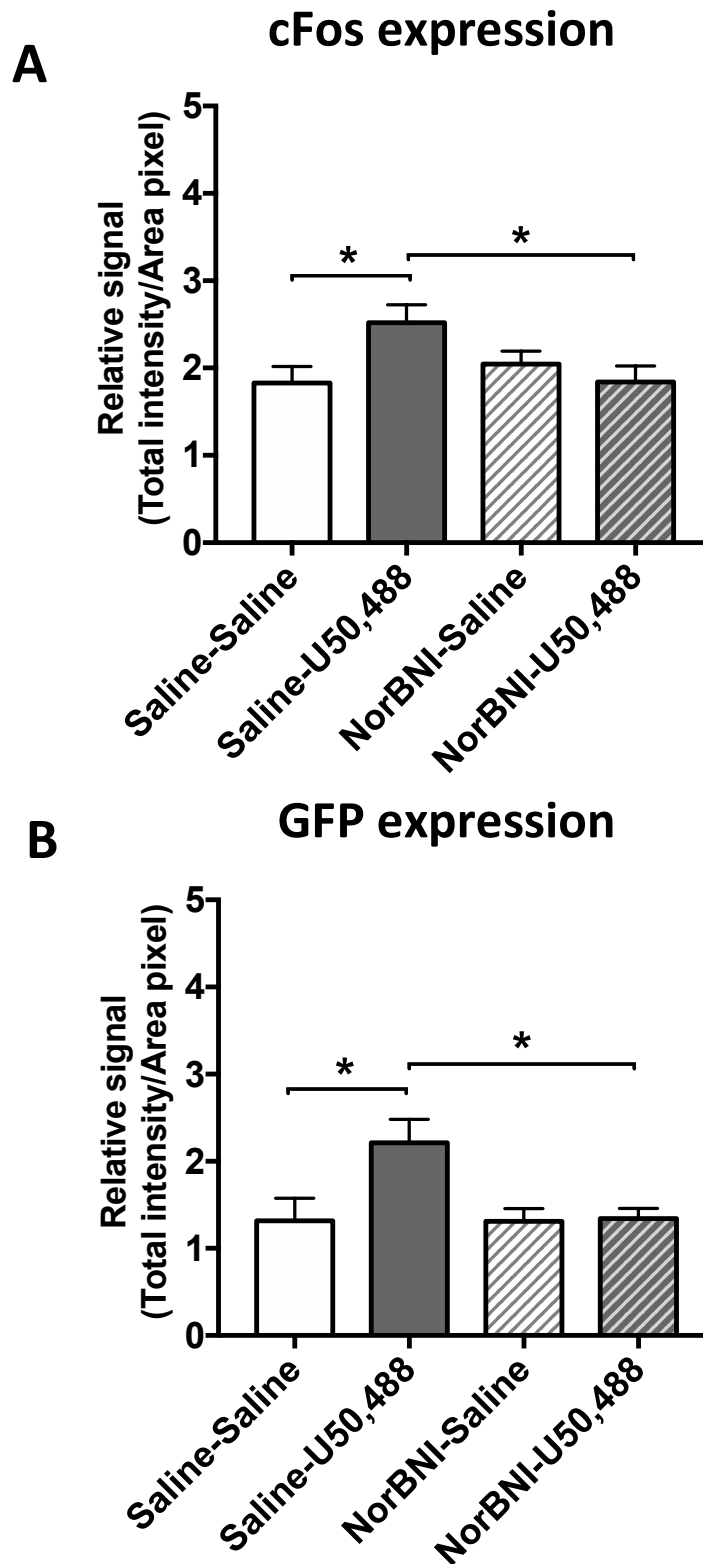


**Figure 4.9C Quantified fluorescent cFos and GFP signals following U50,488 treatment in CeA.**

U50,488 induced both **cFos (A)** or **GFP (B)** signals, which were blocked by the presence of norBNI (10mg/kg). All data are presented as mean  $\pm$  SEM. One-way ANOVA post-hoc Sidak's test, \* =  $P < 0.05$ ,  $n = 6$  animals per treatment group.

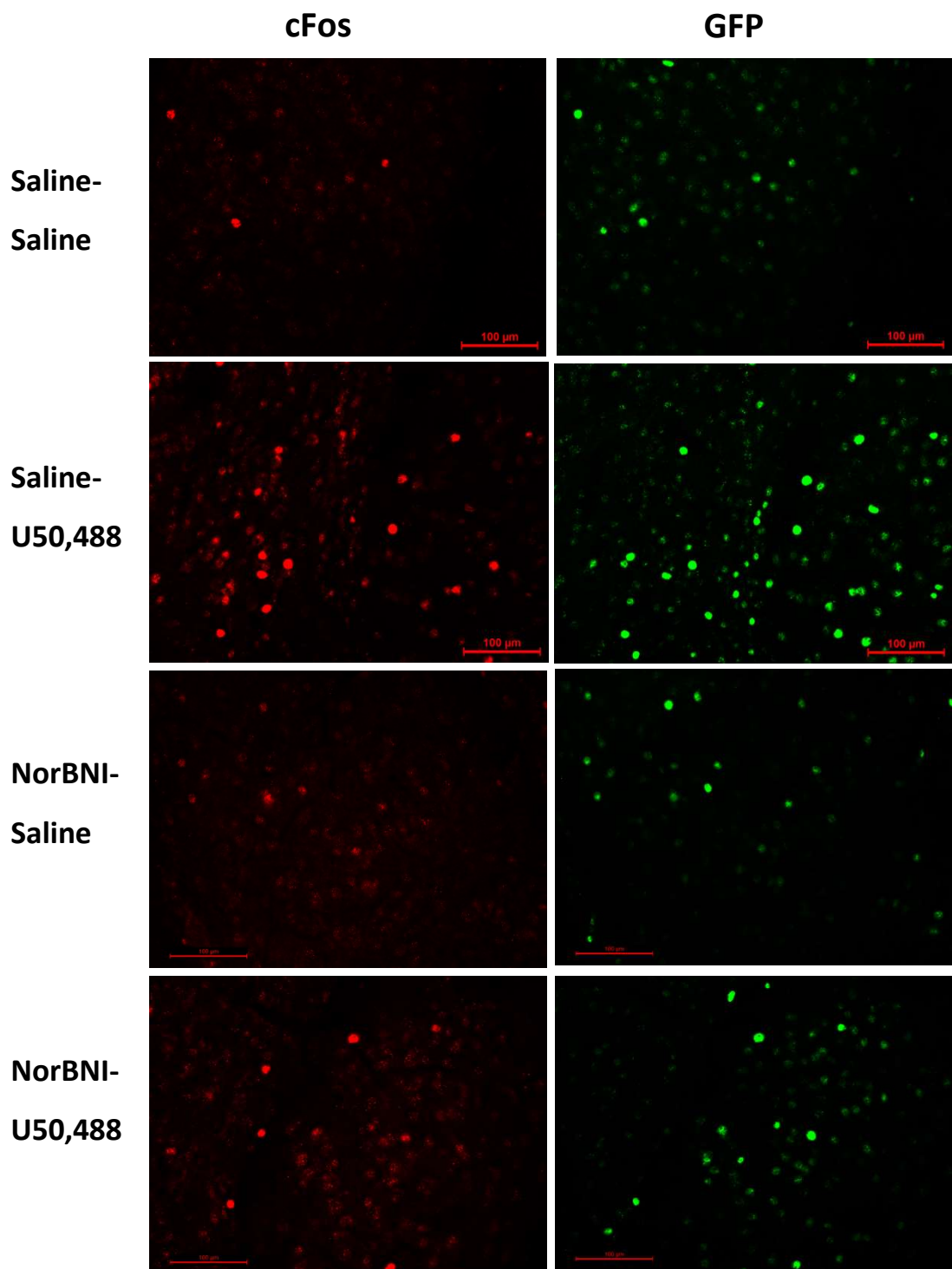


**Figure 4.9D** Fluorescent images of cFos and GFP expression in BLA (Bregma -1.94 mm) after a single U50,488 (20mg/kg) administration.

U50,488 significantly induced both cFos and GFP, compared to the control saline-treated groups, an effect that was inhibited by pretreatment with norBNI. Scale bar = 100μm.

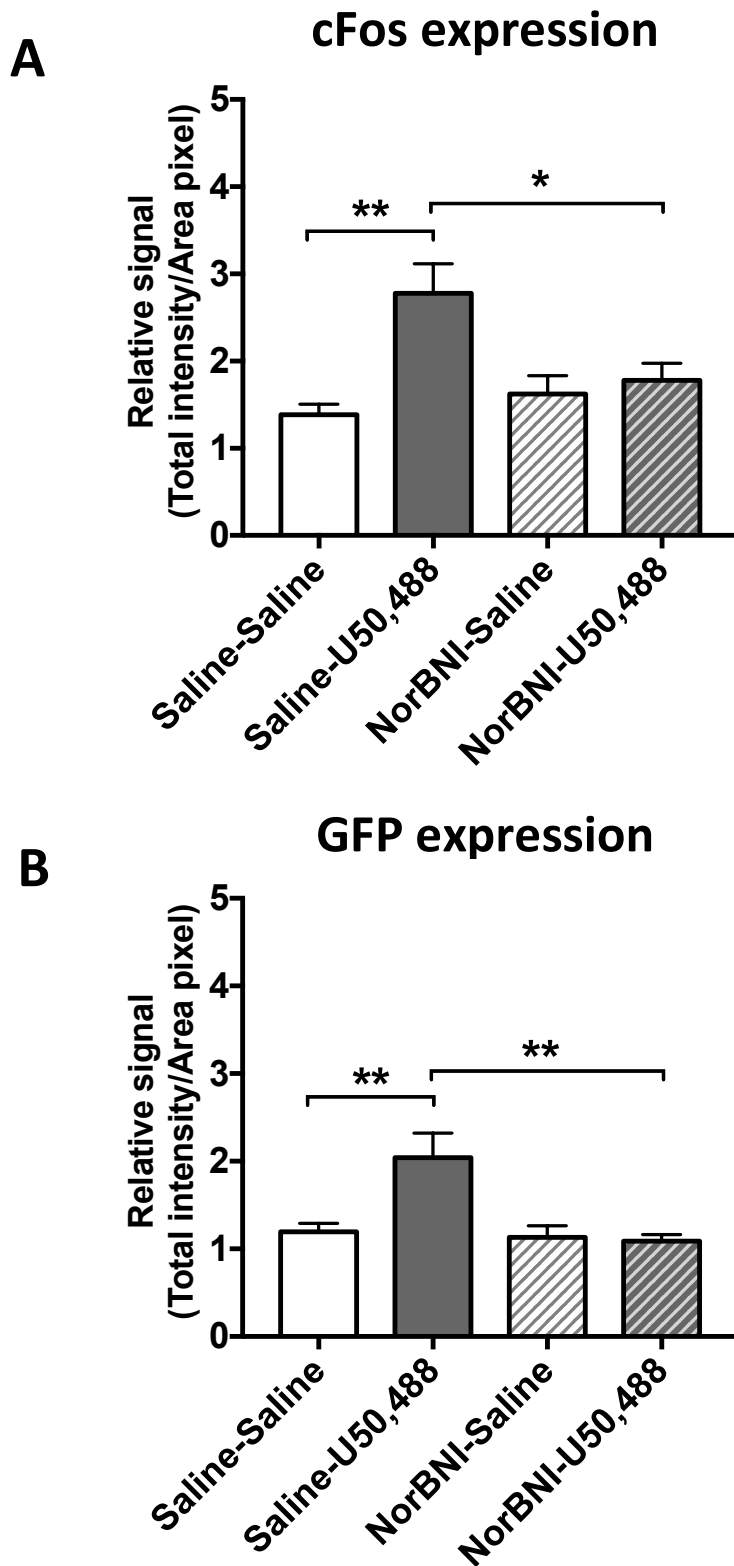


**Figure 4.9E Quantified fluorescent cFos and GFP signals following U50,488 treatment in BLA.**

U50,488 induced both **cFos (A)** or **GFP (B)** signals, which were blocked by the presence of norBNI (10mg/kg). All data are presented as mean  $\pm$  SEM. One-way ANOVA post-hoc Sidak's test, \* =  $P < 0.05$ , \*\* =  $P < 0.01$ ,  $n = 6$  animals per treatment group.

### 4.3.9 The effect of FSS in male amygdala

As the previous section showed KOPr activation (U50,488 treatment) induced significant effects on cFos expression in both the central (CeA) and basolateral amygdala (BLA), the same experiment was repeated with an *in vivo* stressor (FSS). Sample fluorescent images were shown in figure 4.10A, 4.10C.

Interestingly, FSS caused no increased expression in cFos or cFos-driven GFP in the CeA (Figure 4.10B), which is different to the increase in both cFos and GFP expression after U50,488 treatment (Section 4.3.8). In contrast, in the BLA, FSS induced both cFos and cFos-driven GFP signals (Figure 4.10D), but these effects were not significantly inhibited by pre-administration of norBNI. These findings in the BLA suggest that both KOPr activation and FSS induce cFos expression in that brain region, but the the FSS-induced cFos expression is unlikely to be mediated by KOPrs activation.



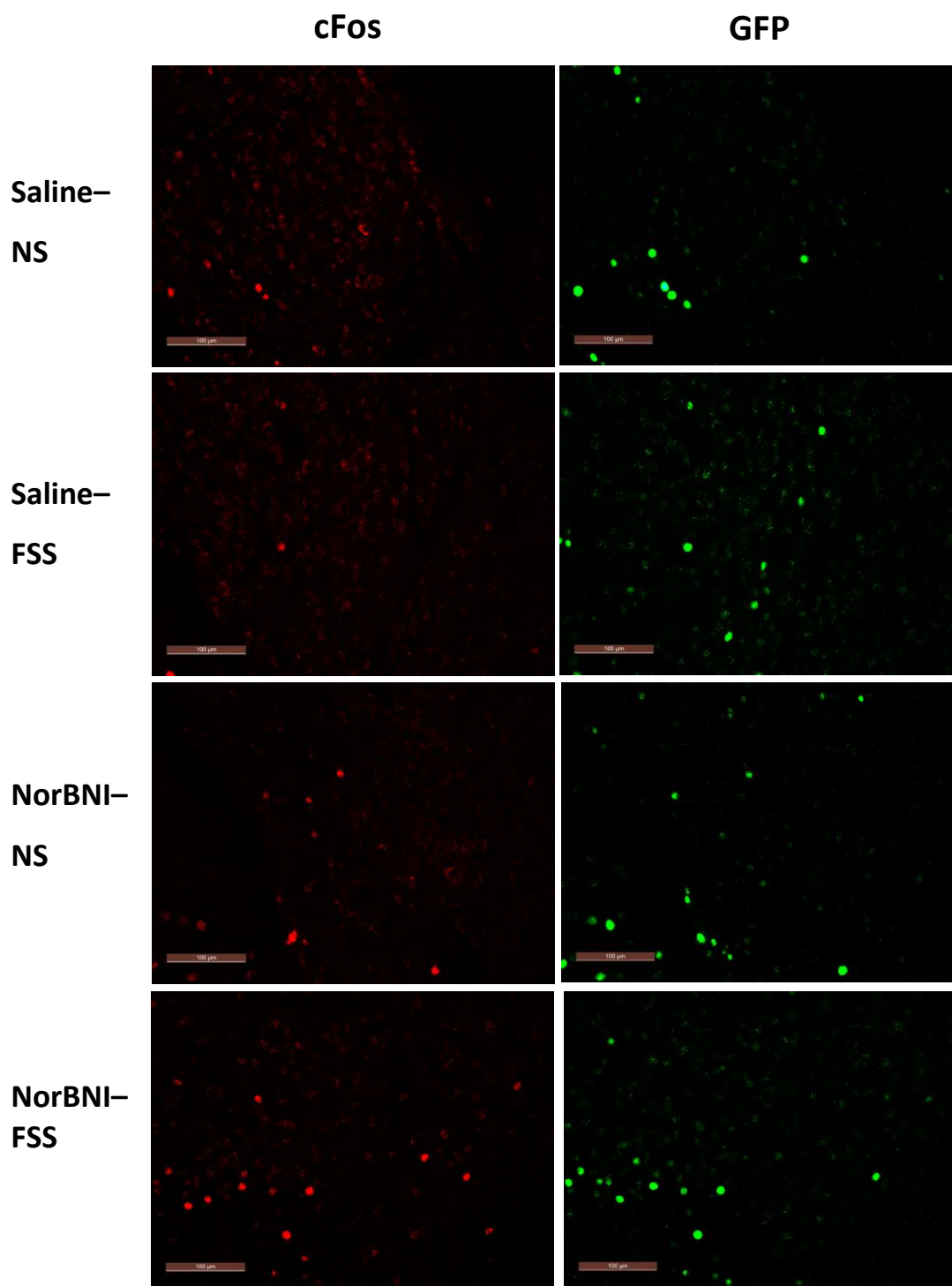


**Figure 4.10A** Fluorescent images of cFos and GFP expression in CeA (Bregma -1.94 mm) following FSS.

Both cFos and GFP expression were not affected by FSS or by pre-administration of norBNI in CeA. Scale bar = 100μm.

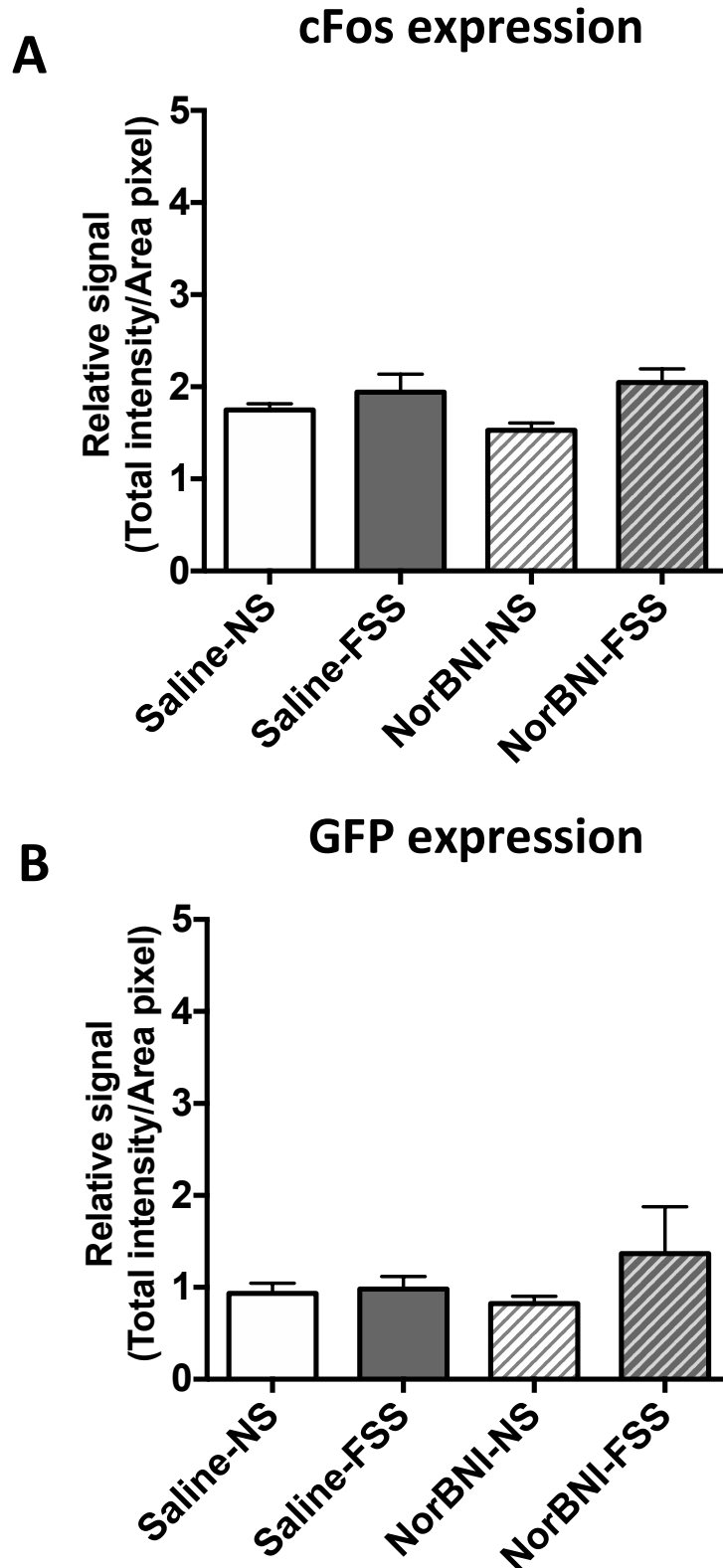


**Figure 4.10B** Quantified fluorescent cFos and GFP signals following 15-minute FSS in CeA.

FSS did not significantly alter either **cFos (A)** or **GFP (B)** signals in the absence or presence of norBNI (10mg/kg). All data are presented as mean  $\pm$  SEM. One-way ANOVA post-hoc Sidak's test,  $n = 6$  animals per treatment group.

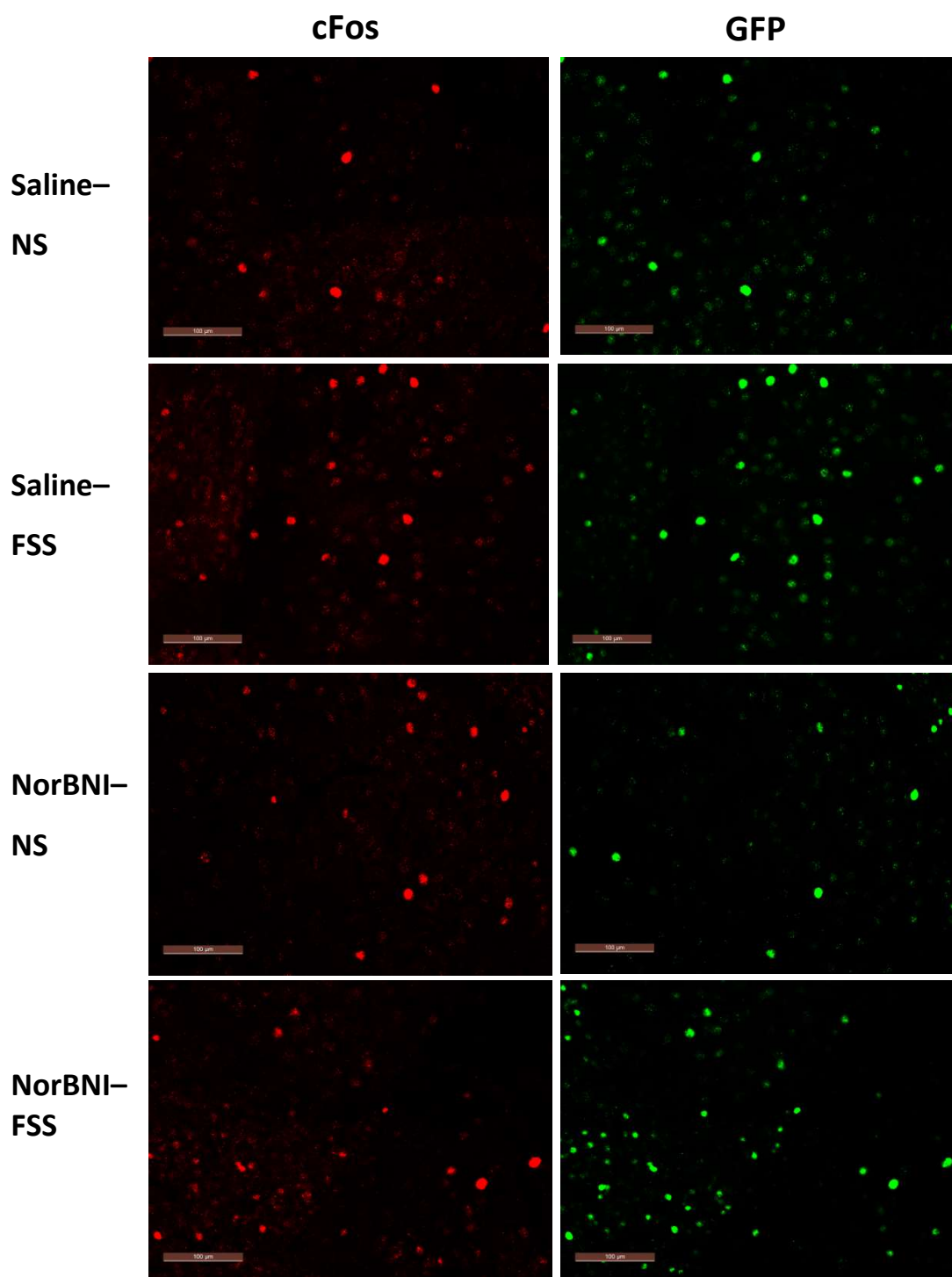


**Figure 4.10C** Fluorescent images of cFos and GFP expression in BLA (Bregma -1.94 mm) following FSS.

Both cFos and GFP expression were induced by FSS in BLA. No significant effect of norBNI was seen. Scale bar = 100µm.

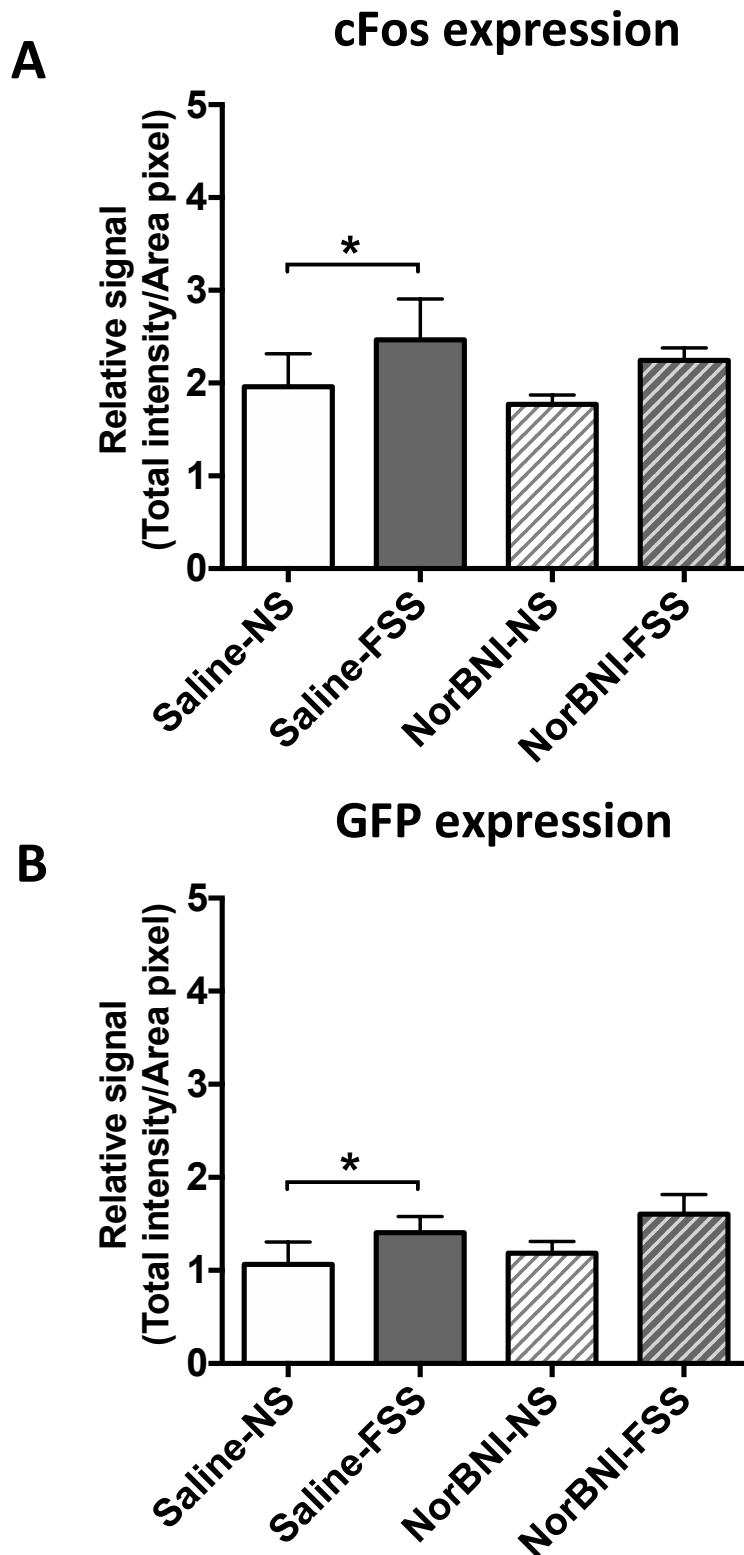


**Figure 4.10D Quantified fluorescent cFos and GFP signals following 15-minute FSS in BLA.**

FSS significantly induced both **cFos (A)** and **GFP (B)** signals in BLA. Pretreatment with norBNI did not significantly inhibit cFos or GFP expression. All data are presented as mean  $\pm$  SEM. One-way ANOVA post-hoc Sidak's test, \* =  $P < 0.05$ ,  $n = 6$  animals per treatment group.

#### 4.3.10 Summary of different stimuli in male mice

As discussed in Chapter 1, PFCx, NAc, hippocampus and amygdala are four important regions that are involved in stress responses, affective-related disorders and addiction-related behaviours. The effects of KOPr activation and *in vivo* stressor (FSS) on neuronal activity in these regions are summarised in Table 4.1. Apart from the dentate gyrus region in the hippocampus, all the regions showed similar effects in response to U50,488 treatment. In contrast, FSS only induced cFos expression in PFCx, NAc and BLA, not in hippocampus and CeA. In each case, if cFos expression was significantly increased, cFos-driven GFP expression was also significantly increased.

The KOPr antagonist, norBNI, was effective in blocking all of the U50,488-induced increases in cFos and cFos-driven GFP effects. In general, norBNI did not significantly inhibit FSS-induced effects in these brain regions, with the exception of the NAc, where FSS-induced cFos expression was significantly inhibited.

	<b>U50,488 (20mg/kg)</b>			
	<b>cFos</b>	<b>norBNI</b>	<b>GFP</b>	<b>norBNI</b>
<b>PFCx</b>	↑ ↑	**	↑	*
<b>NAc</b>	↑ ↑	**	↑	**
<b>Hippocampal CA1</b>	↑	*	↑ ↑	**
<b>Hippocampal DG</b>	ns	ns	ns	ns
<b>Central Amygdala (CeA)</b>	↑	*	↑	*
<b>Basolateral Amygdala (BLA)</b>	↑ ↑	*	↑ ↑	**
	<b>FSS (15 minutes)</b>			
	<b>cFos</b>	<b>norBNI</b>	<b>GFP</b>	<b>norBNI</b>
<b>PFCx</b>	↑ ↑	ns	↑ ↑	ns
<b>NAc</b>	↑ ↑	*	↑ ↑	ns
<b>Hippocampal CA1</b>	ns	ns	ns	ns
<b>Hippocampal DG</b>	ns	ns	ns	ns
<b>Central Amygdala (CeA)</b>	ns	ns	ns	ns
<b>Basolateral Amygdala (BLA)</b>	↑	ns	↑	ns

**Table 4.1. Summary of cFos and cFos-induced GFP expression in different brain regions following KOR activation, U50,488 and in vivo forced swim stress (FSS).** Prefrontal cortex (PFCx), nucleus accumbens (NAc), CA1, dentate gyrus region of hippocampus (Hippocampal CA1, DG), basolateral amygdala (BLA), central amygdala (CeA), ↑ < 0.05; \* < 0.05; ↑↑ < 0.01; \*\* < 0.01; ns = not significant.

## 4.4 Discussion

All the images and figures 4.2-4.5 showed a common pattern, in that there was increased cFos and cFos-driven GFP expression, in both PFCx and NAc, following KOPr stimulation by a single injection of U50,488 or 15-minute *in vivo* FSS. These findings indicate that KOPr activation and FSS both enhance neuronal activity in these brain regions.

### **U50,488 increased neuronal activity in male PFCx and NAc**

Our data (Section 4.3.1, 4.3.3) firstly showed increased neuronal activity in PFCx following KOPr agonist U50,488 administration, which was effectively blocked by the pre-treatment of norBNI (10mg/kg, i.p.), these novel findings confirm that the increased expression in cFos and GFP by U50,488 was caused by KOPr activation. Similar effects were observed in NAc following U50,488 treatment, which is consistent with previous evidence that U50,488-induced cFos expression in NAc in rats (Russell *et al.*, 2014). KOPrs are widely distributed throughout the mouse brain and it has been shown that while the NAc has high density of KOPr expression, the PFCx only expresses KOPr with low density (Le Merrer *et al.*, 2009). Therefore, although the U50,488-induced increase in cFos and GFP expression could result from activation of KOPrs within the PFCx or NAc, it may be as a result of KOPr activation in other brain regions that in turn project to the PFCx or NAc.

### **FSS increased neuronal activity in male PFCx and NAc**

As shown in Section 4.3.2 and 4.3.4, FSS also significantly enhanced cFos and cFos-driven GFP expression in PFCx and NAc. These findings support previous studies that acute social stress, restraint stress or forced swim increased cFos expression in various brain regions, including PFCx and NAc. For example, Funk and colleagues showed that exposure to environmental stressors, such as 10-minute foot shock, 30-minute restraint stress or social defeat significantly increased cFos expression in medial prefrontal cortex and NAc in male rats (Funk *et al.*, 2006). Other studies on male mice also demonstrated that acute (6 minutes) FSS significantly increased cFos expression in the prelimbic region of the PFCx and NAc (Briand *et al.*, 2010). However,

Ons and colleagues reported that exposure of 30 minutes of FSS or immobilization stress in male rats did not increase cFos expression in the NAc shell, only in the prefrontal cortical areas (Ons *et al.*, 2004), whereas our data showed a significant increase in cFos expression following 15 minutes of FSS in NAc core, suggesting that stress-induced neuronal activity within the NAc is region specific (core or shell), and NAc core may play a more important role in stress-induced neuronal activation.

In contrast to U50,488, pre-administration of norBNI did not significantly reduce either stress-induced cFos or GFP expression in the PFCx (Figure 4.3B). This could be due to the complex and multifactored mechanism of stress responses. There are multiple signaling pathways activated and various signaling molecules secreted following stress exposure e.g. corticotropin-releasing factor (CRF), adrenocorticotrophic hormone (ACTH), hypothalamic-pituitary-adrenal (HPA) axis and activation of the autonomic nervous system (McEwen *et al.*, 2015). Although KOPrs have been implicated in mediating stress responses, it is unclear precisely what the mechanism of this interaction is. Therefore, pre-administration of norBNI may only partially block FSS-induced effects. However, MacLaughlin et al. showed that pre-treatment of the KOPr antagonist norBNI (10mg/kg, i.p.) not only inhibited the forced swim stress-induced analgesia and significantly reduced immobility in C57Bl/6 mice, but also blocked FSS-induced potentiation of cocaine CPP (MacLaughlin et al., 2003). In addition, other animal behavioural studies have shown that administration of norBNI (10mg/kg, i.p.) effectively prevent FSS-induced immobility and impaired learning and memory performance in adult male mice (Carey *et al.*, 2009). These studies suggest that FSS-induced immobility, analgesia and impaired cognitive functions are mediated by KOPr system, and stress-induced KOPr activation may be sufficient to cause deficits in learning and memory.

Notably, FSS-induced cFos expression in the NAc was effectively blocked by norBNI (10mg/kg, i.p.), indicating that the FSS-induced neuronal activation in NAc is largely mediated by KOPrs, or is downstream of KOPr activation (Figure 4.5B).



Overall, these results might suggest either that stress responses in the NAc, but not in the PFCx, are largely mediated by KOPrs or are downstream of KOPr activation. Alternatively, as only a single dose of norBNI was used in these experiments, it could mean that insufficient norBNI was administered to block any KOPr-mediated stress responses in the PFCx. It is possible that increasing doses of norBNI pretreatment could reveal inhibitory effects of norBNI in the PFCx following stress.

### **Overlapping expression of cFos and GFP in PFCx and NAc**

If the relative proportion of GFP to cFos increases, this might mean that cells had been activated a long time prior to sectioning, allowing time for cFos to be activated first and degraded, with GFP expression persisting. Our immunocytochemistry images (Figure 4.6A, 4.6B) showed a different pattern of overlapping expression of cFos and cFos-driven GFP following different stimuli in PFCx and NAc. In particular, after FSS, there was a much higher proportion of cFos + GFP-positive neurons in the PFCx compared with in the NAc, even though both cFos and GFP expression overall was increased in both brain regions, which might suggest that FSS activates neurons in NAc first, and transiently, then activates PFCx later. After FSS, there was also a higher proportion of cFos + GFP-positive neurons in the PFCx than that of following U50,488 treatment, suggesting that FSS might activate the PFCx more slowly than U50,488 activates the PFCx. Whereas in NAc, the opposite effects were seen, i.e. the cFos + GFP-positive neurons after FSS is lower than that of U50,488 treatment, suggesting that FSS activates the NAc faster than U50,488 activates the NAc, or FSS activates neurons in the NAc only transiently.

The reason for this is unclear at present but could reflect the different temporal expression of cFos and GFP. This might be as a result of the different temporal expression of cFos and GFP. cFos is a transient immediate early gene with a short half-life, whereas GFP is more stable with a longer half-life (Barth *et al.*, 2004). Therefore, cFos-driven GFP expression would be expected to persist longer than cFos expression itself. In all of these studies, brains were taken at a single time-point after either U50,488 or FSS treatment. Therefore, as FSS increased cFos + GFP-positive neurons in the PFCx but increased GFP-only neurons to a greater extent in NAc, FSS

might activate NAc before it activates PFCx, or, FSS activates the NAc transiently, but activates the PFCx more persistently. There are no studies in the literature that have examined this, but, future experiments could be designed to take brain sections at different time-points after U50,488 or FSS treatments to further test this hypothesis.

Conversely, U50,488 treatment increased the proportion of cFos-only neurons in the NAc, but not the PFCx. For the same reason as above, this could be due to U50,488 treatment activating the PFCx prior to activation of the NAc.

### **The effect of U50,488 and FSS in other brain regions**

Our data showed increased cFos expression in both central (CeA) and basolateral amygdala (BLA) following U50,488 (20mg/kg, i.p.), but FSS only induced cFos expression in BLA, not CeA, which conflicts with a previous study showing that a single injection of U50,488 (10mg/kg, i.p.) significantly increased cFos activation in CeA, but no effect was observed in BLA in male rats (Russell *et al.*, 2014). However, other studies demonstrated the region-specific cFos expression pattern in the amygdala after a single social stress, where CeA exhibited the least change in cFos expression (Martinez *et al.*, 1998). Also, the FSS-induced effect in BLA supports previous studies, which showed fear conditioning increased KOPr mRNA only in BLA, not in CeA in male rats, highlighting the important role of BLA involved in anxiety-related behaviours (Knoll & Carlezon, 2010). As introduced in chapter 1, the amygdala is a brain region well-known for its regulatory role in response to stress and emotional perception (Bennur *et al.*, 2007). Our results showed that the stress-induced cFos expression was significantly increased only in BLA, where BLA is the major region in amygdala that has been shown an increase in spines density and expansion of dendrites following acute or chronic stress (McEwen *et al.*, 2016).

Our data showed that administration of KOPr agonist (U50,488, i.p.), but not FSS, significantly increased cFos expression in the CA1 region of hippocampus. The dentate gyrus region of the hippocampus was not activated following U50,488 or FSS treatment. The finding with KOPr agonist is a novel one, with no previous studies describing cFos expression following a single administration of KOPr agonist.

However, the finding that FSS does not induce cFos expression in the hippocampus conflicts with one of the early studies in male rats, indicating that restraint or immobilisation stress profoundly induced cFos expression in both the CA1 and dentate gyrus regions in the hippocampus in a time dependent manner (Titze-de-Almeida *et al.*, 1994). Other studies further support this by demonstrating that 60 minutes of restraint stress in male rats produced high levels of cFos expression in the CA1-CA3 regions in the hippocampus (Fevurly *et al.*, 2004). In addition, it has been shown that a combination of acute 30 minutes restraint stress and 5 minutes forced swim stress specifically increased cFos-positive neuronal density in the CA1 region of the dorsal hippocampus in male mice, leading to impaired long-term spatial memory (Yu *et al.*, 2018). That our data conflicted with these studies could be due to various potential factors, such as the different animal species, different nature of stressors and durations. Previous studies successfully demonstrated stress-induced cFos expression in the hippocampus after at least 30 minutes of restraint stress or in combination with other stressor (e.g. FSS) time-dependently, which suggests that FSS (15 minutes) in this study might not be strong and persistent enough to induce cFos expression in the hippocampus.

Overall, in most brain regions studied, there was a general overlap between the effects of a single administration of KOPr agonist, and an acute *in vivo* stressor. In general, although pretreatment of norBNI block U50,488-induced neuronal activity in different brain regions, it did not effectively block FSS-induced effects, except in NAc. This suggests either that stress responses are, in part, mediated by activation of KOPrs in NAc, or that activation of KOPr in NAc share similar neuronal network effects to an acute stressor. Other overlapped brain regions that are involved in both KOPr activation and *in vivo* stressor responses could be mediated by different mechanisms, i.e. FSS-induced effects in other brain regions are mediated by non-KOPr systems. Two brain regions that diverged in their responses were the hippocampal CA1 region and the central amygdala. This suggest that KOPr activation in these brain regions is not involved in the stress response.

As outlined in the introduction, there is growing evidence for sex differences in behavioural responses to both KOPr agonists and stress. In the following chapter, we investigated this further.

## **Chapter 5 The effect of kappa opioid receptor activation and in vivo stressor in female mice**

## 5.1 Introduction

Chapter 4 showed that, in male mice, KOPr activation (with a single injection of U50,488) increased neuronal activity in various brain regions, specifically in the PFCx, NAc, hippocampus and amygdala, as shown by increased cFos and cFos-driven GFP expression. These effects were blocked by pre-administration of the KOPr antagonist, norBNI.

Following an acute *in vivo* stressor (FSS), cFos and cFos-driven GFP expression were also increased in the PFCx, NAc and BLA. In the CA1 region of the hippocampus and CeA, however, although U50,488 increased cFos and GFP expression, FSS had no effect. NorBNI was largely ineffective in inhibiting cFos and cFos-driven GFP expression after FSS, except in NAc.

KOPrs have been implicated in the effects of stress, anxiety and depression, and addiction-related behaviours, and KOPr antagonists have been proposed as potential treatments for both anxiety/depression and addiction (Shirayama *et al.*, 2004). In humans, women have higher prevalence of depression and anxiety than men, with statistics showing that women are more likely to be affected by affective disorders (Albert 2015). However, the majority of previous preclinical studies on the KOPr system and the effects of KOPr antagonists have been performed in male rodents. There is increasing evidence demonstrating sex differences in the analgesic effects of opioid receptor activation (Liu *et al.*, 2013, Abraham *et al.*, 2018). Further, recent studies have demonstrated that behavioural effects of stress and KOPr agonists are sex-dependent (See Chapter 1 & Russell *et al.*, 2014), but sex differences in opioid receptor activation in response to stress at molecular level are less understood.

The aim of this chapter is to compare the effects of different stimuli (FSS and U50,488 administration) on cFos and cFos-driven GFP expression in different brain regions in female mice. We will investigate if there is a sex difference in the effects of KOPr activation and *in vivo* stressor at the molecular levels in different brain regions, and

whether the pre-administration of KOPr antagonist, norBNI would block the U50,488 and FSS-induced effects in a similar way in male mice.

It is hypothesised that the effects of KOPr activation and *in vivo* stressor are different between the sexes. We have repeated the experiment in chapter 4, using KOPr agonist, U50,488 (20mg/kg) and 15-minute FSS to investigate the neuronal activity in these brain regions in female cFos-GFP transgenic C57BL/6J mice.

## 5.2 Methods

### 5.2.1 Immunohistochemistry

The immunohistochemistry (described in chapter 2, section 2.10) was repeated in this chapter with adult female (9-13 weeks old, 20-25g) cFos-GFP transgenic mice (n = 6 animals per treatment group). Before immunohistochemistry, the female mice were treated with the same procedures (KOPr agonist, U50,488 or *in vivo* 15-minute forced swim stress) as shown in chapter 4, illustrated in figure 4.1.

The coronal sections (40µm) of PFCx (Bregma +2.22 mm), NAc (Bregma +1.34 mm), amygdala (Bregma -1.94 mm) and CA1 region and dentate gyrus in dorsal hippocampal (Bregma -1.94 mm) slices were prepared on a vibratome. For each mouse, one slice was taken for each brain region. These slices were co-stained with anti-cFos and anti-GFP antibodies (section 2.3), followed by incubation of fluophore-labelled secondary antibodies: goat anti-rabbit antibody Alexa Fluor 568 (diluted 1:500) and goat anti-chicken antibody Alexa Fluor 488 (diluted 1:500) (section 2.3).

The fluorescent immunoreactivity was detected by Leica DMI4000B inverted wide-field fluorescent microscopy at 200X magnification. The relative fluorescent signals for each brain region on each slice were the average values of the left and right signals, which were quantified in ImageJ software (section 3.2.5). The data were analysed with one-way (treatment) ANOVA followed by Sidak's test. All data are presented as mean  $\pm$  SEM and significance levels were  $P < 0.05$ .

## 5.3 Results

### 5.3.1 The effect of U50,488 and FSS in female PFCx

Figures 5.1A & 5.1B show the effects of U50,488 in female mice. Sample fluorescent images are shown in figure 5.1A. Data are quantified in figure 5.1B. These data show that in female cFos-GFP transgenic mice, U50,488 had no effect on cFos or cFos-driven GFP expression in the PFCx. This is indirect contrast to the effect seen in male mice (see Figures 4.2B & 4.2C).

Figures 5.1C & 5.1D show the results from similar experiments where female mice were exposed to a single FSS session before brain sectioning. Sample fluorescent images are shown in figure 5.1C. Data are quantified in figure 5.1D. As with the effects of U50,488 (Figures 5.1A & 5.1B), FSS had no effect on cFos or cFos-driven GFP expression in PFCx in female mice. Again, this is in direct contrast to the robust increase in both cFos and cFos-driven GFP expression seen in male mice, using an identical experimental procedure (Figures 4.3A & 4.3B).

NorBNI had no effect on cFos or GFP expression in PFCx in female mice.

The effects of KOPr agonist, U50,488 and *in vivo* stress, FSS on the PFCx of both male and female cFos-GFP transgenic mice are summarised in table 5.1. Together, these data suggest that the PFCx is primary not involved in mediating stress responses and responses to KOPr agonists in female mice, as well as providing evidences for sex difference in the effects of stress and KOPr agonists in the PFCx.

	Male		Female	
	cFos	GFP	cFos	GFP
U50,488 treatment	↑↑	↑	ns	ns
15-minute FSS	↑↑	↑↑	ns	ns

**Table 5.1.** Comparison between male and female cFos-GFP mice on cFos and GFP expression in **PFCx** following U50,488 or FSS treatment. ↑;  $P < 0.05$ , ↑↑;  $P < 0.01$  vs saline/no stress, ns = not significant.



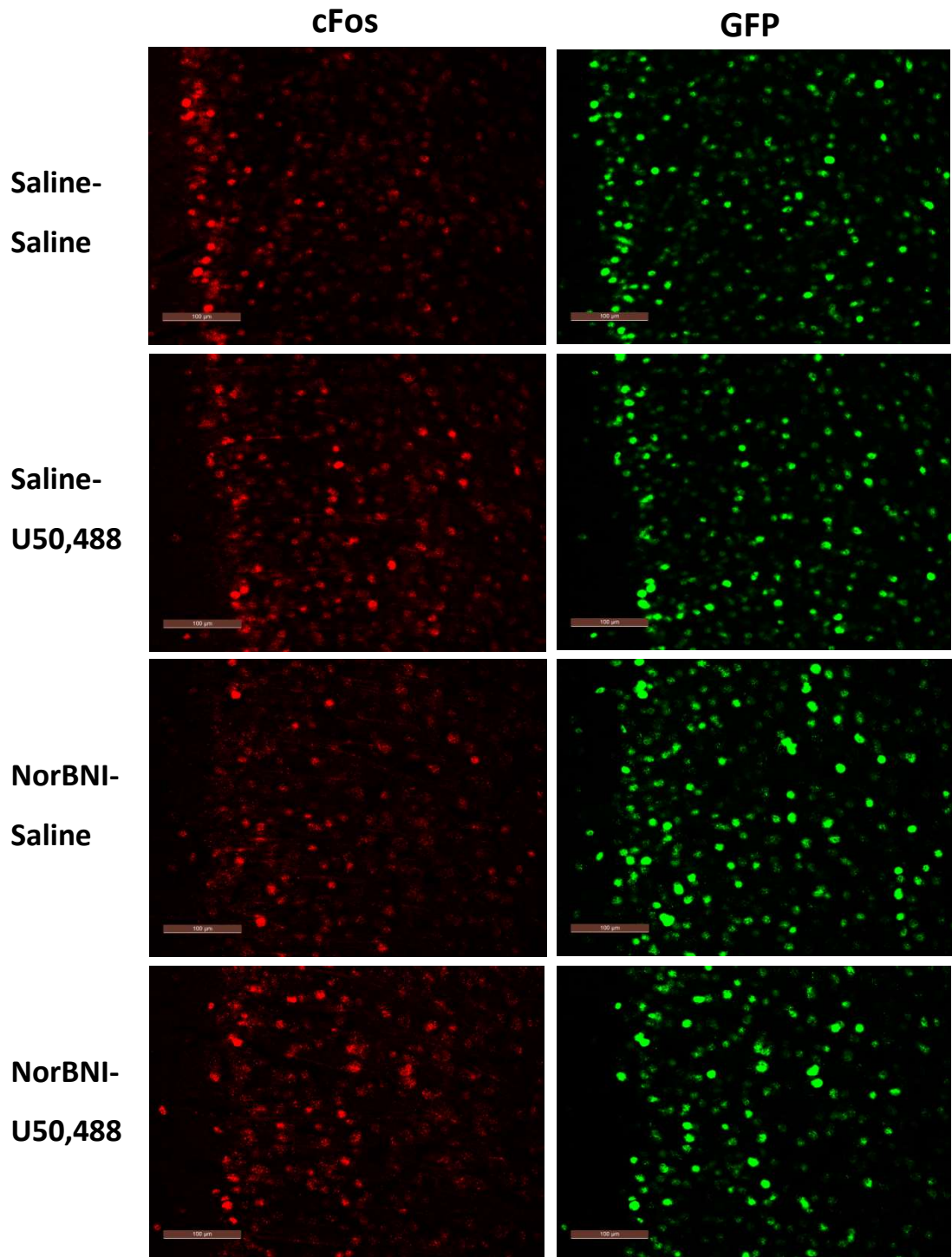


**Figure 5.1A** Fluorescent images of cFos and GFP expression in female PFCx after U50,488 treatment.

Neither cFos or cFos-driven GFP expression were affected by U50,488 treatment or pre-administration of norBNI in female PFCx. Scale bar = 100μm.

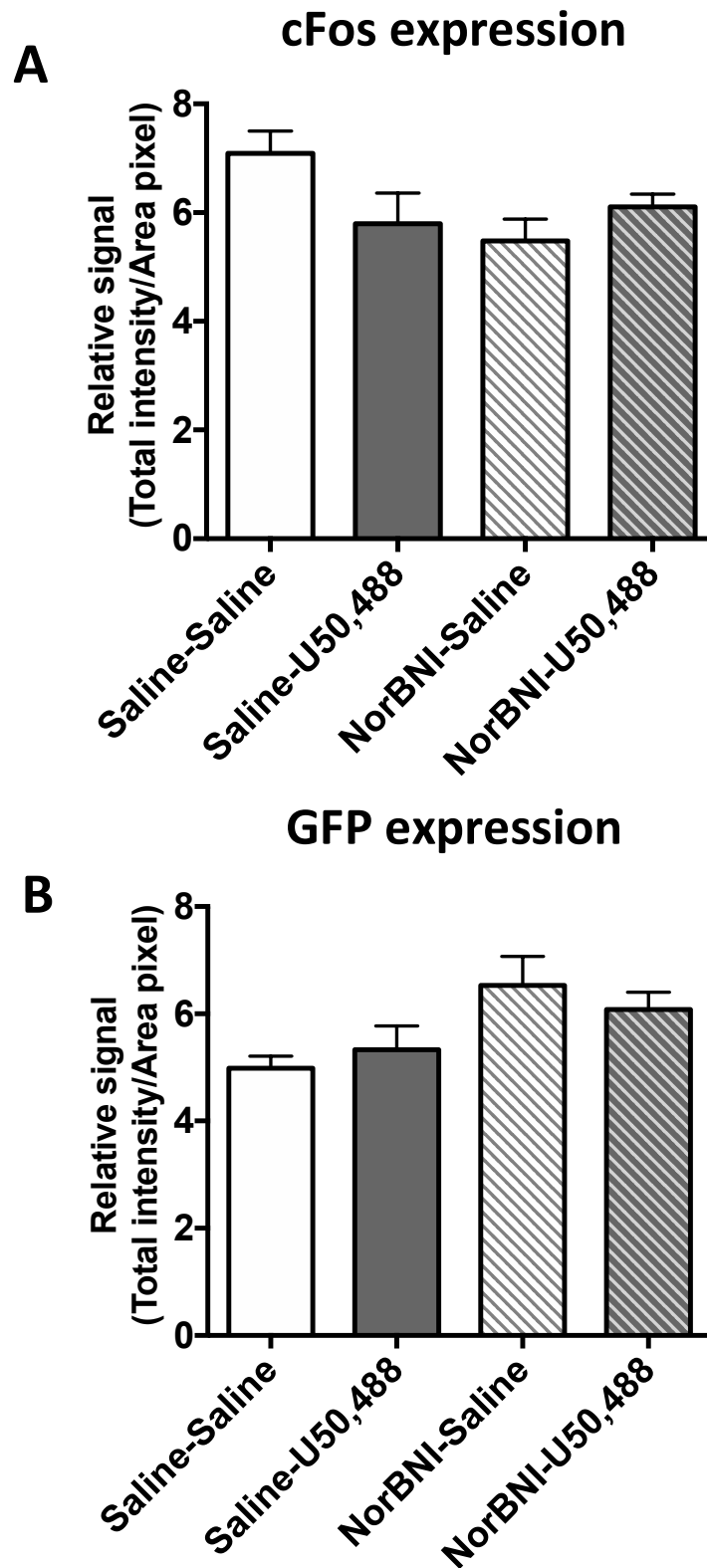


**Figure 5.1B Quantification of fluorescent cFos and GFP signals following U50,488 in female PFCx.**

cFos (A) and GFP (B) signals in female PFCx were unaffected by treatment in the absence and presence of norBNI. All data are shown as mean  $\pm$  SEM. N = 6 animals per treatment group.

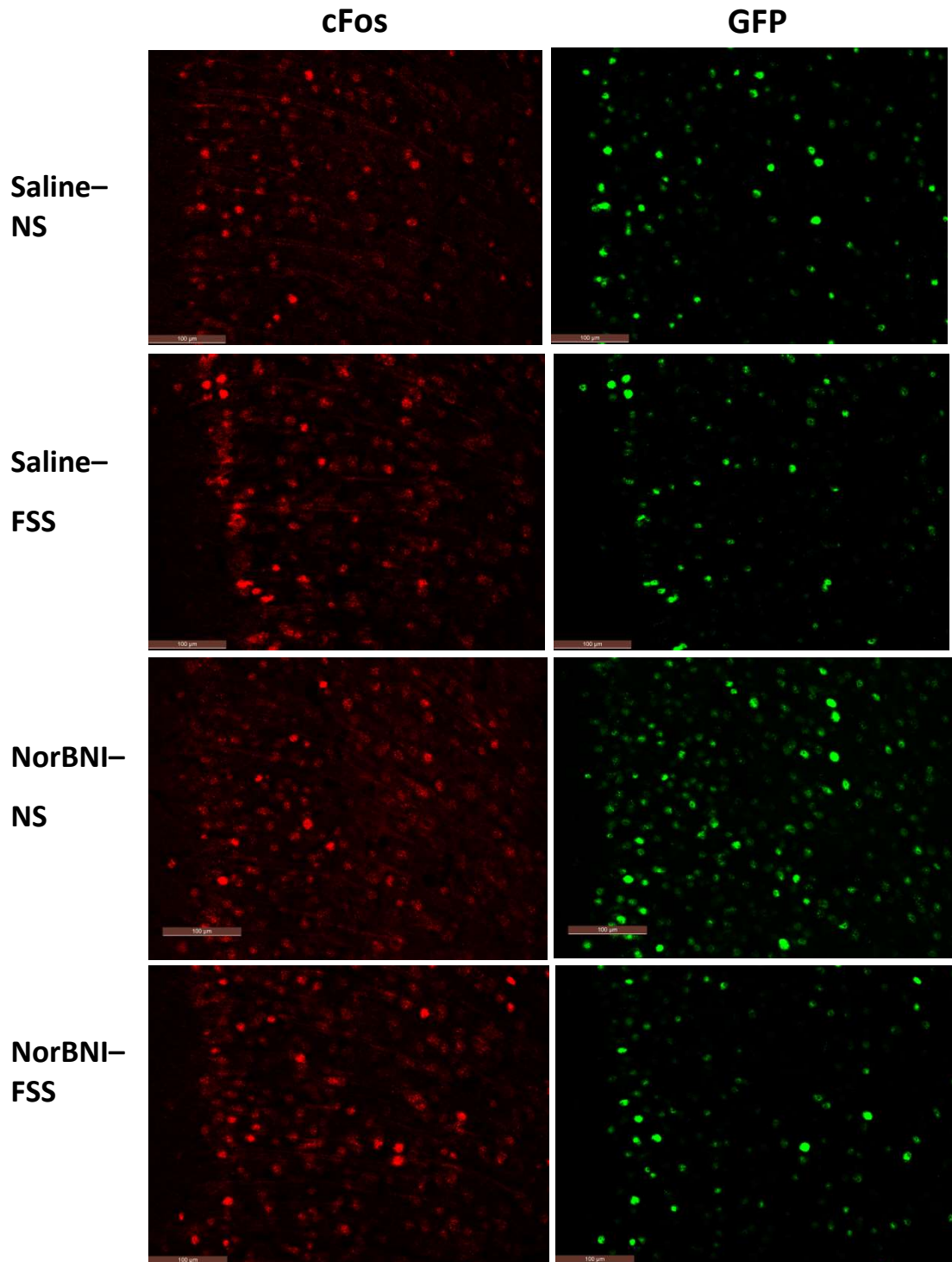


**Figure 5.1C** Fluorescent images of cFos and GFP expression in female PFCx after 15-minute FSS.

FSS did not affect either cFos or GFP expression in female PFCx, which were also insensitive to pre-administration of norBNI. Scale bar = 100µm.

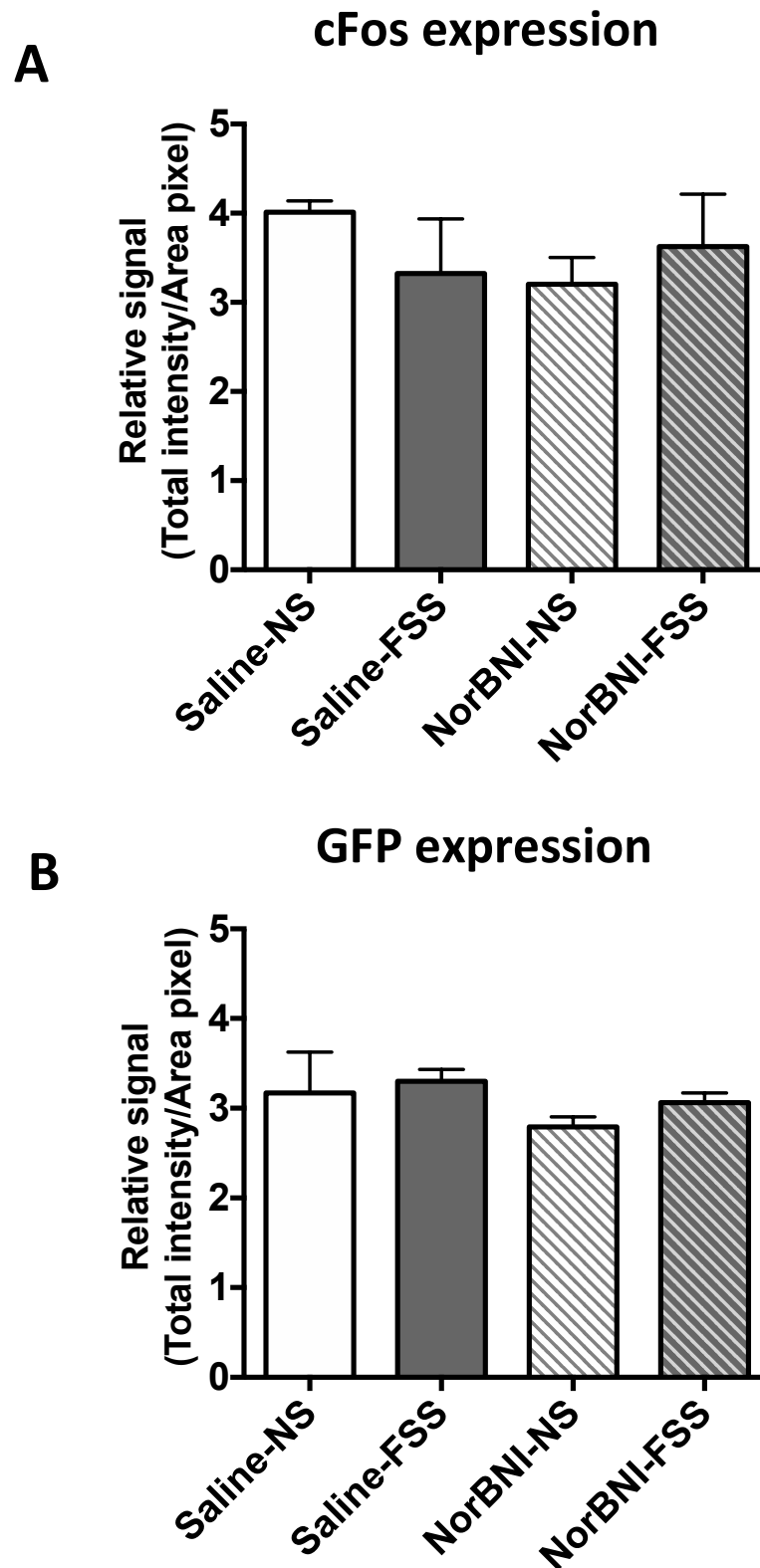


**Figure 5.1D Quantification of fluorescent cFos and GFP signals following FSS in female PFCx.**

FSS did not affect levels of **cFos (A)** or **GFP (B)** in female PFCx in the absence and presence of norBNI. All data are shown as mean  $\pm$  SEM. N = 6 animals per treatment group.

### 5.3.2 The effect of U50,488 and FSS in female NAc

Section 5.3.1 suggests a sex difference in the effect of U50,488 injection and FSS in the PFCx, in that no cFos expression was seen in female mice, whereas robust cFos expression was seen in male mice (Chapter 4). We next investigated the effects of KOPr agonist- and FSS-induced activation of cFos in the NAc region of female mice.

Sample fluorescent images following U50,488 injection and FSS are shown in figure 5.2A and 5.2C respectively. In the NAc region from female mice, a single injection of U50,488 also did not induce either cFos or GFP expression, an effect that was similar to the effects observed in the PFCx from female mice (Figure 5.2B). This finding again suggests that neuronal activity induced by U50,488 is sex dependent as the same treatment resulted in a robust increase in cFos expression in the NAc region in male mice (see Figure 4.4).

In contrast to the effect of U50,488, 15-minute FSS did induce both cFos and GFP expression in the NAc region of female mice (Figure 5.2D), similar to the effect previously shown in the same brain region in male mice (see Figure 4.5). The effects of KOPr agonist- and FSS-induced cFos activation in both male and female NAc are summarised in table 5.2. Furthermore, although there was a trend for decrease in effect of cFos with pre-administration of norBNI, there was no significant effect of norBNI.

	Male		Female	
	cFos	GFP	cFos	GFP
U50,488 treatment	↑↑	↑	ns	ns
15-minute FSS	↑↑	↑↑	↑↑	↑

**Table 5.2.** Comparison between male and female cFos-GFP mice on cFos and GFP expression in **NAc core** following U50,488 or FSS treatment. ↑;  $P < 0.05$ , ↑↑;  $P < 0.01$  vs saline/no stress, ns = not significant.

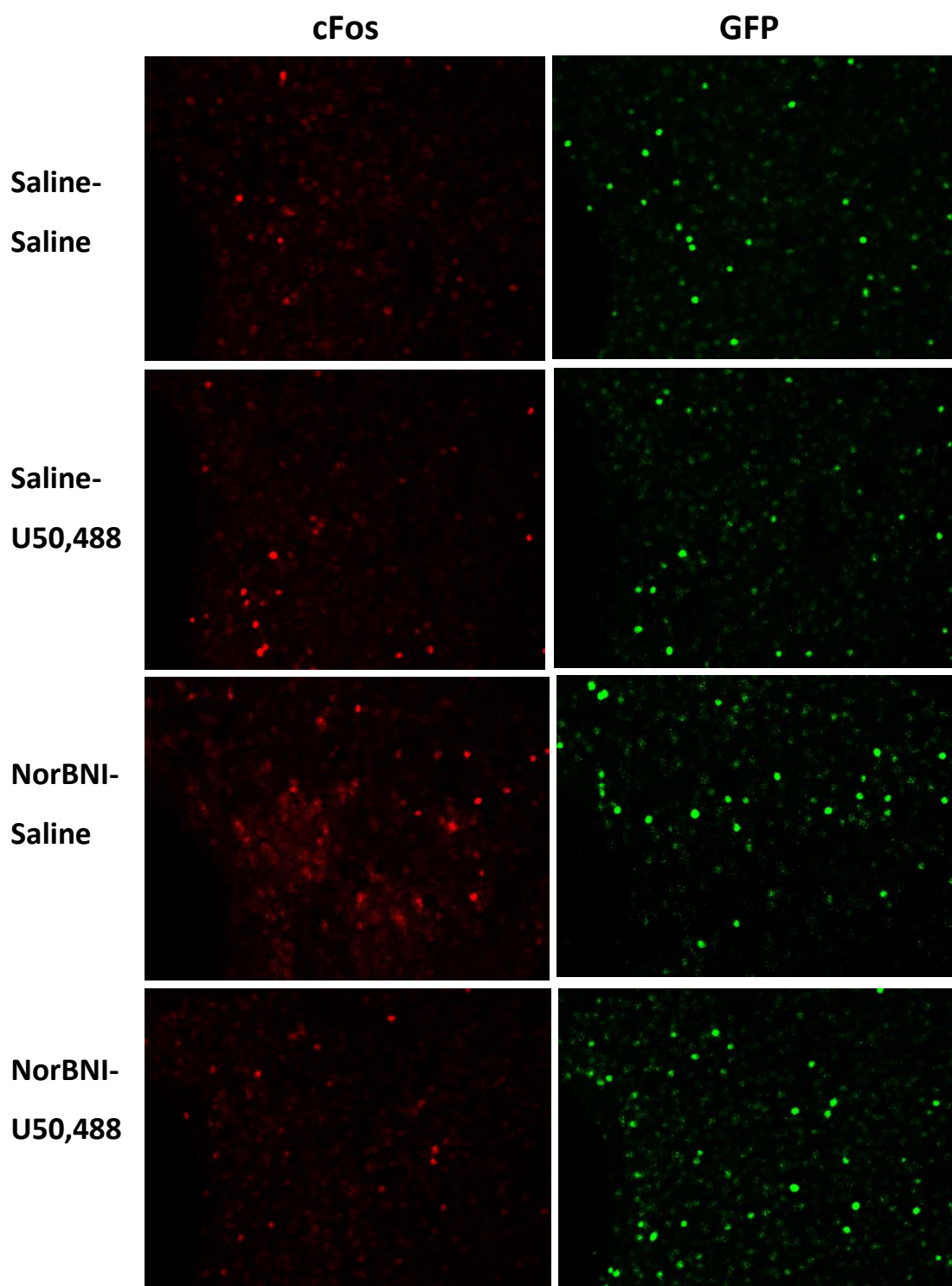


**Figure 5.2A** Fluorescent images of cFos and GFP expression in female NAc core after U50,488 injection.

cFos or GFP expression were not affected by U50,488 treatment in female NAc with or without pre-administration of norBNI. Scale bar = 100 $\mu$ m.

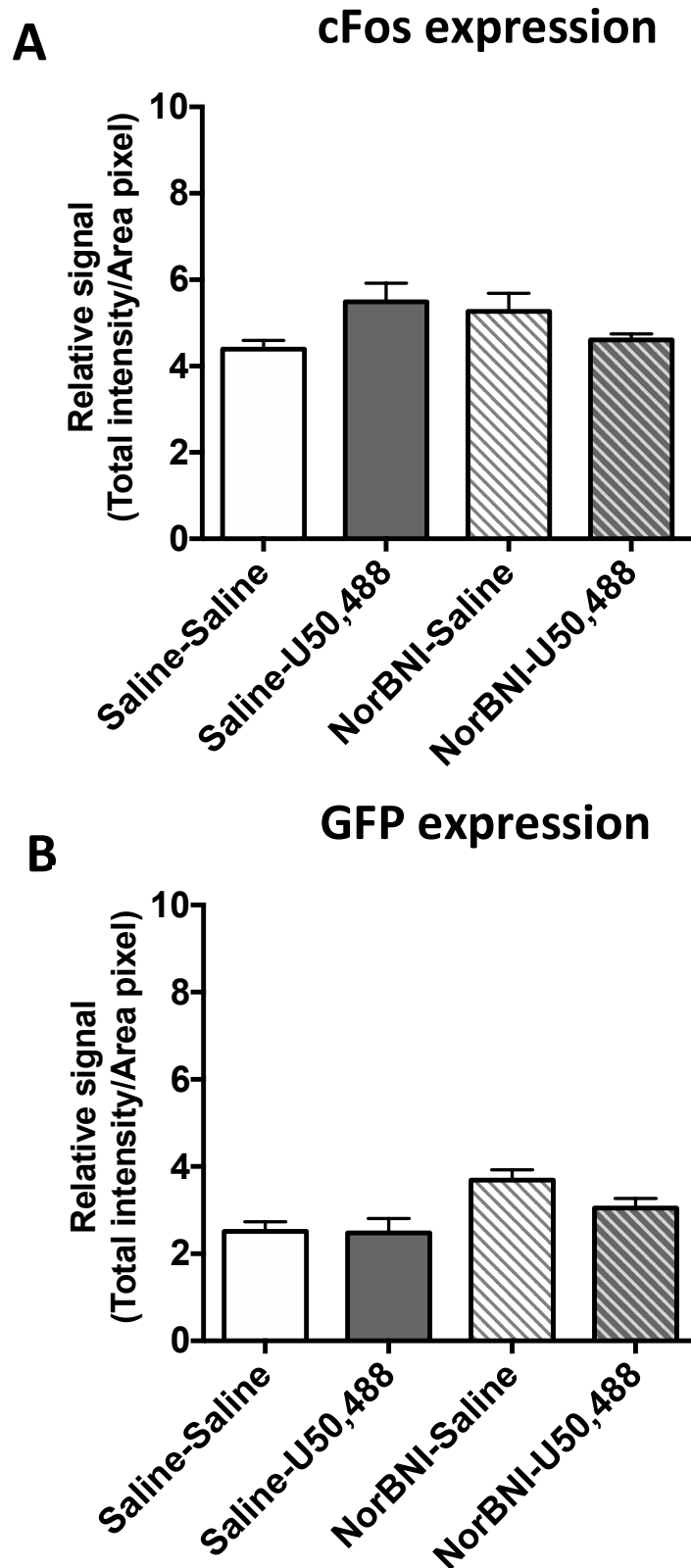


**Figure 5.2B** Quantification of fluorescent cFos and GFP signals following U50,488 in female NAc core.

**cFos (A)** and **GFP (B)** signals in female PFCx were unaffected by U50,488 treatment in the absence and presence of norBNI. All data are presented as mean  $\pm$  SEM. N = 6 animals per treatment group.



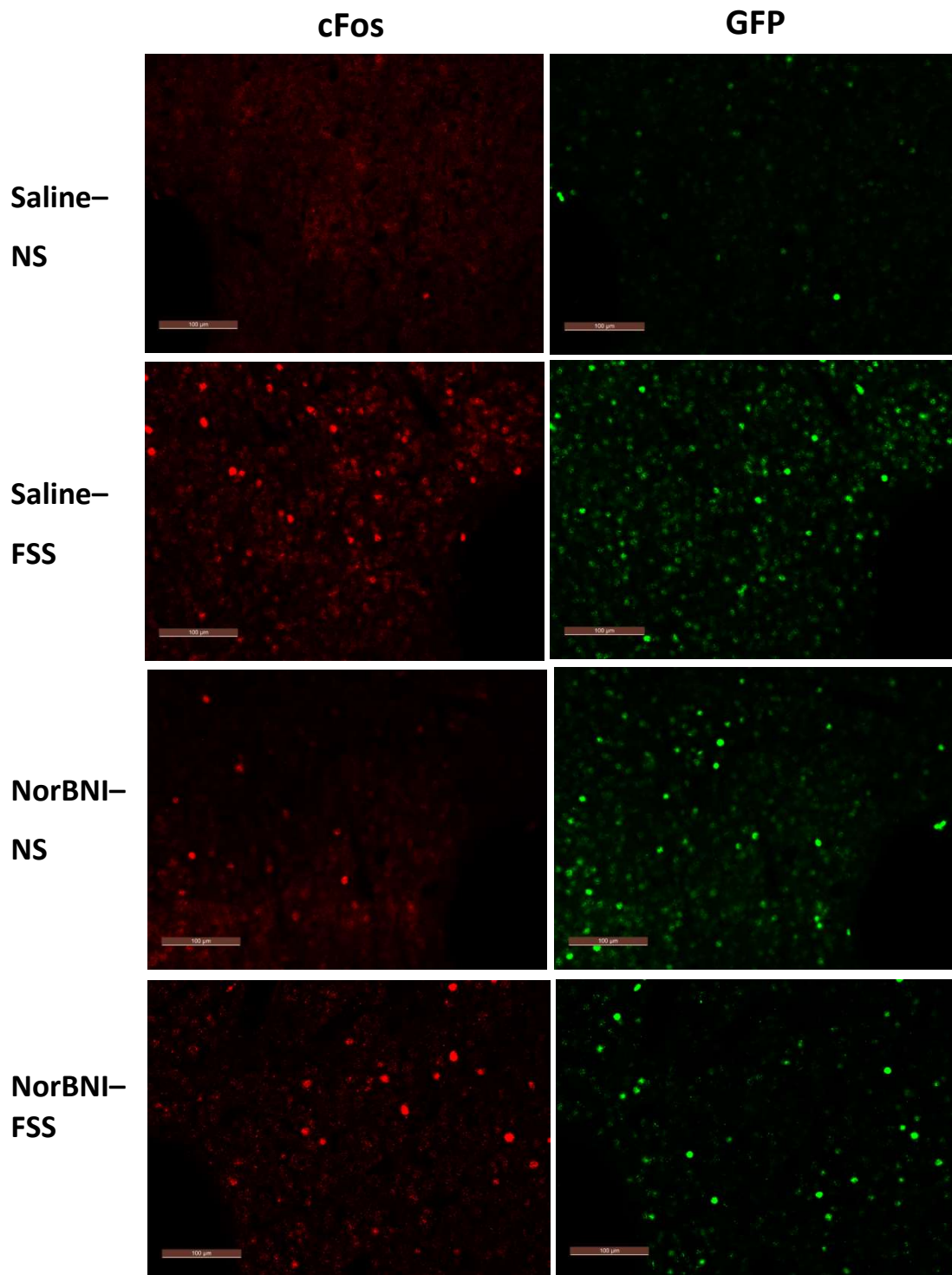


**Figure 5.2C** Fluorescent images of cFos and GFP expression in female NAc core after FSS.

cFos and GFP signals were increased following FSS. Pre-administration of norBNI had no statistically significant effect. Scale bar = 100µm.



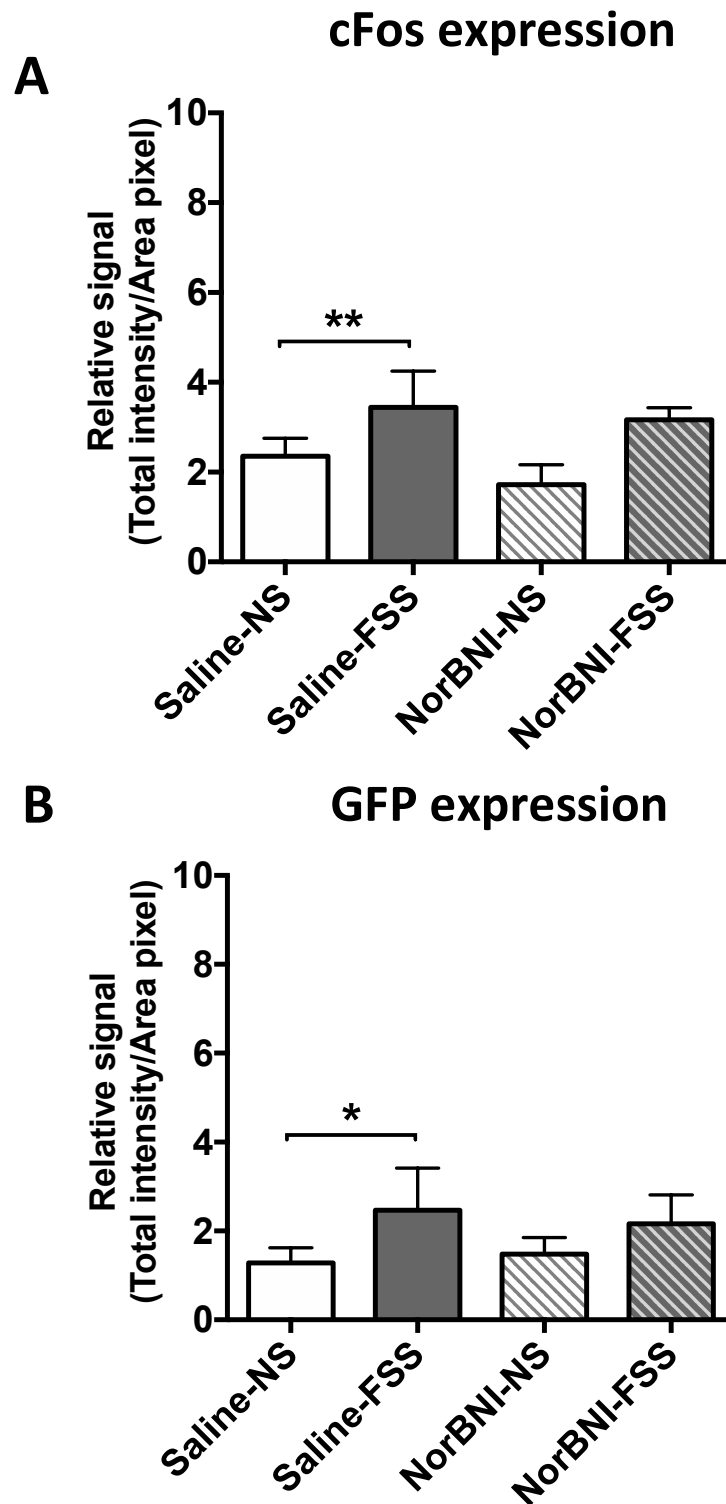


**Figure 5.2D Quantification of fluorescent cFos and GFP signals following FSS in female NAc core.**

cFos (A) and GFP (B) expression were increased by FSS in female NAc. Pre-treatment with norBNI did not have a statistically significant effect. \* =  $P < 0.05$ , \*\* =  $P < 0.01$ . All data are presented as mean  $\pm$  SEM. One-way ANOVA post-hoc Sidak's test,  $n = 6$  animals per treatment group.

### **5.3.3 The effect of U50,488 and FSS in female hippocampus**

Chapter 4 showed different effects of U50,488 and FSS in the CA1 region of the hippocampus in male mice (Sections 4.3.6 & 4.3.7) in that U50,488 treatment, but not FSS, increased both cFos and cFos-driven GFP expression neuronal activity in that region. No effects were seen in the dentate gyrus following either U50,488 treatment or FSS.

To investigate potential sex differences in the hippocampus, the same experiment was repeated in female mice. Sample images following U50,488 and FSS in the CA1 region are shown in figure 5.3A and figure 5.3C. Figure 5.3E and 5.3G shows the fluorescent images in dentate gyrus following U50,488 and FSS respectively.

Quantified signals demonstrated that KOPr activation stimulates neuronal activity in the CA1 region of hippocampus (Figure 5.3B), as seen by an increase in cFos expression, although no significant increase in cFos-driven GFP expression was seen. The increase in cFos expression by U50,488 was inhibited by pre-administration of the KOPr antagonist, norBNI. In contrast, in the FSS treatment group (Figure 5.3D), there was no increase in cFos expression or cFos-driven GFP expression in the CA1 region of the female hippocampus. Both the effect of U50,488 and FSS treatment in the female hippocampus are similar to those previously observed in the male hippocampus. Furthermore, as previously seen in the dentate gyrus region from male mice, there was no increase in cFos expression in the dentate gyrus region from female mice, either following U50,488 injection or FSS treatment (Figure 5.3F, 5.3H). The effects of U50,488 or FSS on cFos expression in CA1 region of hippocampus between male and female mice are summarised in table 5.3, and dentate gyrus in table 5.4.

Overall, similar cFos expression patterns were observed between male and female mice suggesting that the neuronal activity in the hippocampus in response to KOPr activation or stress is not sex-dependent.

	Male		Female	
	cFos	GFP	cFos	GFP
U50,488 treatment	↑	↑↑	↑↑↑	ns
15-minute FSS	ns	ns	ns	ns

**Table 5.3.** Comparison between male and female cFos-GFP mice on cFos and GFP expression in **CA1 region of hippocampus** following U50,488 or FSS treatment. ↑; P < 0.05, ↑↑; P < 0.01, ↑↑↑; P < 0.001 vs saline/no stress, ns = not significant.

	Male		Female	
	cFos	GFP	cFos	GFP
U50,488 treatment	ns	ns	ns	ns
15-minute FSS	ns	ns	ns	ns

**Table 5.4.** Comparison between male and female cFos-GFP mice on cFos and GFP expression in **dentate gyrus** following U50,488 or FSS treatment, ns = not significant vs saline/no stress.

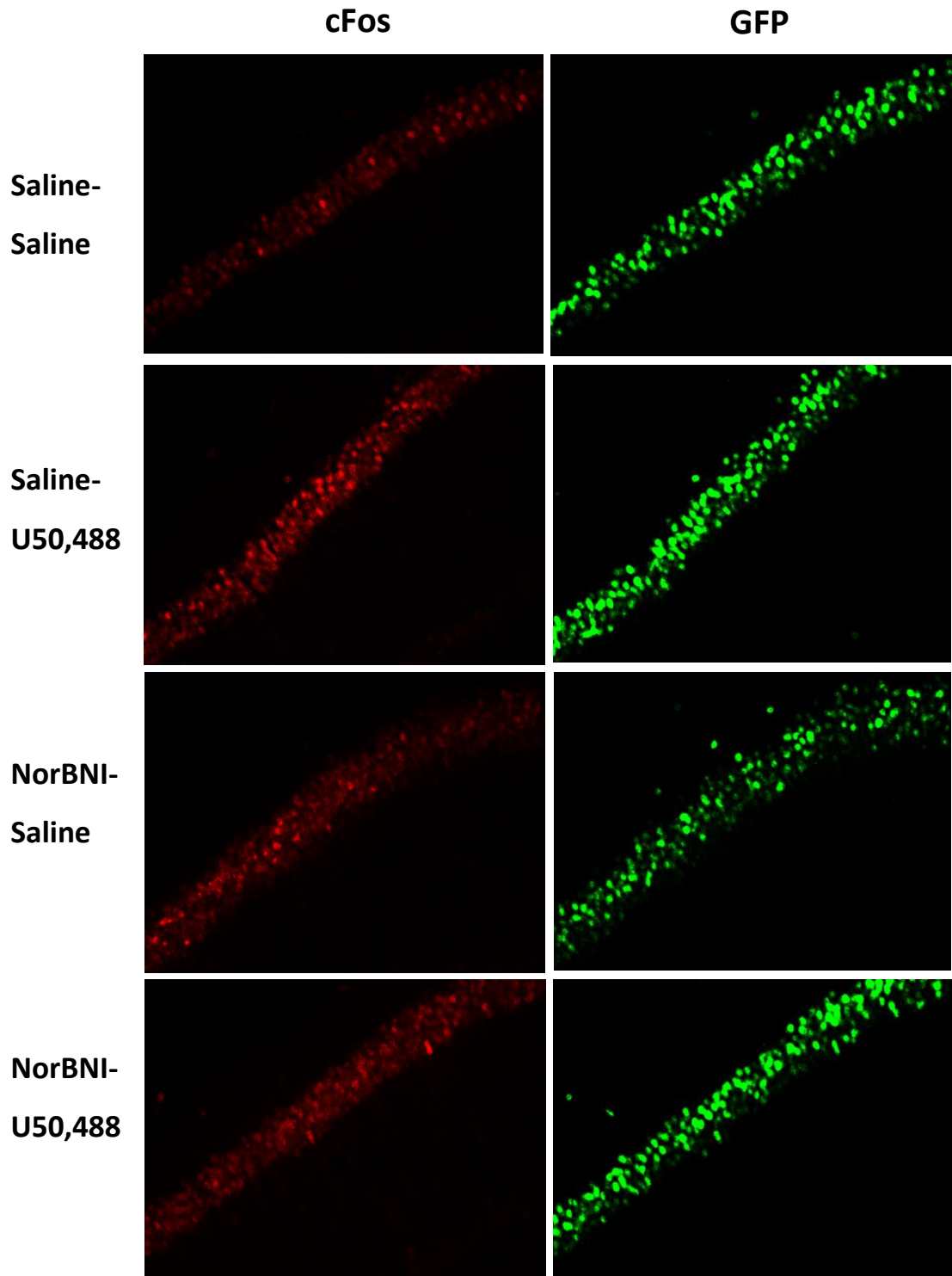


**Figure 5.3A** Fluorescent images of cFos and GFP expression in female CA1 region of hippocampus after U50,488 injection.

U50,488 treatment increased cFos expression, but not in cFos-driven GFP expression, in the hippocampal CA1 region in female mice. Scale bar = 100 $\mu$ m.

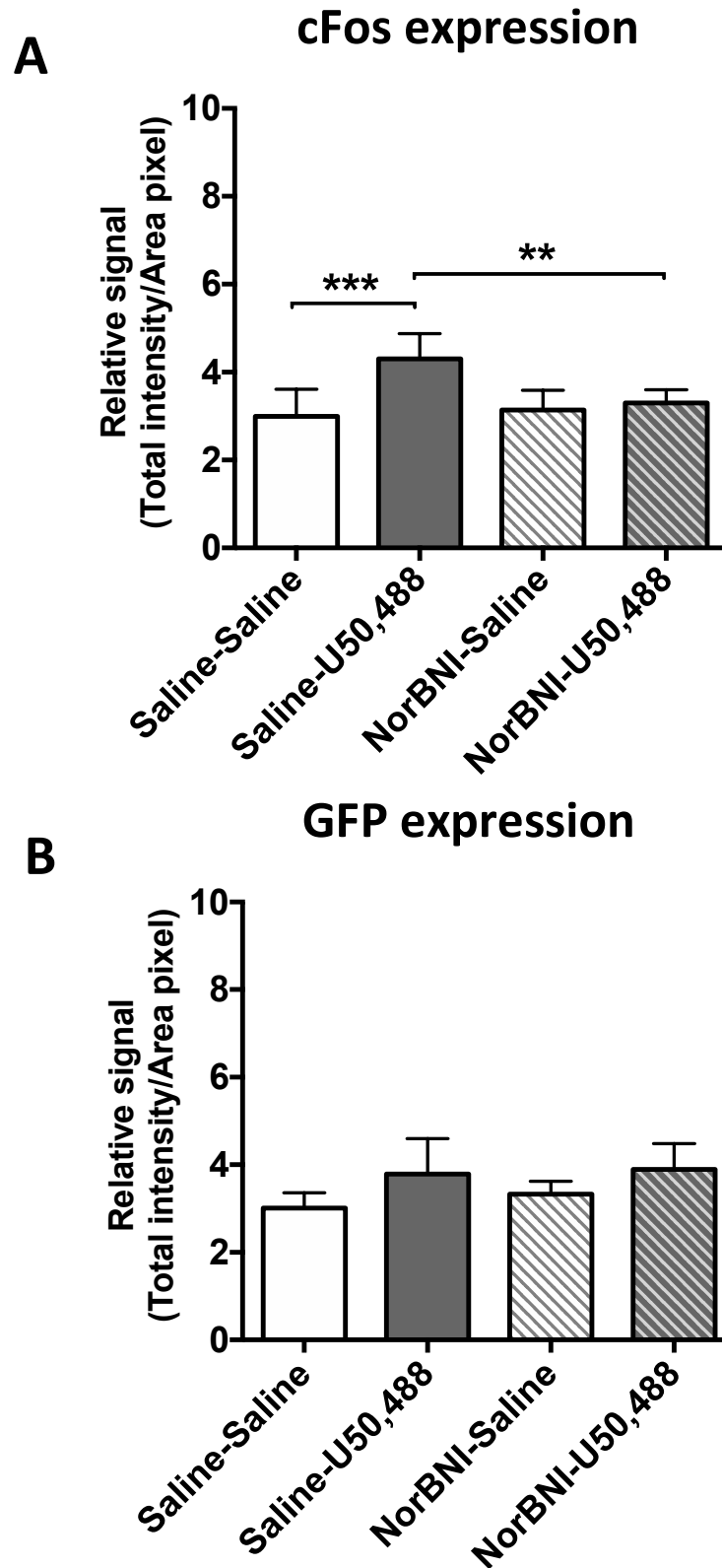


**Figure 5.3B Quantification of fluorescent cFos and GFP signals following U50,488 in female hippocampal CA1.**

U50,488 increased expression of **cFos** (**A**) but did not significantly increase cFos-driven **GFP** expression (**B**) in the hippocampal CA1 in female mice. \*\* =  $P < 0.01$ , \*\*\* =  $P < 0.001$ . All data are shown as mean  $\pm$  SEM. One-way ANOVA post-hoc Sidak's test,  $n = 6$  animals per treatment group.

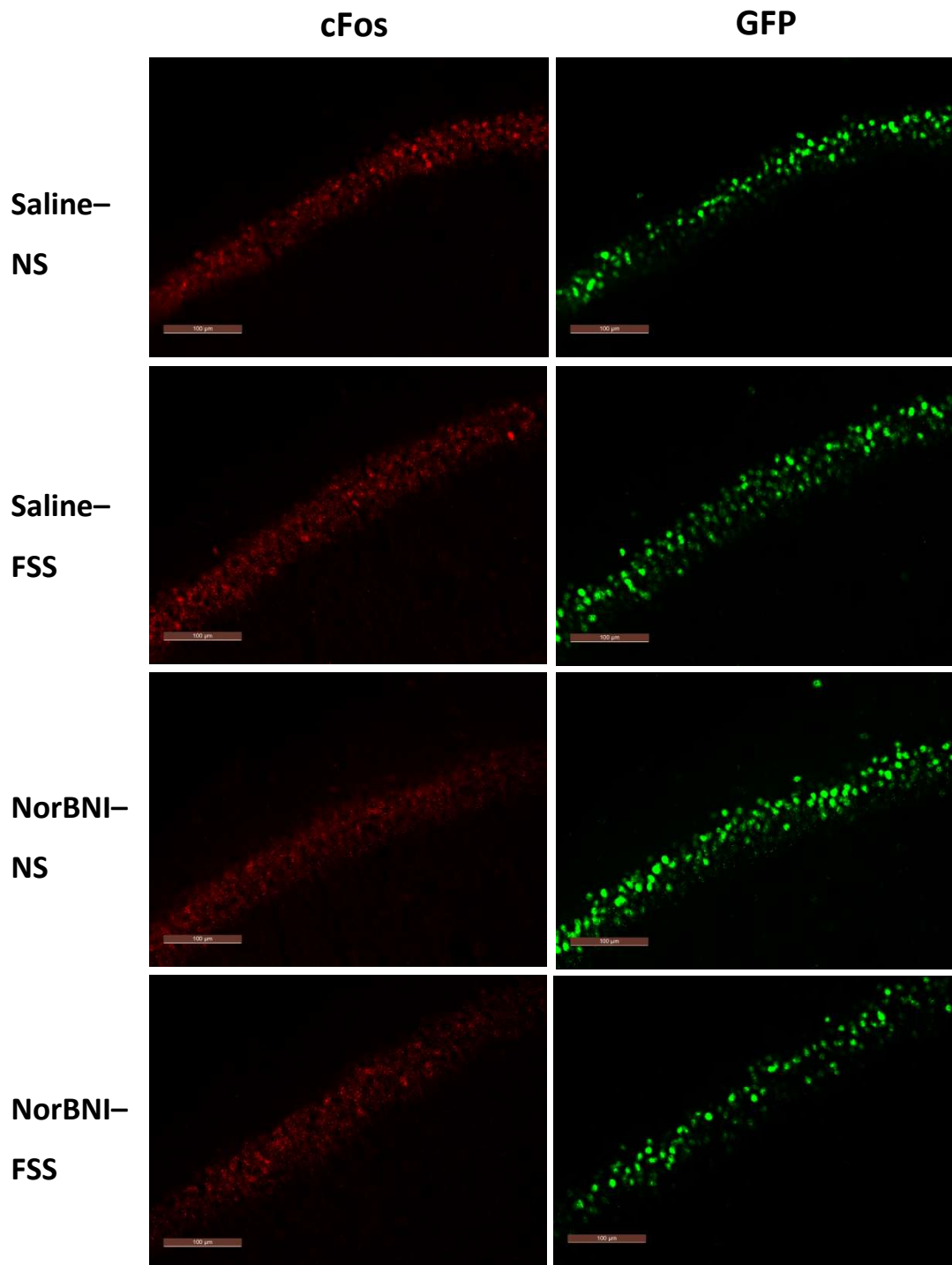


**Figure 5.3C** Fluorescent images of cFos and GFP expression in female hippocampal CA1 region after FSS.

FSS did not affect either cFos or GFP signals. NorBNI pretreatment also had no effect on either cFos or GFP expression. Scale bar = 100μm.

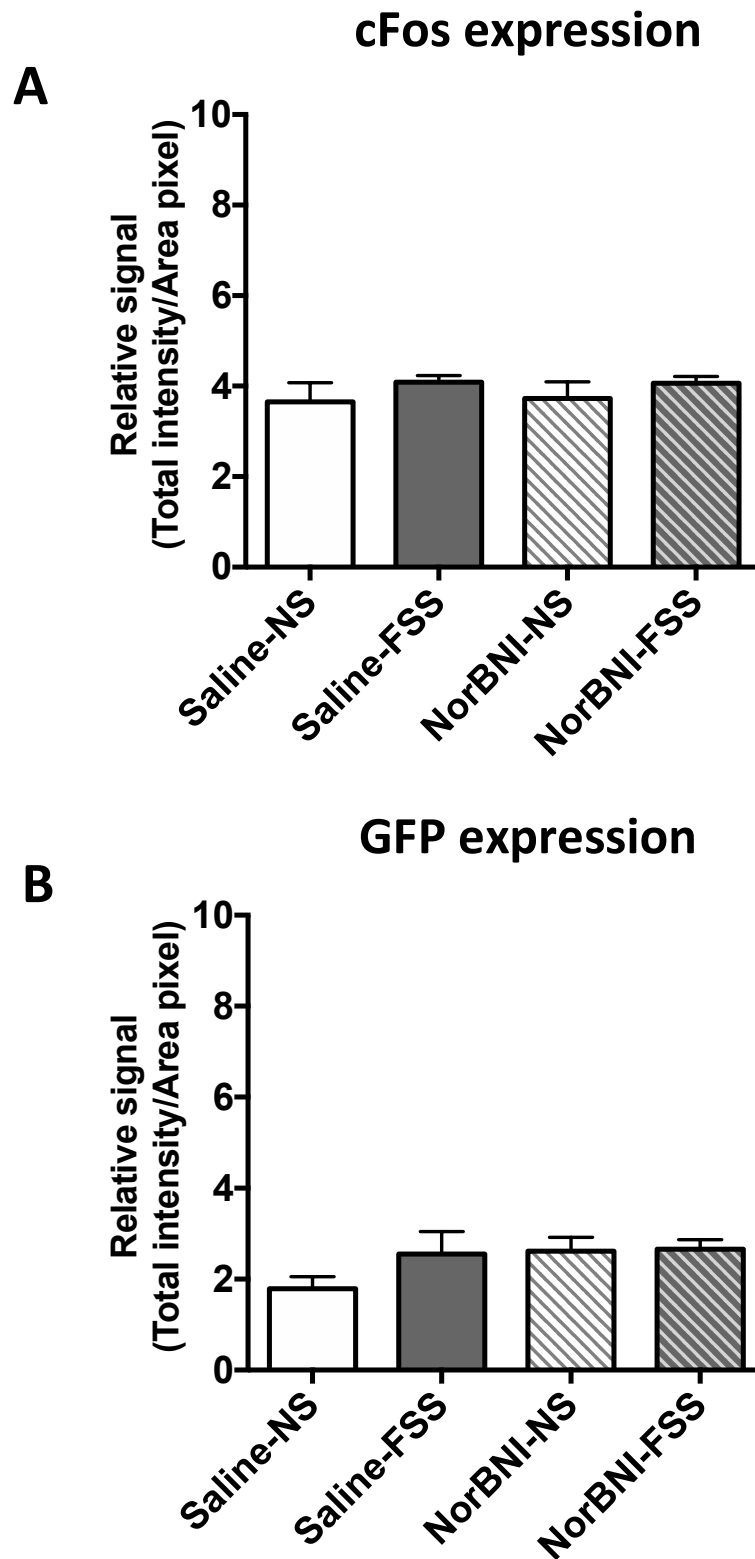


**Figure 5.3D Quantification of fluorescent cFos and GFP signals following FSS in female hippocampal CA1 region.**

**cFos (A) and GFP (B)** signals in the hippocampal CA1 region of female mice were not affected by FSS. All data are shown as mean  $\pm$  SEM. N = 6 animals per treatment group.

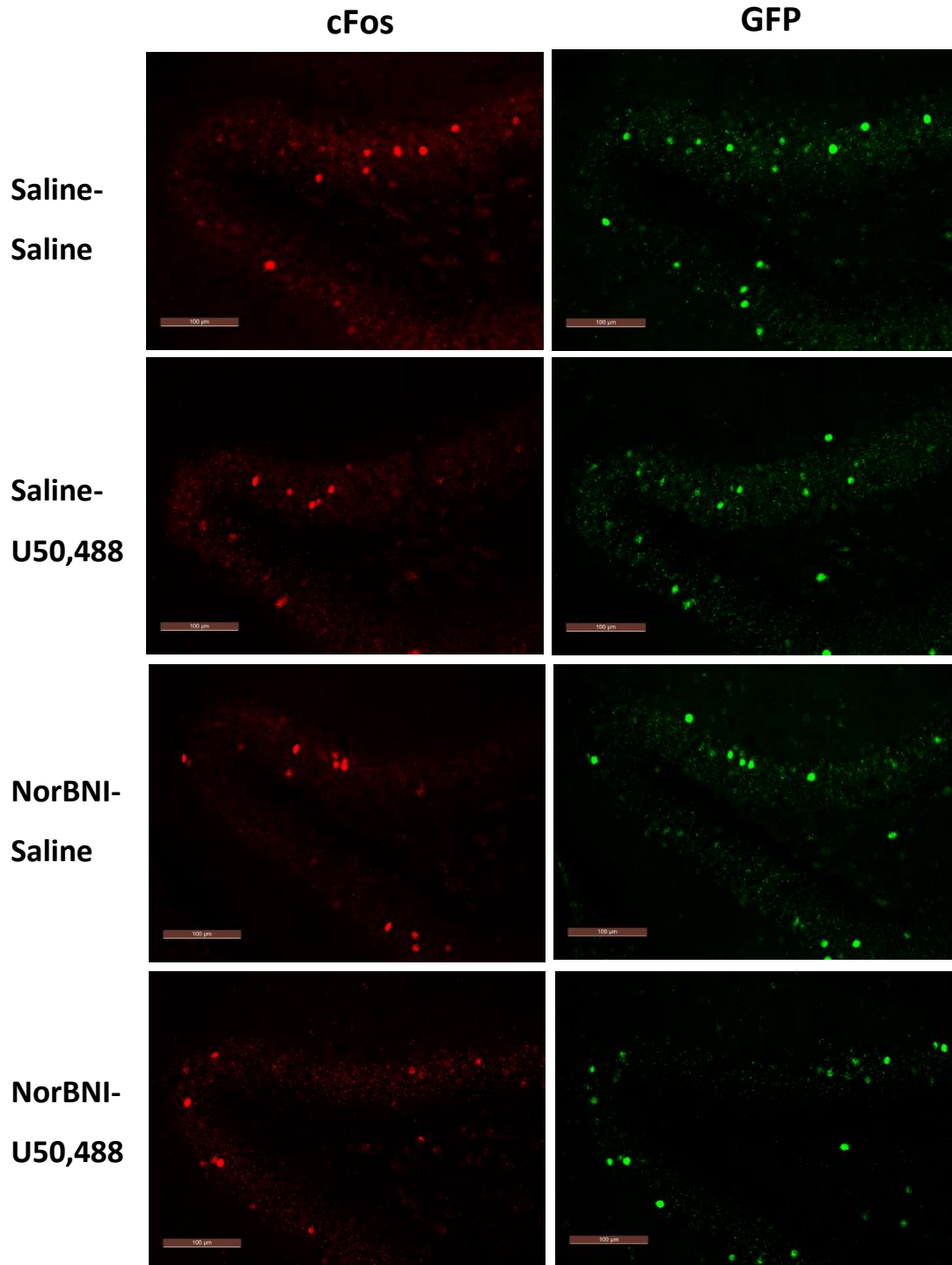


**Figure 5.3E** Fluorescent images of cFos and GFP expression in female dentate gyrus region of hippocampus after U50,488 injection. Neither cFos nor GFP expression was affected by U50,488 treatment in female hippocampal dentate gyrus region. Scale bar = 100 $\mu$ m.



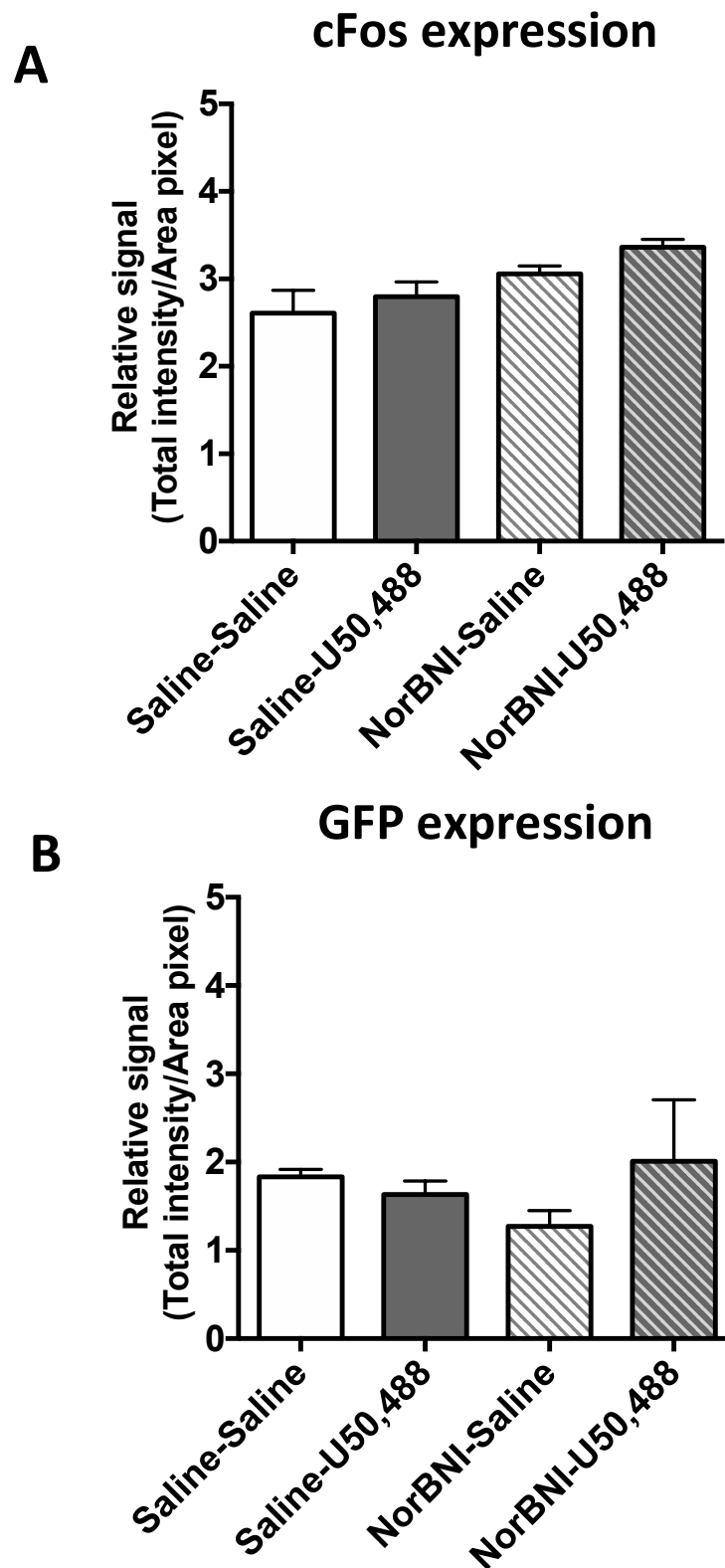


**Figure 5.3F** Quantification of fluorescent cFos and GFP signals following U50,488 in female hippocampal dentate gyrus.

**cFos (A)** signals and **GFP (B)** signals were not affected by U50,488 in female hippocampal dentate gyrus. All data are presented as mean  $\pm$  SEM. N = 6 animals per treatment group.

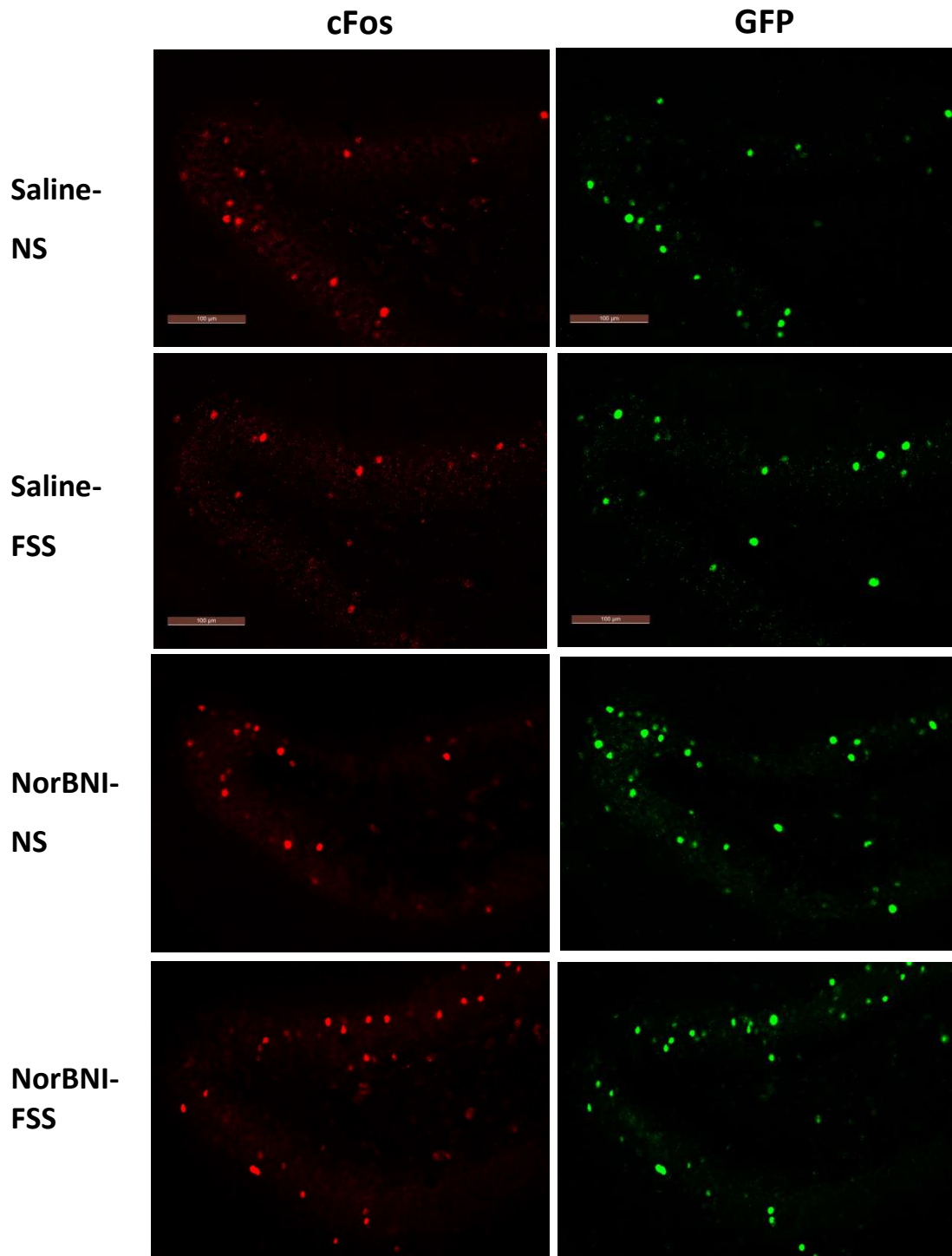


**Figure 5.3G** Fluorescent images of cFos and GFP expression in female dentate gyrus region of hippocampus FSS.

Neither cFos nor GFP expression was affected by 15-minute FSS in female hippocampal dentate gyrus region. Scale bar = 100μm.

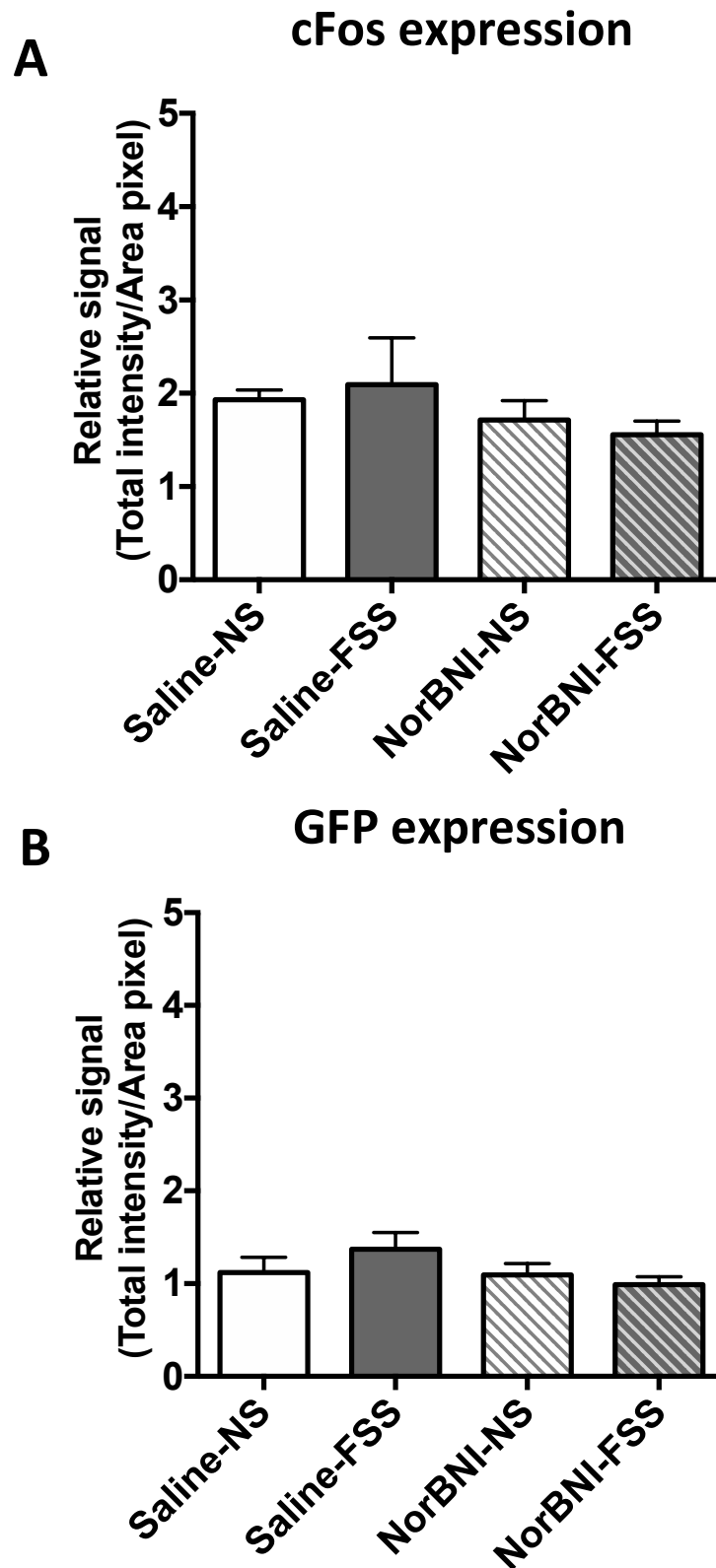


**Figure 5.3H** Quantification of fluorescent cFos and GFP signals following FSS in female hippocampal dentate gyrus.

**cFos (A)** signals and **GFP (B)** signals were not affected by FSS in female hippocampal dentate gyrus. All data are expressed as mean  $\pm$  SEM. N = 6 animals per treatment group.

### 5.3.4 The effect of U50,488 and FSS in female amygdala

It was previously demonstrated (Chapter 4) that both U50,488 and FSS induced cFos and cFos-driven GFP expression in the basolateral amygdala (BLA) in male mice, but different effects were observed following U50,488 and FSS treatment in the central amygdala (CeA) in that U50,488, but not FSS, induced cFos and GFP expression in male mice (Sections 4.3.8 & 4.3.9).

In order to test if there are any sex differences in the amygdala, the experiment was repeated in female mice. Fluorescent images showing the effects of U50,488 and FSS on CeA are shown in figures 5.4A & 5.4C and sample images in BLA are shown in figures 5.4E & 5.4G. The fluorescent signals were quantified and illustrated in Figure 5.4B, 5.4D, 5.4F & 5.4H.

In the CeA, KOPr activation significantly induced both cFos and cFos-driven GFP expression, and the effects was significantly inhibited by norBNI pre-treatment (Figure 5.4B), whereas no increase in cFos and GFP expression were seen after FSS treatment (Figure 5.4D). These findings in the female CeA are similar to that of in the CeA in male mice (Table 5.5). In addition, similar to the effects observed in male mice, both U50,488 and FSS treatment significantly increased cFos and GFP expression in the BLA in female mice (Figure 5.4F, 5.4H), which were also significantly reduced by the pre-administration of norBNI. The U50,488- or FSS-induced effects on CeA in both male and female mice are summarised in table 5.5, while these effects in BLA between male and female mice are summarised in table 5.6.

Overall, the effects of U50,488 and FSS on both CeA and BLA in female mice are similar to the effects observed in male amygdala, indicating that there is no sex difference in response to KOPr activation and *in vivo* stress in the amygdala.

	Male		Female	
	cFos	GFP	cFos	GFP
U50,488 treatment	↑	↑	↑	↑↑
15-minute FSS	ns	ns	ns	ns

**Table 5.5.** Summary of U50,488 or FSS-induced effects in **CeA** in both male and female cFos-GFP mice. ↑; P < 0.05, ↑↑; P < 0.01 vs saline/no stress, ns = not significant.

	Male		Female	
	cFos	GFP	cFos	GFP
U50,488 treatment	↑↑	↑↑	↑↑↑	↑↑
15-minute FSS	↑	↑	↑↑↑	↑

**Table 5.6.** Summary of U50,488 or FSS-induced effects in **BLA** in both male and female cFos-GFP mice. ↑; P < 0.05, ↑↑; P < 0.01, ↑↑↑; P < 0.001 vs saline/no stress.

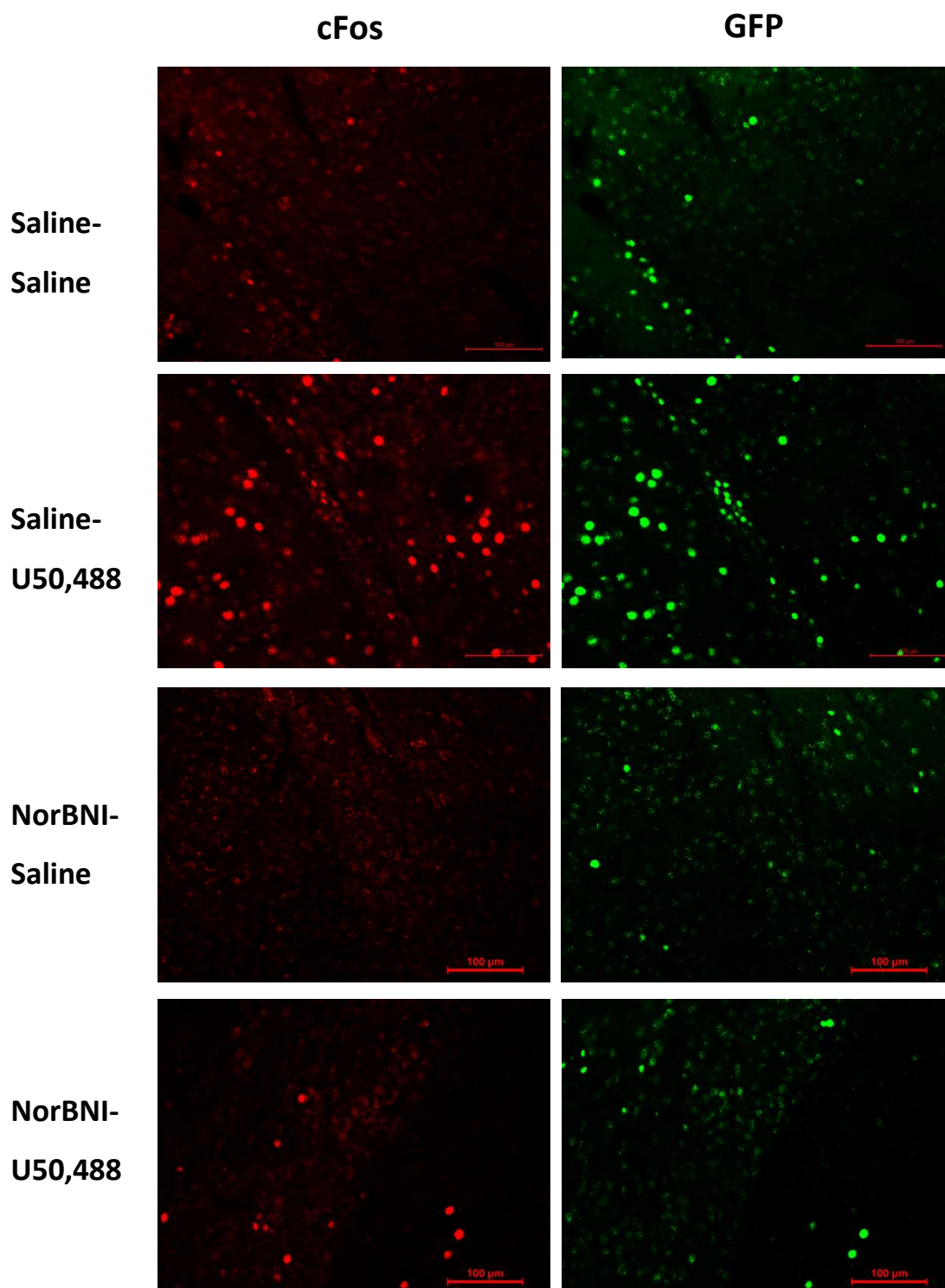


**Figure 5.4A** Fluorescent images of cFos and GFP expression in CeA following a single U50,488 (20mg/kg) administration.

Expression of both cFos and GFP was increased after U50,488 treatment, compared to the control saline-treated groups. The effects were inhibited by pretreatment with norBNI. Scale bar = 100μm.

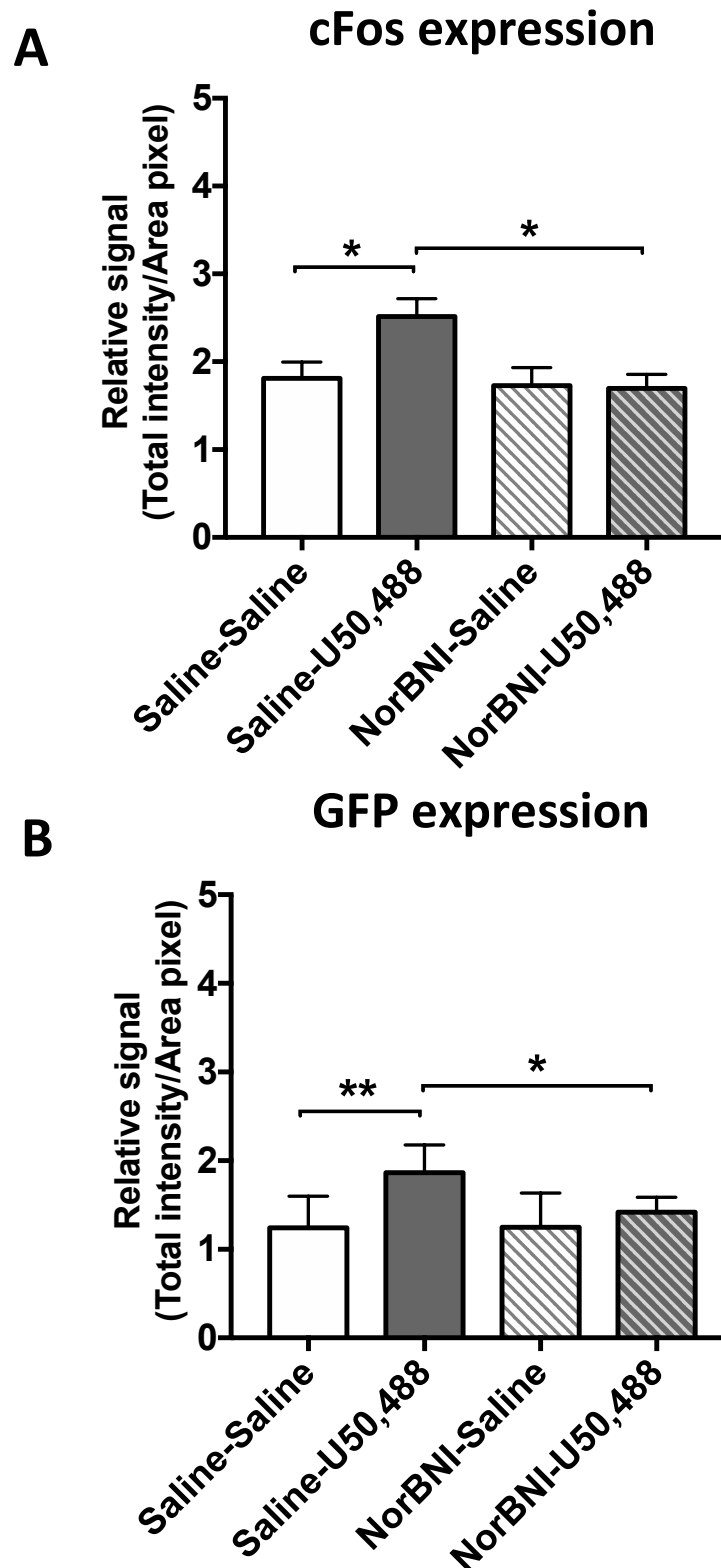


**Figure 5.4B** Quantified fluorescent cFos and GFP signals following U50,488 treatment in CeA in female mice.

U50,488 increased both cFos (A) and GFP (B) signals. The effect was blocked by norBNI (10mg/kg) pre-administration. Data are expressed as mean  $\pm$  SEM. One-way ANOVA post-hoc Sidak's test, \* =  $P < 0.05$ , \*\* =  $P < 0.01$ ,  $n = 6$  animals per treatment group.

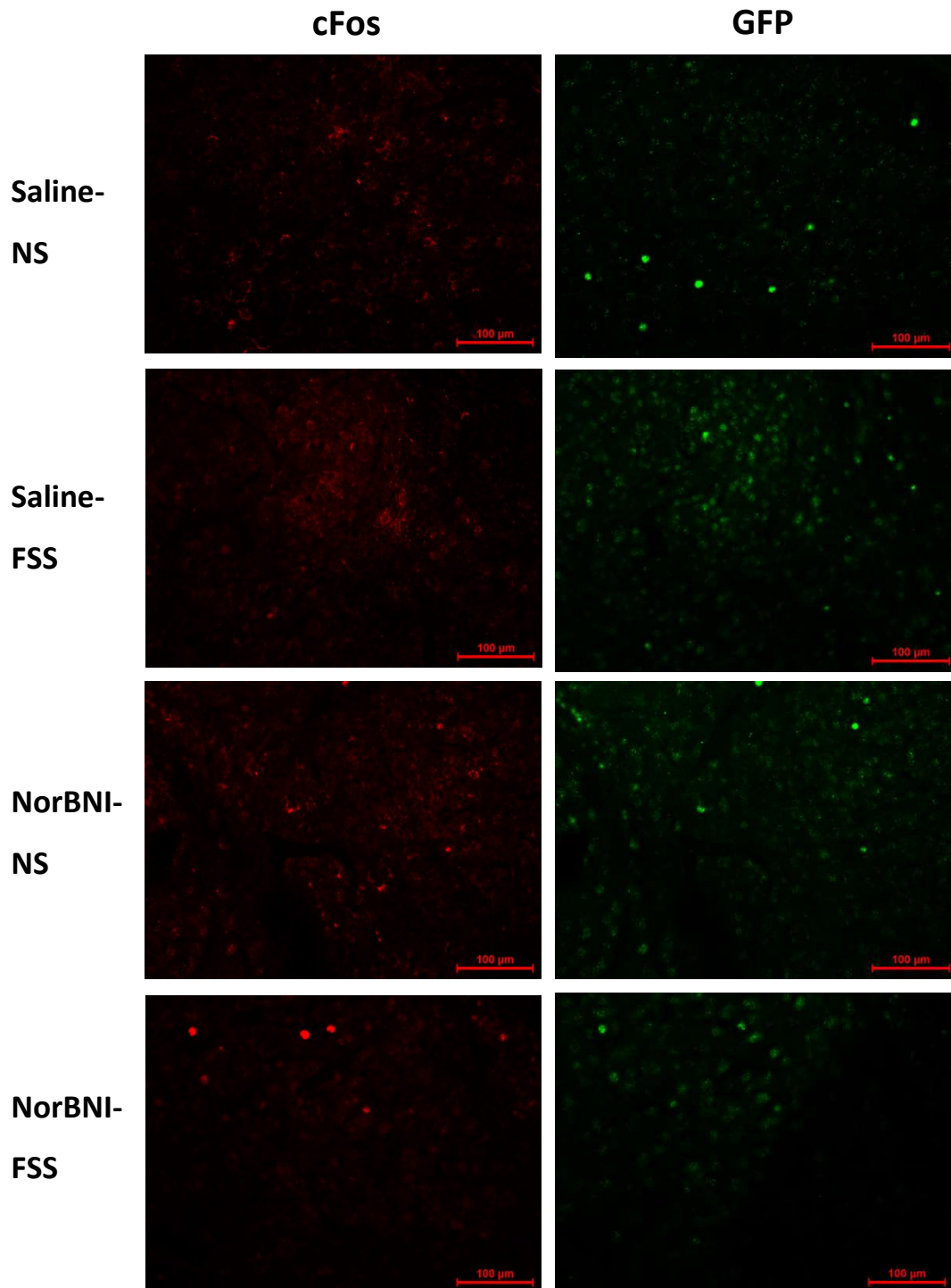


**Figure 5.4C** Typical expression pattern of cFos and GFP in CeA from female mice after FSS.

No changes in the expression of cFos and GFP were seen following FSS in the absence and presence of norBNI pre-treatment. Scale bar = 100 $\mu$ m.



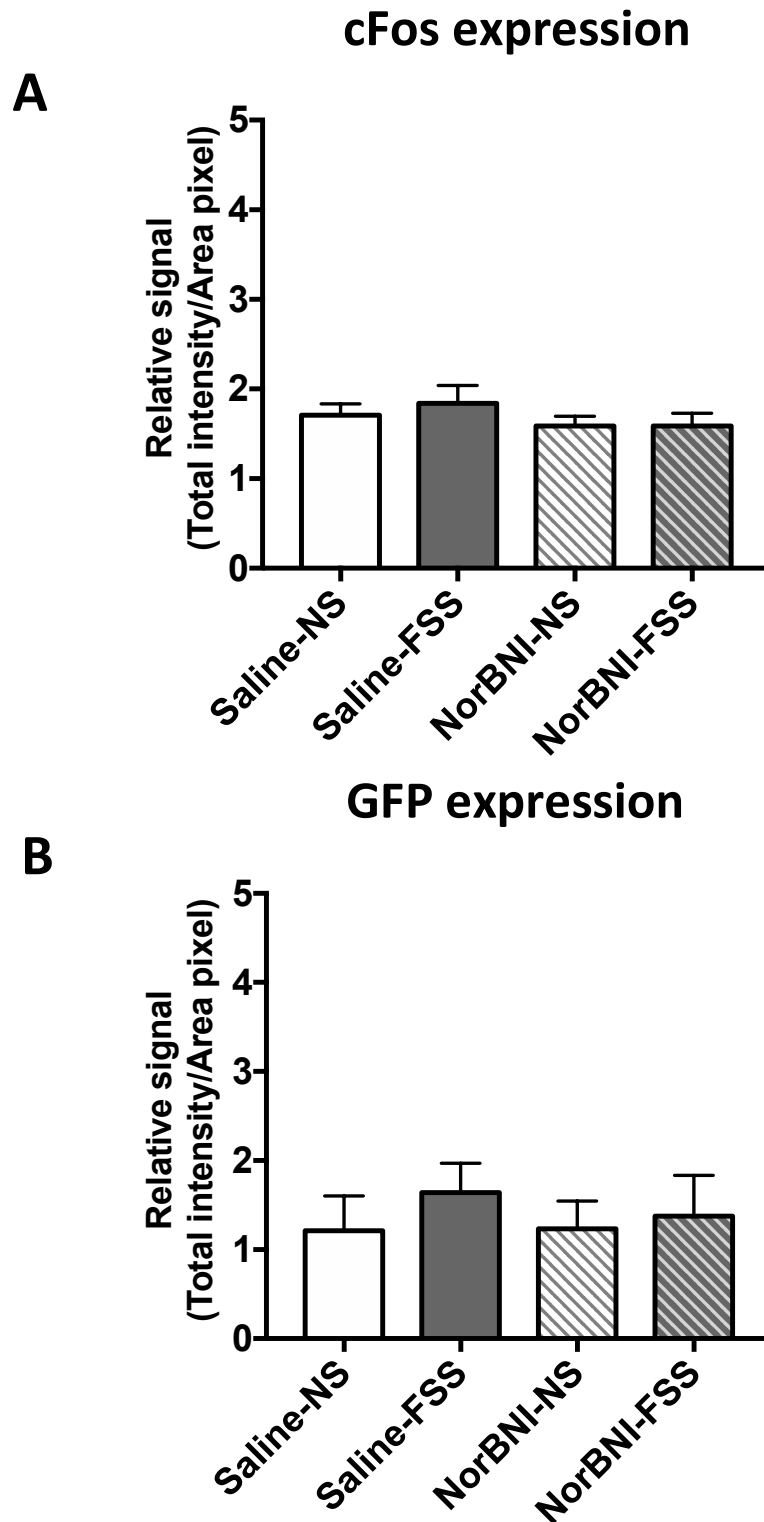


**Figure 5.4D Quantified fluorescent cFos and GFP signals following FSS in CeA in female mice.**

FSS did not change **cFos (A)** or **GFP (B)** signals in the absence and presence of norBNI (10mg/kg) pre-administration. Data are expressed as mean  $\pm$  SEM. N = 6 animals per treatment group.

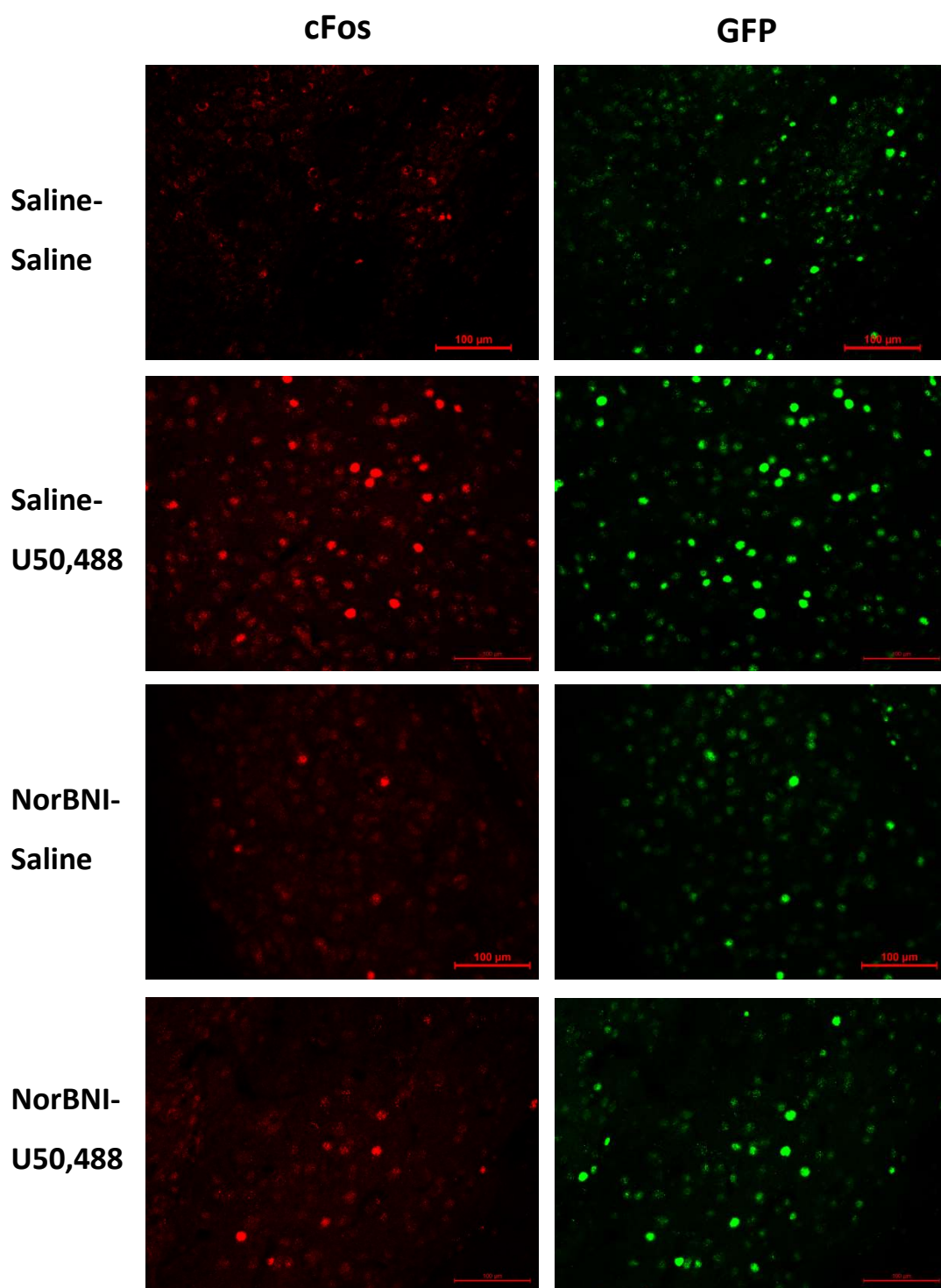


**Figure 5.4E** Fluorescent images of cFos and GFP expression in BLA of female mice following a single U50,488 (20mg/kg) treatment.

U50,488 increased both cFos and GFP expression, compared to the control saline-treated groups. The effects was inhibited by norBNI pre-treatment. Scale bar = 100μm.

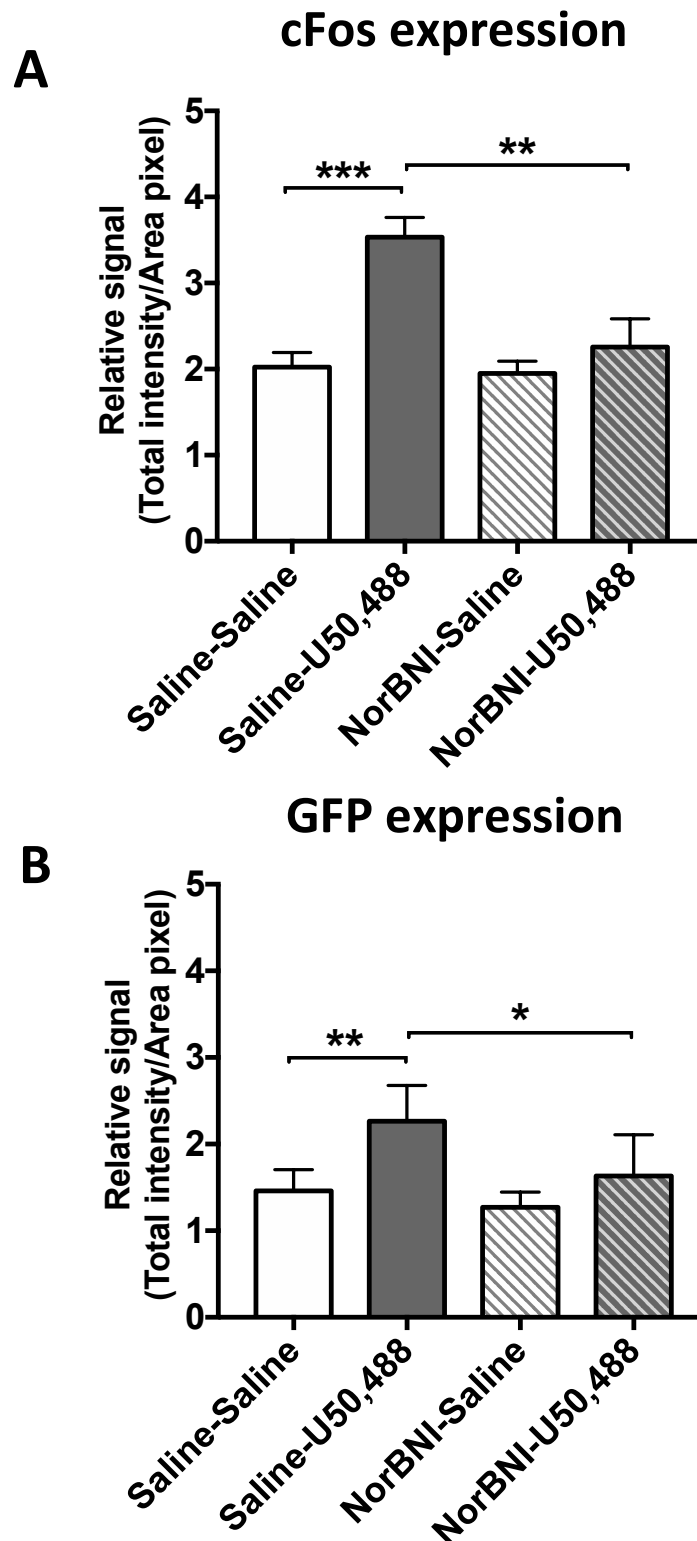


**Figure 5.4F** Quantified fluorescent cFos and GFP signals following U50,488 injection in BLA of female mice.

Both cFos (A) or GFP (B) signals were significantly increased by U50,488 treatment. The effects was significantly inhibited by norBNI (10mg/kg) pre-treatment. Data are expressed as mean  $\pm$  SEM. One-way ANOVA post-hoc Sidak's test, \* =  $P < 0.05$ , \*\* =  $p < 0.01$ , \*\*\* =  $p < 0.001$ ,  $n = 6$  animals per treatment group.

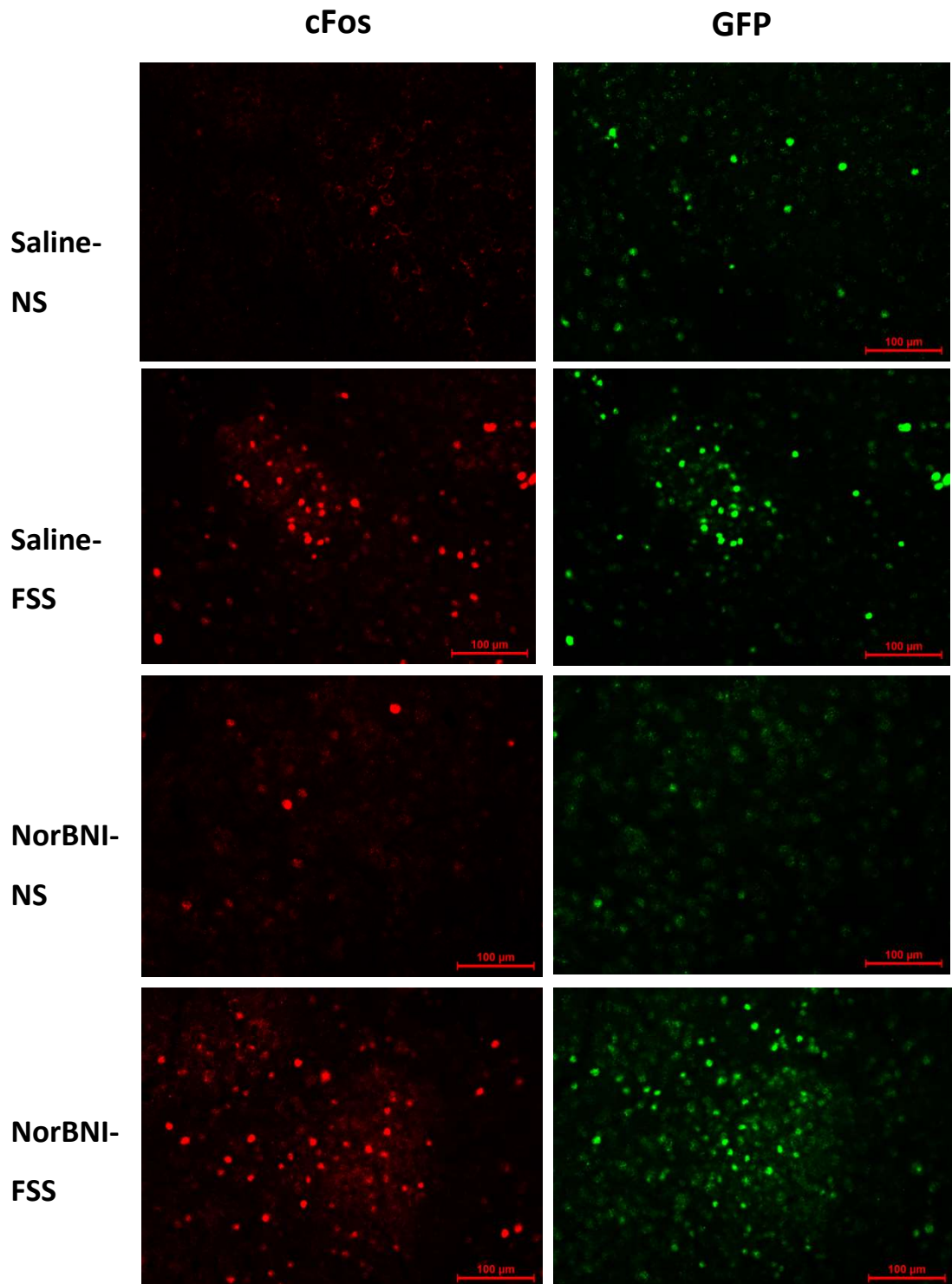


**Figure 5.4G** Fluorescent images of cFos and GFP expression pattern in BLA of female mice after FSS.

FSS significantly increased both cFos and GFP expression following FSS, Pretreatment of norBNI had no effect. Scale bar = 100 $\mu$ m.

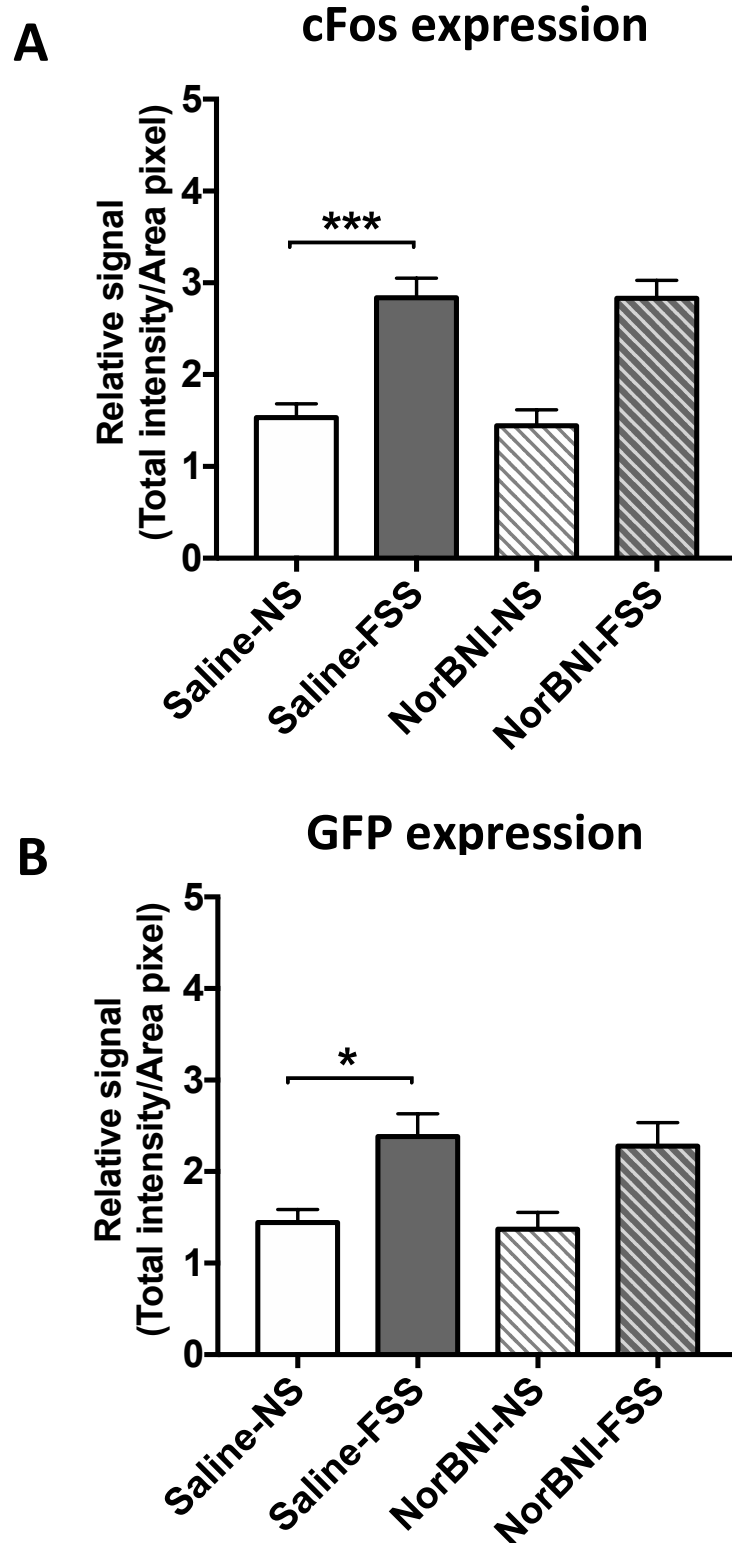


**Figure 5.4H** Quantification of fluorescent signals following FSS in BLA in female mice.

FSS increased both **cFos (A)** or **GFP (B)** signals. These stress-induced effects were not blocked by norBNI pre-treatment. Data are expressed as mean  $\pm$  SEM. One-way ANOVA post-hoc Sidak's test, \* =  $P < 0.05$ , \*\*\* =  $p < 0.001$ ,  $n = 6$  animals per treatment group.

## 5.4 Discussion

The effects of KOPr activation and an *in vivo* stressor in different brain regions in female mice are summarised in Table 5.7.

	U50,488 (20mg/kg)			
	cFos	norBNI	GFP	norBNI
PFCx	ns	ns	ns	ns
NAcc	ns	ns	ns	ns
Hippocampal CA1	↑↑↑	**	ns	ns
Hippocampal DG	ns	ns	ns	ns
Central Amygdala (CeA)	↑	*	↑↑	*
Basolateral Amygdala (BIA)	↑↑↑	**	↑↑	*
	FSS (15 minutes)			
	cFos	norBNI	GFP	norBNI
PFCx	ns	ns	ns	ns
NAcc	↑↑	ns	↑	ns
Hippocampal CA1	ns	ns	ns	ns
Hippocampal DG	ns	ns	ns	ns
Central Amygdala (CeA)	ns	ns	ns	ns
Basolateral Amygdala (BIA)	↑↑↑	ns	↑	ns

**Table 5.7. Summary of cFos and cFos-induced GFP expression in different brain regions in female mice following KOPr activation (U50,488) and *in vivo* stress (FSS).** Prefrontal cortex (PFCx), nucleus accumbens (NAc), CA1, dentate gyrus region of hippocampus (Hippocampal CA1, DG), basolateral amygdala (BLA), central amygdala (CeA), ↑ < 0.05; \* < 0.05; ↑↑ < 0.01; \*\* < 0.01; ↑↑↑ < 0.001; ns = not significant.

A single administration of KOPr agonist U50,488 induced cFos expression in the CA1 region of the hippocampus, central amygdala and basolateral amygdala, with no increase in cFos expression seen in the dentate gyrus region of the hippocampus. These effects were inhibited by pre-administration of the KOPr antagonist, norBNI.

Surprisingly, in the CA1 region of the hippocampus, U50,488 induced a robust and highly significant increase in cFos expression, but no significant increase in cFos-driven GFP expression. As outlined in Chapter 4, in these mice, we would expect cFos expression from a given stimulus to occur first, before cFos-driven GFP expression, and for cFos-driven GFP expression to persist longer than cFos expression. Therefore,

as there is cFos, but not GFP expression in the CA1 region of the hippocampus following U50,488 administration, however, both cFos and GFP expression is seen in the amygdala of the same animals. The different cFos and cFos-driven GFP expression pattern between hippocampus and amygdala might suggest that U50,488 induces neuronal activation in the amygdala before the hippocampus.

Further, this pattern of cFos and GFP expression in the CA1 region of the female hippocampus is different to that seen in males, and, there are more profound differences between the patterns of cFos and GFP expression between male and female animals. These are summarized in Table 5.8.

	<b>U50,488 (20mg/kg)</b>		<b>FSS (15 minutes)</b>	
	<b>cFos</b>	<b>GFP</b>	<b>cFos</b>	<b>GFP</b>
<b>PFCx</b>	□ □	□	□ □	□ □
<b>NAc</b>	□ □	□	□ □ □ □	□ □ □
<b>Hippocampal CA1</b>	□ □ □ □	□ □		
<b>Hippocampal DG</b>				
<b>Central Amygdala (CeA)</b>	□ □ □	□ □ □		
<b>Basolateral Amygdala (BLA)</b>	□ □ □ □ □	□ □ □ □ □	□ □ □ □ □	□ □ □ □ □

**Table 5.8. Summary of the sex differences in the expression of cFos and GFP following U50,488 and FSS treatment.** Prefrontal cortex (PFCx), nucleus accumbens (NAc), CA1, dentate gyrus region of hippocampus (Hippocampal CA1, DG), basolateral amygdala (BLA), central amygdala (CeA). The number of sex symbols indicate the level of significance; ♂, ♀ < 0.05; ♂♂, ♀♀ < 0.01; ♂♂♂, ♀♀♀ < 0.001.

In the hippocampal CA1 region, in male mice U50,488 administration increased both cFos and cFos-driven GFP expression. In contrast, in female mice, only an increase in cFos expression was observed. As mentioned before, GFP is only induced following cFos expression, meaning that cFos is induced first, GFP occurs later than cFos expression. For the reasons outlined above, a potential explanation for this is that KOPr activation activates CA1 neurons in male mice sooner than in female mice, i.e. there was no time for GFP to be expressed in female mice. There are no previous studies that have shown these effects, but this hypothesis could be supported by extending the time-points where c-Fos expression is investigated following U50,488 treatment.

Table 5.8 also shows more profound, and surprising, differences in neuronal activation between male and female mice. Although U50,488 induces neuronal activation in the PFCx and NAc in male mice (as seen by both increased expression of both cFos and cFos-driven GFP), the same treatment had no effect in the same brain regions in female mice.

Following FSS, again sex-dependent patterns of neuronal activation were seen. In both male and female mice, FSS induced cFos and cFos-driven GFP in both the NAc and BLA. However, neuronal activation in the PFCx was only seen in male mice, not in female mice.

These findings show sex differences in response to KOPr and stress in these brain regions, which may contribute to the sex differences in the behavioural responses to both KOPr activation and stress (discussed in Chapter 8). The majority of previous studies examining cFos activation following KOPr activation or stress have been performed in male animals (see Introduction & Chapter 4), however, two studies have investigated cFos expression in both male and female mice following KOPr activation. Russell and colleagues reported that KOPr activation, U50,488 (10mg/kg, i.p.) significantly induced cFos expression in the NAc core and shell of both male and female rats (Russell *et al.*, 2013). However, sex-dependent increases in cFos expression were seen in the BNST where cFos expression was increased in female rats compared with in male rats, an effect that was dependent on the stage of the oestrus cycle.

Another study showed that in the NAc shell, U50,488 increased phosphor-p38 cells immunoreactivity in both male and female California mice in a dose dependent manner, but no significant increases in phosphor-p38 immunoactivity in the NAc core in both sexes (Robles *et al.*, 2014). Although there were no profound differences in phosphor-p38 expression between the sexes, U50,488 had effects in male rats at lower doses than in females, suggesting that the male rats were more sensitive to the KOPr effect, similar to the effect seen in the present study. Again, as in the previous paper mentioned, sex differences were seen in the BNST, but the effects



were opposite to that shown by Russell and colleagues, with phosphor-p38 expression increased in males, but not in females. As it has been shown that activation of phosphorylated p38 MAP kinase is the key mechanism mediating dysphoric effect in response to stress-induced KOPr activation, which could be used as indirect marker for KOPr activation within neurons (Bruchas *et al.*, 2007). These findings suggest that the effect of KOPr activation, U50,488 on neuronal activity in the NAc is not sex-dependent, which conflicted with our data showing an increase cFos expression in the NAc was only seen in male mice after U50,488 (20mg/kg, i.p.) treatment, but not in female cFos-GFP transgenic mice. There are possible reasons that may underly these conflicting data in KOPr activation-induced effects, our studies only used cFos-GFP mice, whereas previous studies used rats or California mice. As different animal species could exhibit different expression levels of KOPr throughout the brain, resulting in differences in broader network mechanisms. No previous studies have investigated the effects of KOPr agonist on cFos expression in either PFCx or hippocampus in both male and female mice.

In terms of previous studies demonstrating sex differences in cFos activation following an acute *in vivo* stressor. Bland *et al.* (2005) examined the effects of acute restraint stress (100-minute duration) on cFos mRNA expression in both male and female rats. cFos mRNA was increased in the prelimbic and infralimbic regions of the PFCx in both male and female rats, compared to the non-stressed controls. However, the increase seen in male rats was significantly greater than that seen in female rats, similar to the data presented in this study. Interestingly, the sex-dependent effects were only seen immediately after the stressor (100 minutes after initiation of the stressor), but there was no difference in cFos mRNA levels between male and female animals at 60 minutes post-stress (i.e. 160 minutes after initiation of the stressor), indicating that the time point post-stress is an important factor to affect stress-induced effects in PFCx. While our data only focused on one time-point (2 hours) post-stress or post- KOPr agonist treatment, which could be the potential reason that underlies the differences observed in this study.

In addition to acute stress, a more recent study in mice revealed that chronic mild stress (2 or 4 weeks in duration) induced changes in cFos expression that were sex-dependent (Shepard *et al.*, 2016). In NAc core, chronic mild stress induced a significant decrease in cFos expression in male mice, but not in female mice. In contrast, a decrease in cFos expression was observed in both the PFCx and the basomedial amygdala in female mice, but not in male mice. Interestingly, this study also demonstrated that the decrease in cFos expression in the PFCx of female mice was correlated with an increase in markers of GABAergic transmission (parvalbumin-positive neurons and parvalbumin mRNA), suggesting that chronic stress-induced decrease in cFos expression in female PFCx could result from increased GABAergic signaling within the PFCx, which may underlie the sex differences in the effects of stress on neuronal activity, as well as high prevalence of stress-related affective disorders in females. However, care must be taken when interpreting data from chronic stress models with respect to acute stress models (as used here) because of adaptive responses taking place during chronic stress (Melia *et al.*, 1994, Mohammad *et al.*, 2000).

A further study used two different models of stress in rats and observed sexually dimorphic effects on cFos expression (Sood *et al.*, 2018). Acute immobilisation stress (2 hours) induced similar amounts of cFos expression between males and females in the prelimbic cortex, but less cFos expression in female infralimbic cortex compared with in males. In the dentate gyrus region of the hippocampus, acute immobilisation stress did not alter cFos expression but, surprisingly, and in contrast to the findings presented here, acute stress caused a decrease in cFos expression in female animals. Similarly, in the CA1 region of the hippocampus, sex differences were seen following acute stress with an increase in cFos expression in males, with no change in females. In the amygdala, no sex differences were seen, with acute stress inducing similar amounts of cFos expression in the basolateral, central and basomedial subregions of the amygdala. Furthermore, when the effects of a different stressor was examined, different patterns of cFos expression were seen. Using a subchronic forced swim stress paradigm (15 min on day 1, 5 min on day 2), increases in cFos expression were seen in the prelimbic cortex, infralimbic cortex and CA1 region of the hippocampus

in both male and female rats. In the dentate gyrus, cFos expression was increase in female rats, but not in male rats. This shows a different pattern of expression between the two types of stressor used in this study, as well as differences between the patterns of cFos expression we observed. As, in our data, a single acute FSS (15 minutes) did not induce cFos expression in the PFCx, CA1 region, dentate gyrus of hippocampus and central amygdala in either males or females, which is in contrast to the findings shown previously (Sood *et al.*, 2018), as Sood and colleagues showed that different *in vivo* stressors e.g. AIS and FSS affect neuronal activity differently, suggesting the effects of stress on various brain regions depend on sex and nature of stressors. The differences observed between our study and previous studies in different brain regions could result from different animal species, stressor natures, duration and intensity of the stressor.

Our data showed sex differences in the effects of U50,488 treatment and FSS in the PFCx and NAc. There are a number of potential factors underlying the sex differences. First, the different circulating gonadal hormones between sexes could affect pharmacological effects of U50,488, although previous findings have stated that the effects of U50,488 in mice were independent of the phases of the estrous cycle (Craft and Bernal 2001, Russell *et al.*, 2014). In future studies, the effect of gonadal hormones on sex differences in KOPr systems could be further investigated by vaginal lavage. Second, the sex chromosomes might also affect the KOPr activation, since early evidence has showed sex chromosome contributes to sex differences in nociception and analgesia in mice (Gioiosa *et al.*, 2008). Third, different KOPr distribution in the brain or different KOPr coupling efficiencies could also underlie the sex differences. Wang *et al.*, (2011) examined KOPr expression and KOPr agonist-induced GTP $\gamma$ S levels in male and female guinea pigs. Although some sex-dependent differences in KOPr expression were observed (e.g. in periaqueductal grey, substantia nigra), none were seen in the hippocampus, amygdala or NAc, and the prefrontal cortex was not studied. More profound changes were seen with KOPr agonist-induced GTP $\gamma$ S expression, however, with less GTP $\gamma$ S binding in females in the somatosensory and insular cortices (prefrontal cortex was not examined), and more KOPr agonist-induced GTP $\gamma$ S expression in the dentate gyrus. Although there

was a trend for decreased KOPr agonist-induced GTP $\gamma$ S expression in the amygdala and hippocampus, the effect was not statistically significant. No change was seen in the NAc. This study suggests complex sex-dependent differences in both KOPr expression and KOPr agonist-induced GTP $\gamma$ S in guinea pigs. It is possible that similar differences may underlie the sex-dependent changes in cFos expression seen here in mice.

Overall, this study showed novel findings that the effects of KOPr activation on neuronal activity in PFCx and hippocampus are sex-dependent in mice. NAc and PFCx are two important regions showed sex differences in response to KOPr activation and acute stress, particularly in female PFCx, which was insensitive to either KOPr activation nor acute stress. The conflicting data between this study and the previous evidence highlight the importance of potential factors, such as the nature of stressors, stress duration and intensity, different post-stress or post-KOPr activation time-points that may underlie different sex-dependent effects.

## **Chapter 6 Identification of activated neurons in response to stress**

## 6.1 Introduction

Chapters 4 & 5 showed increased cFos expression in various brain regions following KOPr activation and *in vivo* stressor, indicating the recent neuronal activity in response to stress in different brain areas. To attempt to identify the type(s) of neurons where cFos expression is enhanced following stress or KOPr activation, we now use GAD-GFP transgenic mice, where the enhanced green fluorescent protein (eGFP) gene is controlled by Gad1 (GAD67) gene promoter, thus GFP is expressed only in GABAergic neurons (Tamamaki *et al.*, 2003). GAD-GFP transgenic mice enable us to identify if the activated neurons are GABAergic or non-GABAergic neurons by overlaying cFos-positive and GFP-positive images together i.e. co-localisation of cFos and GFP-positive neurons indicate GABAergic neurons were being activated and different localisation of cFos and GFP-expressing neurons implies activated neurons were non-GABAergic neurons.

In this chapter we focus on PFCx and NAc, regions of particular interest as previous chapters showed sex-specific effects of stress and KOPr agonist administration. In PFCx, the primary output neurons are glutamatergic pyramidal neurons, although there is also evidence, in mice, for GABAergic neurons that project to the NAc, as well as GABAergic interneurons (Lee *et al.*, 2014). In NAc, the primary output neurons are GABAergic medium spiny neurons, as well as cholinergic interneurons (Meredith *et al.*, 1993). Although there is evidence that KOPrs are expressed both in the PFCx and in the NAc (Fan *et al.*, 2002), neuronal activation induced by an *in vivo* stressor or systemic administration of KOPr agonists could be due to network activity, and activation of KOPr elsewhere in the brain that in turn affects neuronal activation in the PFCx and NAc. The data presented here constitute a first attempt to identify the specific neurons where cFos is activated following KOPr agonist administration or *in vivo* stressor.

## 6.2 Methods

### 6.2.1 Immunohistochemistry

In this chapter, the immunohistochemistry (section 2.10) was repeated with adult (9-13 weeks old) male (25-30g) and female GAD-GFP transgenic mice (20-25g). Before immunohistochemistry, the GAD-GFP mice were treated with the same procedures (KOPr agonist, U50,488 or *in vivo* forced swim stress) as shown in chapter 4, illustrated in figure 4.1.

The coronal sections (40µm) of PFCx (Bregma +2.22 mm) and NAc (Bregma +1.34 mm) of both male and female GAD-GFP mice were cut on a vibratome and proceed to immunohistochemistry. For each mouse, one slice was taken for PFCx and NAc. These slices were dual labelled with anti-cFos and anti-GFP antibodies (section 2.3) on the first day, followed by incubation of fluophore-labelled secondary antibodies on the second day, including: goat anti-rabbit antibody Alexa Fluor 568 (diluted 1:500) and goat anti-chicken antibody Alexa Fluor 488 (diluted 1:500) (section 2.3). The fluorescent immunoreactivity was detected and quantified exactly the same way as shown in chapter 4 and 5.

All data were analysed with one-way (treatment) ANOVA followed by Sidak's test and presented as mean  $\pm$  SEM and significance levels were  $P < 0.05$ .

## 6.3 Results

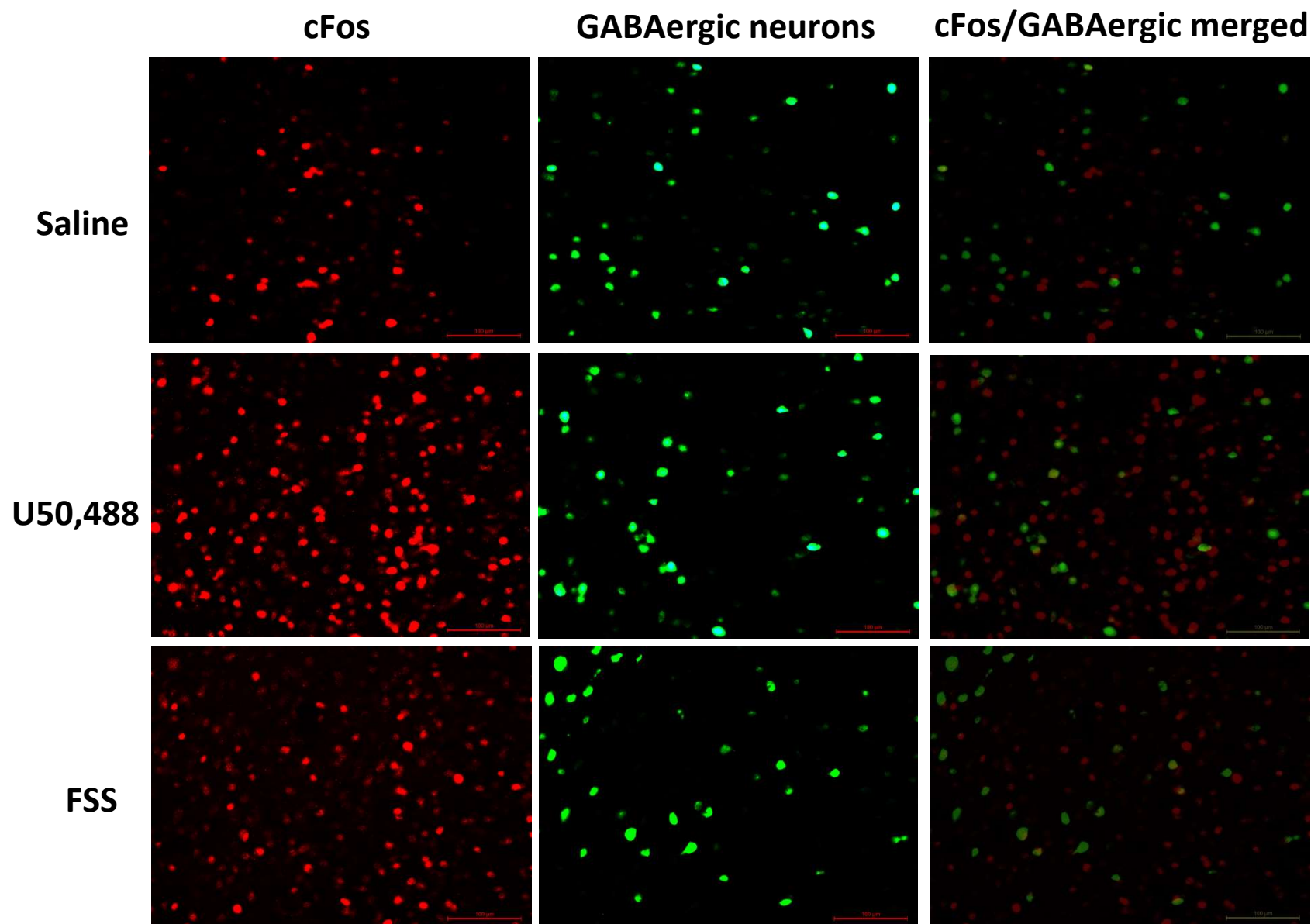
*In vivo* treatments and immunohistochemical imaging techniques were performed exactly as in Chapter 4 & 5 (although GAD-GFP mice were used instead of cFos-GFP mice); male and female mice were administered a single dose of KOPr agonist, U50,488, or a single *in vivo* stressor (FSS). Mice were then killed and sections of PFCx and NAc taken for immunohistochemical imaging.

Figure 6.1 shows typical cFos expression patterns in PFCx from male mice following FSS and KOPr activation, alongside merged cFos/GABAergic images. Signal from the cFos antibody is shown in red. In these mice, GFP is only expressed in GAD67-positive neurons (GABAergic neurons), therefore green signal denotes GABAergic neurons. Figure 6.2 shows typical cFos expression patterns in NAc from male mice following U50,488 administration and FSS, alongside merged cFos/GABAergic images. Quantified data are shown in Figure 6.3. As in Chapter 4, both U50,488 and FSS significantly increased cFos expression in both the PFCx and NAc regions. An indication of whether cFos-positive neurons are GABAergic or not can be gained by examining neurons that exhibit cFos expression with those that are GFP-positive (and are therefore GABAergic neurons). As seen in the merged images (where red signal largely does not overlap with green signal), minimal overlap is shown between cFos- and GFP-positive neurons. Indeed, less than 5% of neurons express both cFos and GFP. Furthermore, the percentage of neurons that are positive for both cFos and GFP did not increase after KOPr activation or *in vivo* stress (see grey bars in Figure 6.3). Collectively, these data suggest that cFos expression, induced by either an *in vivo* stressor or KOPr agonist administration, does not take place in GABAergic neurons.

Figure 6.4 & 6.5 show representative images from female mice showing cFos and GFP expression patterns in PFCx (Figure 6.4) and NAc (Figure 6.5) following KOPr activation and FSS. Quantified data are shown in Figure 6.6. As in Chapter 5, neither U50,488 or FSS caused an increase in cFos expression in PFCx, and FSS (but not U50,488) induced a significant increase in cFos expression in NAc. As in male mice (Figure 6.1 - 6.3) the green signal derived from cFos was largely separate from the



red signal derived from GFP (driven by GAD expression); less than 5% of neurons express both cFos and GFP. Further, the increase in cFos expression in female NAc following FSS did not cause an increase in neurons that were both cFos- and GFP-positive. As in male mice, these data suggest that cFos expression in both the PFCx and NAc in female mice is largely expressed in non-GABAergic neurons.



**Figure 6.1** Fluorescent images of cFos-expressing neurons (red), GABAergic neurons (green) and cFos/GABAergic neurons overlapping in **male PFCx** following U50,488 and FSS. Both U50,488 and FSS increased cFos expression, compared to saline-treated group, the majority of cFos-expressing neurons do not overlap with GABAergic neurons.

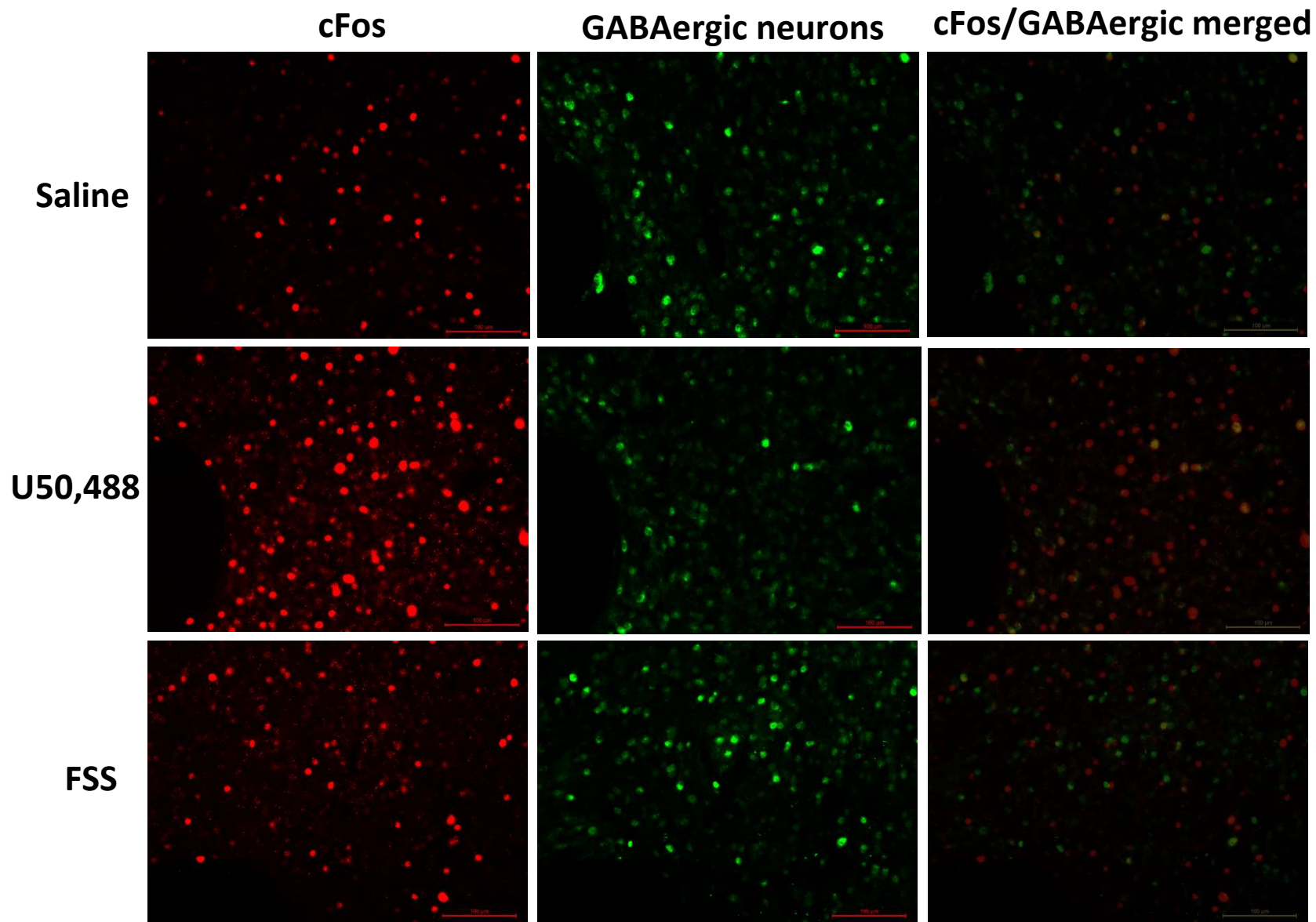


**Figure 6.2** Fluorescent images of cFos-expressing neurons (red), GABAergic neurons (green) and cFos/GABAergic neurons overlapping in **male NAc** following U50,488 and FSS. In male NAc, both U50,488 and FSS increased cFos expression, compared to saline-treated group, the majority of cFos-expressing neurons do not overlap with GABAergic neurons.

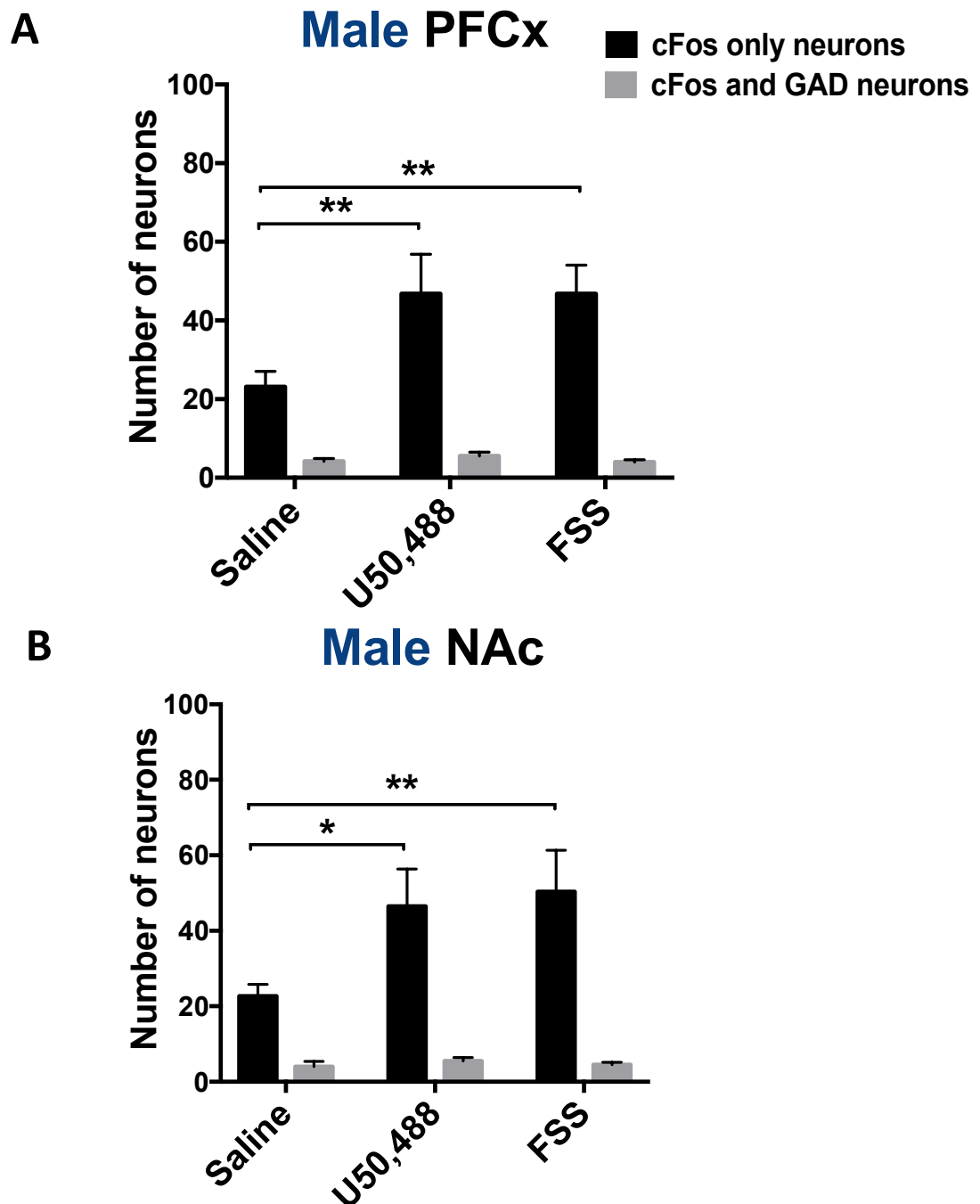


**Figure 6.3** Total number of cFos-expressing neurons that were induced by U50,488 or FSS in male PFCx and NAc. Comparison with GFP-positive neurons. In male PFCx (**A**) and NAc (**B**), cFos expression was significantly induced by both stimuli, compared to saline-treated group. Less than 5% of the neurons were both cFos and GFP-positive. Data are expressed as mean  $\pm$  SEM. N = 6 animals per treatment group. \*P < 0.05, \*\*P < 0.01.

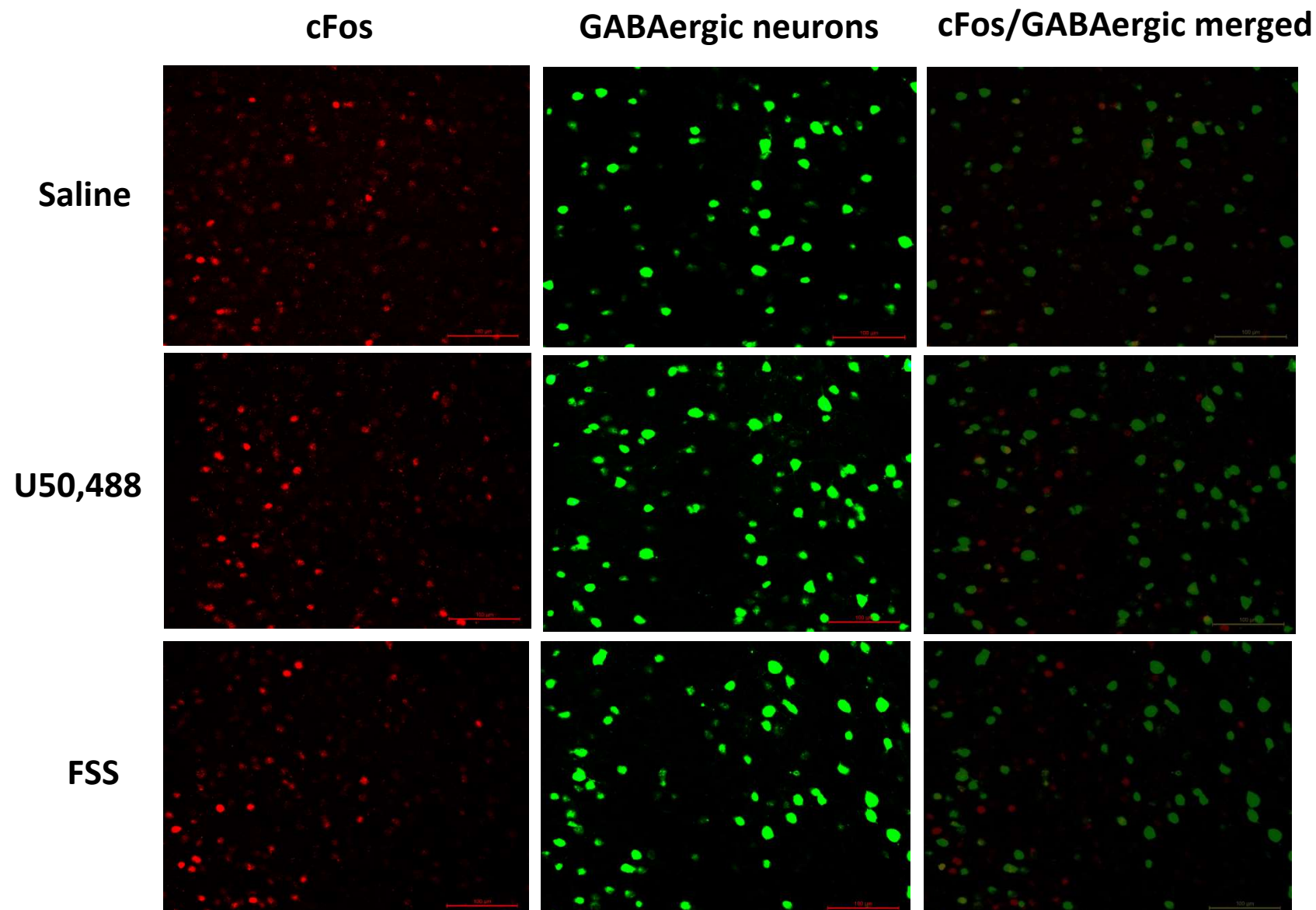


**Figure 6.4** Fluorescent images of cFos-expressing neurons (red), GABAergic neurons (green) and cFos/GABAergic neurons overlapping in **female PFCx** following U50,488 and FSS. Neither U50,488 nor FSS increased cFos expression, compared to saline-treated group, the majority of cFos-expressing neurons do not overlap with GABAergic neurons.



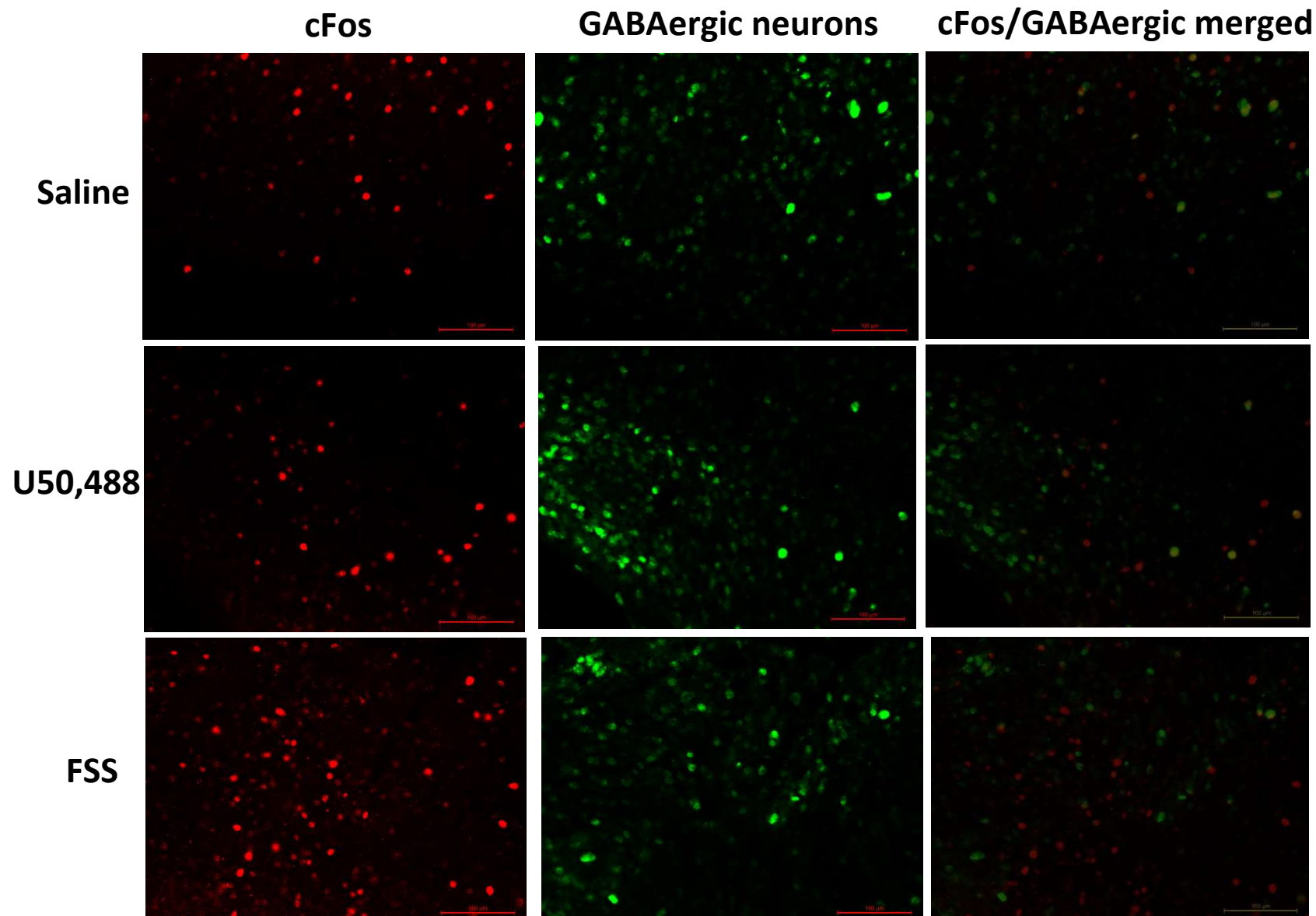


**Figure 6.5** Fluorescent images of cFos-expressing neurons (red), GABAergic neurons (green) and cFos/GABAergic neurons overlapping in **female NAc** following U50,488 and FSS. FSS, but not U50,488 increased cFos expression, compared to saline-treated group, the majority of cFos-expressing neurons do not overlap with GABAergic neurons.

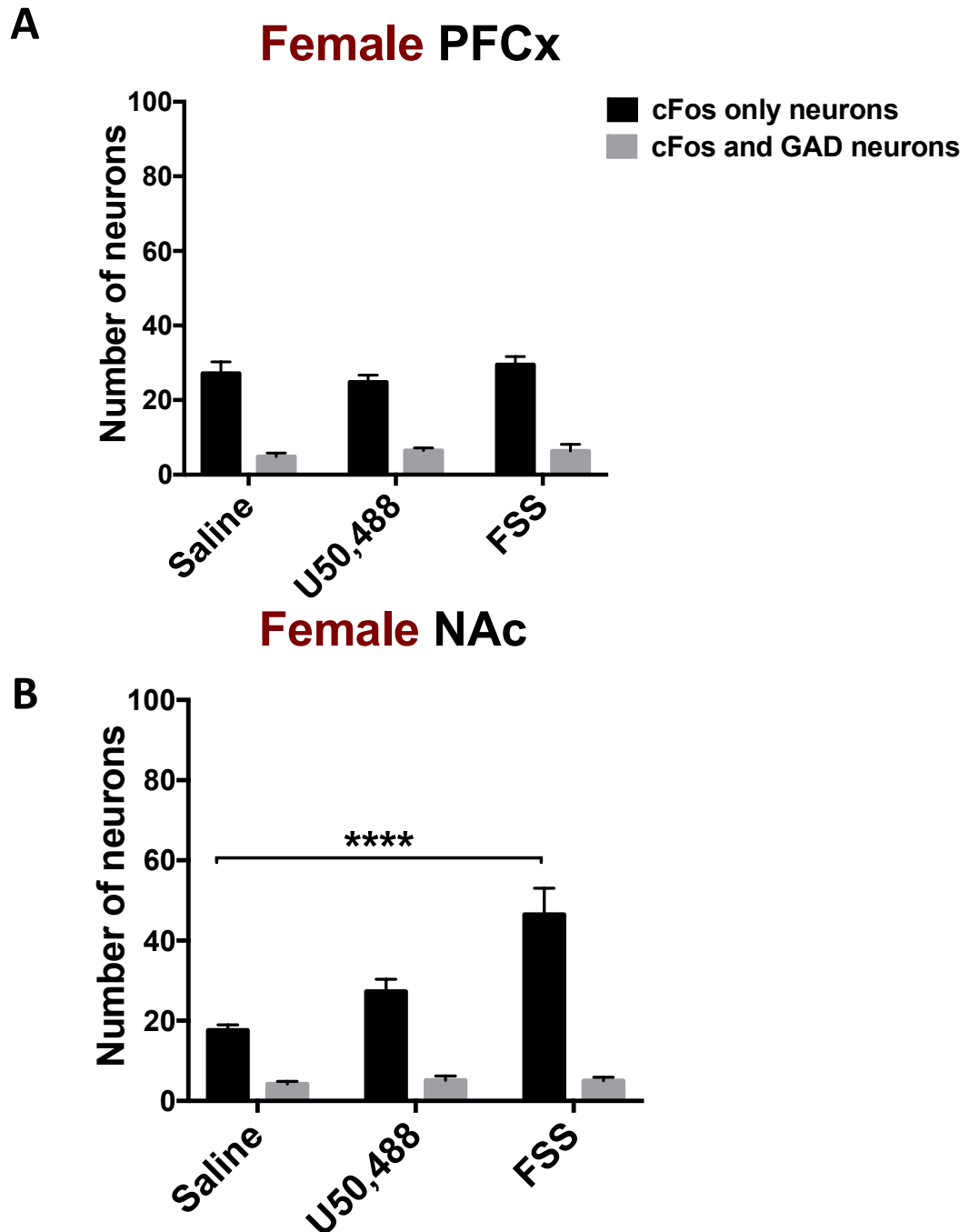


**Figure 6.6 Total number of cFos-expressing neurons that were induced by U50,488 or FSS in female PFCx and NAc. Comparison with GFP-positive neurons.** In female PFCx (**A**), neither U50,488 or FSS increased cFos expression. In NAc FSS (**B**), but not U50,488, increased cFos expression when compared to the control group. Less than 5% of the neurons were both cFos and GFP-positive. Data are expressed as mean  $\pm$  SEM. N = 6 animals per treatment group. \*\*\*\*P < 0.0001.

## 6.4 Discussion

This chapter shows the first attempt to further characterise the specific neurons that are activated in response to activation of KOPr or an *in vivo* stressor.

In Chapter 4 & 5, cFos-GFP transgenic mice were used, to enable co-staining of cFos and cFos-driven GFP. Here, GAD-GFP mice were used, to enable co-staining of cFos and GFP selectively expressed in GABAergic neurons, to enable us to identify whether cFos is expressed in GABAergic neurons following administration of KOPr agonist or *in vivo* stressor.

First, key findings from Chapter 4 & 5 are repeated here, in that both U50,488 and FSS increased the number of cFos-positive neurons in both NAc and PFCx in male mice. In female mice, neither FSS or U50,488 increased cFos expression in PFCx, and FSS increased cFos expression in NAc, but not in PFCx. Although the GAD-GFP and cFos-GFP mice are on the same background strain (C57/BL6) of mice, the data shown here indicate that the sex differences in cFos expression shown in the previous chapters are robust and repeatable, in a different substrain and cohort of mice.

The overall aim of the experiments shown here were to identify the neurons where cFos is activated following U50,488 or FSS. If cFos was activated in GABAergic neurons, we would have expected the percentage of cFos AND GFP-positive neurons to increase in brain regions where cFos expression has increased. In each treatment group, however, this was not the case. Indeed, the overall percentage of neurons that were both cFos and GFP-positive under these conditions was less than 5%. Overall, this indicates that the primary neurons in which activated by U50,488 or FSS are not GABAergic neurons.

In the PFCx, KOPrs are largely located pre-synaptically on nerve terminals, both dopaminergic inputs, as well as glutamatergic and GABAergic inputs. Electrophysiological studies in rats have shown that the KOPr agonist, U69,593 significantly inhibited dopaminergic neurons projecting to the PFCx (Margolis *et al.*,



2005). This finding was further supported by *in vivo* microdialysis in mice and rats, demonstrating that direct administration of the KOPr agonist, U69,593 into PFCx significantly reduced the local dopamine, glutamate and GABA levels, which could be reversed by KOPr antagonist, norBNI. Further, mice lacking KOPr in dopaminergic neurons showed that KOPr activation inhibits dopamine levels by directly acting on dopaminergic neuronal terminals in PFCx (Tejeda *et al.*, 2013). These results are similar to previous evidence in rats, showing that the KOPr agonist, U50,488, largely inhibited electrically evoked dopamine release in the PFCx, which was effectively prevented by KOPr antagonist, norBNI (Heijna *et al.*, 1990). All these results suggest that KOPrs are largely expressed on dopaminergic, glutamatergic and GABAergic neurons in PFCx, although our studies have shown the neurons activated by *in vivo* stress and KOPr activation are non-GABAergic neurons, further identification of the types of the neurons is required.

In the NAc, a number of studies have shown that KOPrs are located pre-synaptically on both dopaminergic and glutamatergic inputs and KOPrs contribute to modulation of dopamine, glutamate and GABA release and neurotransmission. Similar to the findings in PFCx, the systemic administration of KOPr agonist, U50,488 significantly inhibited electrically induced release of dopamine in the rat NAc, which was fully blocked by norBNI (Heijna *et al.*, 1990). This effect of KOPr activation on dopamine levels in rats NAc was further confirmed by another KOPr agonist, BRL52537, which demonstrated that single stimulus pulse-evoked overflow of dopamine was inhibited by application of BRL52537, an effect that was reversed by administration of norBNI. It was confirmed that this inhibitory effect of KOPr on dopamine release results from direct actions on presynaptic KOPrs located at dopaminergic nerve terminals in the NAc (Britt and McGehee, 2008). *In vivo* microdialysis studies showed that administration of KOPr agonist, U69,593 could reduce the release of dopamine and glutamate in rats NAc (Gray *et al.*, 1999) and *in vitro* electrophysiology studies revealed that U69,593 reduced glutamatergic neurotransmission in the presynaptic terminals in the NAc of rats (Hjelmstad and Fields 2001). In addition to inhibiting glutamate release in the NAc, whole-cell voltage-clamp studies in rat brain slices showed that KOPr activation by the KOPr agonist U59,593 also showed reduced

GABA release in the NAc by directly acting on GABAergic neuronal terminals (Hjelmstad and Fields 2003). Overall, these studies provide evidence that activation of KOPr reduces dopamine, glutamate and GABA release by directly acting on the KOPrs on terminals of these dopaminergic, glutamatergic and GABAergic neurons in both PFCx and NAc regions, at least in male animals.

Our data in both male and female mice showed that the majority of stress or KOPr activation-induced cFos expression was not merged with GFP-expressing neurons, which indicates that KOPr activation- or stress-activated neurons were mostly non-GABAergic neurons. The use of GAD-GFP transgenic mice only allow us to identify the KOPr activation or stress-activated neurons are GABAergic or non-GABAergic neurons, and they are unable to identify the specific types of the neuron following stress or KOPr activation. In order to further characterise individual neurons that are activated by stress or KOPr activation, electrophysiology techniques can be used in further experiments (further discussed in Chapter 8).

**Chapter 7 Effect of acute stress and kappa opioid  
receptor activation on plasma corticosterone in  
adult male and female mice**

## 7.1 Introduction

The data in previous chapters showed neurons in the PFCx, NAc, hippocampus and amygdala were activated in response to acute stress and KOR activation in a sex dependent manner. As describe in chapter 1, corticosterone is one of the glucocorticoids produced and secreted by the cortex of the adrenal glands in stress responses through activation of the hypothalamo-pituitary-adrenocortical (HPA) axis (Chapter 1). Previous evidence showed that forced swim stress significantly increased dynorphin immunoreactivity in the NAc and hippocampus (Shirayama *et al.*, 2004), also elevated plasma corticosterone levels in wildtype male C57BL/6N mice (Wittmann *et al.*, 2009). The stress-induced increased in corticosterone levels were significantly attenuated by pre-treatment of KOR antagonist, norBNI (10mg/kg) in wildtype mice and in male prodynorphin knockout mice (dyn<sup>-/-</sup>), suggesting the facilitatory role of endogenous dynorphin and KOR system in regulating corticosterone release in HPA axis in response to stress (Wittmann *et al.*, 2009). The important role of dynorphin in stress-induced corticosterone responses was also supported by similar study in Sprague-Dawley male rats, which showed that stress-induced high levels of plasma corticosterone were reduced by KOR antagonism, norBNI (20mg/kg) (Allen *et al.*, 2013). The direct correlation between dynorphin/KOR system and glucocorticoid levels was reported by early studies, which showed that KOR agonist, U50,488 significantly increased rats plasma corticosterone in a dose dependent manner (Hayes and Stewam 1985, lyengar *et al.*, 1986).

The exact mechanism of which dynorphin/KOR activation induces corticosterone levels in HPA axis still remains unclear, but it likely depends on the activation of corticotropin-releasing hormone (CRH) release in the hypothalamus. As in (dyn<sup>-/-</sup>) mice, CRH mRNA was reduced by almost 30% in the paraventricular nucleus of the hypothalamus (Wittmann *et al.*, 2009). Further evidence showed that intracerebroventricular injection of CRH induces aversion, which was blocked by dynorphin gene disruption and KOR antagonism, norBNI treatment, suggesting the possible mechanism of dynorphin/KOR system in corticosterone responses is CRH dependent (Land *et al.*, 2008).

To identify whether stress and KOR activation produce effects on plasma corticosterone levels. Blood samples were collected from male and female cFos-GFP transgenic mice following acute forced swim stress and U50,488 in the absence and presence of norBNI. To investigate the response to stress, it is involved that blood samples are collected carefully. The tail incision method, in which a small nick is made in the lateral tail vein, and it has been validated as a refined method for single or repeated blood sampling in adult mice (Sadler *et al.*, 2013).

It is hypothesised that plasma corticosterone levels would be significantly increased in response to forced swim stress and a single injection of U50,488 treatment, and pre-treatment of norBNI would block, at least in part, stress-induced elevated plasma corticosterone levels.

## **7.2 Methods**

### **7.2.1 Animals**

In this chapter, both male (25-30g) and female (20-25g) adult (9-13 weeks old) cFos-GFP transgenic mice were used, which were originally purchased from Jackson Laboratories (Bar Harbor, Maine, USA) (section 2.1).

### **7.2.2 FSS and KOPr ligand treatment**

The blood samples were collected for baseline corticosterone levels measurements before norBNI (10mg/kg, i.p.) or saline (10ml/kg, i.p.) injections on the day 1. The following day, the mice were treated with either FSS (section 2.5) or KOPr agonist, U50,488 (20mg/kg, i.p.) (section 2.6) to investigate if stress or KOPr activation could affect the plasma corticosterone levels, after 30 minutes, the blood samples were collected for corticosterone measurements, the experiment timeline is illustrated in figure 7.1.

### **7.2.3 Blood collection and corticosterone analysis**

The blood samples were collected using the tail incision method and corticosterone levels measurements were determined using ELISA kit (IBL International, Hamburg, Germany), details were described in chapter 2, section 2.11 and 2.12.

### **7.2.4 Statistical analysis**

All data are presented as mean  $\pm$  SEM for each treatment group. All corticosterone levels were analysed using a two-way ANOVA with factors 'treatment' and 'time' followed by post hoc Sidak's test for each stress or KOPr activation experiment in male and female mice group.  $P < 0.05$  was used to indicate the significance difference.

## 7.3 Results

The blood collection and corticosterone analysis methods are described in Chapter 2, Section 2.11. In order to confirm HPA activation in response to acute FSS and a single injection of U50,488, and the effect of KOR antagonist on plasma corticosterone levels, the experimental design is illustrated in Figure 7.1. Blood samples were collected at baseline (24 hours pre-stress), and mice were then treated with either saline or KOR antagonist, norBNI (10mg/kg). After 24 hours, male or female mice were treated with either U50,488 (20mg/kg) administration or 15 minutes FSS, blood samples were collected 30 minutes after U50,488 treatment, as previous evidence showed 30 minutes post KOR activation (U50,488) significantly induces corticosterone levels in rats (Hayes and Stewart 1985), blood samples were also collected 30 minutes after exposure to FSS, in order to allow the corticosterone levels reach its peak (Connor *et al.*, 1997) (Figure 7.1). The collected plasma corticosterone levels were determined by ELISA (Section 2.12).

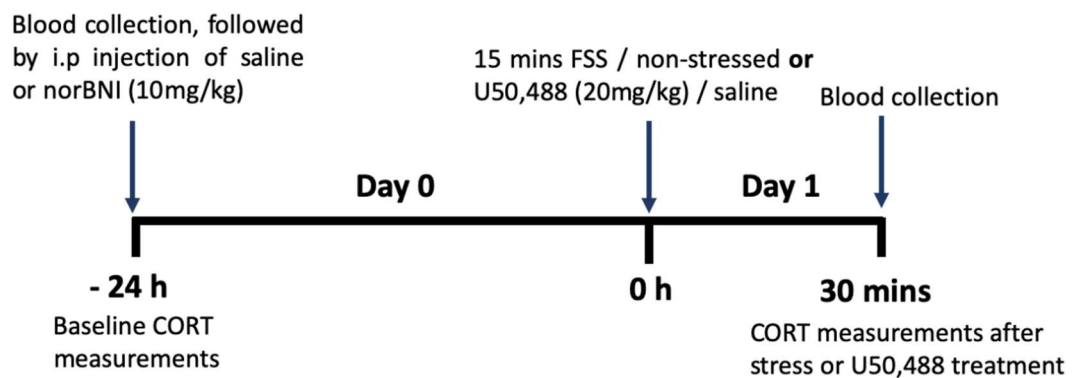


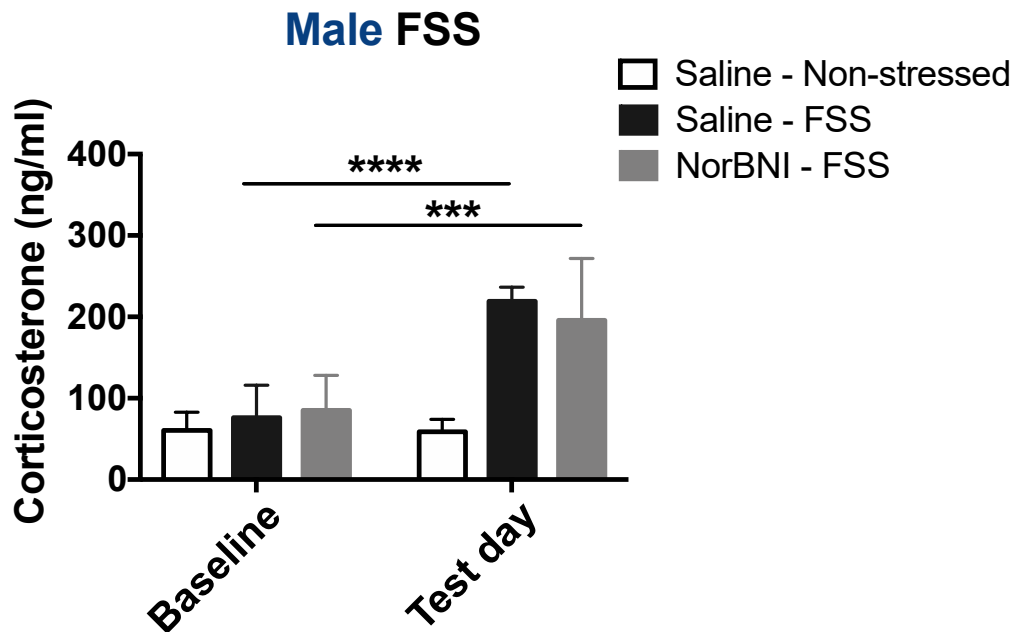
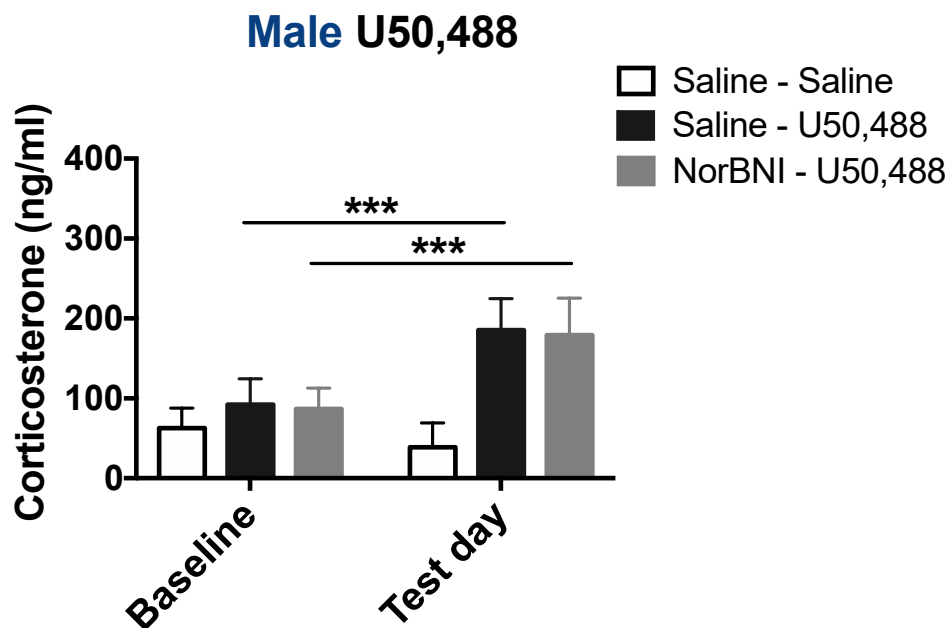
**Figure 7.1** Experimental design for male and female mice treated with either stress (15 mins FSS) or KOR agonist (U50,488) in the presence or absence of norBNI pre-treatment. CORT, corticosterone, FSS, forced swim stress.

In adult male mice, there were no differences between non-stressed control groups and stressed groups at baseline corticosterone levels, the mean baseline values  $\pm$  SEM, ( $n = 5/\text{group}$ ) are  $60 \pm 10$  ng/ml,  $76 \pm 18$  ng/ml,  $85 \pm 19$  ng/ml. Forced swim stress produced a significant increase by almost 200%, compared to baseline measurements ( $F_{(1,24)} = 30.87$ ,  $P < 0.0001$ ). These FSS-induced plasma levels of

corticosterone were not affected by pretreatment of norBNI (10mg/kg) (Figure 7.2A). U50,488 administration also produced a significant increase in plasma corticosterone levels ( $F_{(1,24)} = 18.69$ ,  $P = 0.0002$ ), compared to the baseline measurements (200% of baseline control) (Figure 7.2B). Surprisingly, pretreatment of norBNI also did not block elevated corticosterone levels in U50,488 treatment groups (Figure 7.2B).

In adult female mice, similar to the measurements in male mice, there were no differences between control and treated groups at baseline corticosterone levels, the mean baseline values  $\pm$  SEM, ( $n = 5/\text{group}$ ) are  $75 \pm 12$  ng/ml,  $98 \pm 10$  ng/ml,  $97 \pm 17$  ng/ml. The plasma corticosterone levels were also significantly increased by FSS by 160%, compared to baseline measurements ( $F_{(1,24)} = 46.77$ ,  $P < 0.0001$ ) (Figure 7.3A). Similarly, U50,488 administration produced a significant increase in plasma corticosterone ( $F_{(1,24)} = 37.83$ ,  $P < 0.0001$ ), 350% compared to the baseline levels, which was not blocked by pre-treatment with norBNI (Figure 7.3B).



**A****B**

**Figure 7.2 Effect of forced swim stress (FSS) and U50,488 (20mg/kg) on corticosterone levels in male cFos-GFP transgenic mice.** Blood samples were collected on day 0 as baseline levels. On day 1, blood samples were taken 30 minutes after swimming and administration of U50,488. Blood samples were also collected for non-stressed and saline-treated mice as control groups. All data are presented as mean  $\pm$  SEM. N=5 per treatment group, Two-way ANOVA with Sidak's test. \*\*\* $P < 0.001$ , \*\*\*\* $P < 0.0001$ . For FSS treatment (i.e. saline vs FSS:  $F_{(1,24)} = 46.77$ ,  $P < 0.0001$ ), and time (i.e. baseline vs test day:  $F_{(2,24)} = 15.58$ ,  $P < 0.0001$ ). For U50,488 treatment (i.e. saline vs U50,488:  $F_{(1,24)} = 37.83$ ,  $P < 0.0001$ ), and time (i.e. baseline vs test day:  $F_{(2,24)} = 17.1$ ,  $P < 0.0001$ ).

**A**

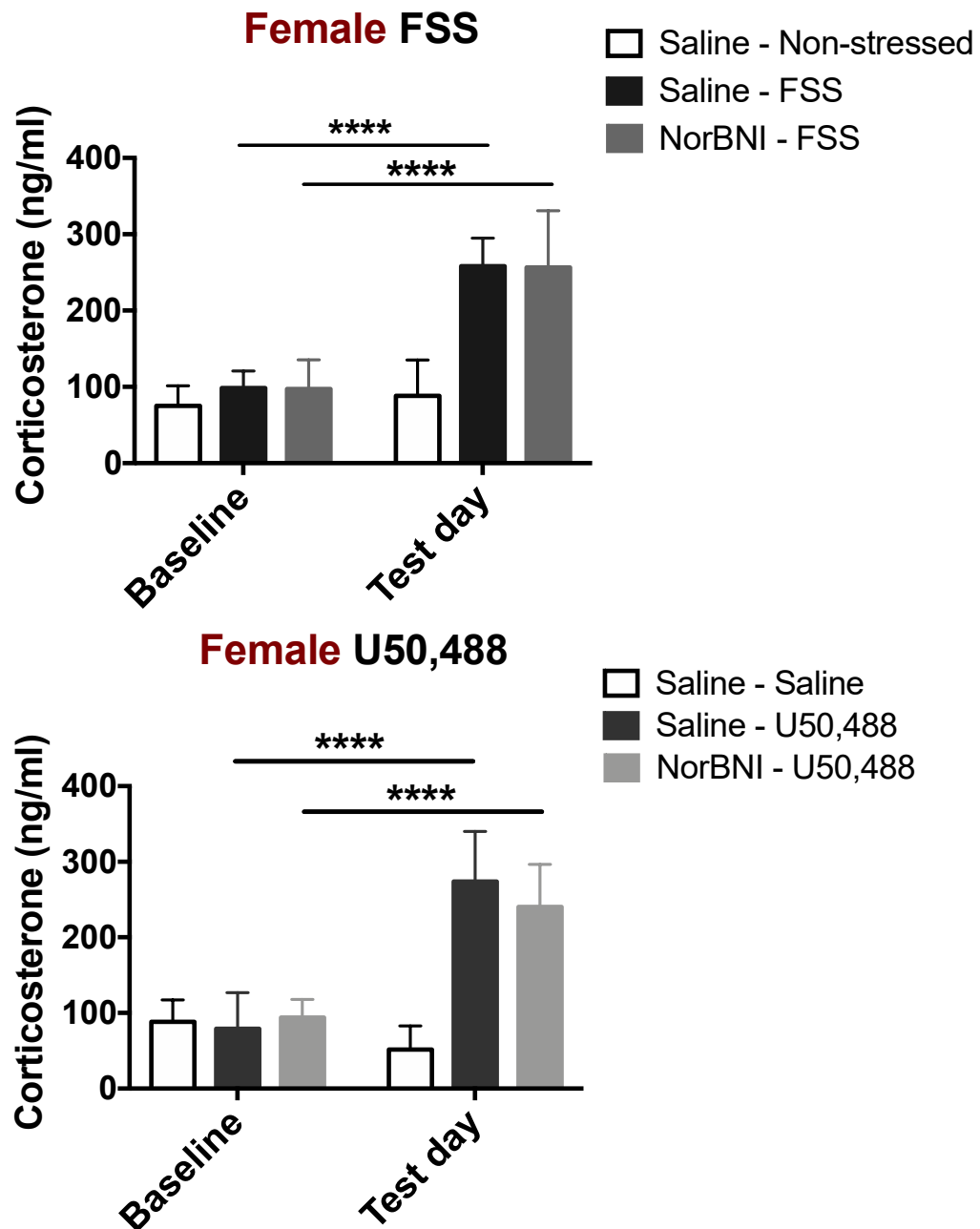


**Figure 7.3 Effect of forced swim stress (FSS) and U50,488 (20mg/kg) on corticosterone levels in female cFos-GFP transgenic mice.** Blood samples were collected on day 0 as baseline levels. On day 1, blood samples were taken 30 minutes after swimming and administration of U50,488. Blood samples were also collected for non-stressed and saline-treated mice as control groups for comparison. All data are presented as mean  $\pm$  SEM. N=5 per treatment group, Two-way ANOVA with Sidak's test. \*\*\*\*P<0.0001. For FSS treatment (i.e. saline vs FSS:  $F_{(1,24)} = 30.87$ ,  $P < 0.0001$ ), and time (i.e. baseline vs test day:  $F_{(2,24)} = 13.93$ ,  $P < 0.0001$ ). For U50,488 treatment (i.e. saline vs U50,488:  $F_{(1,24)} = 18.69$ ,  $P = 0.0002$ ), and time (i.e. baseline vs test day:  $F_{(2,24)} = 20.72$ ,  $P < 0.0001$ ).

## 7.4 Discussion

Our studies have shown the baseline, swim stress-induced and U50,488-induced plasma corticosterone levels in both adult male and female C57Bl/6J mice. The mean basal corticosterone levels for male and female mice are 75 ng/ml and 90 ng/ml respectively, suggesting that female mice have higher baseline corticosterone levels than males. Direct comparison of baseline data with other studies is complicated by the method of blood collection which may influence the values obtained, however, similar findings are in the literature. For example, Malisch *et al.* (2007) showed mean baseline plasma corticosterone levels in females (115 ng/ml) were almost twice as high in males (59 ng/ml) in CD1 mice, with blood samples taken by retro-orbital sinus puncture.

In response to acute FSS, our data showed a significant increase in corticosterone levels by almost 200% in male mice and 160% in females, compared to baseline corticosterone levels. These effects were similar to effects revealed in a previous study, demonstrating that two hours restraint stress significantly induced high levels of corticosterone concentrations by 220% over baselines in C57BL/6 male mice (Sadler & Bailey, 2016). Acute 30 minutes restraint stress produced a significant increase in both male and female C57BL/6 mice by over 500% and reached over 700 ng/ml in males and over 800 ng/ml in females (Romeo *et al.*, 2013). These restraint stress-induced corticosterone levels were much higher than the corticosterone levels we determined following 6 minutes FSS in our study, which could result from the nature and duration of the stressors. In addition, acute 40 minutes restraint stress produced a significant increase in corticosterone levels by almost 400% in male mice and 300% over baseline levels in female mice, resulting in elevated corticosterone levels approximately 300 ng/ml in males and 460 ng/ml in females (Malisch *et al.*, 2006). In that study, there was a higher percentage increase in stress-induced corticosterone levels in males, but because of the higher baseline levels in females, the final stress-induced corticosterone levels were higher in female mice than in male mice. The sex-dependent differences in corticosterone levels in response to stress was proposed to result from, at least in part, the involvement of gonadal steroids

such as estrogen in regulating corticosterone secretion and clearance rate in the HPA axis (Handa *et al.*, 1994).

Following U50,488 with a dose of 20 mg/kg treatment, our data showed a significant 2-fold increase (200% of control) in plasma corticosterone levels in male mice and approximately 3-fold increase (350% of baseline control) in female C57BL/6 mice. Early studies showed that U50,488 at 5 mg/kg largely produced a 300% increase in plasma corticosterone in adult male rats (Hayes and Stewam 1985). Others reported that U50,488 at only 2 mg/kg induced elevated corticosterone levels (200% of control) in adult male rats (Iyengar *et al.*, 1986). Dose-dependent increases in corticosterone in response to U50,488 induced KOPr activation have been shown in rats. U50,488 at 8 mg/kg increased corticosterone levels to 550% and 16 mg/kg increased to 500% of controls, suggesting that 8 mg/kg is the dose to induce the maximum HPA activity and corticosterone responses, and corticosterone responses could be blunted with more than 8 mg/kg of U50,488 treatment (Iyengar *et al.*, 1986). These changes seen in rats, albeit at lower doses, are similar to the corticosterone responses determined in mice in this study with 20 mg/kg of U50,488. In this study, the U50,488-induced percentage increase in corticosterone levels were greater in females than that of males, suggesting that female mice may be more sensitive to KOPr activation inducing increased in corticosterone response.

As described above, both FSS and U50,488 treatment produced significant effects on plasma levels of corticosterone in both male and female C57BL/6 mice in this study. However, these stress-induced elevated plasma corticosterone levels were not blocked by pretreatment of KOR antagonist norBNI. These results were consistent with previous studies on the effects of restraint stress on corticosterone levels, which showed 10mg/kg of norBNI was unable to block restraint stress-induced increase in plasma corticosterone levels in male CD1 mice (Almatroudi *et al.*, 2017). In addition, other studies also showed that neither the presence of norBNI in wildtype mice nor prodynorphin knockout mice affect FSS-induced elevated corticosterone in C57BL/6 mice (McLaughlin *et al.*, 2006). In rats, it has also been reported that norBNI pre-administration (10mg/kg) did not block elevated corticosterone levels following FSS

in male Sprague-Dawley rats, suggesting that FSS-induced increase in corticosterone was independent of KOPr activation signaling (Polter *et al.*, 2014). However, a number of studies demonstrated contradictory data, for example, Allen and colleagues reported that pre-administration of norBNI (20mg/kg) effectively reduced the elevated plasma corticosterone levels after food restriction in Sprague-Dawley rats (Allen *et al.*, 2013). In addition, another group showed that the presence of norBNI (10mg/kg) reduced basal levels of plasma corticosterone in wild type C57/BL6 mice, as well as in prodynorphin knockout mice, indicating the dynorphin/KOPr activity is involved, at least in part, in regulating corticosterone levels in the HPA axis activation (Wittmann *et al.*, 2009).

Overall, this study showed that the methodology used here to induce stress was stressful to the mice as the FSS procedure produced an increase in plasma corticosterone levels in both male and female mice. Similarly, this study confirmed that U50,488 (20 mg/kg) induced an increase in plasma corticosterone levels, as has been reported previously, in both male and female mice. However, norBNI did not reduce plasma corticosterone levels following FSS, which may suggest that FSS-induced corticosterone levels were independent of KOPr system, although norBNI and other KOPr antagonists have been shown to effectively blocked stress-induced behaviours (Shirayama *et al.*, 2004, Almatroudi *et al.*, 2018). Moreover, norBNI did not effectively block U50,488-induced increase in plasma corticosterone in our study, which could perhaps result from an insufficient dose of norBNI or alternatively U50,488-induced increase in corticosterone levels are independent of KOPr activation.

## **Chapter 8 General Discussion**

The overall aims of this project were to determine which brain regions are activated by stress and KOPr activation, to help determine whether there is overlap between brain regions activated by both behavioural stimuli. As previous studies have shown sex differences in behavioural responses to physical stressors and KOPr activation, we also sought to determine whether there were sex differences in the brain regions activated by these *in vivo* stimuli.

The key results in this thesis are that in male cFos-GFP transgenic mice there was considerable overlap in brain regions that were activated by both a physical stressor (FSS) and KOPr activation, with significant increases in cFos and cFos-driven GFP expression in the PFCx, NAc and basolateral amygdala. In the CA1 region of the hippocampus and central amygdala KOPr activation significantly increased cFos expression, whereas FSS was without effect.

Surprisingly, there was a very different pattern of cFos expression seen in female mice undergoing the same experimental procedures. In the PFCx, neither KOPr activation nor FSS increased cFos expression. In the NAc, FSS but not KOPr activation increased cFos expression. In the CA1 region of the hippocampus, central amygdala and basolateral amygdala similar patterns of cFos expression were seen between male and female mice following both KOPr activation and FSS.

Although in some brain regions there was cFos expression following both KOPr activation and FSS, pretreatment of animals with norBNI significantly inhibited cFos activation by KOPr, but generally had no effect against the FSS-induced increase in cFos expression.

This chapter will discuss the potential factors that underlie these sex differences to the effects of KOPr activation and stress. Also, the limitations of these studies and how these could be addressed in the future experiments.

## 8.1 Sex differences in KOPr expression

Our data demonstrated sex-dependent cFos expression in PFCx and NAc following U50,488 treatment, but not in hippocampal CA1 and amygdala, i.e. male mice exhibited a significant increase in cFos expression in the PFCx and NAc after KOPr activation, an effect that was not seen in females. This could directly result from different expression levels of KOPrs in different brain regions between male and female mice. To our knowledge, there have been no previous studies examining sex differences in KOPr expression in male and female mice, but this hypothesis could be supported by previous evidence in guinea pigs (Wang *et al.*, 2011). Using *in vitro* autoradiography with the KOPr agonist, U69,593, they showed that in some brain regions (somatosensory cortex, insular cortex, claustrum, endopiriform cortex, periaqueductal grey, substantia nigra), there was significantly less KOPr binding in female brains compared with male brains. Of the two brain regions that showed the most profound sex-dependent effect in our study (PFCx and NAc), there was no significant difference in KOPr expression seen in the NAc, and the PFCx was not studied.

Moreover, recent studies reported the sex differences in KOPr distribution in healthy human subjects *in vivo* using PET imaging scanning (Vijay *et al.*, 2016), which revealed that males had higher KOPr availability than that of females in multiple brain regions, including the frontal cortex and amygdala, with no sex-dependent differences seen in the hippocampus and amygdala (the NAc was not studied) (Vijay *et al.*, 2016). These studies suggest that there are sex-dependent differences in KOPr expression. Similar future studies in mice are required before the sex-dependent differences in cFos expression shown in our study can be ascribed to differences in KOPr expression. There are also other potential explanations for our findings, and for the sex-dependent differences in KOPr agonist-induced behaviour in rodents.



## 8.2 Sex differences in KOPr activation and signaling

In addition to the differences in expression levels of KOPrs in different brain regions between males and females, it is also hypothesised that the sex differences observed in KOPr-induced cFos expression is caused, at least in part, by differences in KOPr-mediated G protein activation in different brain regions. As well as investigating sex-dependent differences in KOPr expression, Wang and colleagues also reported that G protein activation stimulated by the KOPr agonist, U69,593, was significantly greater in male guinea pigs than females in various brain regions, including somatosensory cortex and insular cortex, with no differences seen in the hippocampus or NAc (the PFCx was not investigated). In contrast, in the dentate gyrus in the hippocampus, there was significantly greater U69,593-stimulated G protein activity in females than in males (Wang *et al.*, 2011). Moreover, by combining KOPr expression level data and KOPr-agonist stimulated G protein activation data an index of 'Receptor-G protein coupling efficiency' was derived, showing significantly lower coupling efficiency in female guinea pigs in several brain areas (cingulate cortex, somatosensory cortex, insular cortex, claustrum, medial geniculate nucleus and cerebellum), with significantly higher coupling efficiency in females in one brain area: the dentate gyrus. No difference was seen in NAc, hippocampus or amygdala, and the PFCx was not studied. Overall, although these studies do suggest that sex-dependent differences in KOPr coupling efficiency may exist, they do not directly correlate with sex-differences in KOPr agonist-induced cFos expression presented here as no changes were seen in the NAc, and significant differences were seen in the dentate gyrus, where, in our study, KOPr activation did not increase cFos expression in either male or female animals. However, as these studies were performed in guinea pigs, further similar studies are required in mice to determine whether sex-dependent differences in receptor coupling efficiency underlie the sex-dependent effects of KOPr activation presented in this thesis.

Another recent study (Abraham *et al.*, 2018) also demonstrated sex-dependent differences in KOPr signaling, comparing the effects of the KOPr agonist, U50,488, in male and female mice. As in previous studies, U50,488 was a less effective analgesic

in female mice compared with male mice, but, this was shown to be oestrogen-dependent, as the sex-dependent effect was absent in ovariectomised animals, and there was a small, but significant, increase in KOPr agonist-induced analgesia in female animals in oestrus compared to those not in oestrus. Further investigations into the mechanisms underlying this effect showed that although KOPr agonist-induced phosphorylation of p38 MAP kinase in males and females were equivalent, KOPr agonists induced phosphorylation of ERK1/2 only in males, with no effect seen in females. P38 MAP kinase phosphorylation is thought to be arrestin-mediated, following activation of KOPr, phosphorylation of the receptor by GRK2/3, and subsequent binding of arrestin to KOPr (Bruchas *et al.*, 2006). In contrast, ERK1/2 phosphorylation is thought to be mediated by activation of the  $\beta\gamma$  subunits of the G-protein. One of the effects of GRK2 is to bind to  $\beta\gamma$  subunits of the G-protein and inhibit them (Daaka *et al.*, 1997). Furthermore, oestrogen has been shown to enhance GRK2 levels, thereby decreasing KOPr signaling through  $G\beta\gamma$  in females (Dominguez *et al.*, 2009). A similar mechanism is one potential mechanism that may underlie the sex differences in cFos expression observed in our data, showing that female mice were less sensitive to U50,488 treatment in different brain regions, especially in PFCx and NAc.

All of the evidence so far considered above is that the sex differences shown in this study might be because of altered KOPr expression or signaling in the brain regions involved (PFCx, NAc etc). However, the effects seen in this study were differences in cFos activation that are likely to be caused by activation of neurons. KOPrs are generally inhibitory, and so would be unlikely to cause direct activation of neurons on which they are expressed, but, KOPr activation could cause activation of neurons via changes in excitation within neuronal networks. For example, KOPrs are coupled to the  $G_{ai/o}$  protein and activation of KOPr located at nerve terminals has been shown to inhibit neurotransmitter release, resulting in altered neuronal activity. Neurons are connected in complex neuronal networks, and so KOPr-induced inhibition of neurons in a brain region distinct from those investigated in this study could produce

disinhibition effects of these circuits, resulting in increased neuronal activity in the brain regions studies here (e.g. NAc, PFCx etc).

For example, accumulating evidence has shown that there is a complex network effects in response to systemic KOPr agonist administration. In the PFCx, it has been shown that in male mice and rats, systemic administration of KOPr agonist, U50,488 or intra-mPFCx administration U69,593 reduced extracellular dopamine, glutamate and GABA concentrations in the PFCx (Heijna *et al.*, 1990, Tejeda *et al.*, 2013), and it was confirmed that KOPr activation-induced decrease in dopamine overflow in the PFCx by directly activating KOPr on dopaminergic terminals (Tejeda *et al.*, 2013). Additionally, local infusion of KOPr agonists into the VTA also reduced dopamine levels in the PFCx, showing that KOPr on dopaminergic afferents from the VTA could also regulate dopamine release in specific region e.g. PFCx. Thus, it is becoming clear that KOPrs are largely located presynaptically on nerve terminals of dopaminergic inputs, as well as at nerve terminals of glutamatergic and GABAergic inputs (Shippenberg *et al.*, 2001, Tejeda *et al.*, 2013). In the NAc, KOPrs are located presynaptically on dopaminergic inputs and glutamatergic inputs (Shippenberg *et al.*, 2001, Britt & McGehee, 2008). Activation of KOPr by systemic administration of U50,488 also reduced electrically-evoked dopamine release in the NAc in male adult rats (Heijna *et al.*, 1990). In addition to decreasing dopamine release in the NAc, another study reported that KOPr agonist, U69,593 also inhibits glutamate and GABA releases in the NAc in male rats (Hjelmstad *et al.*, 2003).

Electron microscopy studies found KOPr-immunoreactivity on dopaminergic-positive neurons in the NAc (Svingos *et al.*, 2001), and KOPrs are also expressed, at least in part, on serotonergic (5-HT) neurons and presynaptic glutamatergic cortical neurons in the NAc (Schindler *et al.*, 2012, Hjelmstad *et al.*, 2003). The effects of KOPr activation on different brain regions could be even more complicated, with a recent study showing that KOPr-induced inhibition on presynaptic terminal reduces the excitatory of dopamine D1 receptor activity, whereas presynaptic KOPr activation on inhibitory D2 receptor enhances excitatory activity (Tejeda *et al.*, 2017), suggesting that KOPr activation effects not only depend on expression levels and localisation of

the KOPrs, but also on the types of neurons that KOPrs are expressed on. However, all the above studies were performed in male rodents, similar investigations on the effects of KOPr activation on neuronal transmission in female rodents have not been performed, nor have studies investigating the precise neuronal localization of KOPrs in female animals.

Moreover, it is known that glial cells have an important role in regulating and supporting neurotransmitter metabolism and synaptic neurotransmission. Altered function of glial cells, particularly astrocytes, can be induced by both drugs of abuse and stress, leading to the suggestion that altered glial cell function may contribute to the development of drug addiction and psychological stress-related disorders (Miguel-Hidalgo, 2009). Furthermore, there are several studies demonstrating that KOPr activation is involved in regulating of  $\text{Ca}^{2+}$  channels and phospho-p38 immunoactivity in astrocytes (Eriksson *et al.*, 1993, Gurwell *et al.*, 1996, Bruchas *et al.*, 2006). This hypothesis was also supported by a study that reported the presence of KOPr mRNA in cortical, striatal and hippocampal glial cultures, confirming the expression of KOPrs in astrocytes in specific brain regions (Ruzicka *et al.*, 1995). Therefore, a further possible mechanism that may underlie the sex-dependent patterns of cFos activation seen in this study may be because of sex-dependent differences in KOPr activation or signaling in astrocytes, rather than in neurons.

### **8.3 Sex differences in stress-induced cFos expression**

Our study showed that an acute *in vivo* stressor, FSS, significantly induced cFos expression in a brain-region-dependent manner in both male and female mice. Similar to the effects of U50,488, FSS also significantly induced cFos expression levels in various brain regions, including PFCx, NAc and BLA in male mice. Whereas U50,488 induced a significant increase in cFos expression in the CA1 region of the hippocampus and CeA, FSS had no effect in these brain regions. The pattern of cFos expression was similar in female mice, with the exception of PFCx where no FSS-induced cFos activation was observed. As previously discussed in Chapter 1, stress

induces the release of the DYN, which is an endogenous ligand of KOPrs. Studies have shown that the prodynorphin gene is associated with drug addiction development in a sex-dependent manner. In mice, alcohol consumption in female mice was reduced in mice lacking the prodynorphin gene, with no effect in male mice (Blednov *et al.*, 2006). Similarly, a human study investigated single nucleotide polymorphisms (SNPs) in the prodynorphin gene and observed an interaction between distribution of prodynorphin SNPs and opioid dependence only in females, not in males (Clarke *et al.*, 2009). These studies suggest sex differences in the roles of the prodynorphin gene (and thus the dynorphin/KOPr system), which in turn may underlie sex differences in stress-induced neuronal activity and behaviour.

In our study, generally, the stress-induced cFos expression effects were not blocked by pretreatment with norBNI (KOPr antagonist), although a blocking effect trend towards significance was seen in some brain regions. In our data, norBNI significantly blocked stress-induced cFos only in the NAc in male mice, the blocking effect of norBNI was not observed in female mice and other brain regions in male mice. In behavioural studies, norBNI effectively blocked stress-induced analgesia, impaired learning and memory and reduced stress-induced immobility in male adult mice (McLaughlin *et al.*, 2003, Carey *et al.*, 2009). This could mean that these behaviours are largely mediated by KOPr activation in NAc, although this is unlikely, as NAc is thought to largely mediated euphoria/dysphoria, not analgesia. An alternative explanation is that the dose of norBNI used in this study is insufficient to fully block KOPrs. The main difference between KOPr activation following stress and KOPr activation following administration of U50,488 is the KOPr agonist used, with stress causing release of endogenous neurotransmitter dynorphin. Dynorphin is known to be highly efficacious, and previous studies have demonstrated spare KOPrs such that the effects of dynorphin can be seen at very low receptor occupancy (Chavkin and Goldstein, 1981).

There have been few studies directly examining the effects of KOPr antagonists on stress-induced cFos expression in rodents, and the findings are somewhat conflicting. Carr and colleagues examined cFos expression after stress or norBNI in two rat strains:

Sprague Dawley and Wistar Kyoto. In Wistar Kyoto rats, norBNI induced an antidepressive-like phenotype (decreased immobility and increased swimming in the Forced Swim test), an effect that was absent in Sprague Dawley rats. In animals that had undergone the Forced Swim procedure, norBNI induced an increase in cFos expression in the NAc, with no effect in the CA1, CA3 or dentate gyrus regions of the hippocampus (PFCx was not studied). When comparing cFos activation between control animals and those that had undergone Forced Swim, cFos expression in the NAc was increased in the Forced Swim animals (Carr *et al.*, 2010). Overall, this shows that Forced Swim can increase cFos expression (as shown in the present study), but that norBNI increases cFos expression even further. The mechanism underlying this is unknown, but it suggests that dynorphin release and KOPr activation is just one component of stress. Two caveats when comparing Carr *et al* with the present study are that this study was performed in rats, not mice, and the Forced Swim procedure was repeated in Carr *et al* (1x 15 min, 1x 5min) rather than a single 15 min stressor as performed here.

A further study that investigated the effect of norBNI on stress-induced cFos activation is Nygard *et al* (2016) who examined yohimbine-induced reinstatement of nicotine conditioned place preference in male C57 mice (Nygard *et al.*, 2016). NorBNI pretreatment effectively inhibited stress-induced reinstatement, and stress-induced reinstatement was similarly blocked in both KOPr and dynorphin knockout mice. Stress-induced reinstatement increased cFos expression in all brain regions investigated (BLA, CeA, Bed Nucleus Stria Terminalis, Dorsal Raphe nucleus), with norBNI inhibiting cFos activation only in the BLA and Dorsal Raphe nucleus (Nygard *et al.*, 2016). This study utilizes a very different stressor from the one used in the present study but does show that although cFos expression is increased in multiple brain regions, norBNI is only effective in inhibiting this increase in some brain regions. Again, this suggests either that stress involves more components in addition to dynorphin release and KOPr activation (as discussed in Chapter 1), and/or the dose of norBNI used was insufficient to block all KOPrs in some brain regions.

Lastly, our data revealed that KOPr activation by U50,488 significantly induced cFos expression in the NAc only in male mice, not in female mice, indicating KOPr-activated neuronal activity is greater in males than females in these brain regions. As previously mentioned in Chapter 1, U50,488 effectively produced decreases in motivational behaviours in intracranial self-stimulation paradigm in male rats, but significantly less effects were observed in female rats (Russell *et al.*, 2014), and U50,488 was also shown to suppress dopamine release in the NAc more effectively in male mice, compared to females (Conway *et al.*, 2019), which further suggests that female mice are less sensitive than males to KOPr activation. These neurochemical and behavioural responses correlate with our study, which showed a significant increase in cFos expression in the NAc in the male mice, not in females, suggesting that KOPr-mediated effects are less sensitive in females than males, and may explain the sex dependent motivational behaviours in response to KOPr activation.

Similar KOPr-induced cFos expression pattern between sexes was observed in the PFCx, i.e. greater cFos induction in males than females PFCx. The PFCx plays an important role in decision making and memory (McEwen, 2010), which is more difficult to assess in a behavioural paradigm than in motivational behaviours for NAc. Future investigations in neurochemical changes in the PFCx or cognitive behaviours following KOPr activation could help to understand how these sex dependent cFos expression observed in the PFCx underlie the behavioural responses to stress and KOPr activation.

## **8.4 Future work**

### **Are there any sex differences in DYN release, KOPr expression levels and activation?**

As introduced in Chapter 1, KOPrs are widely expressed throughout the brain, in numerous brain region that play key roles in cognition, emotion, mood and motivational behaviours, including VTA, PFCx, hippocampus, NAc, substantia nigra, hypothalamus and amygdala. However, KOPr expression levels and distribution between male and female animals are not fully understood. Although previous

studies (Wang *et al.*, 2011) showed differences in regional distribution of KOPrs in male and female guinea pig brains (Section 8.1.1), and PET imaging studies have taken place in humans, no studies have examined sex-dependent KOPr expression in rodents. Future experiments could investigate KOPr expression levels and distribution between male and female C57 mice by using quantitative *in vitro* autoradiography or immunohistochemistry (Shirayama *et al.*, 2004, Wang *et al.*, 2011). Since DYN is one of the key neuropeptides released in response to stress and primarily activate on KOPrs, measuring DYN release following stress in both males and females using microdialysis could facilitate better understanding of mechanisms that underlying the sex differences in stress responses, and whether there are differences in DYN release between males and females that could explain the sex differences in cFos activation seen in the present study (Rocha *et al.*, 1997). As Section 8.1.2 described, KOPr-mediated G protein activity may also underlie the sex differences in KOPr-induced neuronal activity, future studies including radioligand binding or GTP $\gamma$ S binding assays could be used to determine the binding properties and activation levels of KOPrs following KOPr activation between male and female C57 mice. Immunolabelling of the KOPr activation-dependent phosphor-p38 activity following KOPr agonist treatment could be used to compare the KOPr-activated G protein activity in male and female rodents (Bruchas *et al.*, 2006).

#### **What types of neurons that are activated following stress or KOPr agonist?**

As Section 8.1.2 discussed, KOPr activation produces different effects on neuronal transmission, depending on the types of neurons expressing KOPr, as well as the location of KOPr expression, e.g. pre or post-synaptically. Previous studies suggest that KOPrs are likely expressed presynaptically on nerve terminals of dopaminergic, glutamatergic and GABAergic inputs in many brain regions including NAc and PFCx (Section 8.2 & Chapter 6). Initial studies to investigate precisely which neurons have cFos activation following KOPr agonist administration or stress (Chapter 6) showed that U50,488 and forced swim stress-activated neurons induced cFos in non-GABAergic-neurons. Future dual-labelling immunocytochemistry could be used to identify the types of neurons that were activated in response to KOR activation or stress. For example, glutamatergic neurons could be identified using an antibody



against Vesicular Glutamate Transporter 2 (VGLUT2) (Halasz *et al.*, 2006), and dopaminergic neurons could be identified using an antibody against Tyrosine Hydroxylase (TH) (Procaccini *et al.*, 2011). Therefore, using a similar approach to that used in Chapter 6, dual-labelling of brain sections with cFos and either anti-VGLUT2 or anti-TH antibodies could help identify in which neurons cFos is activated.

It is also possible that cFos is activated in glial cells following KOPr activation or stress. Glial cells are abundantly expressed in the central nervous system, and glial fibrillary acidic protein (GFAP) is found in astrocyte cells, anti-GFAP antibody is widely and specifically used as astrocyte marker, which could be used alongside anti-cFos antibody to test whether KOPr agonist-activated neurons are neuronal or non-neuronal glial cells (Herrera *et al.*, 1998). However, dual-labelling approaches have certain limitations, which would not allow us to determine the exact neuronal type in which cFos is located, therefore using the cFos-GFP transgenic mouse, electrophysiological recordings could be performed from GFP-positive neurons (hence, only from neurons where cFos has been activated by KOPr activation or stress). Electrophysiology could be used not only to determine the phenotype of neuron in which cFos is activated (glutamatergic, GABAergic etc), but also whether that neuron expressed KOPr itself, or if the cFos activation from systemic KOPr agonist administration was via neuronal network effects (Barth *et al.*, 2004, Dai *et al.*, 2009). A final possible method that could be used to identify in which neurons cFos are activated following KOPr agonist activation or stress is FACS sorting of neurons from the cFos-GFP transgenic mouse, where neuronal phenotype could be determined, as well as potential molecular alterations in cFos-positive neurons (Liu *et al.*, 2014).

### **Are the KOPr activation-induced effects influenced by sex chromosomes and gonadal hormones?**

It is thought that sex differences in KOPr activation-mediated effects could result from, at least in part, chromosomal and hormonal factors (Gioiosa *et al.*, 2008, Rasakham *et al.*, 2011). Although how the gonadal hormones regulate stress responses and KOPr function is not fully understood, there are studies that have

reported the important role of gonadal hormones in regulating KOPr function in mice. For example, estradiol treatment significantly reduced DYN expression in adult female C57BL/6 mice, thus affected KOPr activation in response to stress (Gottsch *et al.*, 2009). It also has been shown that DYN is co-expressed with estrogen receptor alpha (ER $\alpha$ ) in the spinal cord of adult female rats. Oestrogen or progesterone treatment increased this co-expression, resulting in elevated DYN release upon ER $\alpha$  activation, which in turn affected KOPr function in response to stress in female animals (Gintzler *et al.*, 2008). As mentioned previously, Abraham *et al.* (2018) showed altered KOPr signaling in females that was oestrogen-dependent, as the response in ovariectomised animals was the same as in male animals. Although this study shows an overall effect of oestrogen in KOPr activation, the effect of the oestrus cycle was much less than the effect of ovariectomy. Similarly, Russell & colleagues showed neuronal activation in the NAc (core and shell) and amygdala (central and basolateral) following U50,488 in female rats was independent of oestrous cycle stage (Russell *et al.*, 2014). However, early animal studies in Swiss-Webster male and female mice showed that swim stress-induced analgesia is dependent the effects of gonadectomy, showing that ovariectomised females demonstrated reduced stress-induced analgesia (Mogil *et al.*, 1993). Other studies in CD1 mice using the open-field assay of anxiety-like behaviours demonstrated that social stressed female mice spent significant less time in the open field only at oestrous and dioestrous stages, but not in proestrous stage, suggesting that stress-induced anxiety-like behaviours is dependent on the oestrous cycle (Palanza *et al.*, 2001).

In this study we did not determine what stage in the oestrus cycle the animals were in during experimentation, future work could incorporate vaginal lavage to assess the correlation between oestrus cycle and sex-dependent effects of KOPr activation and stress.

### **Are there any sex differences after chronic stress or KOPr activation?**

In this study, acute forced swimming stress and a single injection of U50,488 were used, but the effect of acute stress and chronic stress differ significantly at both the

molecular level and behavioural level. For example, it has been shown that chronic stress induced dendritic shrinkage in the hippocampus and PFCx, resulting in impaired memory and cognition (Radley *et al.*, 2004, McEwen *et al.*, 2016), whereas acute restraint stress rapidly increases extracellular levels of glutamate in the hippocampus, enhanced excitability and improved memory (Lowy *et al.*, 1993, McEwen *et al.*, 2016). In addition, acute immobilisation stress largely increased cFos mRNA in the paraventricular nucleus (PVN) of rat hypothalamus, compared to the non-stressed control rats, but rats displayed significantly lower cFos mRNA signal after chronic stress (Bonaz & Rivest 1998). Similarly, chronic treatment of KOPr agonist, U50,488 not only induces prolonged KOPr phosphorylation and analgesic tolerance, but also modulates NMDA receptors in the hippocampus (McLaughlin *et al.*, 2004, Dogra *et al.*, 2016). All the studies suggest that the effects of stress on neuronal activity at molecular levels or behaviours are dependent on the stress duration. Therefore, future work could investigate whether chronic stress induces similar neuronal activity in various brain regions, whether this effect is sex-dependent as we have shown with acute stress, and how KOPrs play different roles in chronic stress responses.

In summary, our data demonstrate an apparent sex difference in brain regions that are activated by acute stressors and KOPr activation. In particular, only in male mice was their neuronal activation in the PFCx following either an acute stressor or KOPr activation. Further, although there were some common effects seen in both sexes (eg. hippocampal CA1 region and central and basolateral amygdala), in the NAc both KOPr activation and acute stress induced neuronal activation in male mice, only acute stress had that effect in female mice. As there is behavioural evidence that male and female rodents respond differently to acute stress and to KOPr activation, these data suggest that the PFCx and NAc may be key brain regions that mediate that sex difference.

This work highlights the challenges for developing effective therapeutics for psychiatric disorders between men and women patients. Future work could focus on: identifying which specific neuronal types are activated in these brain regions

following acute stress and/or KOPr activation; whether the effect of chronic stress differs to that of acute stress; where KOPrs are expressed in these brain regions, and that expression differs between the sexes.

## References

- Abraham, A. D., Schattauer, S. S., Reichard, K. L., Cohen, J. H., Fontaine, H. M., Song, A. J., Johnson, S. D., Land, B. B., Chavkin, C., 2018. Estrogen Regulation of GRK2 Inactivates Kappa Opioid Receptor Signaling Mediating Analgesia, But Not Aversion. *J Neurosci* 38, 8031-8043.
- Adinoff, B., 2004. Neurobiologic processes in drug reward and addiction. *Harv Rev Psychiatry* 12, 305-320.
- Albert 2015. Why is depression more prevalent in women? *J Psychiatry Neurosci*. 40, 219-221.
- Albert, P. R., 2015. Why is depression more prevalent in women? *J Psychiatry Neurosci* 40, 219-221.
- Alim, T. N., Lawson, W. B., Feder, A., Iacoviello, B. M., Saxena, S., Bailey, C. R., Greene, A. M., Neumeister, A., 2012. Resilience to meet the challenge of addiction: psychobiology and clinical considerations. *Alcohol Res* 34, 506-515.
- Allen, C. P., Zhou, Y., Leri, F., 2013. Effect of food restriction on cocaine locomotor sensitization in Sprague-Dawley rats: role of kappa opioid receptors. *Psychopharmacology (Berl)* 226, 571-578.
- Almatroudi, A., Ostovar, M., Bailey, C. P., Husbands, S. M., Bailey, S. J., 2018. Antidepressant-like effects of BU10119, a novel buprenorphine analogue with mixed  $\kappa/\mu$  receptor antagonist properties, in mice. *Br J Pharmacol* 175, 2869-2880.
- Back, S. E., Waldrop, A. E., Saladin, M. E., Yeatts, S. D., Simpson, A., McRae, A. L., Upadhyaya, H. P., Contini Sisson, R., Spratt, E. G., Allen, J., Kreek, M. J., Brady, K. T., 2008. Effects of gender and cigarette smoking on reactivity to psychological and pharmacological stress provocation. *Psychoneuroendocrinology* 33, 560-568.
- Bailey, S. J., Toth, M., 2004. Variability in the benzodiazepine response of serotonin 5-HT<sub>1A</sub> receptor null mice displaying anxiety-like phenotype: evidence for genetic modifiers in the 5-HT-mediated regulation of GABA(A) receptors. *J Neurosci* 24, 6343-6351.
- Bals-Kubik, R., Ableitner, A., Herz, A., Shippenberg, T. S., 1993. Neuroanatomical sites mediating the motivational effects of opioids as mapped by the conditioned place preference paradigm in rats. *J Pharmacol Exp Ther* 264, 489-495.
- Bangasser, D. A., Curtis, A., Reyes, B. A., Bethea, T. T., Parastatidis, I., Ischiropoulos, H., Van Bockstaele, E. J., Valentino, R. J., 2010. Sex differences in corticotropin-releasing factor receptor signaling and trafficking: potential role in female vulnerability to stress-related psychopathology. *Mol Psychiatry* 15, 877, 896-904.

- Barr, J. L., Forster, G. L., Unterwald, E. M., 2014. Repeated cocaine enhances ventral hippocampal-stimulated dopamine efflux in the nucleus accumbens and alters ventral hippocampal NMDA receptor subunit expression. *J Neurochem* 130, 583-590.
- Barth, A. L., Gerkin, R. C., Dean, K. L., 2004. Alteration of neuronal firing properties after in vivo experience in a FosGFP transgenic mouse. *J Neurosci* 24, 6466-6475.
- Bennur, S., Shankaranarayana Rao, B. S., Pawlak, R., Strickland, S., McEwen, B. S., Chattarji, S., 2007. Stress-induced spine loss in the medial amygdala is mediated by tissue-plasminogen activator. *Neuroscience* 144, 8-16.
- Bland, S. T., Schmid, M. J., Der-Avakian, A., Watkins, L. R., Spencer, R. L., Maier, S. F., 2005. Expression of c-fos and BDNF mRNA in subregions of the prefrontal cortex of male and female rats after acute uncontrollable stress. *Brain Res* 1051, 90-99.
- Blednov, Y. A., Walker, D., Martinez, M., Harris, R. A., 2006. Reduced alcohol consumption in mice lacking preprodynorphin. *Alcohol* 40, 73-86.
- Bolea-Alamanac, B., Bailey, S. J., Lovick, T. A., Scheele, D., Valentino, R., 2018. Female psychopharmacology matters! Towards a sex-specific psychopharmacology. *J Psychopharmacol* 32, 125-133.
- Bolla, K. I., Eldreth, D. A., London, E. D., Kiehl, K. A., Mouratidis, M., Contoreggi, C., Matochik, J. A., Kurian, V., Cadet, J. L., Kimes, A. S., Funderburk, F. R., Ernst, M., 2003. Orbitofrontal cortex dysfunction in abstinent cocaine abusers performing a decision-making task. *Neuroimage* 19, 1085-1094.
- Bonaz, B., Rivest, S., 1998. Effect of a chronic stress on CRF neuronal activity and expression of its type 1 receptor in the rat brain. *Am J Physiol* 275, R1438-1449.
- Bremner, J. D., Narayan, M., Anderson, E. R., Staib, L. H., Miller, H. L., Charney, D. S., 2000. Hippocampal volume reduction in major depression. *Am J Psychiatry* 157, 115-118.
- Briand, L. A., Vassoler, F. M., Pierce, R. C., Valentino, R. J., Blendy, J. A., 2010. Ventral tegmental afferents in stress-induced reinstatement: the role of cAMP response element-binding protein. *J Neurosci* 30, 16149-16159.
- Britt, J. P., McGehee, D. S., 2008. Presynaptic opioid and nicotinic receptor modulation of dopamine overflow in the nucleus accumbens. *J Neurosci* 28, 1672-1681.
- Brown, E. E., Finlay, J. M., Wong, J. T., Damsma, G., Fibiger, H. C., 1991. Behavioral and neurochemical interactions between cocaine and buprenorphine: implications for the pharmacotherapy of cocaine abuse. *J Pharmacol Exp Ther* 256, 119-126.

- Bruchas, M. R., Macey, T. A., Lowe, J. D., Chavkin, C., 2006. Kappa opioid receptor activation of p38 MAPK is GRK3- and arrestin-dependent in neurons and astrocytes. *J Biol Chem* 281, 18081-18089.
- Bruchas, M. R., Land, B. B., Aita, M., Xu, M., Barot, S. K., Li, S., Chavkin, C., 2007. Stress-induced p38 mitogen-activated protein kinase activation mediates kappa-opioid-dependent dysphoria. *J Neurosci* 27, 11614-11623.
- Bruchas, M. R., Land, B. B., Lemos, J. C., Chavkin, C., 2009. CRF1-R activation of the dynorphin/kappa opioid system in the mouse basolateral amygdala mediates anxiety-like behavior. *PLoS One* 4, e8528.
- Bruchas, M. R., Land, B. B., Chavkin, C., 2010. The dynorphin/kappa opioid system as a modulator of stress-induced and pro-addictive behaviors. *Brain Res* 1314, 44-55.
- Brunson, K. L., Kramar, E., Lin, B., Chen, Y., Colgin, L. L., Yanagihara, T. K., Lynch, G., Baram, T. Z., 2005. Mechanisms of late-onset cognitive decline after early-life stress. *J Neurosci* 25, 9328-9338.
- Cami, J., Farre, M., 2003 Drug addiction. *The new England Journal of Medicine* 349, 975-986.
- Campioni, M. R., Xu, M., McGehee, D. S., 2009. Stress-induced changes in nucleus accumbens glutamate synaptic plasticity. *J Neurophysiol* 101, 3192-3198.
- Carey, A. N., Lyons, A. M., Shay, C. F., Dunton, O., McLaughlin, J. P., 2009. Endogenous kappa opioid activation mediates stress-induced deficits in learning and memory. *Journal of Neuroscience* 29, 4293-4300.
- Carlezon, W. A., Jr., Beguin, C., DiNieri, J. A., Baumann, M. H., Richards, M. R., Todtenkopf, M. S., Rothman, R. B., Ma, Z., Lee, D. Y., Cohen, B. M., 2006. Depressive-like effects of the kappa-opioid receptor agonist salvinorin A on behavior and neurochemistry in rats. *J Pharmacol Exp Ther* 316, 440-447.
- Carlezon, W. A., Jr., Chartoff, E. H., 2007. Intracranial self-stimulation (ICSS) in rodents to study the neurobiology of motivation. *Nat Protoc* 2, 2987-2995.
- Carr, G. V., Bangasser, D. A., Bethea, T., Young, M., Valentino, R. J., Lucki, I., 2010. Antidepressant-like effects of kappa-opioid receptor antagonists in Wistar Kyoto rats. *Neuropsychopharmacology* 35, 752-763.
- Chavkin, C., Goldstein, A., 1981. Demonstration of a specific dynorphin receptor in guinea pig ileum myenteric plexus. *Nature* 291, 591-593.
- Chefer, V. I., Backman, C. M., Gigante, E. D., Shippenberg, T. S., 2013. Kappa opioid receptors on dopaminergic neurons are necessary for kappa-mediated place aversion. *Neuropsychopharmacology* 38, 2623-2631.

- Chen, Y., Fenoglio, K. A., Dube, C. M., Grigoriadis, D. E., Baram, T. Z., 2006. Cellular and molecular mechanisms of hippocampal activation by acute stress are age-dependent. *Mol Psychiatry* 11, 992-1002.
- Clarke, S., Chen, Z., Hsu, M. S., Pintar, J., Hill, R., Kitchen, I., 2001. Quantitative autoradiographic mapping of the ORL1, mu-, delta- and kappa-receptors in the brains of knockout mice lacking the ORL1 receptor gene. *Brain Res* 906, 13-24.
- Clarke, T. K., Krause, K., Li, T., Schumann, G., 2009. An association of prodynorphin polymorphisms and opioid dependence in females in a Chinese population. *Addict Biol* 14, 366-370.
- Connor, T. J., Kelly, J. P., Leonard, B. E., 1997. Forced swim test-induced neurochemical endocrine, and immune changes in the rat. *Pharmacol Biochem Behav* 58, 961-967.
- Conway, S. M., Puttick, D., Russell, S., Potter, D., Roitman, M. F., Chartoff, E. H., 2019. Females are less sensitive than males to the motivational- and dopamine-suppressing effects of kappa opioid receptor activation. *Neuropharmacology* 146, 231-241.
- Corish, P., Tyler-Smith, C., 1999. Attenuation of green fluorescent protein half-life in mammalian cells. *Protein Eng* 12, 1035-1040.
- Craft, R. M., Bernal, S. A., 2001. Sex differences in opioid antinociception: kappa and 'mixed action' agonists. *Drug Alcohol Depend* 63, 215-228.
- Crowley, N. A., Kash, T. L., 2015. Kappa opioid receptor signaling in the brain: Circuitry and implications for treatment. *Prog Neuropsychopharmacol Biol Psychiatry* 62, 51-60.
- Cryan, J. F., Markou, A., Lucki, I., 2002. Assessing antidepressant activity in rodents: recent developments and future needs. *Trends Pharmacol Sci* 23, 238-245.
- Cullinan, W. E., Herman, J. P., Battaglia, D. F., Akil, H., Watson, S. J., 1995. Pattern and time course of immediate early gene expression in rat brain following acute stress. *Neuroscience* 64, 477-505.
- Curran, T., Franza, B. R., Jr., 1988. Fos and Jun: the AP-1 connection. *Cell* 55, 395-397.
- Daaka, Y., Pitcher, J. A., Richardson, M., Stoffel, R. H., Robishaw, J. D., Lefkowitz, R. J., 1997. Receptor and G betagamma isoform-specific interactions with G protein-coupled receptor kinases. *Proc Natl Acad Sci USA* 94, 2180-2185.
- Dai, Y., Carlin, K. P., Li, Z., McMahon, D. G., Brownstone, R. M., Jordan, L. M., 2009. Electrophysiological and pharmacological properties of locomotor activity-related neurons in cfos-EGFP mice. *J Neurophysiol* 102, 3365-3383.



Deuschle, M., Schweiger, U., Weber, B., Gotthardt, U., Korner, A., Schmider, J., Standhardt, H., Lammers, C. H., Heuser, I., 1997. Diurnal activity and pulsatility of the hypothalamus-pituitary-adrenal system in male depressed patients and healthy controls. *J Clin Endocrinol Metab* 82, 234-238.

Di Chiara, G., Imperato, A., 1988. Drugs abused by humans preferentially increase synaptic dopamine concentrations in the mesolimbic system of freely moving rats. *Proc Natl Acad Sci U S A* 85, 5274-5278.

Dogra, S., Kumar, A., Umrao, D., Sahasrabudhe, A. A., Yadav, P. N., 2016. Chronic Kappa opioid receptor activation modulates NR2B: Implication in treatment resistant depression. *Sci Rep* 6, 33401.

Dominguez, R., Hu, E., Zhou, M., Baudry, M., 2009. 17beta-estradiol-mediated neuroprotection and ERK activation require a pertussis toxin-sensitive mechanism involving GRK2 and beta-arrestin-1. *J Neurosci* 29, 4228-4238.

Endoh, T., Matsuura, H., Tanaka, C., Nagase, H., 1992. Nor-binaltorphimine: a potent and selective kappa-opioid receptor antagonist with long-lasting activity in vivo. *Arch Int Pharmacodyn Ther* 316, 30-42.

Erb, S., Shaham, Y., Stewart, J., 1996. Stress reinstates cocaine-seeking behavior after prolonged extinction and a drug-free period. *Psychopharmacology (Berl)* 128, 408-412.

Eriksson, P. S., Nilsson, M., Wagberg, M., Hansson, E., Ronnback, L., 1993. Kappa-opioid receptors on astrocytes stimulate L-type Ca<sup>2+</sup> channels. *Neuroscience* 54, 401-407.

Evans, J., Macrory, I., Randall, C., 2016. Measuring national wellbeing: Life in the UK, 2016, ONS.

Fan, L. W., Tanaka, S., Park, Y., Sasaki, K., Ma, T., Tien, L. T., Rockhold, R. W., Ho, I. K., 2002. Butorphanol dependence and withdrawal decrease hippocampal kappa 2-opioid receptor binding. *Brain Res* 958, 277-290.

Fevurly R.D., Spencer, R. L., 2004. Fos expression is selectively and differentially regulated by endogenous glucocorticoids in the paraventricular nucleus of the hypothalamus and the dentate gyrus. *Journal of Neuroendocrinology* 16, 970-979.

Funada, M., Suzuki, T., Narita, M., Misawa, M., Nagase, H., 1993. Blockade of morphine reward through the activation of kappa-opioid receptors in mice. *Neuropharmacology* 32, 1315-1323.

- Funk, D., Li, Z., Le, A. D., 2006. Effects of environmental and pharmacological stressors on c-Fos and corticotropin-releasing factor mRNA in rat brain: relationship to the reinstatement of alcohol seeking. *Neuroscience* 138, 236-243.
- Gall, C. M., Hess, U. S., Lynch, G., 1998. Mapping brain networks engaged by, and changed by, learning. *Neurobiol Learn Mem* 70, 14-36.
- Garcia, R., Musleh, W., Tocco, G., Thompson, R. F., Baudry, M., 1997. Time-dependent blockade of STP and LTP in hippocampal slices following acute stress in mice. *Neurosci Lett* 233, 41-44.
- Gear, R. W., Gordon, N. C., Heller, P. H., Paul, S., Miaskowski, C., Levine, J. D., 1996. Gender difference in analgesic response to the kappa-opioid pentazocine. *Neurosci Lett* 205, 207-209.
- Gear, R. W., Miaskowski, C., Gordon, N. C., Paul, S. M., Heller, P. H., Levine, J. D., 1996. Kappa-opioids produce significantly greater analgesia in women than in men. *Nat Med* 2, 1248-1250.
- George, S. R., Zastawny, R. L., Briones-Urbina, R., Cheng, R., Nguyen, T., Heiber, M., Kouvelas, A., Chan, A. S., O'Dowd, B. F., 1994. Distinct distributions of mu, delta and kappa opioid receptor mRNA in rat brain. *Biochem Biophys Res Commun* 205, 1438-1444.
- Gintzler, A. R., Schnell, S. A., Gupta, D. S., Liu, N. J., Wessendorf, M. W., 2008. Relationship of spinal dynorphin neurons to delta-opioid receptors and estrogen receptor alpha: anatomical basis for ovarian sex steroid opioid antinociception. *J Pharmacol Exp Ther* 326, 725-731.
- Gioiosa, L., Chen, X., Watkins, R., Umeda, E. A., Arnold, A. P., 2008. Sex chromosome complement affects nociception and analgesia in newborn mice. *J Pain* 9, 962-969.
- Glick, S. D., Maisonneuve, I. M., Raucci, J., Archer, S., 1995. Kappa opioid inhibition of morphine and cocaine self-administration in rats. *Brain Res* 681, 147-152.
- Goeders, N. E., Smith, J. E., 1983. Cortical dopaminergic involvement in cocaine reinforcement. *Science* 221, 773-775.
- Gottsch, M. L., Navarro, V. M., Zhao, Z., Glidewell-Kenney, C., Weiss, J., Jameson, J. L., Clifton, D. K., Levine, J. E., Steiner, R. A., 2009. Regulation of Kiss1 and dynorphin gene expression in the murine brain by classical and nonclassical estrogen receptor pathways. *J Neurosci* 29, 9390-9395.
- Graziane, N. M., Polter, A. M., Briand, L. A., Pierce, R. C., Kauer, J. A., 2013. Kappa opioid receptors regulate stress-induced cocaine seeking and synaptic plasticity. *Neuron* 77, 942-954.

Gray, A. M., Rawls, S. M., Shippenberg, T. S., McGinty, J. F., 1999. The kappa-opioid agonist, U-69593, decreases acute amphetamine-evoked behaviors and calcium-dependent dialysate levels of dopamine and glutamate in the ventral striatum. *J Neurochem* 73, 1066-1074.

Gurwell, J. A., Duncan, M. J., Maderspach, K., Steine-Martin, A., Elde, R. P., Hauser, K. F., 1996. kappa-opioid receptor expression defines a phenotypically distinct subpopulation of astroglia: relationship to Ca<sup>2+</sup> mobilization, development, and the antiproliferative effect of opioids. *Brain Res* 737, 175-187.

Gutstein, H. B., Mansour, A., Watson, S. J., Akil, H., Fields, H. L., 1998. Mu and kappa opioid receptors in periaqueductal gray and rostral ventromedial medulla. *Neuroreport* 9, 1777-1781.

Halasz, J., Toth, M., Kallo, I., Liposits, Z., Haller, J., 2006. The activation of prefrontal cortical neurons in aggression – A double labeling study, *Behavioural Brain Research* 175, 166-175.

Handa, R. J., Burgess, L. H., Kerr, J. E., O'Keefe, J. A., 1994. Gonadal steroid hormone receptors and sex differences in the hypothalamo-pituitary-adrenal axis. *Hormones and Behavior* 464-476.

Hayes, A. G., Stewart, B. R., 1985. Effect of  $\mu$  and  $\kappa$  opioid receptor agonists on rat plasma corticosterone levels. *European Journal of Pharmacology* 116, 75-79.

Heijna, M. H., Padt, M., Hogenboom, F., Portoghese, P. S., Mulder, A. H., Schoffelmeer, A. N., 1990. Opioid receptor-mediated inhibition of dopamine and acetylcholine release from slices of rat nucleus accumbens, olfactory tubercle and frontal cortex. *Eur J Pharmacol* 181, 267-278.

Herman, J. P., McKlveen, J. M., Ghosal, S., Kopp, B., Wulsin, A., Makinson, R., Scheimann, J., Myers, B., 2016. Regulation of the Hypothalamic-Pituitary-Adrenocortical Stress Response. *Compr Physiol* 6, 603-621.

Herrera, D. G., Maysinger, D., Almazan, G., Funnel, R., Cuello, A. C., 1998. Analysis of c-Fos and glial fibrillary acidic protein (GFAP) expression following topical application of potassium chloride (KCl) to the brain surface. *Brain Res* 784, 71-81.

Hjelmstad, G. O., Fields, H. L., 2001. Kappa opioid receptor inhibition of glutamatergic transmission in the nucleus accumbens shell. *J Neurophysiol* 85, 1153-1158.

Hjelmstad, G. O., Fields, H. L., 2003. Kappa opioid receptor activation in the nucleus accumbens inhibits glutamate and GABA release through different mechanisms. *J Neurophysiol* 89, 2389-2395.

- Hoffman, G. E., Smith, M. S., Verbalis, J. G., 1993. c-Fos and related immediate early gene products as markers of activity in neuroendocrine systems. *Front Neuroendocrinol* 14, 173-213.
- Iwasaki-Sekino, A., Mano-Otagiri, A., Ohata, H., Yamauchi, N., Shibasaki, T., 2009. Gender differences in corticotropin and corticosterone secretion and corticotropin-releasing factor mRNA expression in the paraventricular nucleus of the hypothalamus and the central nucleus of the amygdala in response to footshock stress or psychological stress in rats. *Psychoneuroendocrinology* 34, 226-237.
- Iyengar S., Kim, H. S., Wood, P. L., 1986. Kappa opioid agonists modulate the hypothalamic-pituitary-adrenocortical axis in the rat. *The Journal of Pharmacology and Experimental Therapeutics* 238, 429-436.
- Jochman, K. A., Newman, S. M., Kalin, N. H., Bakshi, V. P., 2005. Corticotropin-releasing factor-1 receptors in the basolateral amygdala mediate stress-induced anorexia. *Behav Neurosci* 119, 1448-1458.
- Kant, G. J., Lenox, R. H., Bunnell, B. N., Mougey, E. H., Pennington, L. L., Meyerhoff, J. L., 1983. Comparison of stress response in male and female rats: pituitary cyclic AMP and plasma prolactin, growth hormone and corticosterone. *Psychoneuroendocrinology* 8, 421-428.
- Kavaliers, M., Innes, D. G., 1987. Sex and day-night differences in opiate-induced responses of insular wild deer mice, *Peromyscus maniculatus triangularis*. *Pharmacol Biochem Behav* 27, 477-482.
- Keller, J., Gomez, R., Williams, G., Lembke, A., Lazzeroni, L., Murphy, G. M., Jr., Schatzberg, A. F., 2017. HPA axis in major depression: cortisol, clinical symptomatology and genetic variation predict cognition. *Mol Psychiatry* 22, 527-536.
- Kessler, R. C., 2003. Epidemiology of women and depression. *J Affect Disord* 74, 5-13.
- Kim, K. S., Han, P. L., 2006. Optimization of chronic stress paradigms using anxiety- and depression-like behavioral parameters. *J Neurosci Res* 83, 497-507.
- Kitchen, I., Slowe, S. J., Matthes, H. W., Kieffer, B., 1997. Quantitative autoradiographic mapping of mu-, delta- and kappa-opioid receptors in knockout mice lacking the mu-opioid receptor gene. *Brain Res* 778, 73-88.
- Knoll, A. T., Carlezon, W. A., Jr., 2010. Dynorphin, stress, and depression. *Brain Res* 1314, 56-73.
- Koob, G. F., Bloom, F. E., 1988. Cellular and molecular mechanisms of drug dependence. *Science* 242, 715-723.

- Koob, G. F., Schulkin, J., 2018. Addiction and stress: An allostatic view. *Neurosci Biobehav Rev.* 18, 30218-30225.
- Kovacs, K. J., 1998. c-Fos as a transcription factor: a stressful (re)view from a functional map. *Neurochem Int* 33, 287-297.
- Kudielka, B. M., Kirschbaum, C., 2005. Sex differences in HPA axis responses to stress: a review. *Biol Psychol* 69, 113-132.
- Kuzmin, A., Chefer, V., Bazov, I., Meis, J., Ogren, S. O., Shippenberg, T., Bakalkin, G., 2013. Upregulated dynorphin opioid peptides mediate alcohol-induced learning and memory impairment. *Transl Psychiatry* 3, e310.
- Lalanne, L., Ayranci, G., Kieffer, B. L., Lutz, P. E., 2014. The kappa opioid receptor: from addiction to depression, and back. *Front Psychiatry* 5, 170.
- Laman-Maharg, A. R., Copeland, T., Sanchez, E. O., Campi, K. L., Trainor, B. C., 2017. The long-term effects of stress and kappa opioid receptor activation on conditioned place aversion in male and female California mice. *Behav Brain Res* 332, 299-307.
- Laman-Maharg, A., Williams, A. V., Zufelt, M. D., Minie, V. A., Ramos-Maciel, S., Hao, R., Ordonez Sanchez, E., Copeland, T., Silverman, J. L., Leigh, A., Snyder, R., Carroll, F. I., Fennell, T. R., Trainor, B. C., 2018. Sex Differences in the Effects of a Kappa Opioid Receptor Antagonist in the Forced Swim Test. *Front Pharmacol* 9, 93.
- Land, B. B., Bruchas, M. R., Lemos, J. C., Xu, M., Melief, E. J., Chavkin, C., 2008. The dysphoric component of stress is encoded by activation of the dynorphin kappa-opioid system. *J Neurosci* 28, 407-414.
- Le Merrer, J., Becker, J. A., Befort, K., Kieffer, B. L., 2009. Reward processing by the opioid system in the brain. *Physiol Rev* 89, 1379-1412.
- Lee, A. T., Vogt, D., Rubenstein, J. L., Sohal, V. S., 2014. A class of GABAergic neurons in the prefrontal cortex sends long-range projections to the nucleus accumbens and elicits acute avoidance behavior. *J Neurosci* 34, 11519-11525.
- Lin, S., Boey, D., Lee, N., Schwarzer, C., Sainsbury, A., Herzog, H., 2006. Distribution of prodynorphin mRNA and its interaction with the NPY system in the mouse brain. *Neuropeptides* 40, 115-123.
- Lin, Y., Ter Horst, G. J., Wichmann, R., Bakker, P., Liu, A., Li, X., Westenbroek, C., 2009. Sex differences in the effects of acute and chronic stress and recovery after long-term stress on stress-related brain regions of rats. *Cereb Cortex* 19, 1978-1989.
- Liu, N. J., Schnell, S., Wessendorf, M. W., Gintzler, A. R., 2013. Sex, pain, and opioids: interdependent influences of sex and pain modality on dynorphin-mediated antinociception in rats. *J Pharmacol Exp Ther* 344, 522-530.

- Liu, Q. R., Rubio, F. J., Bossert, J. M., Marchant, N. J., Fanous, S., Hou, X., Shaham, Y., Hope, B. T., 2014. Detection of molecular alterations in methamphetamine-activated Fos-expressing neurons from a single rat dorsal striatum using fluorescence-activated cell sorting (FACS). *J Neurochem* 128, 173-185.
- Lowy, M. T., Gault, L., Yamamoto, B. K., 1993. Adrenalectomy attenuates stress-induced elevations in extracellular glutamate concentrations in the hippocampus. *J Neurochem* 61, 1957-1960.
- Lu, J., Wu, X. Y., Zhu, Q. B., Li, J., Shi, L. G., Wu, J. L., Zhang, Q. J., Huang, M. L., Bao, A. M., 2015. Sex differences in the stress response in SD rats. *Behav Brain Res* 284, 231-237.
- Mague, S. D., Pliakas, A. M., Todtenkopf, M. S., Tomasiewicz, H. C., Zhang, Y., Stevens, W. C., Jr., Jones, R. M., Portoghesse, P. S., Carlezon, W. A., Jr., 2003. Antidepressant-like effects of kappa-opioid receptor antagonists in the forced swim test in rats. *J Pharmacol Exp Ther* 305, 323-330.
- Maisonneuve, I. M., Archer, S., Glick, S. D., 1994. U50,488, a kappa opioid receptor agonist, attenuates cocaine-induced increases in extracellular dopamine in the nucleus accumbens of rats. *Neurosci Lett* 181, 57-60.
- Malisch, J. L., Saltzman, W., Gomes, F. R., Rezende, E. L., Leske, D. R., Garland, T., 2007. Baseline and stress-induced plasma corticosterone concentrations of mice selectively bred for high voluntary wheel running. *Physiol Biochem Zool* 80, 146-156.
- Margolis, E. B., Lock, H., Chefer, V. I., Shippenberg, T. S., Hjelmstad, G. O., Fields, H. L., 2006. Kappa opioids selectively control dopaminergic neurons projecting to the prefrontal cortex. *Proc Natl Acad Sci USA* 103, 2938-2942.
- Margolis, E. B., Karkhanis, A. N., 2019. Dopaminergic cellular and circuit contributions to kappa opioid receptor mediated aversion. *Neurochem Int* 129, 104504.
- Marrone, G. F., Grinnell, S. G., Lu, Z., Rossi, G. C., Le Rouzic, V., Xu, J., Majumdar, S., Pan, Y. X., Pasternak, G. W., 2016. Truncated mu opioid GPCR variant involvement in opioid-dependent and opioid-independent pain modulatory systems within the CNS. *Proc Natl Acad Sci U S A* 113, 3663-3668.
- Martin, K. P., Wellman, C. L., 2011. NMDA receptor blockade alters stress-induced dendritic remodeling in medial prefrontal cortex. *Cereb Cortex* 21, 2366-2373.
- Martinez, M., Phillips, P. J., Herbert, J., 1998. Adaptation in patterns of c-fos expression in the brain associated with exposure to either single or repeated social stress in male rats. *European Journal of Neuroscience* 10, 20-33.

McEwen, B. S., 1999. Stress and hippocampal plasticity. *Annu Rev Neurosci* 22, 105-122.

McEwen, B. S., 2010. Stress, sex, and neural adaptation to a changing environment: mechanisms of neuronal remodeling. *Ann N Y Acad Sci* 1204, Suppl:E38-59.

McEwen, B. S., Bowles, N. P., Gray, J. D., Hill, M. N., Hunter, R. G., Karatsoreos, I. N., Nasca, C., 2015. Mechanisms of stress in the brain. *Nat Neurosci* 18, 1353-1363.

McEwen, B. S., Nasca, C., Gray, J. D., 2016. Stress Effects on Neuronal Structure: Hippocampus, Amygdala, and Prefrontal Cortex. *Neuropsychopharmacology* 41, 3-23.

McLaughlin, J. P., Marton-Popovici, M., Chavkin, C., 2003. Kappa opioid receptor antagonism and prodynorphin gene disruption block stress-induced behavioral responses. *J Neurosci* 23, 5674-5683.

McLaughlin, J. P., Myers, L. C., Zarek, P. E., Caron, M. G., Lefkowitz, R. J., Czyzyk, T. A., Pintar, J. E., Chavkin, C., 2004. Prolonged kappa opioid receptor phosphorylation mediated by G-protein receptor kinase underlies sustained analgesic tolerance. *J Biol Chem* 279, 1810-1818.

McLaughlin, J. P., Li, S., Valdez, J., Chavkin, T. A., Chavkin, C., 2006a. Social defeat stress-induced behavioral responses are mediated by the endogenous kappa opioid system. *Neuropsychopharmacology* 31, 1241-1248.

McLaughlin, J. P., Land, B. B., Li, S., Pintar, J. E., Chavkin, C., 2006b. Prior activation of kappa opioid receptors by U50,488 mimics repeated forced swim stress to potentiate cocaine place preference conditioning. *Neuropsychopharmacology* 31, 787-794.

Melia, K. R., Ryabinin, A. E., Schroeder, R., Bloom, F. E., Wilson, M. C., 1994. Induction and habituation of immediate early gene expression in rat brain by acute and repeated restraint stress. *J Neurosci* 14, 5929-5938.

Menendez, L., Andres-Trelles, F., Hidalgo, A., Baamonde, A., 1993. Involvement of spinal kappa opioid receptors in a type of footshock induced analgesia in mice. *Brain Res* 611, 264-271.

Meng, I. D., Johansen, J. P., Harasawa, I., Fields, H. L., 2005. Kappa opioids inhibit physiologically identified medullary pain modulating neurons and reduce morphine antinociception. *J Neurophysiol* 93, 1138-1144.

Meredith, G. E., Pennartz, C. M., Groenewegen, H. J., 1993. The cellular framework for chemical signalling in the nucleus accumbens. *Prog Brain Res* 99, 3-24.

Mergl, R., Koburger, N., Heinrichs, K., Szekely, A., Toth, M. D., Coyne, J., Quintao, S., Arensman, E., Coffey, C., Maxwell, M., Varnik, A., van Audenhove, C., McDaid, D., Sarchiapone, M., Schmidtke, A., Genz, A., Gusmao, R., Hegerl, U., 2015. What Are

Reasons for the Large Gender Differences in the Lethality of Suicidal Acts? An Epidemiological Analysis in Four European Countries. *PLoS One* 10, e0129062.

Miguel-Hidalgo, J. J., 2009. The role of glial cells in drug abuse. *Curr Drug Abuse Rev.* 2, 76-82.

Mogil, J. S., Sternberg, W. F., Kest, B., Marek, P., Liebeskind, J. C., 1993. Sex differences in the antagonism of swim stress-induced analgesia: effects of gonadectomy and estrogen replacement. *Pain* 53, 17-25.

Murphy, B. E., 1991. Steroids and depression. *J Steroid Biochem Mol Biol* 38, 537-559.

Nestler, E. J., 1992. Molecular mechanisms of drug addiction. *J Neurosci* 12, 2439-2450.

Nestler, E. J., 2005. Is there a common molecular pathway for addiction? *Nat Neurosci* 8, 1445-1449.

Nestler, E. J., Hyman, S. E., 2010. Animal models of neuropsychiatric disorders. *Nat Neurosci* 13, 1161-1169.

NHS Digital 2017. Statistics on Drug Misuses: England, 2017. National Statistics (<http://digital.nhs.uk/pubs/statdrugs17>).

Nygard, S. K., Hourguettes, N. J., Sobczak, G. G., Carlezon, W. A., Bruchas, M. R., 2016. Stress-Induced Reinstatement of Nicotine Preference Requires Dynorphin/Kappa Opioid Activity in the Basolateral Amygdala. *J Neurosci* 36, 9937-9948.

Ons, S., Marti, O., Armario, A., 2004. Stress-induced activation of the immediate early gene *Arc* (activity-regulated cytoskeleton-associated protein) is restricted to telencephalic areas in the rat brain: relationship to *cFos* mRNA. *Journal of Neurochemistry* 89, 1111-1118.

Pace, T. W., Gaylord, R., Topczewski, F., Girotti, M., Rubin, B., Spencer, R. L., 2005. Immediate-early gene induction in hippocampus and cortex as a result of novel experience is not directly related to the stressfulness of that experience. *Eur J Neurosci* 22, 1679-1690.

Palanza, P., Gioiosa, L., Parmigiani, S., 2001. Social stress in mice: gender differences and effects of estrous cycle and social dominance. *Physiol Behav* 73, 411-420.

Perrotti, L. I., Hadeishi, Y., Ulery, P. G., Barrot, M., Monteggia, L., Duman, R. S., Nestler, E. J., 2004. Induction of *deltaFosB* in reward-related brain structures after chronic stress. *J Neurosci* 24, 10594-10602.



Pettit, H. O., Ettenberg, A., Bloom, F. E., Koob, G. F., 1984. Destruction of dopamine in the nucleus accumbens selectively attenuates cocaine but not heroin self-administration in rats. *Psychopharmacology (Berl)* 84, 167-173.

Pfeiffer, A., Brantl, V., Herz, A., Emrich, H. M., 1986. Psychotomimesis mediated by kappa opiate receptors. *Science* 233, 774-776.

Pliakas, A. M., Carlson, R. R., Neve, R. L., Konradi, C., Nestler, E. J., Carlezon, W. A., Jr., 2001. Altered responsiveness to cocaine and increased immobility in the forced swim test associated with elevated cAMP response element-binding protein expression in nucleus accumbens. *J Neurosci* 21, 7397-7403.

Polter, A. M., Bishop, R. A., Briand, L. A., Graziane, N. M., Pierce, R. C., Kauer, J. A., 2014. Poststress block of kappa opioid receptors rescues long-term potentiation of inhibitory synapses and prevents reinstatement of cocaine seeking. *Biol Psychiatry* 76, 785-793.

Portoghese, P. S., Lipkowski, A. W., Takemori, A. E., 1987. Binaltorphimine and nor-binaltorphimine, potent and selective kappa-opioid receptor antagonists. *Life Sci* 40, 1287-1292.

Procaccini, C., Aitta-aho, T., Jaako-Movits, K., Zharkovsky, A., Panhelainen, A., Sprengel, R., Linden, A. M., Korpi, E. R., 2011. Excessive novelty-induced cFos expression and altered neurogenesis in the hippocampus of GluA1 knockout mice. *Eur J Neurosci* 33, 161-174.

Radley, J. J., Sisti, H. M., Hao, J., Rocher, A. B., McCall, T., Hof, P. R., McEwen, B. S., Morrison, J. H., 2004. Chronic behavioral stress induces apical dendritic reorganization in pyramidal neurons of the medial prefrontal cortex. *Neuroscience* 125, 1-6.

Rasakham, K., Liu-Chen, L. Y., 2011. Sex differences in kappa opioid pharmacology. *Life Sci* 88, 2-16.

Redila, V. A., Chavkin, C., 2008. Stress-induced reinstatement of cocaine seeking is mediated by the kappa opioid system. *Psychopharmacology* 200, 59-70.

Rinaman, L., Stricker, E. M., Hoffman, G. E., Verbalis, J. G., 1997. Central c-Fos expression in neonatal and adult rats after subcutaneous injection of hypertonic saline. *Neuroscience* 79, 1165-1175.

Robinson, S. E., 2006. Buprenorphine-containing treatments: place in the management of opioid addiction. *CNS Drugs* 20, 697-712.

Robles, C. F., McMackin, M. Z., Campi, K. L., Doig, I. E., Takahashi, E. Y., Pride, M. C., Trainor, B. C., 2014. Effects of kappa opioid receptors on conditioned place aversion and social interaction in males and females. *Behav Brain Res* 262, 84-93.

Rocha, L. L., Evans, C. J., Maidment, N. T., 1997. Amygdala kindling modifies extracellular opioid peptide content in rat hippocampus measured by microdialysis. *J Neurochem* 68, 616-624.

Romeo R. D., Kaplowitz, E. T., Ho, A., Franco, D., 2013. The influence of puberty on stress reactivity and forebrain glucocorticoid receptor levels in inbred and outbred strains of male and female mice. *Psychoneuroendocrinology* 38, 592-596.

Russell, S. E., Rachlin, A. B., Smith, K. L., Muschamp, J., Berry, L., Zhao, Z., Chartoff, E. H., 2014. Sex differences in sensitivity to the depressive-like effects of the kappa opioid receptor agonist U-50488 in rats. *Biol Psychiatry* 76, 213-222.

Ruzicka, B. B., Fox, C. A., Thompson, R. C., Meng, F., Watson, S. J., Akil, H., 1995. Primary astroglial cultures derived from several rat brain regions differentially express mu, delta and kappa opioid receptor mRNA. *Brain Res Mol Brain Res* 34, 209-220.

Ryabinin, A. E., Melia, K. R., Cole, M., Bloom, F. E., Wilson, M. C., 1995. Alcohol selectively attenuates stress-induced c-fos expression in rat hippocampus. *J Neurosci* 15, 721-730.

Sadler, A. M., Bailey, S. J., 2013. Validation of a refined technique for taking repeated blood samples from juvenile and adult mice. *Lab Anim* 47, 316-319.

Sadler, A. M., Bailey, S. J., 2016. Repeated daily restraint stress induces adaptive behavioural changes in both adult and juvenile mice. *Physiology and Behavior* 167, 313-323.

Schindler, A.G., Messinger, D.I., Smith, J.S., Shankar, H., Gustin, R. M., Schattauer, S. S., Lemos, J. C., Chavkin, N. W., Hagan, C. E., Neumaier, J. F., Chavkin, C., 2012. Stress produces aversion and potentiates cocaine reward by releasing endogenous dynorphins in the ventral striatum to locally stimulate serotonin reuptake. *J Neurosci* 32, 17582-17596.

Senba, E., Ueyama, T., 1997. Stress-induced expression of immediate early genes in the brain and peripheral organs of the rat. *Neurosci Res* 29, 183-207.

Sershen, H., Hashim, A., Lajtha, A., 1998. Gender differences in kappa-opioid modulation of cocaine-induced behavior and NMDA-evoked dopamine release. *Brain Res* 801, 67-71.

Shah, P. J., Ebmeier, K. P., Glabus, M. F., Goodwin, G. M., 1998. Cortical grey matter reductions associated with treatment-resistant chronic unipolar depression. Controlled magnetic resonance imaging study. *Br J Psychiatry* 172, 527-532.

Shepard, R., Page, C. E., Couellier, L., 2016. Sensitivity of the prefrontal GABAergic system to chronic stress in male and female mice: Relevance for sex differences in stress-related disorders. *Neuroscience* 332, 1-12.

Shippenberg, T. S., Chefer, V. I., Zapata, A., Heidbreder, C. A., 2001. Modulation of the behavioral and neurochemical effects of psychostimulants by kappa-opioid receptor systems. *Ann N Y Acad Sci* 937, 50-73.

Shippenberg, T. S., Zapata, A., Chefer, V. I., 2007. Dynorphin and the pathophysiology of drug addiction. *Pharmacol Ther* 116, 306-321.

Shippenberg, T.S. 2009. The dynorphin/kappa opioid receptor system: a new target for the treatment of addiction and affective disorders? *Neuropsychopharmacology* 34, 247.

Shirayama, Y., Ishida, H., Iwata, M., Hazama, G. I., Kawahara, R., Duman, R. S., 2004. Stress increases dynorphin immunoreactivity in limbic brain regions and dynorphin antagonism produces antidepressant-like effects. *J Neurochem* 90, 1258-1268.

Shors, T. J., Dryver, E., 1994. Effect of stress and long-term potentiation (LTP) on subsequent LTP and the theta burst response in the dentate gyrus. *Brain Res* 666, 232-238.

Sinha, R., 2008. Chronic stress, drug use, and vulnerability to addiction. *Ann N Y Acad Sci* 1141, 105-130.

Smith, J. S., Schindler, A. G., Martinelli, E., Gustin, R. M., Bruchas, M. R., Chavkin, C., 2012. Stress-induced activation of the dynorphin/kappa-opioid receptor system in the amygdala potentiates nicotine conditioned place preference. *J Neurosci* 32, 1488-1495.

Sood, A., Chaudhari, K., Vaidya, V. A., 2018. Acute stress evokes sexually dimorphic, stressor-specific patterns of neural activation across multiple limbic brain regions in adult rats. *Stress* 21, 136-150.

Sousa, N., Lukoyanov, N. V., Madeira, M. D., Almeida, O. F., Paula-Barbosa, M. M., 2000. Reorganization of the morphology of hippocampal neurites and synapses after stress-induced damage correlates with behavioral improvement. *Neuroscience* 97, 253-266.

Spanagel, R., Herz, A., Shippenberg, T. S., 1992. Opposing tonically active endogenous opioid systems modulate the mesolimbic dopaminergic pathway. *Proc Natl Acad Sci U S A* 89, 2046-2050.

Sperling, R. E., Gomes, S. M., Sypek, E. I., Carey, A. N., McLaughlin, J. P., 2010. Endogenous kappa-opioid mediation of stress-induced potentiation of ethanol-

conditioned place preference and self-administration. *Psychopharmacology (Berl)* 210, 199-209.

Starkman, M. N., Gebarski, S. S., Berent, S., Schteingart, D. E., 1992. Hippocampal formation volume, memory dysfunction, and cortisol levels in patients with Cushing's syndrome. *Biol Psychiatry* 32, 756-765.

Svingos, A. L., Chavkin, C., Colago, E. E., Pickel, V. M., 2001. Major coexpression of kappa-opioid receptors and the dopamine transporter in nucleus accumbens axonal profiles. *Synapse* 42, 185-192.

Takahashi, M., Senda, T., Tokuyama, S., Kaneto, H., 1990. Further evidence for the implication of a kappa-opioid receptor mechanism in the production of psychological stress-induced analgesia. *Jpn J Pharmacol* 53, 487-494.

Tamamaki, N., Yanagawa, Y., Tomioka, R., Miyazaki, J., Obata, K., Kaneko, T., 2003. Green fluorescent protein expression and colocalization with calretinin, parvalbumin, and somatostatin in the GAD67-GFP knock-in mouse. *J Comp Neurol* 467, 60-79.

Tejeda, H. A., Counotte, D. S., Oh, E., Ramamoorthy, S., Schultz-Kuszk, K. N., Backman, C. M., Chefer, V., O'Donnell, P., Shippenberg, T. S., 2013. Prefrontal cortical kappa-opioid receptor modulation of local neurotransmission and conditioned place aversion. *Neuropsychopharmacology* 38, 1770-1779.

Tejeda, H. A., Wu, J., Kornspun, A. R., Pignatelli, M., Kashtelyan, V., Krashes, M. J., Lowell, B. B., Carlezon, W. A., Bonci, A., 2017. Pathway- and Cell-Specific Kappa-Opioid Receptor Modulation of Excitation-Inhibition Balance Differentially Gates D1 and D2 Accumbens Neuron Activity. *Neuron* 93, 147-163.

Theodor, M., Gasbos, G.I., Buicu, G.E., Ferencz, M., Gabos, G., Marieta, S.A., Popa, C.O., 2016. Increased Cortisol Levels in Depression: A Comparative Study Evaluating the Correlation of Hypercortisolemia with Prosocial Coping Mechanisms. *Acta Medica Marisiensis*, 62, 68–72.

Titze-de-Almeida, R., Shida, H., Guimaraes, F. S., Del-Bel, E. A., 1994. Stress-induced expression of the c-fos proto-oncogene in the hippocampal formation. *Braz J Med Biol Res* 27, 1083-1088.

Trifilieff, P., Martinez, D., 2013. Kappa-opioid receptor signaling in the striatum as a potential modulator of dopamine transmission in cocaine dependence. *Front Psychiatry* 4, 44.

Uhart, M., Chong, R. Y., Oswald, L., Lin, P. I., Wand, G. S., 2006. Gender differences in hypothalamic-pituitary-adrenal (HPA) axis reactivity. *Psychoneuroendocrinology* 31, 642-652.

Van't Veer, A., Carlezon, W. A., Jr., 2013. Role of kappa-opioid receptors in stress and anxiety-related behavior. *Psychopharmacology (Berl)* 229, 435-452.

Varghese, F. P., Brown, E. S., 2001. The Hypothalamic-Pituitary-Adrenal Axis in Major Depressive Disorder: A Brief Primer for Primary Care Physicians. *Prim Care Companion J Clin Psychiatry* 3, 151-155.

Viau, V., Bingham, B., Davis, J., Lee, P., Wong, M., 2005. Gender and puberty interact on the stress-induced activation of parvocellular neurosecretory neurons and corticotropin-releasing hormone messenger ribonucleic acid expression in the rat. *Endocrinology* 146, 137-146.

Vijay, A., Wang, A., Worhunsky, P., Zheng, M. Q., Nabulsi, N., Ropchan, J., Krishnan-Sarin, S., Huang, Y., Morris, E. D., 2016. PET imaging reveals sex differences in kappa opioid receptor availability in humans, in vivo. *Am J Nucl Med Mol Imaging* 6, 205-214.

Vonvoigtlander, P. F., Lahti, R. A., Ludens, J. H., 1983. U-50,488: a selective and structurally novel non-Mu (kappa) opioid agonist. *J Pharmacol Exp Ther* 224, 7-12.

Vyas, A., Mitra, R., Shankaranarayana Rao, B. S., Chattarji, S., 2002. Chronic stress induces contrasting patterns of dendritic remodeling in hippocampal and amygdaloid neurons. *J Neurosci* 22, 6810-6818.

Wang, Y. J., Rasakham, K., Huang, P., Chudnovskaya, D., Cowan, A., Liu-Chen, L. Y., 2011. Sex difference in kappa-opioid receptor (KOPR)-mediated behaviors, brain region KOPR level and KOPR-mediated guanosine 5'-O-(3-[35S]thiotriphosphate) binding in the guinea pig. *J Pharmacol Exp Ther* 339, 438-450.

Weinstock, M., Matlina, E., Maor, G. I., Rosen, H., McEwen, B. S., 1992. Prenatal stress selectively alters the reactivity of the hypothalamic-pituitary adrenal system in the female rat. *Brain Res* 595, 195-200.

Whitelaw, R. B., Markou, A., Robbins, T. W., Everitt, B. J., 1996. Excitotoxic lesions of the basolateral amygdala impair the acquisition of cocaine-seeking behaviour under a second-order schedule of reinforcement. *Psychopharmacology (Berl)* 127, 213-224.

Winkler, C. W., Hermes, S. M., Chavkin, C. I., Drake, C. T., Morrison, S. F., Aicher, S. A., 2006. Kappa opioid receptor (KOR) and GAD67 immunoreactivity are found in OFF and NEUTRAL cells in the rostral ventromedial medulla. *J Neurophysiol* 96, 3465-3473.

Wise, R. A., Bozarth, M. A., 1987. A psychomotor stimulant theory of addiction. *Psychol Rev* 94, 469-492.

Wittmann, W., Schunk, E., Rosskothén, I., Gaburro, S., Singewald, N., Herzog, H., Schwarzer, C., 2009. Prodynorphin-derived peptides are critical modulators of

anxiety and regulate neurochemistry and corticosterone. *Neuropsychopharmacology* 34, 775-785.

Wong, M. L., Licinio, J., 2001. Research and treatment approaches to depression. *Nat Rev Neurosci* 2, 343-351.

Xu, L., Anwyl, R., Rowan, M. J., 1997. Behavioural stress facilitates the induction of long-term depression in the hippocampus. *Nature* 387, 497-500.

Yu, J. Y., Fang, P., Wang, C., Wang, X. X., Li, K., Gong, Q., Luo, B. Y., Wang, X. D., 2018. Dorsal CA1 interneurons contribute to acute stress-induced spatial memory deficits. *Neuropharmacology* 135, 474-486.

## Published abstracts

Ma, Q., Wonnacott, S., Bailey, S. J., Bailey, C.P., 2016. Investigating the roles of kappa opioid receptors in neurochemical changes caused by stress and drugs of abuse. *pA2Oline*.

Ma, Q., Wonnacott, S., Bailey, S.J., Bailey, C.P., 2017. Gender differences in kappa opioid receptor activated brain networks implicated in the response to stress and drugs of abuse. *Journal of Psychopharmacology*. 31(8), pp. A132.

Ma, Q., Wonnacott, S., Bailey, S.J., Bailey, C.P., 2018. Effects of kappa opioid receptor agonists and acute stress on brain regions implicated in the response to stress and drugs of abuse. *Journal of Psychopharmacology*. 32(8), pp. A124.